

Molecular studies of genomic imprinting using an Angelman syndrome imprinting defect mouse model

Hou, Aihua

2008

Hou, A. H. (2008). Molecular studies of genomic imprinting using an Angelman Syndrome imprinting defect mouse model. Doctoral thesis, Nanyang Technological University, Singapore.

<https://hdl.handle.net/10356/13578>

<https://doi.org/10.32657/10356/13578>



**NANYANG
TECHNOLOGICAL
UNIVERSITY**

**MOLECULAR STUDIES OF GENOMIC IMPRINTING
USING AN ANGELMAN SYNDROME IMPRINTING
DEFECT MOUSE MODEL**

**MOLECULAR STUDIES OF GENOMIC IMPRINTING USING AN
ANGELMAN SYNDROME IMPRINTING DEFECT MOUSE MODEL**

HOU AIHUA

HOU AIHUA

SCHOOL OF BIOLOGICAL SCIENCES

2008

2008

**MOLECULAR STUDIES OF GENOMIC IMPRINTING
USING AN ANGELMAN SYNDROME IMPRINTING
DEFECT MOUSE MODEL**

HOU AIHUA

School of Biological Sciences

A thesis submitted to the Nanyang Technological University
in partial fulfillment of the requirement for the degree of
Doctor of Philosophy

2008

Table of Contents

Acknowledgements	5
Abbreviations	6
Summary.....	9
Chapter I Introduction.....	11
1.1 Epigenetics	11
1.2 Epigenetic mechanisms in human disease	15
1.3 Epigenetic reprogramming during early development in mammals	18
1.4 Function of genomic imprinting in mammals	21
1.5 X-chromosome inactivation and imprinting	23
1.6 Regulation of imprinted genes in the somatic cells.....	24
1.7 Prader-Willi syndrome and Angelman syndrome.....	29
1.8 PWS/AS imprinting domain.....	33
1.9 Epigenetic regulation of PWS/AS imprinting domain.....	38
1.10 Project aims	45
Chapter II Materials and Methods	47
2.1 Genomic DNA extraction from mouse tail	47
2.2 Southern blot	47
2.3 Nucleotide polymorphism analysis	48
2.4 Bisulfite genomic sequencing	50
2.5 Methylation specific PCR (MSP).....	51
2.6 Reverse transcription PCR (RT-PCR) and real time PCR	51
2.7 Chromatin Immunoprecipitation (ChIP)	53
2.8 Chromosome conformation capture (3C).....	57

2.9 ChIP-loop	61
2.10 Bacterial artificial chromosome (BAC) DNA extraction.....	63
2.11 Fluorescence in situ hybridization (FISH)	63
2.11.1 Coating slides with poly-L-lysine.....	63
2.11.2 Cell suspension preparation from mouse liver.....	64
2.11.3 Slides preparation for FISH	64
2.11.4 Hybridization and Wash	65
2.11.5 Probe label and precipitation	66
2.12 Vector construction	66
2.12.1 Bacterial strains, plasmids and enzymes.....	68
2.12.2 Protocols	68
2.12.3 pCMVH6 construction procedure.....	69
2.12.4 Mammalian cell transfection.....	75
2.12.5 X-gal staining.....	76
2.12.6 Western blot.....	76
2.13 Electroporation of mouse embryonic stem cells AB2.2.....	77
2.13.1 STO cell culture and mitomycin C treatment	77
2.13.2 Embryonic stem (ES) cells AB2.2 culture.....	78
2.13.3 DNA preparation for electroporation.....	79
2.13.4 Cells preparation for electroporation	79
2.13.5 Electroporation.....	80
2.13.6 Picking colonies	81
2.13.7 Freezing down 96-well plates containing ES cell colonies	81
2.13.8 Selection of positive ES cell colonies by mini-Southern.....	82
2.13.9 Selection of positive ES cell colonies by PCR	83

2.13.10 Expanding ES colonies out of freeze from 96-well plate	84
2.14 Confirmation of PWS/AS deletion by microsatellite analysis	85
Chapter III Results	87
3.1 Incomplete penetrance reflecting epigenetic instability of AS-IC ^{an} mutation in 129/SvEv background	87
3.2 Nucleotide polymorphisms between 129/SvEv and PWK/PhJ mice in the PWS- IC region.....	95
3.3. Characteristics of AS-IC m ^{an} /p ⁺ imprinting defect mice	98
3.3.1 Complete loss of methylation spans the entire <i>Snurf-Snrpn</i> DMR.....	98
3.3.2 <i>Snurf-Snrpn</i> transcript is biallelically expressed in AS-IC m ^{an} /p ⁺ imprinting defect mice	101
3.3.3 Activation of <i>Snurf-Snrpn</i> upstream transcripts from maternal allele	103
3.3.4 Histone epigenetic modifications on the maternal allele mimic that of the paternal allele	106
3.3.5 Differential replication timing of the PWS/AS domain is decreased	114
3.3.6 Biallelic interaction between the PWS-IC and <i>Ndn</i> in AS imprinting defect mice	117
3.3.7 Human PWS-IC and <i>NDN</i> physically interact.....	120
3.4 Mechanisms causing imprinting defect in AS-IC m ^{an} /p ⁺ mice	125
3.4.1 Effect of inserted active promoter on imprinting.....	125
3.4.2 <i>Snurf-Snrpn</i> upstream exons are spliced with 3' <i>Hprt</i> exons	127
3.4.3 A new targeting vector was constructed to delineate the mechanism of AS-IC ^{an} imprinting defect.....	129
3.5 Confirmation of PWS/AS deletion by microsatellite markers	135
Chapter IV Discussion	158

4.1 The imprinting defect occur during oogenesis or fertilization in AS m^{an}/p^{+} mice	158
4.2 Incomplete penetrance of AS-IC ^{an} in 129/SvEv background may due to strain-specific modifier.....	159
4.3 Characteristics of AS-IC m^{an}/p^{+} imprinting defect mice.....	162
4.4 PGK promoter activity may responsible for the imprinting defect in AS-IC m^{an}/p^{+} mice.....	169
4.5 The new targeting vector has been constructed and the screening protocol for recombinant ES colonies needs further optimization.....	173
4.6 Microsatellite PCR can be used as a routine technique to diagnosis PWS/AS.....	175
Reference	178
Appendices	201

Acknowledgements

I would like to express deeply gratitude to my supervisor Prof. Ken-Shiung Chen from School of Biological Sciences, Nanyang Technological University. His stimulating suggestions, scientific guidance, patience and encouragement helped me during the process of the project and writing of this thesis. This thesis would not appear in its present form without the kind assistance and support from Prof. Ken-Shiung Chen.

I would like to thank my former and present lab colleagues who gave me great help during the 4-year study in the School of Biological Sciences, NTU. I thank Lixia for her generous help in handling mice and ES cell culture, thanks to her good work at ordering. I would like to thank Hai Loon for his help in mini-Southern and Yuk Kien for his help in Western blot. Many thanks should give to Shiyun, who helped me to correct many grammer mistakes in the thesis. I thank Yaming, Wailoon, Angeline, Jappar, Lifang, Daren, Zhenzhen for their useful discussion and encouragement.

I would like to thank Dr. Shuan-Pei Lin who generously provided PWS patients' DNA. I thank Dr. Meikkappan Kailasam, who takes good care of the animal holding. I thank Kalyanasundaram Nageswari, Manimaran s/o Joseph and Manickam Vennila. They keep my mice living a happy life. I would like to thank Miss Yang Caixia for her training in confocal microscope. Many thanks should go to Dr. Jiji Miranda from Applied Biosystems for her generous training in real time PCR, sequencing and genotyping using 310 genetic analyzer. I would like to thank our school secretaries for their sincere help with all the administrative work. Special thanks to Chong Chye Hong May for her prompt offering of a helping hand whenever needed.

I would like to thank examiners' critical reading and suggestions for my thesis.

I am very grateful to my parents and my husband. Thanks for their continuous support, encouragement and faith in me. Especially for my husband, it is important to know that he is always on my side in the journey of life.

Abbreviations

3C	Chromosome Conformation Capture
AS	Angelman Syndrome
AS-IC ^{an}	Angelman Syndrome Imprinting Center anchor mutation
ATR-X	Alpha-Thalassaemia, mental Retardation syndrome, X-linked
ATS	antisense
BAC	Bacterial Artificial Chromosome
BP	breakpoint
bp	base pair
BSA	Bovine Serum Albumin
BWS	Beckwith-Wiedemann Syndrome
cDNA	complementary DNA
CE	Capillary Eletrophoresis
cflar	CASP8 and FADD-like apoptosis regulator
ChIP	Chromatin Immunoprecipitation
chrna1	Cholinergic Receptor Nicotinic Alpha polypeptide 1
churc1	Churchill domain Containing 1
CMV	Cytomegalovirus
Cre	Cyclization recombination Recombinase
CREB	cAMP-Response-Elementt-Binding protein
CTCF	CCCTC-binding Factor
DAPI	4',6-Diamidino-2-phenylindole
DEPC	diethylpyrocarbonate
DHS	Dnase I Hypersensitive Site
DMEM	Dulbecco's Modified Eagle Media
DMR	Differential Methylation Region
DMSO	dimethylsulfoxide
DNMT1	DNA methyltransferase 1
DNMT3a	DNA methyltransferase 3a
DNMT3b	DNA methyltransferase 3b
DNMT3L	DNA methyltransferase 3-like
dpc	days post coitum

DTT	dithiothreitol
E6-AP	E3 ubiquitin protein ligase
EDTA	ethylenediaminetetraacetic acid
EGTA	ethylene glycol bis N,N,N',N',-tetraacetic acid
ES	Embryonic Stem
FBS	Fetal Bovine Serum
FIAU	2'-Fluoro-2'-Deoxy-5-Iodo-1- β -D-Arabinofuranosyluracil
FISH	Fluorescence <i>In Situ</i> Hybridization
HAT	histone acetyltransferase
HMT	histone methyltransferase
HPV	Human Papilloma Virus
HRP	Horseradish Peroxidase
IC	Imprinting Center
ICF syndrome	Immunodeficiency/Centromeric instability/Facial anomalies syndrome
ICR	Imprinting Center Region
K4	lysine 4
K9	lysine 9
kDa	kilodaltons
Kb	kilobases
LB	Luria-Bertani
LD	Large Deletion
MAGE	melanoma antigen
MAR	Matrix Attachment Region
MAPH	Multiple Amplifiable Probe Hybridisation
Mb	megabase
Mecp2	Methyl CpG-binding protein 2
MEM	Minimum Essential Medium
MLPA	Multiple Ligation-dependent Probe Amplification
MSP	Methylation Specific PCR
PBS	Phosphate-buffered Saline
PCI	Phenol: Chloroform: Isoamyl alcohol
PCR	Polymerase Chain Reaction
PGC	Primordial Germ Cells

PGK	Phosphoglycerate Kinase
PVDF	polyvinylidene difluoride
PWS	Prader-Willi Syndrome
RITS	RNAi-induced Transcriptional Silencing complex
RNAi	RNA interference
RT-PCR	Reverse Transcription PCR
SD	Small Deletion
SDS-PAGE	Sodium Dodecyl Sulfate Polyacrylamide Gel Electrophoresis
siRNA	small interfering RNA
snoRNA	small nucleolar RNA
SNP	Single Nucleotide Polymorphism
SRO	Smallest Region of Overlap
SSC	Sodium chloride / Sodium Citrate
STO	S, Sandos inbred mice; T, 6-thioguanine resistant; O, ouabain resistant
TBS-T	Tris-buffered Saline Tween-20
TE	Tris-EDTA
TK	Thymidine Kinase
U exons	<i>Snurf-Snrpn</i> upstream exons
UPD	uniparental disomy
UTR	untranslated region

Summary

Prader-Willi syndrome (PWS) and Angelman syndrome (AS) are distinct neurobehavioral disorders associated with the loss of paternally or maternally expressed imprinting genes within human chromosome 15q11-q13, respectively. The human PWS/AS imprinting domain is under the control of a bipartite imprinting center (IC). To dissect the molecular mechanisms of genomic imprinting concerning AS-IC, an AS-IC^{an} mouse line made with 6 kb duplication and an insertion of *puromycin* driven by PGK promoter has been investigated. It was found that maternal inheritance of the AS-IC^{an} mutation causes AS imprinting defect with incomplete penetrance in the 129/SvEv mouse strain and 129/PWK hybrid. In AS-IC^{an} imprinting defect mice, the differential methylation region (DMR) of *Snurf-Snrpn* is biallelically unmethylated and the *Snurf-Snrpn* gene is biallelically expressed; moreover, the normally silent *Ube3a-ATS* maternal allele is activated, resulting in maternal *Ube3a* silencing. Chromatin immunoprecipitation (ChIP) assay demonstrates that histone H3K4 dimethylation is enriched from both parental alleles, and the enrichment of trimethyl H3K9 from maternal allele is reduced in AS-IC^{an} imprinting defect mice when compared to wild type mice. The differential replication timing of PWS/AS domain is reduced in AS-IC^{an} imprinting defect mice. A paternal-specific physical interaction between PWS-IC and *Ndn* gene is detected in wild type mice. Interestingly, the interaction is detected from both parental alleles in AS-IC^{an} imprinting defect mice. The physical interaction of PWS-IC and *NDN* is also detected in human cell lines providing evidences for a new and evolutionarily conserved imprinting regulation mechanism for the PWS/AS imprinting domain. The inserted *puromycin* gene of the targeting vector only expresses from the cerebellum of AS-IC^{an} imprinting defect mice, even though cerebellum and liver cells have the same DNA

methylation and histone modification patterns. A new targeting vector has been constructed to further elucidate the mechanism. In summary, this study indicates that the expression of a maternally inherited PGK promoter upstream of *Snurf-Snrpn* causes DNA demethylation, histone H3K4 dimethylation, DNA looping, losing of replication timing delay, and activating normally silent paternally expressed genes, thus leading to AS imprinting defect.

Chapter I Introduction

1.1 Epigenetics

Epigenetics was defined at an early age by Conrad Waddington as the study of how genotypes give rise to phenotypes during development (1). Later, Arthur Riggs defined epigenetics as the study of mitotically and/or meiotically heritable changes in gene function which cannot be explained by changes in DNA sequences (2). Recently, Adrian Bird gave a newly revised definition of epigenetic event: the structural adaption of chromosomal regions so as to register, signal or perpetuate altered activity state (3). Development is regulated by epigenetic reprogramming. During development, genes in the genome are active in different tissues and organs, depending on their regulation by different sets or combinations of transcription factors and different epigenetic modifications (4). The epigenetic mechanisms remain unclear, but DNA methylation, histone modification and RNA-associated silencing are certainly involved in the epigenetic regulation of gene expression.

DNA methylation has been recognized as an important epigenetic mark for a long time (5). Cytosine residues among CpG islands can be methylated at the C⁵ position in a symmetrical context (CpG), and this methylation is copied to the new DNA strand upon DNA replication. CpG islands are regions more than 500 bps and with GC content more than 55% (6). About 40% of mammalian genes have CpG islands at their promoter regions; once the CpG islands are methylated, genes usually are silenced and this silencing is heritable. DNA methylation is also important for the silencing of tandem and interspersed repeat elements and for genomic imprinting and X-chromosome inactivation (7). DNA methyltransferase 1 (DNMT1) is regarded as

the maintenance DNA methyltransferase because it is the only DNMT known to exhibit a strong affinity for hemimethylated DNA (8). Mouse embryos which are DNMT^{-/-} die prior to midgestation and exhibit a 95% loss of methylation compared to normal embryos (9). From the first division cycle during very early pre-implantation development, DNMT1o (the oocyte form of DNMT1) keeps the differential methylation status of imprinted genes (10). DNA methyltransferase 3a and 3b (DNMT3a and DNMT3b) transfer methyl groups to hemimethylated or unmethylated substrates, and are regarded as *de novo* methyltransferase. However, DNMT3a and DNMT3b have nonoverlapping functions. DNMT3b is required for the methylation of centromeric minor satellite repeats. Mice lacking Dnmt3a or Dnmt3b display different defects and die at different developmental stages, further supporting that Dnmt3a and Dnmt3b have distinct functions (11). DNA methyltransferase 3-like (DNMT3L) also belongs to the DNMT3 subfamily because of its cysteine rich motif. However, DNMT3L lacks the sequence motifs which are involved in activation of the target cytosine, binding of methyl donor S-adenosyl L-methionine, and sequence recognition (12). DNMT3L has been shown to be a potent stimulator of DNMT3a and DNMT3b by changing their conformation and favouring their binding to S-adenosyl L-methionine and target sequences (13). Furthermore, targeted disruption of *Dnmt3L* causes azoospermia in homozygous males, and heterozygous progeny of homozygous females die before midgestation, indicating the importance of Dnmt3L in both oocytes and male germ cells (14). Interestingly, *de novo* methylation has been found in the *Dnmt3a/b*^{-/-} ES cells, suggesting the existence of Dnmt3a/3b-independent *de novo* methylation. It is still unclear whether it is because of unknown Dnmt or because the Dnmt1 can complement the lacking of Dnmt3a/3b as suggested by Lorincz, M.C. *et al* (15).

Histones are subject to a complex and dynamic set of modifications that are thought to be involved in the regulation of transcription. Post-translational modifications of lysine residues on the amino-terminal of histones include methylation, acetylation, phosphorylation, ubiquitylation and SUMOylation. Lysine methylation can be monomeric, dimeric or trimeric, each of which may provide different information. Similar to methylations, acetylation adds small chemical groups, whereas ubiquitylation and SUMOylation add large chemical groups. Compared to methylation and acetylation, ubiquitylation and SUMOylation may lead to profound changes in chromatin structure. On the other hand, synergistic coupling of histone phosphorylation and acetylation is associated with rapid gene activation in response to external stimulation (16). These variations lead to complex histone codes, which can be read and interpreted by different cellular factors (17, 18). In general, acetylated histones mark transcriptionally active regions, whereas hypoacetylated histones mark inactive euchromatin or transcriptionally silent regions. Histone H3 methylation is associated with both active and inactive chromatin regions. Methylation of histone H3 lysine 9 (H3K9) marks silent chromatin regions and methylation of histone H3 lysine 4 (H3K4) marks active chromatin regions (19). In histone H3 and H4, mono- or dimethylated modifications of arginine residues seems strictly limited to the transcriptionally active regions. Serine/threonine phosphorylation is also involved in transcription. H3S10 phosphorylation correlates with both activated transcription and mitotic chromosome condensation (19). It is now realized that the histone codes are more complex than expected, and different combinations of basic modifications may lead to dynamic functional outcome (17).

More and more evidences indicate that RNA, in the form of antisense transcripts (*Igf2r* antisense transcript *Air*), noncoding RNAs (*Xist*) and RNA interference (RNAi) plays important role in post-transcriptional silencing. The imprinting of *Igf2r* gene is lost when the expression of its antisense transcript *Air* is abrogated by removing the CpG island from which *Air* initiated, indicating that this antisense transcript may be involved in the silencing and methylation of the sense gene (20). Interestingly, all the antisense transcripts described at the imprinted loci are non-coding RNAs transcribed from the paternal allele, although their expression does not always correspond to silencing of the sense gene on the same allele (Table 1-1) (21). In the case of α -thalassaemia, antisense transcript has been shown to lead to DNA methylation and stable silencing of a globin gene (22). Antisense transcripts might direct histone modifications and DNA methylation to specific loci, initiating heritable and stable silencing. It is well known that after X chromosome counting and choice, the non-coding RNA *Xist* is transcribed from the future inactivate X chromosome, and the *Xist* RNA molecules coat the future inactive X chromosome, presumably recruiting silencing partners during the accumulation of the *Xist* RNA molecules (23). Recently, investigations into heterochromatin formation triggered by repeat elements, led to the surprising discovery that the RNAi system is involved in the nucleation and assembly of heterochromatin (24). An RNAi-induced transcriptional silencing complex (RITS) not only contains chromatin-associated proteins and RNAi-associated proteins, but also contains small interfering RNAs (siRNA) derived from *dg* and *dh* repeats presenting at different heterochromatin loci. In *Schizosaccharomyces pombe*, mutations in factors that are involved in RNAi result in defects in heterochromatin assembly (24, 25). It is now clear that interplay of the RNAi and heterochromatin systems is crucial for the maintenance and function of genome (26).

Table 1-1 paternal derived antisense transcripts

Sense/Antisense gene pairs	Human chromosome	Mm chromosome	Sense expression	Antisense expression	reference
<i>Igf2r/Air</i>	6q	17A	maternal	paternal	(20)
<i>MEST(Peg1)/MESTIT1</i>	7q32	6A	paternal	paternal	(27)
<i>Copg2/Copg2AS2</i>	7q32	6D	maternal	paternal	(28),(29)
<i>Igf2/Igf2as</i>	11p	7F	paternal	paternal	(30), (31)
<i>Kcnq1/LIT1</i>	11p	7F	maternal	paternal	(32), (33),(34)
<i>Dio3/Dio3AS</i>	14q32	12F1	maternal	paternal	(35)
<i>Ube3a/Ube3a-AS</i>	15p	7C	maternal	paternal	(36),(37)
<i>Zfp127/Zfp127as</i>	15p	7B	paternal	paternal	(38)
<i>Nesp/Nespas</i>	20q	2H	maternal	paternal	(39),(40),(41)
<i>WT1/WTIAS</i>	11p13	2E	maternal	paternal	(42),(43),(44)

Table adapted from (21).

1.2 Epigenetic mechanisms in human disease

Developmental processes are largely regulated by epigenetics, so most epigenetic lesions will cause serious human diseases (Table 1-2) (19). To date, human diseases involving epigenetic lesions can be categorized into three groups: single-gene disorders, cancers and common complex disorders (45). There are two classes of single-gene epigenetic diseases. One involves genes that are epigenetically regulated, such as imprinted genes; the other involves genes that affect the epigenome as a whole. For example, DNA methyltransferase gene *DNMT3B* mutations lead to Immunodeficiency/Centromeric instability/Facial anomalies (ICF) syndrome (46), and mutations of methyl CpG-binding protein 2 (*Mecp2*) gene, which encodes a protein that binds to methylated DNA sequences, cause Rett syndrome (47). Inappropriate gene silencing may also cause disease, for example, in the patient with α -thalassaemia,

transcription of an antisense RNA leads to silencing of a structurally normal α -globin gene (22). More and more investigations show that epigenetic lesions have a major role in the development of human cancers. Both global and gene-specific hypomethylation and hypermethylation can cause cancers. The global hypomethylation may activate some growth-promoting genes and lead to cancers. For example, activation of human papilloma virus HPV16 by hypomethylation is a major mechanism affecting tumor latency in cervical cancer (48). By contrast, some of the tumor suppressor genes may be inactivated by hypermethylation, causing development of tumors. For example, silencing of *MHL1* gene by methylation of the promoter region of the gene contributes to some of the colorectal cancers (49). In addition to DNA methylation abnormalities, mutations of chromatin might also lead to cancers. Overexpression of H3 lysine-27 histone methyltransferase EZH2 may lead to widespread transcriptional repression and cause metastatic prostate cancer (50). Some of the common complex diseases also have epigenetic lesions involved, for example, in systemic autoimmune disease, aberrant hypomethylation leads to overexpression of lymphocyte function-associated antigen-1 in T cells (51). A better knowledge of the mechanisms, timing and consequences of epigenetic abnormality will lead to a clearer understanding of the development of human diseases and will have a huge impact on management, prevention, diagnosis and treatment of human diseases.

Table 1-2 Human epigenetic diseases

Disease	Symptom	Aetiology	Reference
ATR-X syndrome	Intellectual disabilities, α -thalassaemia	Mutations in <i>ATRX</i> gene, hypomethylation of certain repeats and satellite sequences	(52)
Fragile X syndrome	Chromosome instability, intellectual disabilities	Expansion and methylation of CGG repeats in <i>FMR1</i> 5' UTR, promoter methylation	(53)
ICF syndrome	Chromosome instability, immunodeficiency	<i>DNMT3B</i> mutations, DNA hypomethylation	(46)
Angelman syndrome	Intellectual disabilities	Deregulation of one or more imprinted genes at 15q11–13 (maternal)	(54)
Prader–Willi syndrome	Obesity, intellectual disabilities	Deregulation of one or more imprinted genes at 15q11–13 (paternal)	(55)
BWS	Organ overgrowth	Deregulation of one or more imprinted genes at 11p15.5	(56)
Rett syndrome	Intellectual disabilities	<i>MeCP2</i> mutations	(47)
α -Thalassaemia (one case)	Anaemia	Methylation of $\alpha 2$ -globin CpG island, deletion of <i>HBA1</i> and <i>HBQ1</i>	(22)
Various cancers	Microsatellite instability	<i>De novo</i> methylation of <i>MLH1</i>	(49)
	Disruption of Rb, p53 pathway, uncontrolled proliferation	<i>De novo</i> methylation of various gene promoters	(57)
	Disruption of SWI–SNF chromatin remodelling complex	Mutations in <i>SNF5</i> , <i>BRG1</i> , <i>BRM</i>	(58)
	Overexpression of <i>IGF2</i> , silencing of <i>CDKN1C</i>	Loss of imprinting	(48, 59)
Leukaemia	Disturbed haematopoiesis	Chromosomal translocations involving HATs and HMTs	(60)
Rubinstein–Taybi syndrome	Intellectual disabilities	Mutation in CREB-binding protein (histone acetylation)	(61)
Coffin–Lowry syndrome	Intellectual disabilities	Mutation in <i>Rsk-2</i> (histone phosphorylation)	(61)

ATR-X syndrome, α -thalassaemia, mental retardation syndrome, X-linked; BWS, Beckwith-wiedemann syndrome; CREB, Camp-response-element-binding protein; HAT, histone acetyltransferase; HMT, histone methyltransferase; ICF, immunodeficiency, centromeric region instability and facial anomalies syndrome; UTR: untranslated region. Table adapted from (19).

1.3 Epigenetic reprogramming during early development in mammals

In mammalian embryos, there are two major cycles of epigenetic reprogramming of the genome: during pre-implantation development and during germ cell development. Germ cell reprogramming is specifically important for the imprinted genes, for which imprints will be reset according to individual sex (Figure 1-1).

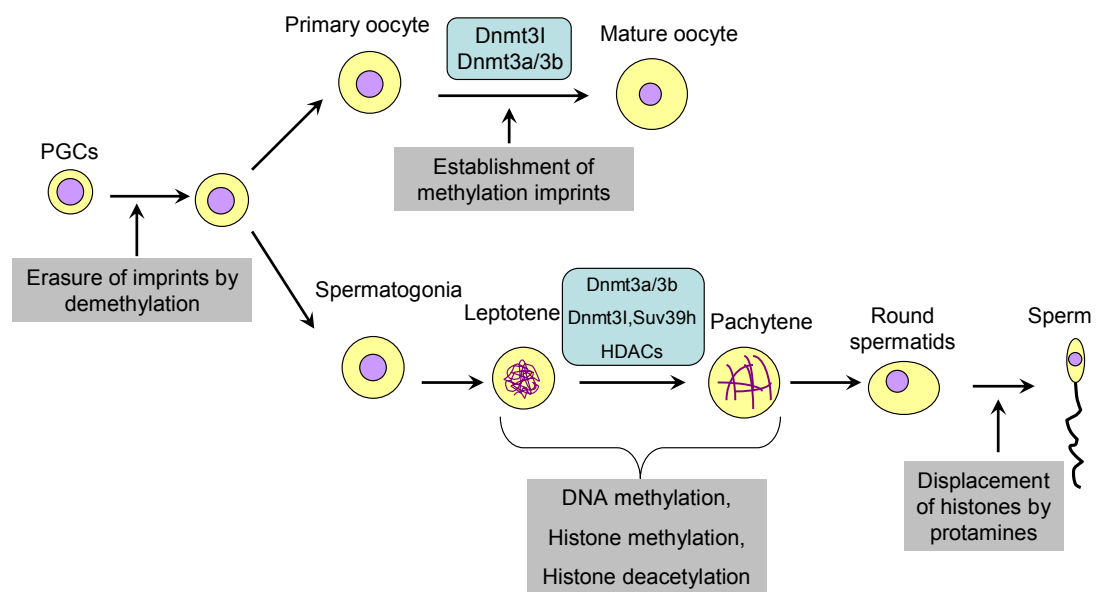


Figure 1-1 Epigenetic reprogramming during gametogenesis of mice Primordial germ cells (PGCs) undergo demethylation at imprinted loci, which erases parental imprinting marks at around embryonic day 11.5–12.5. The female PGCs develop to form primary oocytes. During oocytes growth and maturation, the maternal-specific genomic imprints are re-established through the *de novo* methylation activities of the methyltransferases Dnmt3a and Dnmt3b, and an associated protein Dnmt3l. During spermatogenesis, several factors seem to function during the differentiation of the spermatocytes from the leptotene to pachytene stages of meiosis. During this period, histones are hypoacetylated, and the functions of Suv39h, Dnmt3a and Dnmt3l are essential. The crucial stage when these factors function is not defined. Adapted from (62).

Germ cells are first detected as a founder population of about 45 primordial germ cells (PGCs) in mice at 7.2 days post coitum (dpc). These primordial germ cells then proliferate and migrate into the genital ridges between 10.5-11.5 dpc (63). PGCs continue to proliferate until about 13.5 dpc, when they enter into meiotic prophase in

female gonads and mitotic arrest in male gonads. Many of the epigenetic marks are erased at about the time PGCs arrive at the genital ridges. Imprinted genes are biallelically expressed, and methylation in imprinted genes and single copy genes is erased with the bulk of the demethylation occurring between embryonic day 11.5-12.5 (64, 65). The timing and degree of demethylation are identical in PGCs from female and male embryos, suggesting that the process is unaffected by the sex of the embryo. Incomplete demethylation is observed in both *Line1* and *IAP* families, and this may underlie the epigenetic inheritance, which sometimes occurs at mutant gene loci with transposon insertions (66, 67). The mechanisms of demethylation remain unknown because whether there is a DNA demethylase is still in debate. Szyf's group has suggested that MBD2 binds methylated DNA and possesses DNA demethylase activity (68-70). If MBD2 has DNA demethylase activity, it should be a transcription activator. However, Ng HH *et al* showed that MBD2 does not demethylate DNA and is a transcriptional repressor belonging to the Mecp1 histone deacetylase complex (71). The short form MBD2b has been found to confer transcriptional repression as well as the interaction to Sin3A (72). It has been suggested that rapid global demethylation may occur in response to signals from somatic cells of the undifferentiated bipotential gonadal anlagen when PGCs enter the genital ridge (64). Demethylation in the germ line might reduce the mutation rate caused by deamination of 5-methylcytosine (73).

The establishment of differential methylation takes place several days later after demethylation (74). Most of the maternal DNA methylation is established during oocyte maturation. During this period, both the maternally expressed imprinted genes and the paternally expressed genes are under the control of maternal imprinting

mechanisms that repress paternally expressed genes and activate maternally expressed genes. In contrast, in the male germ line, at the prospermatogonia stage, the paternal DNA methylation is set up although few imprinted genes (*H19*, *Gtl2* and *Rasgrfl*) have paternal DNA methylation (75). It has been shown that the paternal allele of *H19* is remethylated earlier than the maternal one, indicating the presence of other epigenetic marks in the nucleus at prospermatogonia stage (74). Recently, it has been found that the paternally and maternally methylated imprinting center regions (ICRs) are marked by different combinations of histone modifications during spermatogenesis stages preceding histone-to-protamine exchange. H3 acetylation and dimethyl H3K4 are detected at maternally methylated *KvDMR1*, *Igf2r* region 2 and *Hprt1*, but are absent or strongly reduced at paternally methylated *H19*, *Gtl2* and *Rasgrfl* ICRs (76). Dnmt3a is required for the establishment of both maternal and paternal *de novo* methylation imprints in the germ line (77). However, Dnmt3a is not essential for the methylation of all the paternally-imprinted loci examined, suggesting that one or more additional factors are required for gamete-specific differential methylation. Mutations at known DNA methyltransferase genes do not underlie a *trans*-acting imprinting defect that manifests as familial biparental hydatidiform mole, further supporting the presence of such factors (78, 79).

After fertilization, protamines in sperm chromatin are rapidly replaced with acetylated histones (80, 81), closely following which is the initiation of the genome-wide loss of DNA methylation. The demethylation is completed before the beginning of DNA replication in the paternal pronucleus (82). Both the mechanism and the function of paternal genome demethylation are unknown. It is likely that the oocyte cytoplasm contains demethylation factors which are specifically targeted to or excluded from

certain sequence classes in sperm chromatin. Paternal demethylation may have arisen in order to reprogramme paternal germline imprints by the maternally produced oocyte cytoplasm (82). However, heterochromatin in and around centromeres (83), IAP retrotransposons (84) and paternally-methylated imprinted genes (85) do not become demethylated at these stages. The post-fertilization protection of some of the methylated DNA sequences against demethylation in the paternal pronucleus might be due to differential chromatin modifications established during spermatogenesis, testis-specific histone variants being recruited to form specific structures during late spermatogenesis, or a small percentage of the genomic DNA packaged with histones in mature sperm and are protected against paternal DNA demethylation in the zygote (76).

From one cell to blastocyst stage in mouse, there are further changes in global DNA methylation and histone modifications. DNA methylation is reduced progressively with cleavage division; this loss of DNA methylation depends on DNA replication and results in unequally methylated sister chromatids. Many sequences lose methylation at this stage but imprinted genes retain their germ line imprints. It is suggested that *Dnmt1* enters the nucleus at the eight-cell stage to maintain the imprinted gene imprints (10). The precise histone modification reprogramming during passive DNA demethylation is unclear.

1.4 Function of genomic imprinting in mammals

Genomic imprinting is a special epigenetic phenomenon which is unique to mammals. Most of genes are expressed equally from both alleles in mammals, but imprinted

genes are expressed preferentially or exclusively from only one of the parental alleles (86). Imprinted genes do not always display complete monoallelic expression in all tissues; some imprinted genes show tissue-specific or developmental-stage-specific imprinting. Three hypotheses have been developed to identify the selective advantage of genomic imprinting. The first is the evolvability model, which proposes that imprinting provides a population with enhanced adaptability to changing environments by protecting a subset of the alleles in each generation from the full force of natural selection (87). The second is the ovarian-time-bomb hypothesis, which proposes that imprinting has evolved to protect females from the ravages of ovarian trophoblastic disease (88). The third one, conflict theory, has been most extensively developed and can most successfully explain the experimental phenomena (89). Conflict theory proposes that imprinting has evolved because of an evolutionary conflict in individuals between maternally and paternally inherited alleles; the paternally inherited resource-acquisition genes try to extract as many resources from the mother as possible to make a large and fit baby, by contrast, the maternally inherited genes try to keep maternal resources to ensure that these resources are evenly divided among offspring or withheld for future offspring. To date, more than 80 imprinted genes have been found, and most of which have key functions in regulating placental and fetal growth; some of them are important for neonatal adaptations to suckling and metabolism, or have roles in behavior, cognitive functioning and social interactions (90-92). For example, paternal expressed *Igf2* which is transcribed from the placental-specific promoter (P0) regulates the development of the diffusional permeability properties of the mouse placenta. The surface area of the exchange barrier in the labyrinth of the mouse placenta is reduced and the thickness is increased in P0 deleted fetus compared to that of wild type fetus (93). However,

deletion of maternally expressed *Ipl* gene results in a large placenta but normal-sized fetus (94). Another interesting finding is that the female mice lacking the paternal expressed imprinting gene *Peg3* put on fewer reserves during pregnancy and show poor maternal care and impaired milk release (95).

1.5 X-chromosome inactivation and imprinting

So far, imprinted genes have been identified only in placental mammalian species among vertebrates. It is possible that imprinting has coevolved with placentation (90). X-chromosome inactivation is also specific to placenta mammals, moreover, the imprinted X-chromosome inactivation is only limited to the extra-embryonic tissues. Therefore, it is possible that both X-chromosome inactivation and autosomal imprinting have evolved when the evolution of the placenta exerts selective pressure to imprint growth-related genes (96). All of the parental epigenetic marks of X chromosomes in PGCs have been fully erased. After fertilization and in the zygote, both X chromosomes are potentially active. Imprinted inactivation of the paternal X chromosome is established in all cells during the pre-implantation stages, and it is maintained in the placenta and other extra-embryonic tissues, but is erased in the embryonic tissues. Random X-chromosome inactivation is then established in the embryonic cells and maintained throughout adult life, except in the developing germline where the X chromosomes are reprogrammed. It is not yet known if and when a germline imprint is established to differentially mark the parental X chromosome (96). Similar to imprinted X-chromosome inactivation, autosomal imprinting also involves epigenetic marks erasing in PGCs and establishment during gametogenesis. These epigenetic marks can be inherited in the cells of embryo (7,

86). The similarity of molecular mechanisms between imprinted X-chromosome inactivation and autosomal imprinting gene silencing further supports the idea that X-chromosome inactivation and autosomal imprinting may have coevolved. In X-chromosome inactivation of mice, *Xist* encodes a non-coding RNA transcribed only on the paternal X chromosome, to which it targets epigenetic silencing. Maternal copy of *Xist* is prevented from being expressed by an epigenetic imprint (97-99). Maternal-specifically expressed autosomal genes *IC2* and *Igf2r* both contain paternally-expressed non-coding RNA genes, *Kcnq1ot1* in the *IC2* cluster and *Air* in the *Igf2r* cluster. Expression of *Kcnq1ot1* and *Air* silence the paternal alleles of *IC2* and *Igf2r*, respectively. The maternal alleles of *Kcnq1ot1* and *Air* gene are methylated and silenced to prevent silencing of the surrounding genes on the maternal chromosome (100, 101). *Xist* RNA is thought to attract several histone-modifying enzymes to the X chromosome in preimplantation embryos, including histone deacetylases and the polycomb repressive complex 2, which contains the H3K27 histone methyltransferase EZH2 (102). The paternal *Kcnq1ot1* transcript has been thought to recruit histone methyltransferase (Ezh2 and G9a) to the paternal domain, leading to histone methylation *in cis* (103). Similarity of erasing and establishment of epigenetic marks and mechanisms of epigenetic regulation of X-chromosome inactivation and autosomal imprinting supports an evolutionary link between X-chromosome inactivation and autosomal imprinting silencing.

1.6 Regulation of imprinted genes in the somatic cells

Maternally and paternally inherited alleles of imprinted genes are differentially marked during gametogenesis. The imprints are maintained in the early embryo and

fully matured during differentiation, and thus lead to differential gene expression in somatic cells. Epigenetic regulation of imprinted gene expression in somatic cells is well-studied. So far, it has been shown that differential methylation regions (DMRs), imprinting centers (IC), antisense transcriptions, insulators and silencers are the mechanisms involved.

In general, allele-specific DNA DMRs are hallmarks of imprinted genes and are usually located in the promoter regions. Thus, the methylated allele is transcriptionally silenced. It is known that the methyl CpG-binding proteins, Dnmt1 and histone deacetylase form a complex that might lead to a closed chromatin conformation in which transcription factors can't access to the promoter (7). In the DMRs, not only the DNA is differentially methylated, the histone modifications are also allele-specific (18, 104). It is still debatable whether histone modifications or DNA methylation is the primary imprint or they cooperated with each other.

Imprinted genes usually are clustered, and the maternally and paternally expressed genes are under the control of a long range *cis*-acting IC (7, 86). These ICs carry allele-specific epigenetic marks, for example, DNA methylation and histone modification which are established in the germ line and retained thereafter. ICs play important roles in coordinating control of the imprinting clusters by influencing epigenetic modifications of additional *cis*-acting elements. This is important for allele-specific, tissue-specific, or temporal-specific regulation of imprinted genes (105). The famous example is Prader-Willi syndrome (PWS) and Angelman syndrome (AS) imprinting domain (Figure 1-2a). The bipartite IC has two elements, PWS-IC and AS-IC, which control the expression of paternal and maternal imprinting genes,

respectively (106). Deletion of IC impairs the imprint switch in the germ line of all the imprinted genes under its control. For example, deletion of the PWS-IC impairs the establishment of the paternal imprint in the male germ line and the deleted chromosome acquires a maternal methylation imprint in somatic cells (107).

So far, all of the antisense transcripts found at imprinted loci are themselves imprinted and transcribed from the paternal alleles, such as the imprinted gene *Igf2r* and its antisense transcript *Air* (Figure 1-2b). On the paternal allele, *Air* transcript initiates from the intron of *Igf2r* and overlaps the promoter of *Igf2r*, and thus may be responsible for the silencing of the paternal allele of *Igf2r*. On the maternal allele, *Air* is silenced by a methylated DMR at the intron and allows the maternal expression of *Igf2r* (20).

The insulator and silencer model of epigenetic mechanisms regulating imprinted genes come from *Igf2/H19* imprinting domain (Figure 1-3a) (86). Allele-specific methylation at the *H19* promoter contributes to the silencing of its paternal allele; however, the promoter of the silent maternal allele of *Igf2* is unmethylated. A differentially methylated IC located at 2-4 kb upstream of *H19* regulates the reciprocal expression of *H19* and *Igf2* by functioning as a methylation-sensitive insulator. CCCTC-binding factor (CTCF) binds to the unmethylated maternal allele of IC and prevents downstream enhancers from interacting with the upstream maternal *Igf2* promoter. CTCF binding is abolished by DNA methylation of the IC on the paternal allele and allows the downstream enhancers to interact with the paternal *Igf2* promoter (108-111). The insulator model has been suggested to function in the tissues of endoderm. DMR1 of *Igf2* may act as a tissue-specific silencer, probably through the

binding of a repressor protein on the less methylated maternal allele. Deletion of the maternal allele of *Igf2* DMR1 results in biallelic expression of *Igf2* in mesoderm tissues (105, 112, 113). With the progress of investigation of epigenetic mechanisms, variety of control elements, such as enhancers, silencers and chromatin insulators, are thought to regulate imprinted gene expression by establishing and maintaining active and inactive chromatin domains. Recently, a chromatin-looping model has been proposed (Figure 1-3b). In this model, CTCF binding on the maternal *H19* DMR regulates its interaction with matrix attachment region (MAR) 3 and DMR1 of *Igf2*, and thus forming a tight loop around the maternal *Igf2* locus, which may contribute to its silencing in neonatal liver of mice. On the paternal allele, the methylated *H19* DMR is associated with the methylated *Igf2* DMR2 through putative protein factors, moving *Igf2* close to the enhancers downstream of *H19* in the active chromatin domain. *H19* is silenced by DNA methylation although it is in the active domain (114, 115).

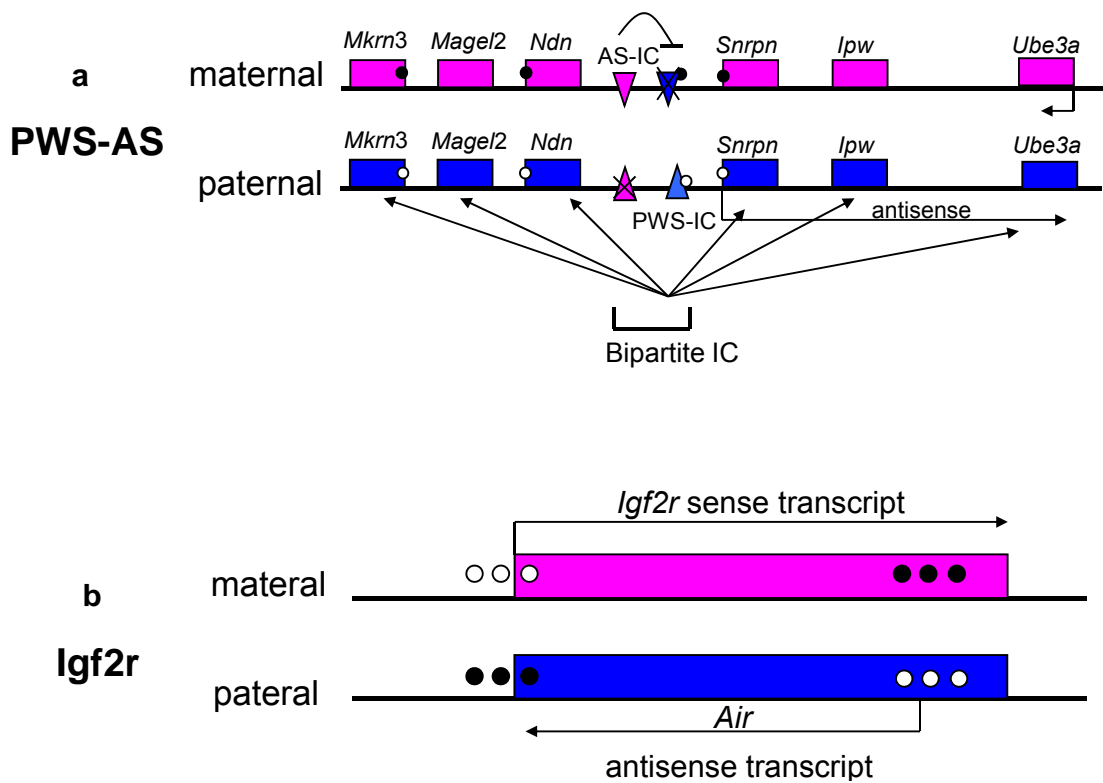


Figure 1-2 Schematic representation of epigenetic regulation at PWS/AS and *Igf2r* imprinted loci

a. At PWS/AS imprinting domain, a bipartite *cis*-acting imprinting center confers long-range imprinting control on the two parental alleles. Female germline transmission of an AS-IC is required for methylation and repression of the maternal alleles of the paternally expressed genes. On the paternal chromosome, this AS-IC is nonfunctional allowing the PWS-IC to confer paternal-allelic expression on upstream and downstream genes. *Ube3a* is expressed from the maternal allele in the brain and appears to be associated with an antisense transcript on the paternal allele in a manner similar to the imprinting of *Igf2r*. **b.** The *Igf2r* locus contains a single imprinted gene regulated by an antisense transcript, which itself is regulated by a differentially methylated germline imprint located in an intron. White circles denote absence of methylation at the differentially methylated region and black circles are methylated regions. Arrows indicate interactions between *cis*-elements on the two parental chromosomes. Drawing is not to scale. Adapted from (86).

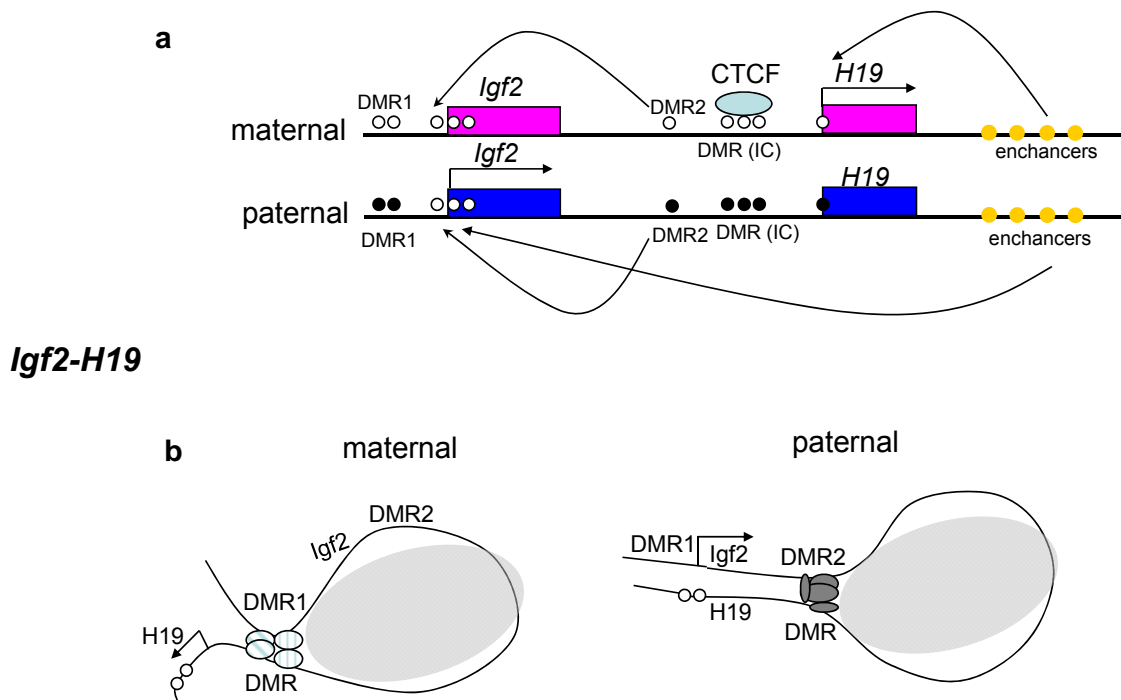


Figure 1-3 Schematic representation of epigenetic regulation at *Igf2/H19* imprinting domain. a. Insulator and enhancer model. The *Igf2-H19* locus contains a pair of reciprocally imprinted and coordinately regulated imprinted genes controlled by an intergenic imprinting center (IC), which binds CTCF (light blue oval) when unmethylated and insulates the *Igf2* fetal promoters from common downstream enhancers (yellow circles) in endoderm. In mesoderm, tissue-specific silencer DMR1 plays a role in *Igf2* regulation. Tissue-specific enhancer (DMR2) upstream of the insulator regulates biallelic activity of *Igf2* in parts of the brain. Adapted from (86). **b.** Chromatin loop model. On the maternal allele, the unmethylated *H19* DMR (which is bound by CTCF and other proteins; open ovals) and *Igf2* DMR1 interact, resulting in two chromatin domains, with *H19* in an active domain with its enhancers (small white circles) and *Igf2* in an inactive domain away from the enhancers (shaded area). On the paternal allele, the methylated *H19* DMR associates with the methylated *Igf2* DMR2 through putative protein factors (filled ovals), moving *Igf2* into the active chromatin domain. The location of DMR2 at the end of *Igf2* positions its promoters in close vicinity to the enhancers downstream of *H19*. *H19* is in the active domain but is silenced by DNA methylation. Drawings are not to scale. Adapted from (115).

1.7 Prader-Willi syndrome and Angelman syndrome

PWS and AS are distinct disorders associated with the loss of gene expression on human chromosome 15q11-q13 from the paternal origin and maternal origin,

respectively (54, 116). Clinical features of PWS patients are characterized by infantile hypotonia, hyperphagia in early childhood, obesity as a result of hyperphagia, high death rate during postnatal period, short stature, small hands and feet, and hypogonadism. Clinical features of AS patients are more serious, including severe mental retardation, lack of speech, seizures, movement disorder, happy disposition, protruding tongue, and wide-spaced teeth (54, 106). So far, growth hormone treatment in young children with PWS is the most efficient way to increase lean body mass accrual, normalize length/height standard deviation scores, faster head growth and decrease percentage body fat, as well as improve language and cognitive abilities (117). To date, there is no report for the therapy of Angelman syndrome patients, but reduction of α CaMKII inhibitory phosphorylation in an AS mouse model with *Ube3a* mutation rescue the neurological deficits (118).

Most PWS and AS patients (65-75%) have a 4 Mb chromosome deletion of 15q11-q13 (106). About 2 Mb of the 4 Mb-deletion contains a cluster of paternally and maternally imprinted genes. Deletion on the paternally inherited chromosome leads to loss of paternally expressed imprinting genes and thus causes PWS; whereas deletion on the maternally inherited chromosome leads to loss of maternally expressed imprinting genes and causes AS. Similar to other contiguous gene deletion syndromes, these gross chromosomal deletions are caused by homologous recombinations between flanking repeat gene clusters (119).

Some of PWS cases (20-30%) arise from maternal uniparental disomy (UPD), and most of which are caused by maternal meiotic nondisjunction followed by mitotic loss of the single paternal chromosome 15 postzygotically. A few AS cases (5%) arise

from paternal uniparental disomy. The likely reason is maternal nondisjunction with postzygotic duplication of the single sperm-derived chromosome (120).

Another 5% of PWS and AS patients have imprinting defect, and some of them are caused by microdeletion of imprinting center. In PWS imprinting defect patients, the paternally inherited chromosome has a maternal epigenotype; by contrast, in AS imprinting defect patients, the maternally inherited chromosome has a paternal epigenotype. Molecular analysis of 51 patients with PWS and 85 patients with AS who have imprinting defect has shown that the vast majority of these defects are epimutations (aberrant epigenetic states) that occur spontaneously in the absence of DNA sequence changes. Transmission disequilibrium test has suggested that common DNA sequence variants of the imprinting center and the *MTHFR* gene are associated with an increased tendency of epimutations in the PWS/AS region (121). Epimutations of the maternal chromosome are often present in a mosaic form, suggesting that in these patients, aberrant DNA methylation occurs after fertilization when the maternal CpG methylation pattern is established. Epimutations of the paternal chromosome appears to occur during male germ cells development (122).

Balanced translocations contribute about 0.1% of PWS cases. To date, 5 cases of paternally derived translocations have been reported and all of which disrupt the SNURF-SNRPN gene in either of two locations. Some of the PWS patients have no deletion, no imprinting defect, no UPD and no translocation, but have the clinical phenotypes of PWS. A study of nine clinical PWS patients with atypical genetics suggests that PWS can result from a stochastic partial change in gene expression, and

even minor disruption of the PWS control region outside the smallest region of overlap (SRO) can still cause PWS (123).

So far, the gene or genes that are responsible for PWS remain elusive, and it is still in debate whether PWS is caused by the loss of function of a single gene or of several genes. By contrast, mutations in *UBE3A* gene cause AS (10% of AS cases) (124, 125). *UBE3A* gene encodes an E3 ubiquitin protein ligase (E6-AP) which transfers ubiquitin to protein substrates in the ubiquitin-proteasome proteolytic pathway. E6-AP can also function as a coactivator for the nuclear hormone receptor superfamily (126). Mutations of *UBE3A* result in defects in the ubiquitin-proteasome protein degradation pathway, but the function of coactivator is intact. Mutation spectrum analysis in AS patients with *UBE3A* mutations shows that two thirds of the mutations are frameshifts caused by deletion or insertion/duplication. Nonsense mutations, caused by slipped mispairing replication errors and deamination of 5-methylcytosine in CpG dinucleotide residues, contribute to 20% of *UBE3A* mutations and create null alleles (127, 128). Some of AS patients (10-15%) have unknown etiology. It is possible that there are epigenetic mutations or genetic disorders of unknown factors which influence *UBE3A* or other related genes (106). Genotype-phenotype analysis of AS patients shows that deletion patients have a more severe phenotype, which may due to the codeletion of genes contributing to AS phenotype. UPD and imprinting defect patients are less severe in most features and have greater tendency for obesity. The severity of the *UBE3A* mutation patients are in the middle of the above groups, indicating that abnormality of *UBE3A* is sufficient for classical features of AS (128).

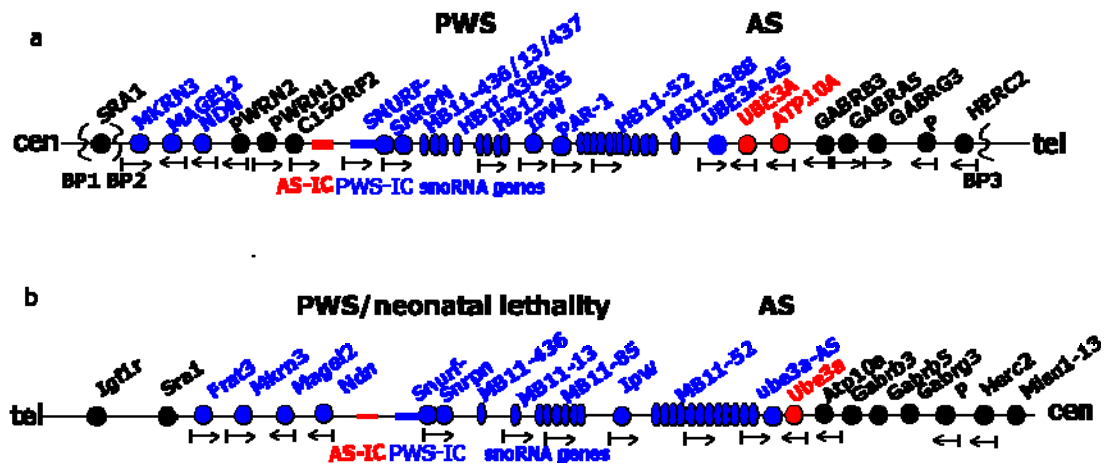


Figure 1-4 Genomic structure of human chromosome 15q11-q13 and its mouse chromosome 7C syntenic region. **a:** Human chromosome 15q11-q13. **b:** Mouse chromosome 7C. blue dots: paternally expressed genes; red dots: maternally expressed genes; black dots: biparentally expressed genes; arrows: transcriptional orientation; red rectangle: AS-IC; blue rectangle: PWS-IC. Adapted from (106).

1.8 PWS/AS imprinting domain

The 2 Mb imprinting region of human chromosome 15q11-q13 contains at least 11 paternally and 2 maternally expressed genes (Figure 1-4a). The paternally expressed genes which are responsible for PWS phenotype maintain the imprint in most or all tissues, while the maternally expressed genes which are associated with AS phenotype are only imprinted in certain cells of brain in both human and mice (106). Studies of evolutionary history indicate that PWS/AS imprinting domain is assembled at about 105-180 million years ago. It arises after fusion of a region bearing *UBE3A* with an unlinked region bearing *SNRPN*, which duplicates from the non-imprinted *SNRPB/B'*. The new region then acquires several retroposed gene copies and arrays of small nucleolar RNAs from different parts of the genome. The studies also suggest that the genomic rearrangement is required for the acquisition of imprinting at PWS/AS domain (129).

The complex *IC-SNURF/SNRPN-snoRNA* polycistronic locus encodes several functions including the element of the *cis*-acting regulatory IC which overlaps with promoter region of *SNURF-SNRPN* transcript, six classes of box C/D small nucleolar RNA (*snoRNA*), and a *UBE3A* antisense (*UBE3A-ATS*) transcript. *SNURF-SNRPN* transcript encodes two independent proteins; exon 1-3 encodes a 71-amino acid protein which is localized in the nucleus and could bind RNA (54, 106); and exon 4-10 encodes protein SmN which is a core spliceosomal protein involved in mRNA splicing in the brain where it replaces constitutively expressed SmB'/B proteins. The mouse models with ablation of *Snurf* have no phenotype, in contrast, in the PWS patients with balanced translocations, *SNURF* is the only gene disrupted. Since *SNURF* is the only gene locus overlaps with IC, it is difficult to explain the functions of *SNURF* (130, 131). In PWS patients and mice with the absence of SmN protein, the SmB'/B isoforms are significantly upregulated, probably to maintain the level of SmN/B'/B in the brain, thus explaining the absence of phenotype in mice with ablation of *Snrpn* (132). The ATG-to-AAG mutation in the initiation codon of *Snurf* can cause 15-fold or more increase in the translation of the downstream ORFs in two fusion constructs, indicating that *SNURF* may regulate *SNRPN* at the translational level both in human and in mice (133).

NDN is a small intronless gene encoding NEDCIN, which is a member of MAGE (melanoma antigen) protein family proposed to act as a neuronal growth suppressor and anti-apoptotic protein in post-mitotic neurons. *NDN* is well-studied because other than *SNURF-SNRPN* it is the most plausible candidate gene contributing to the phenotype of PWS. Unlike *SNURF-SNRPN* which is expressed from the paternal allele in most tissues, *NDN* is expressed exclusively from the paternal allele in brain

and fibroblasts among other tissues, but is silent in blood lymphocytes and derivatives of lymphoblastoid cell line. In mice, *Ndn* is expressed predominantly in a subset of postmitotic neurons, with highest expression level in hypothalamus at late embryonic and early postnatal stages (106). Three *Ndn*-deficient mouse models have been reported independently. One mouse model has no apparent phenotype, and the other two have early postnatal lethality with variable penetrance depending on the mouse strain background (134-136). There is no lethality when the chimeric male is bred with hybrid background females, suggesting that *Ndn*-deficiency phenotype is dependent on genetic modifiers. Surviving mice in all three studies have no obvious phenotype and are fertile and non-obese.

MAGEL2 encodes a small protein of unknown function and has highest sequence similarity to NEDCIN and the MAGE family proteins. *MAGEL2* is expressed from the paternal allele in both human and mice (137). Latest study has found that *Magel2*-null mice exhibit neonatal growth retardation, excessive weight gain after weaning, and increased adiposity with altered metabolism in adulthood, recapitulating fundamental aspects of the PWS phenotype, indicating that *Magel2* might be the PWS responsible gene (138). Another known gene, *MKRN3*, is expressed from the paternal allele in both human and mice, coding the makorin ring finger protein 3, a putative ribonucleoprotein (139). It is still not clear whether *MKRN3* is responsible for the phenotype of PWS.

C15ORF2, *PWRN1* and *PWRN2* are three genes located between *NDN* and *SNURF-SNRPN*. *C15ORF2* encodes an 1156-amino-acid protein which may play a role in primate spermatogenesis because it is present in primates only (140). *C15ORF2*

harbors several genes for PIWI-interacting RNAs, which are believed to regulate spermatogenesis (141-144). *C15ORF2* is expressed in fetal brain and might be subjected to genomic imprinting. So far, *C15ORF2* can't be excluded from playing a role in PWS although it is not conserved in mice. There are five copies of *PWRN1* and *PWRN2*, respectively, spanning a 700 kb region and only one copy of each appears to be transcribed. These genes have no protein-coding potential and are subjected to alternative splicing and polyadenylation. *PWRN1* is biallelically expressed in testis and kidney, but monoallelically expressed in fetal brain. A CpG island at 15 kb upstream of *PWRN1* exon 1 shows absence of methylation in spermatozoa, but is differentially methylated in fetal brain. *PWRN2* is only biallelically expressed in testis (145).

Six classes of box C/D small nucleolar RNA genes (*snoRNA*) have been identified in the PWS/AS imprinting domain. These snoRNAs are processed from introns of *IC-SNURF-SNRPN* transcript. They are brain-specific RNAs imprinted and expressed from the paternal allele only as their host transcript. *PWCR1/HBII-85* and *HBII-52* snoRNAs have 27 and 47 copies, respectively. *HBIII13*, *HBII-436* and *HBII-437* are single copy snoRNAs, and *HBII-438* has two copies in this region. Most C/D box snoRNAs are ubiquitous and function as guide RNAs to direct 2'-O-ribose methylation rRNA; in contrast, the brain-specific snoRNAs in the PWS region lack the usual rRNA complementary and may target cellular mRNAs for methylation or alternative splicing (37). *HBII-437* and *HBII-438* do not have homologs in the mouse, suggesting that these snoRNAs are unlikely to be responsible for the PWS neonatal lethality phenotype. Although *HBII-13* and *HBII-436* are conserved between human and mice, studies of PWS patients with balanced reciprocal chromosome

translocations exclude *HBII-13* and *HBII-436* snoRNA as candidate genes for PWS phenotype (146). In an AS family with a submicrodeletion spanning *UBE3A* and flanking sequences, all 47 copies of *HBII-52* have been deleted. The family members who carry the deletion on their paternal chromosome have no obvious clinical phenotype of PWS, indicating that *HBII-52* snoRNA do not play a major role in PWS (147). Studies of a PWS patient with translocation and a p30^{PUB} mouse model indicate that lack of *PWCRI/HBII-85* snoRNA expression is the most likely cause for the neonatal lethality in PWS patients (146, 148). Recently, microdeletion of snoRNA *HBII-85* has been found in a patient with most or all of the features of PWS (149). Moreover, a mouse model with snoRNA *MBII-85* deletion has been shown to present motor learning deficiency, suggesting an essential role of snoRNA *MBII-85* in neurodevelopment (150).

So far, *UBE3A* and *ATP10C* are the only genes associated with Angelman syndrome. *UBE3A* gene is maternal-specifically expressed in certain cells of brain and is biallelically expressed in the rest tissues of human (124, 125). Studies using mouse primary brain cell cultures suggest that *Ube3a* and *Ube3a-ATS* are cell lineage-specific imprinting. *Ube3a* is biallelically expressed in glial cells and fibroblasts, but expressed exclusively from the maternal allele in neurons, while *Ube3a-ATS* is paternally expressed in neurons but not expressed in other cells where *Ube3a* is biallelically expressed (151). *ATP10C*, encoding a putative aminophospholipid transporting ATPase, is maternally expressed in human brain. It has been suggested that *ATP10C* is a candidate gene for chromosome 15-associated autism and may contribute to AS (152, 153). There are different conclusions about the imprinting status of the mouse ortholog of the human imprinted *ATP10C* gene, *Atp10c*. Results

from one group suggest that *Atp10c* is not imprinted and is biallelically expressed in all the tissues examined, in contrast, another group indicates that *Atp10c* is maternally expressed in the hippocampus and olfactory bulb, which overlaps the region of imprinted *Ube3a* expression (154, 155). The possible explanation for the discrepancy is that *Atp10c* imprinting is genetic background-dependent. Interestingly, it is found that *Atp10c* is functionally imprinted and that loss of the maternal allele causes obesity. The mice which is heterozygous for *Atp10c* gene deletion have nearly twice the body fat when the deletion is inherited maternally as when it is inherited paternally (156).

1.9 Epigenetic regulation of PWS/AS imprinting domain

In somatic cells of human and mouse, DMR exists at the 5' CpG island of *SNURF-SNRPN*, which is heavily methylated on the silent maternal allele and is almost completely unmethylated on the active paternal allele (157, 158). *Ndn* and *MKRN3* also have parental-specific methylation at the promoter regions, and they have the same methylation patterns as *SNURF-SNRPN* promoter (159, 160). The fourth parental-specific methylation region locates at the intron 7 of *SNURF-SNRPN*, which is methylated on the paternal allele (161). The methylation status of the paternally expressed gene *MAGEL2* has not been thoroughly examined so far. Although the snoRNAs lack a direct methylation imprint, they are still under the control of DMR because snoRNAs are processed from *IC-SNURF/SNRPN*-snoRNA transcript which is regulated by *SNURF-SNRPN* DMR. The DMR of *Snurf-Snrpn* is hypermethylated in mouse oocytes and unmethylated in mouse sperm, indicating that maintenance of the gamete-specific methylation patterns account for the methylation patterns in somatic cells (162). However, there are different reports about the methylation status at DMR

of *SNURF-SNRPN* in human oocyte; one said it is heavily methylated, the other said it is unmethylated (163, 164).

The methylated maternal allele of *SNURF-SNRPN* DMR is associated with dimethyl H3K9, whereas the unmethylated paternal allele is associated with dimethyl H3K4 in both human and mice (104, 165, 166). The same histone modification pattern has also been observed at the *NDN* promoter (160). *G9a* encodes the major H3K9 methyltransferase in euchromatic regions of the nucleus. ES cells with *G9a*^{-/-} shows decreased association of dimethyl H3K9, biallelic unmethylation at *Snurf-Snrpn* DMR and biallelic expression of *Snurf-Snrpn*. However, ES cells with *Dnmt1*^{-/-} shows normal association of dimethyl H3K9, biallelic unmethylation at DMR of *Snurf-Snrpn* and monoallelic expression of *Snurf-Snrpn*. These results suggest that maintenance of DMR in ES cells is dependent on H3K9 methylation and maintenance of *Snurf-Snrpn* imprinting requires H3K9 methylation but not DNA methylation (166).

There are two prominent nuclease-hypersensitive sites (DHS) flanking *SNURF-SNRPN* exon 1 (DHS1 at the *SNURF-SNRPN* promoter and DHS2 within intron 1) on the unmethylated active paternal allele. These sites are completely inaccessible to nuclease on the methylated inactive maternal allele. In contrast, there are two maternal nuclease-hypersensitive sites; one of them coincides with the AS shortest region of deletion overlap, the other lies in *SNURF-SNRPN* intron 1 immediately downstream of the paternal-specific hypersensitive site (167). It has been shown that the DHS1 allele-specifically interacts with multiple regulatory proteins, and the DHS2 acts as an enhancer of the *SNURF-SNRPN* promoter and contains highly conserved

regions that show allele-specific interaction with unphosphorylated RNA polymerase II, YY1, Sp1 and NRF-1 (168).

In contrast to the paternally active genes, the maternally active *UBE3A* lacks differential DNA methylation regions. The epigenetic silencing of *UBE3A* has been associated with a brain-specific and paternally expressed *UBE3A-ATS* transcript. In human, the *UBE3A-ATS* extends ~450 kb from *SNURF-SNRPN* promoter region to *UBE3A* and silences the paternal allele of *UBE3A in cis*. In mouse, it has been suggested that *Snurf-Snrpn* upstream exons (U exons) which have different splicing patterns regulate the *Ube3a-ATS*. There are evidences showing that U exons are spliced to *Ube3a-ATS* with the exclusion of *Snurf-Snrpn* and silence the *Ube3a* gene *in cis* (169). However, Lander *et al* shows that the maternal disruption of *Ube3a* leads to increased expression of *Ube3a-ATS*, suggesting that the antisense is modulated by sense rather than the reciprocal model (170). It contradicts with other cases of sense-antisense epigenetic *cis*-interactions.

Paternally and maternally expressed genes in chromosome 15q11-q13 are controlled by a bipartite imprinting center. PWS/AS IC consists of two elements: PWS-IC and AS-IC. Studies of the smallest region of overlap (SRO) in PWS imprinting defect patients suggest that PWS-IC is about 4.3 kb, encompassing the promoter and the first exon region of *SNURF-SNRPN* (107, 171). Studies of the SRO in AS imprinting defect patients have mapped AS-IC to an 880-bp region located 35 kb upstream of *SNURF-SNRPN* promoter (172, 173). Reciprocal methylation and chromatin structure have been observed at the PWS-IC and AS-IC, with the AS-IC unmethylated, sensitive to DNase I and packaged in acetylated histone H3 and H4 on the maternal

allele, and such epigenetic modifications also happened on the paternal allele of PWS-IC (174). Since ortholog of AS-IC in mouse has not been identified, sequences of human AS-IC and PWS-IC, or sequences of human AS-IC and mouse PWS-IC have been used to construct transgenic mouse lines (175, 176). Studies of these kinds of transgenic mouse lines suggest that primary imprinting mark is established on AS-IC in the gametes, and the imprinted AS-IC confers imprinting on PWS-IC post fertilization. The molecular mechanisms are unknown, but *cis*-acting elements and *trans*-acting proteins are thought to provide the machinery for the interactions between AS-IC and PWS-IC (177). It appears that the close proximity and/or the correct orientation of the two IC elements are/is necessary for the establishment of a maternal imprint. Two sibs with AS have a 1-1.5 megabase (Mb) inversion separating the two IC elements, and the inversion impairs maternal imprinting after transmission through the female germline leading to AS (178).

Allele-specific DNA asynchronous replication between homologues during S phase of the cell cycle has been observed in cells from normal individuals and from PWS and AS patients with chromosome 15 deletions, but not in PWS patients with maternal uniparental disomy. At PWS/AS imprinting domain, the paternally derived allele replicates earlier than the maternal allele (179). In mouse, the asynchronous replication timing of *Snurf-Snrpn* region is established in the gametes and maintained during development (180).

Mouse chromosome 7C and its syntenic human chromosome 15q11-q13 region are conserved not only in imprinting features but also in gene order (Figure 1-4b). To date, multiple PWS and AS mouse models have been reported (Table 1-3), but it is

still not clear whether there is conservation of the imprinting control mechanisms between humans and mice. Although PWS-IC is conserved in mice, a murine equivalent to the human AS-IC element has not yet been identified. Considering human AS-IC is mapped to an 880-bp region located 35 kb upstream of *SNURF-SNRPN* promoter, the *Snurf-Snrpn* upstream region of mice was studied by targeting strategy. Three mouse lines have been generated using chromosome engineering approach (Figure 1-5). The large deletion mouse line (LD) has a 1.5-Mb deletion which extends from 100 kb upstream of *Snurf-Snrpn* minimal promoter to *Ndn* gene. The mouse develops PWS when it inherits the deleted chromosome from the paternal origin, and yet its methylation pattern is normal. The IC-anchor mutation mouse line (AS-IC^{an}) carries a targeted insertion vector (pG12H6) located 13 kb upstream from *Snurf-Snrpn* minimal promoter. Interestingly, mice paternally inherited AS-IC^{an} mutations are normal, whereas mice develop AS imprinting defect when the AS-IC^{an} mutation is inherited from the maternal origin. The usually methylated maternal allele of *Snurf-Snrpn* DMR becomes unmethylated and the maternal allele of *Ube3a* gene is silent in cerebellum. The small deletion mouse line (SD) has a chromosome deletion extending 80 kb from the AS-IC^{an} mutation, encompassing the putative AS-IC located upstream of *Snurf-Snrpn* minimal promoter. This mouse develops AS imprinting defect with incomplete penetrance and mosaicism when the mutant allele is inherited from maternal origin (181).

My project focused on the AS-IC^{an} mutation mouse line. To generate the AS-IC^{an} mutant mice, an insertion targeting vector was used to introduce the 3' portion of an *Hprt* selectable cassette, a loxP site, and a *puromycin* selectable marker at a site 13 kb 5' of *Snurf-Snrpn* exon 1; the targeting vector generated a duplication of 6 kb genomic

sequence (Appendix Figure 1). After transmitted to mouse germline, mice with either a paternally or maternally transmitted mutation were viable and fertile on a 129/SvEv and C57BL/6J genetic background. DNA methylation analysis by Southern blot showed that maternal inheritance of AS-IC^{an} mutation resulted in loss of methylation on the maternal allele at DMR of *Snurf-Snrpn*. DNA methylation analysis at DMR of *Ndn* showed an increase in the fraction of unmethylated DNA for heterozygous mice with maternal inheritance of the AS-IC^{an} mutation. These results suggested that maternal inheritance of AS-IC^{an} mutation leads to AS imprinting defect. Decreased expression of UBE3A in the human brain is assumed but not currently proven character of AS imprinting defect. Mice bearing the AS-IC^{an} mutation on their maternal chromosome showed a severe decrease in E6-AP both in the cortex and cerebellum by Western blot (181).

At least three mechanisms may explain the AS imprinting defect among AS-IC^{an} mutation mice. First, the promoter activity from the insertion vector may interfere with the *Snurf-Snrpn* upstream transcripts and perturb its role in establishing and/or maintaining of imprinting marks on the maternally inherited chromosome (169, 182). Second, the insertion of the targeting vector may destroy the element of AS imprinting center and thus leads to AS imprinting defect. Alternatively, the 6 kb duplication generated from homologous recombination may interfere with the AS imprinting process. The 6 kb duplication area is a *HindIII* genomic sequence which is located at 11 kb upstream of *Snurf-Snrpn* exon 1. It is the homology region contained in the insertion-type targeting vector pG12H6. The 6 kb region contains a *SalI* site, which is the insertion site of pG12H6. These mechanisms are not necessary mutually exclusive.

Table 1-3 Mouse models

	Genotype	Phenotype	Reference
PWS mouse model	maternal UPD/paternal deficiency	100% postnatal lethality	(183)
	transgenic insertion/large deletion	paternal 100% lethality maternal AS-like	(184)
	42 kb PWS-IC deletion	paternal 100% lethality on C57BL/6 & 129/SvEv	(107)
	<i>Snrpn</i> to <i>Ube3a</i> deletion	paternal 80% lethality maternal AS-like	(124)
	<i>Ndn</i> null	paternal variable lethality and phenotype	(134)
	<i>Ndn</i> null	Paternal variable lethality and phenotype	(135)
	<i>Snrpn</i> promoter 4.8 kb deletion	paternal 40-50% lethality	(182)
AS mouse model	LD deletion	paternal PWS	Our lab
	<i>Ube3a</i> null	AS	(185)
	IC-anchor mutation	AS imprinting mutation	(181)
	SD deletion	AS imprinting mutation	(181)
	Human PWS-IC replace mouse PWS-IC	PWS and AS imprinting mutation	(186)
None phenotype	<i>SmN</i> null	none	(131)
	<i>Snurf</i> null	none	(130)
	<i>Ndn</i> null	none	(136)
	<i>Snrpn</i> promoter 0.9 kb deletion	none	(182)
	12.8 kb deletion extending from -37kb to -24kb relative to <i>Snrpn</i> exon1	none	(187)
	8.2 kb deletion extending from -37kb to -29kb relative to <i>Snrpn</i> exon 1	none	(187)

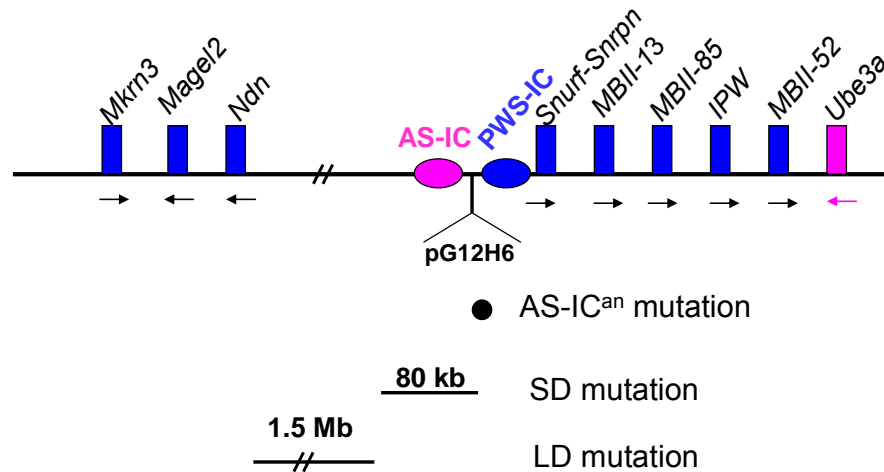


Figure 1-5 Chromosomal engineering of PWS/AS critical region in mice. The IC-anchor mutation mouse line (*AS-IC^{an}*) carries a targeted insertion vector *pG12H6* located at 13 kb upstream of *Snurf-Snrpn* minimal promoter. The small deletion mouse line (*SD*) carries a 80 kb-deletion extending from *AS-IC^{an}* mutation. The large deletion mouse line (*LD*) has a 1.5 Mb deletion which extends from 100 kb upstream of *Snurf-Snrpn* minimal promoter to *Ndn* gene. The paternally expressed genes are labeled in blue and maternally expressed genes are labeled in red. Arrows indicate transcription orientation. blue ellipse, *PWS-IC*; red ellipse, *AS-IC*.

1.10 Project aims

This study aims to develop the molecular mechanism of genomic imprinting for the human disease PWS/AS using an *AS-IC^{an}* mutant mouse line. The methylation status of the entire *Snurf-Snrpn* DMR has been examined by bisulfite sequencing method. Loss of methylation usually leads to gene activation, so that *Snurf-Snrpn* gene expression has been studied by real time PCR. The *Snurf-Snrpn* upstream transcripts may play roles in AS imprinting regulation, so the expression and splicing patterns of the *Snurf-Snrpn* upstream transcripts have also been investigated. Chromatin immunoprecipitation has been carried out to study histone modifications at *Snurf-Snrpn* DMR. Chromosome conformation capture can detect long range chromosome interaction, and it has been performed to detect whether PWS/AS imprinting center confers imprint by direct physical interaction. In addition, a new targeting vector has

been constructed to delineate the mechanisms which lead to AS imprinting defect. Through these experiments, we can develop hypothesis for the molecular mechanism governing genomic imprinting. Establishing hypothesis molecular mechanism may open more new research areas that probably lead to better understanding of human genomic imprinting diseases and ultimately to establish treatment strategies.

Chapter II Materials and Methods

2.1 Genomic DNA extraction from mouse tail

Three mouse strains used in this study were 129/SvEv, PWK/PhJ and C57BL/6J. Mouse tail (1-1.5 cm) was digested overnight at 55 °C in a 1.5 ml tube containing 500 µl of NTES solution [50 mM Tris pH 7.5, 50 mM ethylenediaminetetraacetic acid (EDTA) pH 8.0, 100 mM NaCl, 5 mM dithiothreitol (DTT), 0.5 mM spermidine, 2% sodium dodecyl sulfate (SDS) and proteinase K (0.2 µg/µl)]. Next day, equal volume of phenol was added to the tube, and then the tube was slowly rocked for 30 min followed by centrifugation for 15 min at 13,000 g. The aqueous layer was transferred to a 1.5 ml tube, and then 500 µl of PCI (phenol: chloroform: isoamyl alcohol = 25: 24: 1) solution was added. The tube was slowly shaken for 30 min, and then was centrifuged for 15 min at 13,000 g. The top aqueous layer was transferred to a 1.5 ml tube. Chloroform (500 µl) was added to the tube, and the tube was gently shaken for 30 min followed by centrifugation for 15 min at 13,000 g. The top layer was removed to a 1.5 ml tube again. Isopropanol (500 µl) was added to precipitate DNA. White thread like DNA was observed by inverting the tube slowly. DNA was spooled out and dissolved in 200 µl of solution [180 µl of ddH₂O and 20 µl of Tris-EDTA (TE) buffer] in a 1.5 ml tube at 37 °C overnight. DNA was quantitated by spectrophotometry and stored at 4 °C.

2.2 Southern blot

For genotyping of AS-IC^{an} mouse, genomic DNA (10 µg) was digested overnight with restriction enzyme *SacI*. For methylation studies of the *Snurf-Snrpn* DMR, genomic

DNA (20 µg) was first digested overnight with *Hind*III, and then precipitated with 100% ethanol, and finally was re-dissolved in 20 µl of water. Ten microliter of DNA (10 µg) was taken out and digested overnight with methylation sensitive restriction enzyme *Sac*II. For Southern blot analysis, digested DNA was electrophoresed in a 0.8% agarose gel at 25 V overnight, and then transferred to a Hybond N+ membrane (Amersham). The probe (240 bp) for genotyping of AS-IC^{an} mouse was prepared by polymerase chain reaction (PCR) using mouse BAC CT7-289D17 as template. The primers used for preparing the 240-bp DNA probe were SHF and SHR (Table 1 of Appendices). PCR cycling conditions were: 10 min at 94 °C, then 35 cycles of 30 seconds at 94 °C, 30 seconds at 55 °C and 1 min at 72 °C, followed by 10 min at 72 °C. The Taq polymerase used for PCR was Faststart Taq (Roche). PCR products were purified by QIAquick Gel Extraction Kit (QIAGEN). The probe for methylation analysis of *Snurf-Snrpn* DMR was a 1.3 kb *Bss*HIII-*Eco*RI fragment from plasmid TF11. Labeling and detection of Southern blot were carried out using Gene Images Random Prime Labeling and Detection System (Amersham) according to manufacturer's protocol. Membranes were exposed to Kodak X-ray films.

2.3 Nucleotide polymorphism analysis

PCR reactions were performed using genomic DNA from 129/SvEv, PWK/PhJ and 129/PWK F1 hybrid as templates. The primers used for polymorphism analysis were AH4 and AH5, AH52 and AH53, AH44 and AH53, AH5r and AH45 (Table 1 of Appendices). PCR with primers AH4 and AH5 was performed using Faststart Taq polymerase (Roche) and the PCR conditions were: 10 min at 94 °C, then 35 cycles of 30 seconds at 94 °C, 30 seconds at 53 °C and 1 min at 72 °C, followed by 10 min at 72 °C. PCR with primers AH52 and AH53 was performed using iTaq DNA

polymerase (BioRad) and PCR conditions were: 5 min at 95 °C, then 35 cycles of 30 seconds at 95 °C, 30 seconds at 58 °C and 30 seconds at 72 °C, followed by 7 min at 72 °C. PCR with primers AH44 and AH53 was performed using the same Taq polymerase and the same PCR conditions as primer set AH52 and AH53. PCR with primers AH5r and AH45 was performed using i-starTaq DNA polymerase (i-DNA) and PCR conditions were: 2 min at 94 °C, then 35 cycles of 20 seconds at 94 °C, 10 seconds at 58 °C and 30 seconds at 72 °C, followed by 5 min at 72 °C. PCR products (543 bp) from AH4 and AH5 were electrophoresed in a 2.0% agarose gel and purified by the QIAquick Gel Extraction Kit (QIAGEN), and then were fused to pCR4.0-TOPO vector (Invitrogen) according to manufacturer's protocol with minor modifications as the following: 4 µl of DNA was incubated at room temperature with 1 µl of vector plus 1 µl of salt solution (1.2 M NaCl, 0.06 M MgCl₂) for 30 min, and then 50 µl of TOP 10 competent cells was added. The DNA/cell mixture was incubated on ice for 20 min, and then was heat-shocked at 42 °C for 90 seconds, followed by incubation on ice for 2-3 min. SOC medium (250 µl of 2% tryptone, 0.5% yeast extract, 10 mM NaCl, 2.5 mM KCl, 10 mM MgCl₂, 10 mM MgSO₄, 20 mM glucose) was added into the DNA/cell mixture and mixed. The mixture was spread directly on Luria-Bertani (LB) plates containing 50 µg/ml of kanamycin, and the plates were incubated overnight in a 37 °C incubator. Colonies were inoculated into 3 ml of LB liquid medium with 50 µg/ml kanamycin and cultured in a 37 °C shaking incubator overnight. Plasmids DNA were extracted using QIAprep Spin Miniprep Kit (QIAGEN) and sequenced using T7 primer (Research Biolaboratory). PCR products (145 bp) from AH52 and AH53, PCR products (850 bp) from AH44 and AH53, and PCR products (340 bp) from AH5r and AH45 were electrophoresed in 2.0% agarose gels, and then were purified by the QIAquick Gel Extraction Kit

(QIAGEN) and sequenced directly on 310 Genetic Analyzer (Applied Biosystems) using sequence-specific primers, respectively. Cycle sequencing reactions were carried out using BigDye Terminator v3.1 (Applied Biosystems) and the reaction conditions for these primers sets were: 1 min at 96 °C, then 25 cycles of rapid thermal ramp (1 °C /second) to 96 °C, 10 seconds at 96 °C, rapid thermal ramp to 55 °C (1 °C /second), 5 second at 55 °C, rapid thermal ramp to 60 °C (1 °C /second) and 4 min at 60 °C. After the thermal cycles, EDTA (2.5 µl of 125 mM EDTA) and 25 µl of 100% ethanol were added to the cycle reaction products (10 µl) and mixed well. The mixture was incubated at room temperature for 15 min and centrifuged for 30 min at 4 °C. The aqueous part was removed and the DNA pellet was washed once with 800 µl of 70% ethanol, and then incubated at 65 °C in a vacuum concentrator for 5 min. DNA pellet was resuspended in 20 µl of Hi-Di™ formamide (Applied Biosystem) and sequences were determined using 310 Genetic Analyzer and analyzed using Vector NTI.

2.4 Bisulfite genomic sequencing

Bisulfite treatment of genomic DNA was carried out using the CpGemone™ DNA Modification Kit (Chemicon, international) following manufacturer's instruction. Bisulfite-modified DNA was amplified by nested PCR; primers BIOF and BIOR were used for the first round PCR, primers BIIF and BIIR were used for the second round PCR (Table 1 of Appendices). The first round PCR cycling conditions were: 10 min at 94 °C, then 30 cycles of 30 seconds at 94 °C, 30 seconds at 50 °C and 1 min at 72 °C, followed by 10 min at 72 °C. One microliter of the first round PCR products was used as template for the second round PCR. The cycling conditions of the second round PCR were the same as that of the first round except that the cycle number

increased from 30 to 35 cycles. Faststart Taq polymerase was used for both the first and the second round PCR. PCR products were electrophoresed in a 2.0% agarose gel and purified by the QIAquick Gel Extraction Kit (QIAGEN), and then were fused to pCR4.0-TOPO vector (Invitrogen) and sequenced. Sequencing results were analyzed by Vector NTI.

2.5 Methylation specific PCR (MSP)

Mouse genomic DNA was treated with CpGenomeTM DNA Modification Kit (Chemicon, international) according to the manufacturer's protocol. The bisulfite modified DNA was amplified by methylation specific primers. The methylation specific primers for the DMR of *Snurf-Snrpn* in mice were designed using MethPrimer (188). Primers for amplification of the methylated allele are Mf and Mr. Primers for amplification of the unmethylated allele are Pf and Pr. The sequences of these primers are available in the Table 1 of the appendices. The PCR reactions were performed using Taq polymerase (Applied Biosystem) and the PCR conditions were: 6 min at 95 °C, then 35 cycles of 30 seconds at 95 °C, 30 seconds at 50 °C and 30 seconds at 72 °C, followed by 7 min at 72 °C. PCR products were separated in a 2% agarose gel.

2.6 Reverse transcription PCR (RT-PCR) and real time PCR

Total RNA was isolated from mice liver or cerebellum using TRIzol (Invitrogen) according to the manufacture's instruction. The concentration of RNA was measured by spectrophotometry. Total RNA (100 µg) was treated with RQ1 DNase I (10 U, Promega) at 37 °C water bath for 1 hour in the presence of RNase Inhibitor (40 U,

Invitrogen). The reaction mixture was extracted by equal volume of phenol/chloroform, and then RNA was precipitated by 0.25 volume of 7.5 M ammonium acetate and 2.5 volume of 100% ethanol. DNase I treated RNA was dissolved in diethylpyrocarbonate (DEPC) treated ddH₂O. Reverse transcription reactions were performed with random hexamer for the first strand complementary DNA (cDNA) synthesis using SuperScript First-Strand Synthesis System (Invitrogen). For the preparation of cDNA for real time PCR of *puromycin* gene, dimethylsulfoxide (DMSO, 10%) was added into the reverse transcription reaction mixture.

Gene specific primers for the *Snurf-Snrpn* exon 3 were AH10 as described before by Bressler *et al* as primer b (182). Gene specific primer for *Snurf-Snrpn* upstream exon 7 was AH11 and for upstream exon 5 was AH12 which were designated as primers u7b and u5 (169). The gene specific primer for 3' Hprt exons was Hprt. The sequences of primers are provided in the Table 1 of appendices. PCR reactions were performed using Faststart Taq polymerase and PCR conditions were the same as described previously. The annealing temperatures of PCR cycling conditions varied according to primers combinations. Annealing temperature for AH10 and AH11 was 56 °C, for AH10 and AH12 was 58 °C. PCR products were fused to pCR4.0-TOPO vector and sequenced. Sequencing results were analyzed by Vector NTI.

Real time PCR was performed using SYBR Green PCR master mix (Applied Biosystems) by standard curve method. *Beta-actin* was used as the endogenous control. Gene specific primers for *Snrpn* were ksc3 and ksc4, for *puromycin* were purof and puror, and for *β-actin* were actinF and actinR. The sequences of primers are available in the Table 1 of the appendices. Real time PCR cycling conditions were: 2

min at 50 °C, 40 cycles of 15 seconds at 95 °C and 1 min at 60 °C (also the data collection step), followed by a dissociation stage. Each assay was carried out in triplicates on an ABI 7500 real time PCR system (Applied Biosystems).

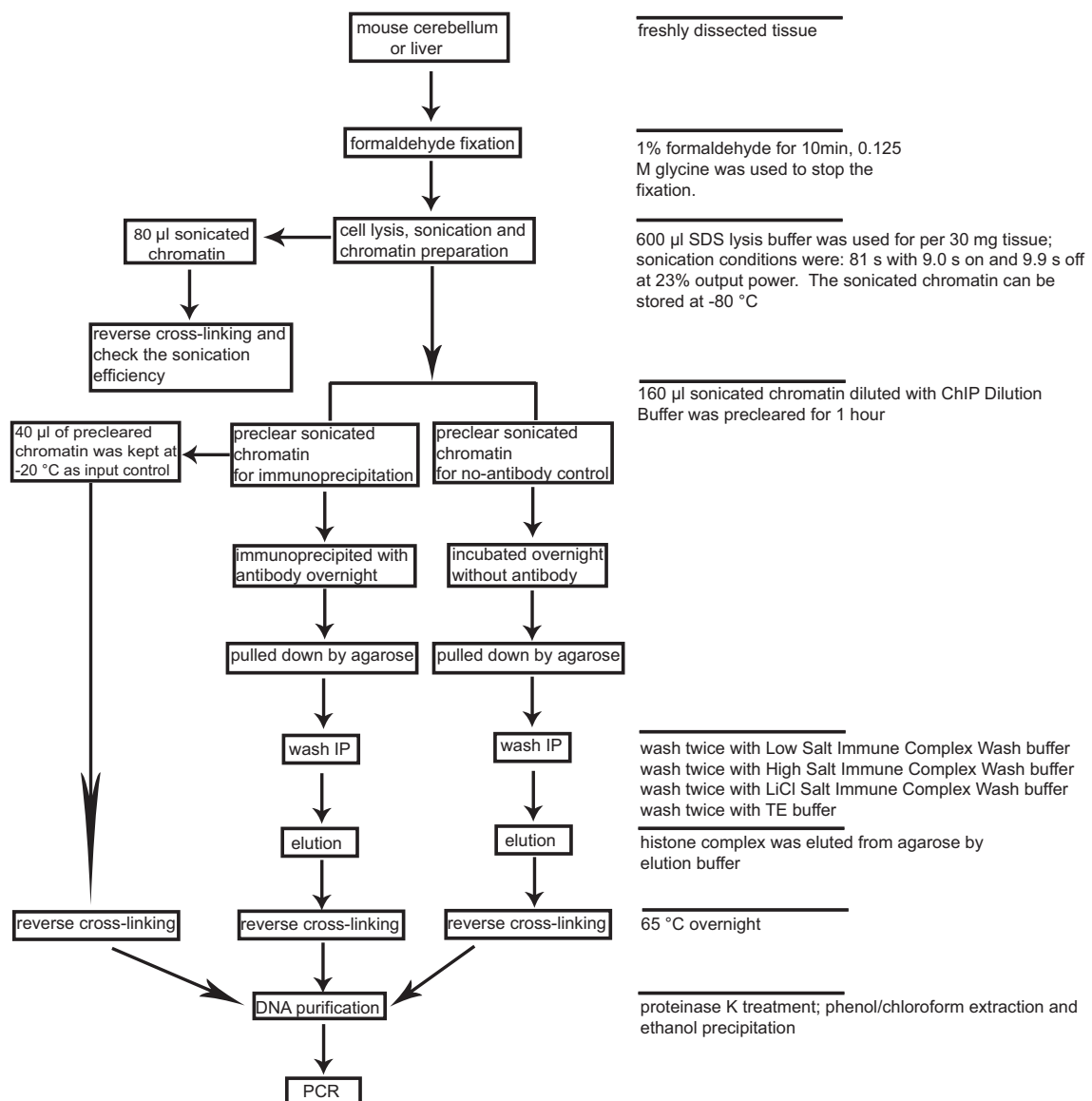


Figure 2-1 Flow chart of ChIP

2.7 Chromatin Immunoprecipitation (ChIP)

The flow chart of ChIP is shown in Figure 2-1. Liver or cerebellum (30 mg) from (129/SvEv × PWK/PhJ reciprocal matings) F1 mice was minced into small pieces in a 2 ml tube containing 1 ml of 1× Phosphate-Buffered Saline (PBS) buffer, and then the

tissues were fixed by 1% formaldehyde for 10 min with rotation at room temperature. The reaction of formaldehyde was stopped by adding 2.5 M glycine to a final concentration of 0.125 M. The fixed samples were centrifuged at 100 g for 30 seconds at 4 °C. The aqueous layer was removed and the pellet was washed by 1 ml of ice cold 1× PBS, and then was resuspended in 600 µl of SDS lysis buffer (1% SDS, 10 mM EDTA, 50 mM Tris-Cl pH 8.1). The pellet was sonicated after incubation on ice for 10 min. The sonication was performed using a 750 W, 20 kHz sonicator (Sonics & Materials, In., Model: VC750) and the conditions were 81 s with 9.0 s on and 9.9 s off at 23% output power. The sonication was paused for 5 min per 27 s to minimize heat-generation. The sonicated samples were centrifuged at 13,000 g for 10 min at 4 °C, and the supernatant was transferred to a new 2 ml tube. The sonicated supernatant was kept at -80 °C.

A small volume (80 µl) of sonicated supernatant was transferred to a 1.5 ml tube, and then 3.2 µl of 5 M NaCl was added to the tube. The mixture was incubated at 65 °C for 4 hours to reverse cross-linking. DNA was recovered by equal volume of phenol/chloroform extraction and fractionized in 1% agarose gel to visualize sonication efficiency with 20 µl of sample per lane.

Sonicated supernatant (160 µl) was diluted by 1440 µl of ChIP Dilution Buffer (0.01% SDS, 1.1% Triton X-100, 1.2 mM EDTA, 16.7 mM Tris-Cl pH 8.1, 167 mM NaCl) with protease inhibitor cocktail (Roche) in a 2 ml tube. An additional sample was prepared as a no-antibody immunoprecipitation control. The diluted samples were pre-cleared with 80 µl of Salmon Sperm DNA/Protein A Agarose -50% Slurry (Upstate) for 1 hour at 4 °C with agitation, and then agarose was pelleted by

centrifugation at 100 g for 2 min at 4 °C. The supernatant fraction was transferred to a new 2 ml tube. An aliquot of supernatant (40 µl) was kept at -20 °C as input control. Immunoprecipitation was carried out using the rest supernatant with diluted (1:400) anti-dimethyl-histone H3 lys4 (Upstate), anti-dimethyl-histone H3 lys9 (Upstate) and anti-trimethyl-histone H3 lys9 (Abcam) antibodies. The immunoprecipitation process was performed overnight at 4 °C with rotation. The no-antibody immunoprecipitation control was also rotated overnight at 4 °C. The next day, the antibody/histone complex was pulled down by adding 80 µl of Salmon Sperm DNA/Protein A Agarose -50% Slurry for 1 hour at 4 °C with rotation. The agarose was pelleted by gentle centrifugation at 100 g for 2 min at 4 °C and washed twice with 1 ml of Low Salt Immune Complex Wash buffer (0.1% SDS, 1% Triton X-100, 2 mM EDTA, 20 mM Tris-Cl pH 8.1, 150 mM NaCl) for 10 min each on a rotating platform at room temperature. The agarose was pelleted by centrifugation at 100 g for 2 min at 4 °C, and then washed twice with 1 ml of High Salt Immune Complex Wash buffer (0.1% SDS, 1% Triton X-100, 2 mM EDTA, 20 mM Tris-Cl pH 8.1, 500 mM NaCl) for 10 min each time on a rotating platform at room temperature. The agarose was pelleted again and washed twice with 1 ml of LiCl Immune Complex Wash Buffer (0.25 M LiCl, 1% IGEPAL-CA630, 1% deoxycholic acid, 1 mM EDTA, 10 mM Tris-Cl pH 8.1) at the same conditions as above. Finally, the agarose was washed twice with 1 ml of TE buffer (pH 8.0). To elute the histone complex from the agarose, 250 µl of elution buffer (1% SDS, 0.1 M NaHCO₃) was added to the pelleted protein A agarose/antibody/histone complex, and the mixture was incubated at room temperature for 15 min with rotation, followed by centrifugation at 100 g for 2 min at 4 °C. The supernatant fraction was carefully transferred to a new 2 ml tube. The elution step was repeated for one more time and the eluates were combined. To

reverse histone-DNA cross-linking, 5 M NaCl was added to the combined eluates and the input control to a final concentration of 0.2 M. The samples were incubated at 65 °C overnight, followed by adding 10 µl of 0.5 M EDTA, 20 µl of 1 M Tris-Cl (pH 6.5) and 1 µl of 20 mg/ml proteinase K (Roche), and then the mixture was incubated at 45 °C for 1 hour. Equal volume of phenol/chloroform was added to each sample to extract DNA by centrifugation at 13,000 g for 10 min. The aqueous fraction was transferred to a 2 ml tube and 2.5 volume of 100% ethanol was added to precipitate DNA at -20 °C overnight, with 20 µg of yeast tRNA as inert carrier. The next day, DNA was pelleted by centrifugation at 13,000 g for 10 min at room temperature and washed once with 70% ethanol, and then was air-dried and dissolved in 30 µl of TE buffer.

DNA recovered from antibody-immunoprecipitated materials and input materials were amplified by PCR with allele-specific primers in the presence of [α -³²P] dCTP for 32 cycles. One-fourth microliters, 1 µl and 2 µl of original DNA samples were used for PCR to ensure the PCR amplification was still in the linear range. Primers specific for PWK/PhJ allele amplification are AH20a and AH21a. Primers specific for 129/SvEv allele amplification are AH22a and AH23a. PCR cycling conditions were: 5 min at 95 °C, 35 cycles of 30 seconds at 95 °C, 30 seconds at 60 °C and 30 seconds at 72 °C, followed by 7 min at 72 °C. PCR products (10 µl) were separated in 12% nondenaturing polyacrylamide gels and visualized by autoradiography to X-ray films after drying of gels.

For the DNA precipitated with anti-trimethyl histone H3K9 from mouse liver, real time PCR was performed using SYBR Green PCR master mix (Applied Biosystems)

by standard curve method. *D13Mit55* was used as the endogenous control. Primers AH20a, AH21a, AH22a and AH23a were used for real time PCR for amplification of PWK/PhJ allele and 129/SvEv allele, respectively. AH24a and AH25a were primers for amplification of *D13Mit55*. Real time PCR cycling conditions were: 2 min at 50 °C, 40 cycles of 15 seconds at 95 °C and 1 min at 60 °C (also the data collection step), followed by a dissociation stage. Each assay was carried out in triplicates on an ABI 7500 real time PCR system (Applied Biosystems). The sequences of primers for ChIP are available in the Table 2 of the appendices.

2.8 Chromosome conformation capture (3C)

The human fibroblast cell lines used for the 3C were GM00364, GM04503, GM09255 (Coriell Cell Repositories). Cells from one T-75 flask at 70-80% confluency were trypsinized with 4 ml of 0.05% trypsin/0.53 mM EDTA for 7 min, and then the trypsinization was stopped by adding 5 ml of culture medium [Minimum Essential Medium (MEM), 2× essential amino acid (Invitrogen, Cat. No.11130), 2× non-essential amino acid (Invitrogen, Cat. No.11140), 2× Vitamin (Invitrogen, Cat. No.11120), 2 mM L-glutamine, 15% of uninactivated fetal bovine serum (FBS)]. For each cell line, cells from three T-75 flasks were combined and collected by centrifugation at 800 g for 3 min. Cells were resuspended in 25 ml of culture medium. For mouse tissues, freshly dissected cerebellum was mashed (about 4×10^7 cells) through a 70-µm nylon cell strainer (BD Falcon) into a 50 ml tube containing 25 ml of Dulbecco's Modified Eagle Media (DMEM) (Invitrogen) supplemented with 10% of FBS.

Cell suspension was fixed by 2% formaldehyde for 10 min at room temperature with rotation. The fixation reaction was quenched by adding 2 M glycine to a final concentration of 0.125 M. The cells were pelleted by centrifugation at 4500 g for 10 min at 4 °C and resuspended in 25 ml of ice cold lysis buffer (10 mM Tris-Cl pH 8.0, 10 mM NaCl, 0.2% Nonidet P-40 and Roche protease inhibitor cocktail) to be lysed on ice for 90 min with stir. Nuclei were pelleted by centrifugation at 3250 g for 15 min at 4 °C, and then resuspended in 2 ml of 1× restriction enzyme buffer (New England Biolabs, NEB) with 0.3% SDS (30 µl of 20% SDS), and incubated at 37 °C for 1 hour with rotation. Triton X-100 (180 µl of 20% Triton X-100) was added to the nuclei mixture to make a final concentration of 1.8% to sequester the SDS, and the mixture was incubated for one hour at 37 °C with rotation. Nuclei were counted on a haemocytometer and an aliquot (about 1×10^6 nuclei, ~ 15 µg) was digested within a total volume of 800 µl by 1200 U of enzyme *Bgl*II, *Pst*I, *Bam*HI, *Sac*I, *Xba*I, *Nde*I, *Sph*I or *Nco*I at 37 °C overnight with rotation. All the restriction enzymes were from NEB. An aliquot of nuclei (about 100 µl) was kept at 4 °C as the non-digestion control. The next day, restriction enzyme reaction was inactivated by adding 20% SDS to a final concentration of 1.6% and was heated at 65 °C for 20 min. An aliquot of enzyme reaction mixture (2 µg) was made up to 800 µl with ligation buffer (80 µl), 20% Triton X-100 (40 µl) and appropriate volume of ddH₂O, and was incubated at 37 °C for 1 hour. T4 DNA ligase (30 Weiss units, Promega) was added to the mixture after the temperature being cooled down, and then the mixture was incubated at 16 °C for 16 hours. An aliquot of enzyme reaction mixture (100 µl) was kept at 4 °C as the post-digestion control. The next day, proteinase K (100 µg/ml final) was added to the ligation mixture, the non-digestion control and the post-digestion control samples. The samples were incubated at 65 °C overnight. All of the samples were treated with

RNase A (0.5 µg/ml) at 37 °C for 30 min, and extracted by equal volume of phenol/chloroform, and then were precipitated by adding 2.5 volume of 100% ethanol. Finally, TE buffer (40 µl) was used to dissolve DNA. Ten microliters of DNA was electrophoresed in a 1% agarose gel. One microliter of 3C DNA was used in two rounds PCR and PCR products were electrophoresed in a 2% agarose gel. The PCR products with expected size were purified by QIAquick Gel Extraction Kit (QIAGEN). The purified PCR products were sequenced directly or fused to pCR4.0-TOPO vector for sequencing. Sequencing results were analyzed by BioEdit. The sequences of primers used in 3C are available in the Table 3 of the appendices.

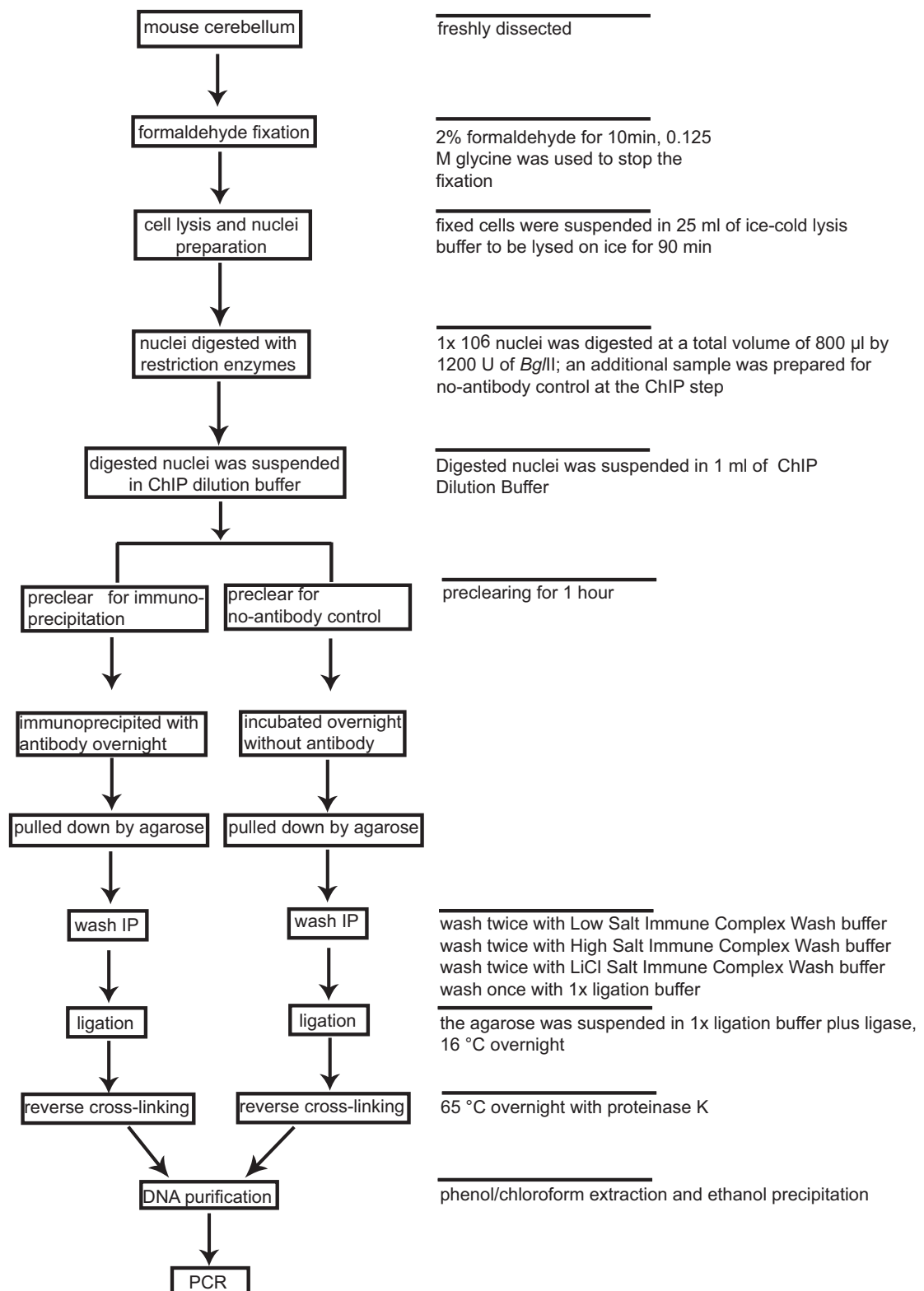


Figure 2-2 Flow chart of ChIP-loop

2.9 ChIP-loop

ChIP-loop is a combination of ChIP and 3C assay. Flow chart of ChIP-loop is shown in Figure 2-2. Cell suspension from mice cerebellum was fixed by 2% formaldehyde for 10 min at room temperature with rotation. The fixation reaction was quenched by adding 2 M glycine to a final concentration of 0.125 M. The cells were pelleted at 4500 g for 10 min at 4 °C, and then were resuspended in 25 ml of ice cold lysis buffer (10 mM Tris-Cl pH 8.0, 10 mM NaCl, 0.2% Nonidet P-40 and protease inhibitor cocktail) to be lysed on ice for 90 min with stir. The nuclei were pelleted by centrifugation at 3,250 g for 15 min at 4 °C, and then were resuspended in 2 ml of 1× restriction enzyme buffer (NEB) with 0.3% SDS (30 µl of 20% SDS), followed by incubation at 37 °C for 1 hour with rotation. Triton X-100 (180 µl of 20% Triton X-100) was added to the nuclei mixture to make a final concentration of 1.8% to sequester the SDS, and the mixture was incubated for one hour at 37 °C with rotation. The nuclei were counted on a haemocytometer. A nuclei aliquot (about 1×10^6 nuclei, ~ 15 µg) was digested at a total volume of 800 µl by 1200 U of *Bgl*/II (NEB) at 37 °C overnight with rotation. The next day, the restriction enzyme reaction was heat-inactivated at 65 °C for 20 min. The digested nuclei was collected by centrifugation for 10 min at 2,500 g and suspended in 1 ml of the ChIP dilution buffer (0.01% SDS, 1.1% Triton X-100, 1.2 mM EDTA, 16.7 mM Tris-Cl pH 8.1, 167 mM NaCl and protease inhibitor cocktail). An additional sample was prepared as a no-antibody immunoprecipitation control. Diluted samples were pre-cleared with 80 µl of Salmon Sperm DNA/ Protein A Agarose -50% Slurry for 1 hour at 4 °C with agitation. The agarose was pelleted by centrifugation at 100 g for 2 min at 4 °C. Supernatant fraction was transferred to a new 1.5 ml tube and diluted (1:200) anti-Mecp2 (Upstates) was added. The immunoprecipitation process was performed overnight at

4 °C with rotation. The no-antibody immunoprecipitation control was also rotated overnight at 4 °C. The antibody/protein complex was pulled down by adding 80 µl of the Salmon Sperm DNA/ Protein A Agarose -50% Slurry for 1 hour at 4 °C with rotation. The agarose was pelleted by gentle centrifugation at 100 g for 2 min at 4 °C, and washed twice with 1 ml of Low Salt Immune Complex Wash buffer (0.1% SDS, 1% Triton X-100, 2 mM EDTA, 20 mM Tris-Cl pH 8.1, 150 mM NaCl) for 10 min each time on a rotating platform at room temperature. The agarose was pelleted by centrifugation at 100 g for 2 min at 4°C, and then washed twice with 1 ml of the High Salt Immune Complex Wash buffer (0.1% SDS, 1% Triton X-100, 2 mM EDTA, 20 mM Tris-Cl pH 8.1, 500 mM NaCl) for 10 min each time on a rotating platform at room temperature. The agarose was pelleted again and washed twice with 1 ml of the LiCl Immune Complex Wash Buffer (0.25 M LiCl, 1% IGEPAL-CA630, 1% deoxycholic acid, 1 mM EDTA, 10 mM Tris-Cl pH 8.1) at the same conditions as above. Finally, the agarose was washed once with 800 µl of 1× ligation buffer (Promega) for 10 min on a rotated platform at room temperature, and then was suspended in 100 µl of 1× ligation buffer and ligase (30U, Promega). The ligation reaction was performed at 16 °C overnight. The next day, proteinase K (100 µg/ml) was added to the ligation mixture tube and the tube was incubated at 65 °C overnight. The next day, RNase A (0.5 µg/ml) was added to the tube and the tube was incubated at 37 °C for 30 min. Equal volume of phenol/chloroform was added to the tube and mixed, and then was centrifuged at 13,000 g for 15 min. The aqueous layer was transferred to a 1.5 ml tube. Sodium acetate (0.3 M) and 2.5 volume of 100% ethanol were added to the tube to precipitate DNA by centrifugation at 13,000 g for 10 min at room temperature. The DNA pellet was washed with 70% ethanol and air-dried, finally was resuspended in 20 µl of TE buffer. One microliter of DNA from the ChIP-

loop was used for PCR. Primers flanking *Bgl*III sites at PWS-IC, *Ube3a* gene and putative AS-IC of mice were used for PCR reactions. The sequences of primers are available in the Table 3 of the appendices.

2.10 Bacterial artificial chromosome (BAC) DNA extraction

A single BAC colony was inoculated into 100 ml of the LB medium containing 12.5 µg/ml chloramphenicol and cultured overnight with vigorous shaking (250 rpm/min) at 37 °C. Bacteria were harvested by centrifugation at 6,000 g for 15 min at 4 °C and then the BAC DNA was extracted using QIAGEN Plasmid Midi Kit (QIAGEN) following the manufacturer's instruction with minor modifications. To ensure bacteria cells were lysed completely, the volumes of the buffer P1, P2 and P3 were increased to two fold for each sample. The DNA was eluted from the QIAGEN-tip 100 column by adding 5 aliquots of the 1 ml pre-warmed (65 °C) elution buffer QF.

2.11 Fluorescence *in situ* hybridization (FISH)

2.11.1 Coating slides with poly-L-lysine

The poly-L-lysine solution (5 ml of 0.1% w/v) (Sigma P8920) was diluted by 45 ml of ultrafiltered water in a 50 ml conical tube to make a working solution. The slides were first cleaned by dipping in the acetone for 5 min, and then were removed from the acetone and wiped with a kimwipe. The air-dried slides were dipped in the poly-L-lysine working solution for 15 min and air-dried at an angle on the paper towels. The coated slides were marked, and then were put into 55 °C oven for 1 hour.

2.11.2 Cell suspension preparation from mouse liver

Freshly dissected liver were mashed through a 70- μ m nylon cell strainer (BD Falcon) into 25 ml of DMEM supplemented with 10% of foetal calf serum. The cells were pelleted at 4,500 g for 10 min and washed twice with 20 ml of 1 \times PBS, and then were resuspended in 10 ml of 0.075 M KCl hypotonic buffer and incubated at 37 °C for 10 min. The hypotonic cells were collected by centrifugation at 800 g for 3 min and resuspended in 1 ml of freshly prepared fixative solution (methanol : acetic acid= 3:1), and then were transferred to a 1.5 ml microcentrifuge tube. The cells were pelleted at 3,000 g for 2 min and resuspended in 1 ml of fixative solution. This step was repeated for one more time. The cells were counted on a haemocytometer and resuspended in proper volume of fixative solution. The cell suspension was divided into 0.5 ml aliquots and kept at -20 °C. When needed, the cells were spin down and washed once with fresh fixative, and then were suspended in the same volume of fresh fixative. The cells were ready for slides preparation.

2.11.3 Slides preparation for FISH

The coated slides were passed through a hot steam of a 75 °C water bath for 2-3 seconds to moisturize the surface of the slides. The cell suspension (30 μ l) was placed on the slides. When the surfaces of the slides became grainy, the slides were placed cell-side down into the hot steam again for 1-3 seconds, and then were dried on a 70 °C hot plate. The dried slides were kept at the room temperature overnight and incubated at 60 °C for 4 hours the next day. The slides were ready for FISH; alternatively, they were stored in the 100% ethanol or in a slide box at -20 °C.

2.11.4 Hybridization and Wash

The dried slides were rehydrated in 1× PBS for 5 min at room temperature, and then were dipped into 0.005% pepsin solution (0.01 N HCl and 0.005% pepsin) at 37 °C for 10 min. The slides were rinsed briefly in 1× PBS and incubated 5 min each in 70% and 100% ethanol at room temperature, and then were air-dried. One hundred and fifty microliters of solution [70% formamide, 2× Sodium chloride/Sodium citrate buffer (SSC)] was placed on each slide and then the slides were covered with coverslips. The slides were gradually (within 90 seconds) heated to 75 °C and kept at 75 °C for 120 seconds, and then were gradually (90 seconds) cooled to room temperature. The coverslips were removed from the slides and the slides were incubated for 3 min each in 70% and 100% ethanol at room temperature and air-dried. Probes were placed on the slides at the place with cells, and then the slides were covered with coverslips and sealed with parafilm, followed by incubation in a humid chamber to hybrid overnight at 37 °C. The next day, the coverslips were washed off from the slides with plenty of 50% formamide/2× SSC buffer. The slides were washed 3 times in 50% formamide/2× SSC buffer for 5 min each at 37 °C and washed another 3 times in 2× SSC for 5 min each at 37 °C. Ten microliters of 0.1 mg/ml of 4',6-Diamidino-2-phenylindole (DAPI) was placed on each slide to stain nuclei for 4 min, and then was washed off from the slides by 2× SSC at room temperature. At last, the slides were mounted with 14 µl of mounting medium (90% glycerol, 0.1× PBS, 0.1% p-phenylenediamine, pH 9), covered with coverslips and sealed with nail polish. The slides were observed under Zeiss LSM 510 Laser Scanning Confocal Microscope and pictures were taken by LSM 510 Meta software.

2.11.5 Probe label and precipitation

The DNA of mouse BAC RP23-59P20 and CT7-289D17 was extracted and labeled by the Nick Translation Kit (Vysis, Inc.) following the manufacturer's instructions. The RP23-59P20 and CT7-289D17 DNA (1 µg) were labeled with the SpectrumGreenTM (Vysis, Inc.) in the 50 µl of reaction volume, respectively. An aliquot (9 µl) of labeled probe was electrophoresed in a 2% agarose gel to determine the size of labeled probe. The labeled probe (5 µl) was put into a 1.5 ml microcentrifuge tube, together with 5 µg of mouse COT-1 DNA (Invitrogen) and 10 µg of salmon sperm DNA (Invitrogen), and adjusted to final volume to 24 µl with ddH₂O. One-tenth volume of 3 M sodium acetate and 2.5 volume of 100% ethanol were added to the tube, and then the tube was placed at -80 °C for 15 min and centrifuged at 13,000 g for 30 min at 4 °C to pellet the DNA. The DNA pellet was washed twice with 1 ml of 70% ethanol and dried for 2-3 min under a vacuum at ambient temperature, and finally was dissolved in 7 µl of formamide. The probe was denatured for 5 min in a 75 °C water bath and chilled on ice for 1 min, and then was put into 37 °C water bath for 30-60 min for competition. Seven microliters of 2× hybridization buffer [4× SSC, 20% dextran sulfate, 2 mg/ml bovine serum albumin (BSA)] was mixed with the probe before hybridization.

2.12 Vector construction

The vector construction strategy of pCMVH6 is shown in the Figure 2-3. The primers used for the construction are listed in the Table 4 of the appendices.

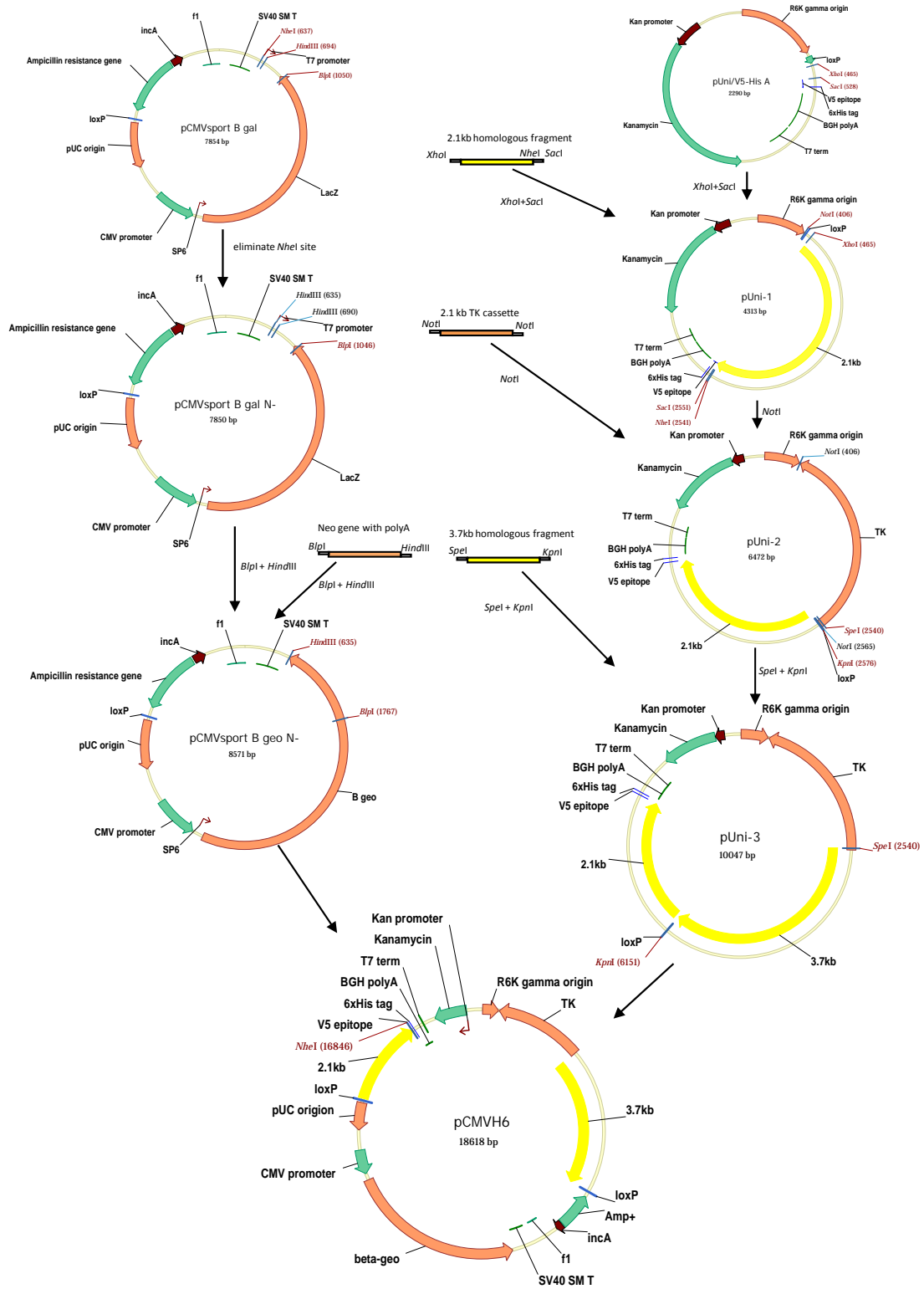


Figure 2-3 Construction strategy of pCMVh6

2.12.1 Bacterial strains, plasmids and enzymes

E. coli strains: all of the following strains are from Invitrogen.

DH5 α : F⁻ ϕ 80*lacZ* Δ M15 Δ (*lacZYA-argF*) U169 *recA1 endA1*
hsdR17(r_k⁻, m_k⁺) *phoA supE44* λ ⁻ *thi-1 gyrA96 relA1*

Pir1: F- Δ *lacI69 rpoS*(Am) *robA1 creC510 hsdR514 endA recA1*
uidA(Δ MluI)::*pir-116*

TOP10: F- *mcrA* Δ (*mrr-hsdRMS-mcrBC*) ϕ 80*lacZ* Δ M15 Δ *lacX74 recA1*
araD139 Δ (*araleu*) 7697 *galU galK rpsL* (StrR) *endA1 nupG*

Plasmids: pUni/v5-HisA (Invitrogen), pCMV-sport- β gal (Invitrogen), pSA β geo (lab collection), pMC1TK-6 (lab collection)

Enzymes: *NheI*, *BlnI*, *HindIII*, *XhoI*, *SacI*, *NotI*, *SpeI*, *KpnI*, T4 DNA ligase, Mung bean nuclease, Antarctic phosphatase and Cyclization recombination recombinase (Cre), were from New England Biolabs.

2.12.2 Protocols

Plasmid mini-, midi- and maxi-preparation were performed using QIAprep Spin Miniprep Kit (Cat. No. 27106), QIAGEN Plasmid Midi Kit (Cat. No.12143) and QIAGEN Plasmid Max Kit (Cat. No. 12163), respectively, following the manufacturer's instructions.

All the restriction enzyme digestion reactions were carried out following the manufacturer's instructions.

Restriction enzyme digested DNA was electrophoresed in agarose gels and then purified by QIAquick Gel Extraction Kit (Cat. No. 28706) or was directly purified by QIAquick PCR Purification Kit (Cat. No. 28106).

To prevent self-ligation of cloning vectors, DNA was dephosphorylated by the Antarctic phosphatase following manufacturer's instruction. The reaction was inactivated at 65 °C for 3 min.

DNA ligation was performed using T4 DNA ligase following the manufacturer's instructions. Reaction mixture was incubated at 16 °C overnight. The molecular ratio of fragments to vector was 3:1.

The standard chemical transformation protocol was used to transform *E. coli*. (Refer to Molecular Cloning: a laboratory manual, Third Edition).

PCR amplification was carried out using Expand Long Template PCR System (Roche).

2.12.3 pCMVH6 construction procedure

Plasmid pCMVSPORTβgal was digested with *NheI* and the linearized DNA was treated with Mung bean nuclease to blunt the sticky ends. The plasmid was transformed into

E. coli DH5 α after self-ligation. The potentially *NheI*-eliminated plasmids extracted from 8 colonies were digested with *NheI* using original pCMVSPORT β gal as a control (Figure 2-4a). Comparing to lane 1 which was *NheI*-digested pCMVSPORT β gal, the *NheI* sites in plasmids No.6 and No.9 (lane 6 and lane 9 in Figure 2-4a) might be eliminated successfully. The plasmids were further confirmed by restriction digestion with *EcoRI* plus *Bam*HI and *NheI*, respectively (Figure 2-4b). The plasmids No.6 and No.9 (lane 2 and lane 3 in Figure 2-4b) had the same restriction pattern as pCMVSPORT β gal (Figure 2-4b, lane 1) *EcoRI* and *Bam*HI digestion. Plasmid pCMVSPORT β gal could be linearized by *NheI* (Figure 2-4b, lane 4), while the plasmids No.6 and No.9 couldn't (Figure 2-4b, lane 5 and lane 6). The region containing *NheI* site in the plasmids No.6 and No. 9 were sequenced. The sequencing results showed that *NheI* site was eliminated and a new *Hind*III site was generated in both No.6 and No. 9 plasmids. The plasmid without the *NheI* site was named pCMVSPORT β galN⁻.

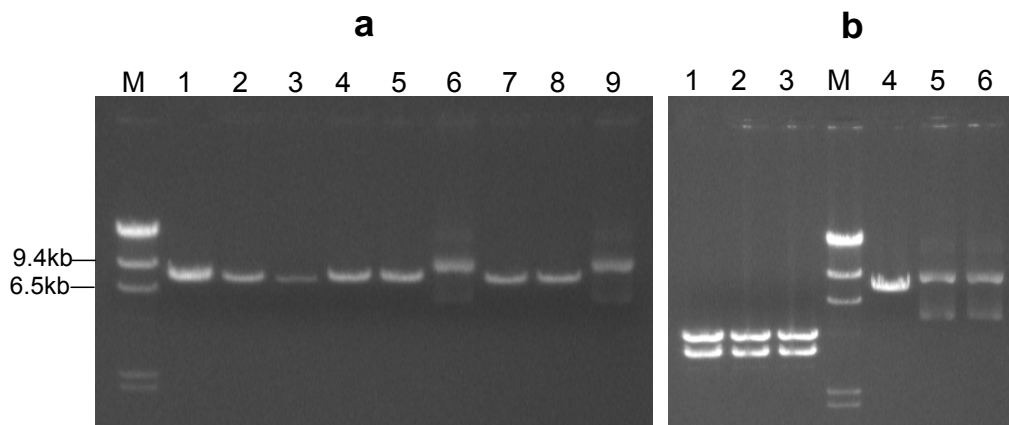


Figure 2-4 Elimination of *NheI* site from pCMVSPORT β gal **a.** Plasmids digested with *NheI*. lane 1: pCMVSPORT β gal/*NheI*, lanes 2-9: potential pCMVSPORT β galN⁻/*NheI*. Plasmids in lane 6 and 9 could be candidate plasmids; **b.** pCMVSPORT β galN⁻ further confirmation, lane 1: pCMVSPORT β gal/*EcoRI*+*Bam*HI, lanes 2,3: No.6 and No.9/ *EcoRI*+*Bam*HI, lane 4: pCMVSPORT β gal/*NheI*, lanes 5,6: No.6 and No. 9/*NheI*. M: λ DNA/*Hind*III

To fuse the neomycin resistant gene with the β -galactosidase gene of pCMVsport β galN⁻, primers (neopAF and neopAR) containing *B*lpI and *H*indIII sites, respectively, were designed to amplify a 1.1-kb neomycin resistant gene fragment from pSA β geo (189) (Figure 2-5a). The PCR products and pCMVsport β galN⁻ were both digested with *B*lpI and *H*indIII. The digested PCR products and the 7.4 kb pCMVsport β galN⁻ fragments were ligated together, fusing neomycin resistant gene in frame with β -galactosidase gene. The expected size of the recombinant plasmid is 8.5 kb. Plasmids extracted from six colonies which were randomly picked up were digested with *B*lpI and *H*indIII. All of the 6 plasmids had 1.1 kb insertion (Figure 2-5b). The sequencing results with primer galA showed that the neomycin resistant gene was fused in framed with the β -galactosidase gene. The new plasmid was named pCMVsport β geoN⁻.

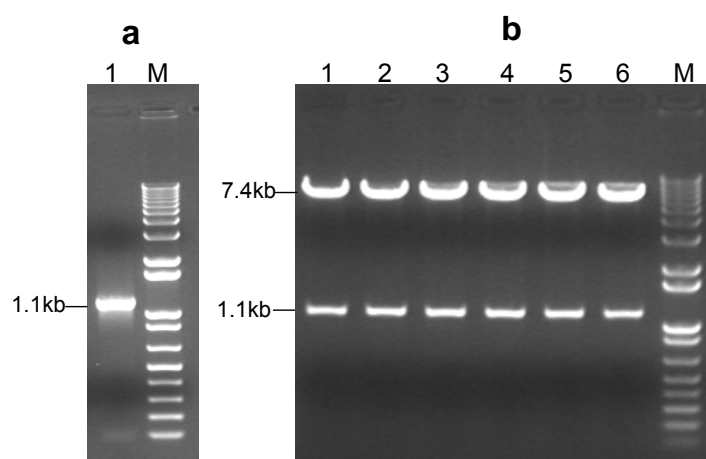


Figure 2-5 Fusion of neomycin phosphotransferase gene with β -galactosidase gene of pCMVsport β galN⁻ a. PCR amplification of 1.1-kb *B*lpI-*H*indIII neomycin resistant gene fragment; b. Confirmation of the putative clones carrying the 1.1-kb insertion by double digestion with *B*lpI and *H*indIII. M: 1 kb ladder.

Primers 2.3f-2 and 2.3R were used to amplify 2.1 kb genomic region from 129/SvEv mouse genomic DNA (Figure 2-6a). The 2.1-kb PCR products and the 2.2-kb plasmid

pUni/V5-HisA were both digested with *Xho*I and *Sac*I, and then ligated to generate the 4.3 kb pUNI-1, which contains R6K γ origin and can only be replicated in Pir1 strain carrying the replication protein π coding gene *pir*. Plasmids extracted from 12 colonies which were randomly picked up were digested with *Not*I which is a single site on the recombinant plasmid (Figure 2-6b). Nine out of twelve plasmids were 4.3 kb as expected, and these nine plasmids released 2.2 kb and 2.1 kb fragments when they were digested with *Xho*I and *Sac*I (Figure 2-6c). Primer 2.3f-2 contains a *Nhe*I site and all of the 9 plasmids could be linearized by *Nhe*I (Figure 2-6d), indicating that the *Nhe*I site was inserted into the new plasmid successfully.

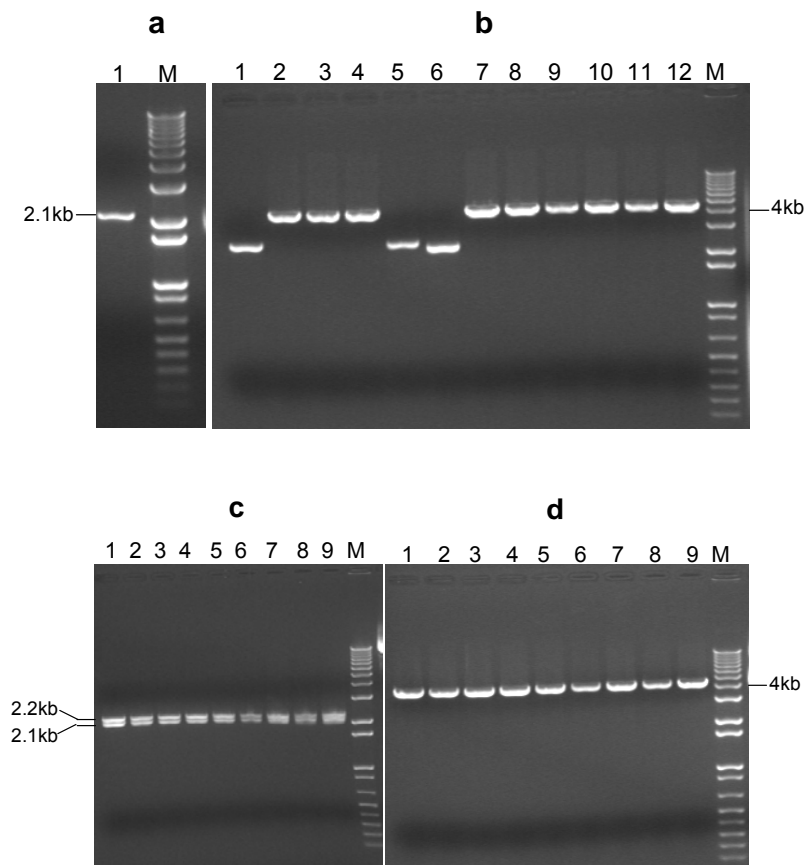


Figure 2-6 Fusion of 2.1 kb genomic region with pUni/V5-HisA **a.** PCR amplification of 2.1 kb 129/SvEv genomic region **b.** Twelve putative recombinant plasmids were digested with *Not*I, and 9 out of 12 plasmids appear to have the expected insertion. **c.** The nine recombinant plasmids were digested with *Xho*I and *Sac*I, all of them could be digested into 2.2 kb and 2.1 kb fragments. **d.** The nine recombinant plasmids could be digested by *Nhe*I, indicating that *Nhe*I site was inserted. M: 1 kb ladder.

Thymidine kinase (TK) expression cassette was released as a 2.1-kb *NotI* DNA fragment from pMC1TK-6 (190) (Figure 2-7a), and inserted into the *NotI* site of pUNI-1, and then transformed into the *E. coli* strain Pir1. Plasmids extracted from 11 colonies were digested with *NotI* and all of them were confirmed to carry both of the 4.3 kb and the 2.1 kb *NotI* fragment (Figure 2-7b). Since the insertion fragments and the acceptor vector were digested by single enzyme, the TK cassette can be inserted into pUNI-1 with either orientation, but only one insertion orientation is desired. The 11 plasmids were digested with the *SpeI* plus *KpnI* to select the plasmids with insertion at the correct orientation (Figure 2-7c). Among 11 plasmids, 9 of them (except lane 2 and lane 3) were confirmed to have correct orientation by sequencing with primer 2.1R. The new plasmid was named pUNI-2.

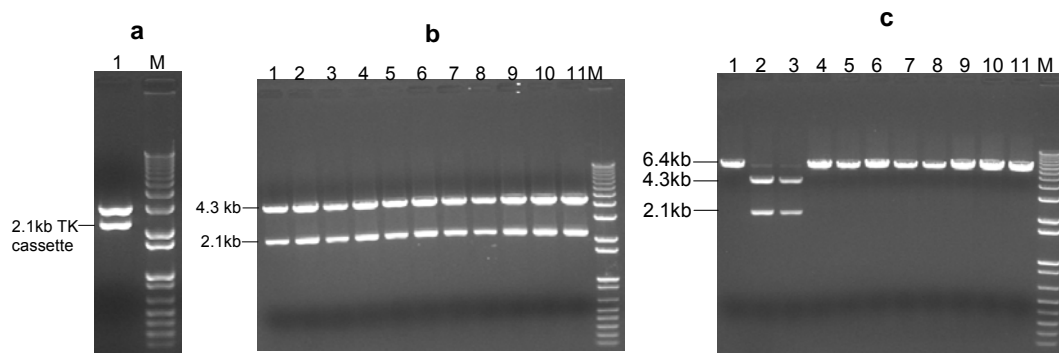


Figure 2-7 Fusion of TK cassette with pUNI-1 **a.** TK containing plasmid pMC1TK-6 was digested with *NotI* to release the 2.1 kb TK cassette. **b.** Recombinant plasmids (11) were digested with *NotI*. All of them are recombinants of TK cassette and pUNI-1. **c.** Recombinant plasmids (11) were digested with *SpeI* plus *KpnI* to confirm the orientation of TK cassettes. All of the plasmids carry the TK cassette in desired orientation except plasmids from lane 2 and lane 3. M: 1 kb ladder.

Primers 3.7F and 3.7R were used to amplify 3.7 kb genomic region from 129/SvEv mouse genome DNA (Figure 2-8a). The PCR products were digested with the *SpeI* and *KpnI* and fused with pUNI-2 which was also digested with the *SpeI* and *KpnI*.

The expected size of the recombinant plasmid is 10.1 kb. The ligation mixture was transformed into the *E. coli* strain Pir1. Plasmids extracted from 10 colonies were digested with the *SpeI* plus *KpnI*, and 2 (Figure 2-8b, lane 5 and 6) out of 10 plasmids showed the expected restriction patterns. The new plasmid was named pUNI-3 and further confirmed by sequencing.

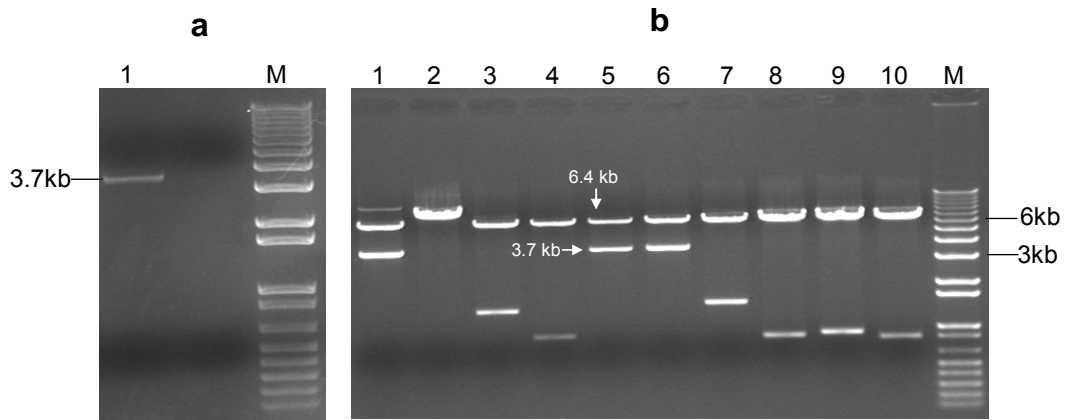


Figure 2-8 Fusion of 3.7 kb genomic fragment with pUNI-2 **a.** PCR amplification of 3.7 kb genomic fragment from 129/SvEv mouse genomic DNA. **b.** Recombinant plasmids (10) were confirmed by restriction digestion with *SpeI* and *KpnI*. Plasmids of lane 5 and 6 had expected restriction patterns. M: 1 kb ladder.

To fuse pCMVsport β geoN⁻ and pUNI-3, we took advantage of the loxP sites presence in both plasmids. The two plasmids can be fused together by *in vitro* Cre-loxP reaction. Plasmid pUNI-3 has R6K γ replication origin and can replicate in the *E. coli* strain Pir1, but can not replicate in the *E. coli* strain TOP10 which don't have *pir* gene. Plasmid pUNI-3 also carries kanamycin resistant gene, so the *E. coli* cells containing pUNI-3 can grow on the LB agar plates containing kanamycin. Plasmid pCMVsport β geoN⁻ has ampicillin resistant gene and can replicate in the *E. coli* strain TOP10. Therefore, pCMVsport β geoN⁻ and pUNI-3 fusion plasmid can be selected by transforming Cre mediated recombinant DNA into the TOP10 competent cells in the presence of kanamycin. Several rounds of selection were performed using the above strategies and finally a fusion plasmid was identified. The fusion plasmid is 18.6 kb

and can be linearized by *NheI* (Figure 2-9a). For further confirmation, the plasmid was digested with *EcoRI* and *HindIII*, respectively. The restriction patterns were as expected (Figure 2-9b). The fusion plasmid was also confirmed by sequencing using primers 3.7Fr and 2.1R. The ultimate targeting vector was named pCMVH6.

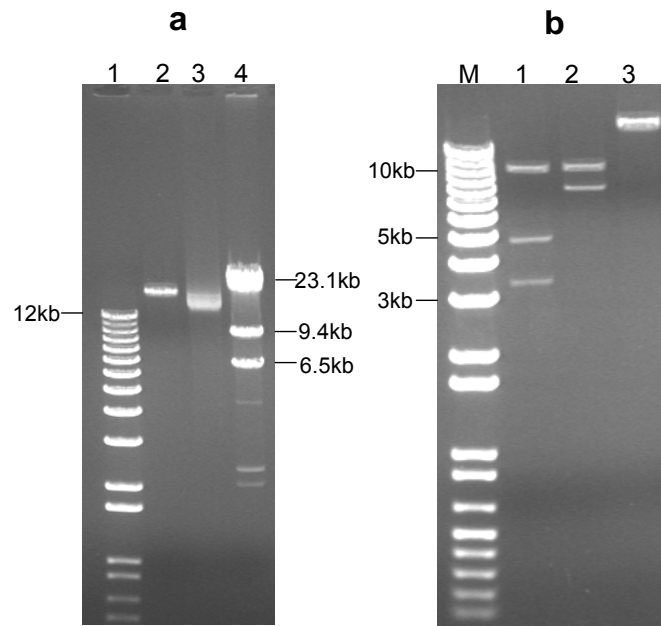


Figure 2-9 Fusion of pCMVsportβgeoN⁻ with pUNI-3 **a.** pCMVH6 was digested with *NheI*, lane 1: 1 kb ladder; lane 2: pCMVH6/*NheI*; lane 3: pCMVH6; lane 4: λ DNA/*HindIII*. **b.** pCMVH6 further confirmation, M: 1 kb ladder; lane 1: pCMVH6/*EcoRI*; lane 2: pCMVH6/*HindIII*; lane 3: pCMVH6/*NheI*.

2.12.4 Mammalian cell transfection

HEK293 (human embryonic kidney, Invitrogen) and COS7 (Africa green monkey kidney, ATCC) cells transfection were performed using Lipofectamine™ 2000 (Invitrogen). The cells (1×10^5 /well) were seeded into 6-well plates 24 hours before transfection. The plasmids (pCMVH6 and pCMVsportβgal, 4 μg for each) and the 10 μl of Lipofectamine™ 2000 were diluted in 250 μl of serum-free medium, respectively. The mixtures were incubated at room temperature for 5 min, and then

the diluted DNA and the diluted Lipofectamine™ 2000 were combined and incubated at room temperature for 20 min before adding into the 6-well plates. The plates were mixed by rocking back and forth. The transfected cells were incubated for 18-48 hours in a 37 °C incubator supplemented with 5% CO₂ before transgene expression was determined.

2.12.5 X-gal staining

The β -galactosidase gene expression was visualized by X-gal staining. The transfected cells were washed twice with PBS and covered with 0.5% glutaraldehyde (Sigma) for 5 min at room temperature, and then were washed twice again with PBS. The cells were then covered with the developing solution (2 mg/ml X-gal, 0.5 mM potassium ferricyanide, 0.5 mM potassium ferrocyanide, 0.2 mM MgCl₂) and incubated at least 1 hour at 37 °C until the cells were visibly stained. The stained cells were visualized with a phase contrast microscope and photographed using Nikon digital camera DXM 1200F with software ACT-1.

2.12.6 Western blot

The transfected cells were lysed in the lysis buffer [0.1% Triton X-100, 25 mM Tris-Cl pH 7.5, 150 mM NaCl, 1 mM DTT, 1 mM EDTA, 1 mM ethylene glycol bis N,N,N',N'-tetraacetic acid (EGTA), 10 mM NaF, 20 mM β -glycerophosphate, 1 mM Na₃VO₄, Roche complete proteases inhibitor cocktail tablet]. The proteins were isolated by centrifugation at 14,500 g for 10 min at 4 °C. The supernatant (20 μ l) was used for the SDS- polyacrylamide gel electrophoresis (SDS-PAGE, 7.5%) and the proteins were transferred onto the polyvinylidene difluoride (PVDF, GE healthcare)

membrane by the semi-dry blotting (Bio-Rad) following the manufacturer's instructions. The PVDF membrane was blocked for 1 hour at room temperature with 2% BSA in TBS-T (Tris-Buffered Saline Tween-20), and incubated for 1 hour with diluted (1:2000) anti- β -galactosidase antibody. Following washed 3 times with TBS-T, the PVDF membrane was incubated for one more hour with the diluted (1:1000) secondary antibody conjugated to horseradish peroxidase (HRP) at room temperature. After washed 3 times with TBS-T, the membrane was stained by the enhanced chemiluminescence (ECL plus, GE healthcare) and exposed to X-ray film (Kodak).

2.13 Electroporation of mouse embryonic stem cells AB2.2

2.13.1 STO cell culture and mitomycin C treatment

Three 10-cm tissue culture plates were gelatinized for 1 hour with 6 ml of 0.1% gelatin at the room temperature. STO (S, SIM; T, 6-thioguanine resistant; O, ouabain resistant) cell vial was brought out from liquid nitrogen and thawed quickly in a 37 °C water bath with gentle shaking. Cell suspension from the vial was put into 10 ml of the STO cell media (ES cell DMEM, 10% fetal calf serum, 1% glutamine and 1% penicillin plus streptomycin) in a 15 ml tube. The tube was spin at 72 g for 5 min and the media was removed. Fresh STO cell media (24 ml) was used to resuspend the STO cells in a 50 ml tube. Gelatin was removed from the 10-cm plates and 8 ml of the STO cells was seeded into each plate. The STO cells were cultured in a 37 °C incubator supplemented with 5% CO₂. At day 2, the STO cells were fed with new STO cell media. At day 4, media was removed from the plates and 6 ml of mitomycin C media (0.01 mg/ml mitomycin C in the STO cell media) was added and the plates were incubated in a 37 °C incubator for 2.5 hours. The mitomycin C media was

removed from the plates and PBS was used to wash the plates for three times, 10 ml of PBS for each time, and then trypsin [0.25% (w/v) trypsin- 0.53 mM EDTA] solution (2 ml) was added into each plate and the plates were incubated at room temperature for 1 min. The STO cell media (5 ml per plate) was added to inactivate the trypsin. The cell suspension from one plate was transferred to a 15 ml tube and collected by spinning at 72 g for 5 min. The cells from three 10-cm plates were combined and resuspended into 6 ml of the STO media. The cells were counted on a haemocytometer and seeded into the pre-gelatinized plates or wells at a density of $5 \times 10^4/\text{cm}^2$ for ES cells culture.

2.13.2 Embryonic stem (ES) cells AB2.2 culture

STO cells were seeded into a pre-gelatinized 6-well plate 2 days before starting ES cells culture. An ES cell vial was brought out from liquid nitrogen and thawed quickly in a 37 °C water bath with gentle shaking. Cell suspension from the vial was put into 10 ml of ES cell media M15 [ES cell DMEM, 15% fetal bovine serum, 1% glutamine, 1% penicillin plus streptomycin, $1 \times$ non-essential amino acid (Invitrogen, cat. No. 111400), 55 mM β -mercaptoethanol] in a 15 ml tube. The tube was spin at 72 g for 5 min and the media was removed. Fresh M15 (3 ml) was added to the tube to resuspend the ES cells. STO cell media was removed from the 6-well plate and 3 ml of the ES cells was seeded into each well. The ES cells were cultured in a 37 °C incubator supplemented with 5% CO₂ and the media was replaced with 3 ml of M15 every day. At day 3, the media of the ES cells was replaced with fresh M15 and removed 2 hours later, and then the ES cells were washed twice with PBS, 3 ml of PBS for each time, followed by adding 400 μ l of trypsin to each well. The plate was incubated at 37 °C for 5 min followed by adding 4 ml of M15 to each well to

inactivate the trypsin. The cells were resuspended up and down for at least 40 times to make single cell suspension. The single cell suspension (1 ml) was added to each 10-cm plate containing mitomycin C treated STO cells and 7 ml of the M15. The media of the ES cells was replaced with 7 ml of M15 every day. At day 3, the media of the ES cells was replaced with fresh M15 and removed 2 hours later, and then the ES cells were washed twice with PBS, 8 ml of PBS for each time, followed by adding 2 ml of trypsin to each plate. The plates were incubated at 37 °C for 5 min followed by adding 6 ml of the M15 to inactivate the trypsin. The ES cells were resuspended up and down for at least 40 times to make single cell suspension. The cells were collected by centrifugation at 72 g for 5 min at 4 °C. The cells were counted on a haemocytometer and seeded into 10-cm STO cell containing plates with a density of 1500 cells per plate.

2.13.3 DNA preparation for electroporation

Plasmid pCMVH6 DNA was digested with restriction enzyme *NheI* at 37 °C overnight. A small aliquot (0.5 µg) was electrophoresed in a 1% agarose gel to determine the digestion. The large-scale digested DNA was extracted once with an equal volume of phenol/chloroform and once with an equal volume of chloroform, and then was precipitated with 2.5 volumes of 100% ethanol. The DNA was resuspended in appropriate volume of sterilized 0.1× TE buffer at a concentration of 1 µg/µl.

2.13.4 Cells preparation for electroporation

ES cells (80% confluency) on the 10-cm plates were passaged 1:2 the day before electroporation. The next day, the media of the ES cells was replaced with fresh M15 and removed 4 hours later, and then the ES cells were washed twice with PBS, 8 ml of PBS for each time, followed by adding 2 ml of trypsin to each plate. The plates were incubated at 37 °C for 5 min followed by adding 10 ml of M15 (cells from two 10 cm plates were combined in a total volume of 10 ml in a 15 ml tube). The cells were pelleted at 72 g for 5 min and resuspended in 10 ml of PBS. Total number of cells was determined by counting on a haemocytometer. The cells were pelleted and resuspended in PBS at a density of 1.1×10^7 cells/ml.

2.13.5 Electroporation

The linearized pCMVH6 DNA and cells were mixed together in a 15 ml tube (25 µg of DNA and 0.9 ml of cells for each electroporation). The cell and DNA mixture was incubated at room temperature for 5 min and aliquoted into the electroporation cuvettes with 0.9 ml per cuvette. The cuvettes were placed in the electroporation holder with the foil electrodes in contact with the metal holding clips. ECM 630 (BTX, a Division of Genetronics, Inc.) was set at 230V, 500 µF for the electroporation. Time constant was between 5.6 and 7.0. The cuvettes were left at room temperature for 5 min. The electroporated ES cells were seeded at a density not more than 2×10^7 cells into 10-cm plates containing STO cells. About 24 hours later, cells were fed with fresh M15 containing 0.2 mg/ml G418 and 0.2 µM FIAU (2'-fluoro-2'-Deoxy-5-Iodo-1-β-D-Arabinofuranosyluracil). From now on, the media of the ES cells was replaced every day with fresh M15 containing G418 and FIAU. At day 10 to 14, colonies were picked.

2.13.6 Picking colonies

STO cells were seeded into the gelatinized 96-well plates 2 days before ES cell colonies were picked. The media of the STO cells was changed to M15 (100 µl/well) at the day of picking colonies. Trypin (25 µl/well) was put into one U-bottom 96-well plate and M15 (75 µl/well) was put into a second U-bottom 96-well plate. The media of the ES cells was replaced with fresh M15 and removed 2 hours later. The ES cells were washed once with 10 ml of PBS. PBS (7 ml) was put into the plates again, and the plates were ready for picking colonies. Colonies were picked from the STO cell monolayer using pipetteman with yellow tips and put into the trypsin in the U-bottom plate by pipetting up and down. Every 25 min, the ES cells in trypsin were put into a 37 °C incubator for 5 min and pipetted up and down for 20 times. The M15 media from the second U-bottom 96-well plate was put into the U-bottom plate with ES cells and pipetted up and down for 40 times, and then the ES cells were transferred to the 96-well plate containing STO cells. This step was repeated till all the colonies were picked. At last, the 96-well plates with the ES cells were put into a 37 °C incubator supplemented with 5% CO₂. The media of the ES cells was replaced every other day with 150 µl of M15 per well.

2.13.7 Freezing down 96-well plates containing ES cell colonies

Appropriate numbers of 96-well plates (2 plates, A and B, for each ES cell plate to be frozen down) were gelatinized at least 1 hour before freezing, and then gelatin was removed from the plates and M15 was put into plate A (75 µl/well) and plate B (100 µl/well). The media of the ES cells were replaced with fresh M15 and removed 2 hours later. The ES cells were washed twice with PBS, 100 µl/well PBS for each

time. Trypsin (50 µl/well) was added to the ES cell plates and then the plates were incubated in a 37 °C incubator for 8 min. Freezing media (50 µl/well of 60% DMEM, 20% fetal calf serum and 20% DMSO) was added into the ES cell plates. Cell clusters were broken up by pipetting up and down for at least 40 times to make single cell suspension. An aliquot (25 µl/well) was transferred to the plate A. The original 96-well plates containing the remaining ES cells were sealed with Alumaseal II Films (Gold Eagle Co.) and put into a -80 °C freezer. The ES cells in the plate A were pipetted up and down, and then was transferred from plate A (50 µl/well) to plate B. M15 (100 µl/well) was added into the plate A to bring to a total volume of 150 µl/well. The plates (A and B) were incubated in a 37 °C incubator with 5% CO₂. The media of the ES cells were changed every other day with M15 (150 µl/well). The ES cells were ready for DNA extraction at confluency.

2.13.8 Selection of positive ES cell colonies by mini-Southern

M15 was removed from the 96-well plates A and B, and the ES cells were washed twice with PBS (100 µl/well for each time). Lysis buffer (10 mM Tris-Cl pH 7.5, 10 mM EDTA pH8.0, 10 mM NaCl, 0.5% Sarcosyl and 1 mg/ml proteinase K) was added to the plates with 50 µl/well. The plates were incubated overnight at 60 °C in a humid chamber. The next day, 75 mM NaCl in ethanol (100 µl/well) was added to the plates and the plates were incubated at room temperature for 20 min. The plates were inverted to discard the NaCl solution and 70% ethanol was added to the plates (100 µl/well) to wash the plates for three times, and then the plates were air-dried for a few minutes at room temperature. *Bam*HI restriction enzyme mixture (1× *Bam*HI buffer, 1 mM spermidine, 100 µg/ml BSA and 25 units of enzyme) was added to the

plates (40 µl/well) and mixed by pipetting up and down, and then the plates were sealed before incubation in a 37 °C humid chamber overnight. For Southern blot analysis, digested DNA was electrophoresed in 1% agarose gels at 25 V overnight, and then transferred to a Hybond N+ membrane (Amersham). The probe (240 bp) for selection of positive ES colonies was prepared by PCR with primers SHF and SHR using 129/SvEv genomic DNA as template (Table 1 of appendices). The PCR products were purified by the QIAquick Gel Extraction Kit (QIAGEN) following manufacturer's instructions. The probe was labeled with [α -³²P] dCTP by Klenow enzyme (New England Biolabs) using random hexamer as primers. The labeling and detection protocols were followed the standard methods (191). Membranes were exposed to Kodak X-ray films.

2.13.9 Selection of positive ES cell colonies by PCR

M15 ES cell media was removed from the 96-well plates A and B, and the ES cells were washed twice with PBS (100 µl/well for each time). Lysis buffer (10 mM Tris-Cl pH 7.5, 10 mM EDTA pH8.0, 10 mM NaCl, 0.5% Sarcosyl and 1 mg/ml freshly added proteinase K) was added to plates (60 µl/well) and the plates were incubated overnight at 60 °C in a humid chamber. The next day, cell lysate (10 µl/well) was removed to a new 96-well plate. DNA was precipitated by adding 75 mM NaCl in ethanol (20 µl/well) to the plates and the plates were incubated at room temperature for 20 min. The plates were inverted to discard the NaCl solution and 70% ethanol (50 µl/well) was added to wash the plates for three times, and then the plates were air-dried for a few minutes at room temperature. TE buffer (0.1× TE buffer) was added to the plates (50 µl/well) to dissolve DNA. One microliter of DNA was used for PCR

with primers galA and galB. The DNA samples which had PCR products of galA and galB was subjected to PCR with primers AHF1 and AHR1, and then the DNA samples which had PCR products of AHF1 and AHR1 was subjected to PCR with primers AHF2 and AHR2. Finally, DNA samples which had PCR products of AHF2 and AHR2 was subjected to PCR with primers AHF2 and BXR4. The PCR conditions for primer sets galA and galB, AHF1 and AHR1, AHF2 and AHR2 were: 5 min at 95 °C, then 35 cycles of 30 seconds at 95 °C, 30 seconds at 55 °C and 30 seconds at 72 °C, followed by 7 min at 72 °C. The PCR conditions for primer sets AHF2 and BXR4 were: 5 min at 95 °C, then 35 cycles of 30 seconds at 95 °C, 30 seconds at 55 °C and 3 minutes at 72 °C, followed by 10 min at 72 °C. All of the PCR products were electrophoresed in 2% agarose gels. The sequences of primers are available in the Table 4 of the appendices.

2.13.10 Expanding ES colonies out of freeze from 96-well plate

M15 (2 ml/well) was added to a 24-well plate containing STO cells. The 96-well plate containing ES cells was brought out from -80 °C freezer and warmed in a 37 °C incubator for 20 min. The entire contents from the wells containing putative targeted colonies were transferred to the 24-well plate. The media of the 24-well plate was replaced every day with 1 ml/well of M15. At day 3, the media was changed to fresh M15 and removed 2 hour later. The ES cells were washed twice with PBS (1 ml/well), and trypsinized (200 µl/well) at 37 °C for 5 min, followed by adding M15 (2 ml/well) to inactivate the trypsin. The cell suspension was pipetted up and down for at least 40 times, and then transferred to a new 24-well plate (1 ml/well) containing STO cells. The media of the new 24-well plate was replaced every day with 1 ml/well of M15. At day 3, the media was changed to fresh M15 and removed 2 hours later.

The ES cells were washed twice with PBS (1 ml/well) and trypsinized (200 µl/well) at 37 °C for 5 min. The trypsinized cells were mixed with M15 (4 ml/well) in a 15 ml tube by pipetting up and down for at least 40 times. The cell suspension of one colony was seeded into 2 wells (2 ml/well) on a 6-well plate containing STO cells. The media of the 6-well plate was replaced every day with 3 ml/well of M15. At day 3, the media was changed to fresh M15 and removed 2 hours later. The ES cells were washed twice with PBS (3 ml/well) and trypsinized (500 µl/well) at 37 °C for 5 min. The cells from one colony were mixed with ES cell media (4 ml/colony) in a 15 ml tube by pipetting up and down for at least 40 times. The cell suspension (400 µl/well) was seeded into a new 6-well plate containing M15 (2 ml/well). The rest of cell suspension was pelleted at 72 g for 5 min and resuspended in 1 ml of M15. Freezing media (1 ml of 60% DMEM, 20% FCS and 20% DMSO) was added to the cells and mixed by pipetting up and down. The cell suspension was aliquoted to cryogenic vials with 1 ml per vial. The vials were put into a -80°C freezer for one day and transferred to liquid nitrogen the next day. The media of the new 6-well plate was replaced with 3 ml/well of M15 every other day. The ES cells were lysed and DNA was extracted when the cells were confluent.

2.14 Confirmation of PWS/AS deletion by microsatellite analysis

The DNA samples of PWS patients and their parents were generously provided by Dr. Shuan-pei Lin. For each DNA samples, 16 sets of primers were used to amplify 16 microsatellite markers covering the 4 Mb PWS/AS breakpoints region. The sequences of primers are available in the Table 5 of the appendices. All the forward primers were labeled with fluorescence tags. PCR master mix without primers was prepared

and aliquoted into 16 PCR tubes. The primers were added to each tube, respectively. PCR reactions were divided into 4 groups according to the annealing temperatures of their primers, respectively. The annealing temperature of group 1 (D15S165, D15S1019, D15S1010, D15S115) is 52 °C, group 2 (D15S1048) is 53.7 °C, group 3 (D15S1031, D15S126, D15S541, D15S543, D15S11, D15S1002, D15S1043 and D15S113) is 55.1 °C, group 4 (D15S542, D15S984) is 60 °C. The 16 PCR reactions were performed on a gradient PCR machine. PCR reaction conditions were: 5 min at 95 °C, then 35 cycles of 30 seconds at 95 °C, 30 seconds at 52 °C, 53.7 °C, 55.1 °C or 60 °C and 30 seconds at 72 °C, followed by 7 min at 72 °C. The original PCR products were diluted 15 times and 0.3 µl of diluted PCR products were used for capillary electrophoresis. PCR products were mixed with 0.5 µl of GeneScan™-500LIZ™ size standard (Applied Biosystems) and 9.5 µl of Hi-Di™ formamide (Applied Biosystems). The mixture was heated at 95 °C for 3 min to denature DNA and then was fractionized by capillary electrophoresis on a 310 genetic analyzer. POP4™ (Applied Biosystems) and capillary (47 cm × 50 µm, Applied Biosystems) were used. The signals were collected by 310 data collection software and analyzed by GeneMapper 4.0.

Chapter III Results

3.1 Incomplete penetrance reflecting epigenetic instability of AS-IC^{an} mutation in 129/SvEv background

In human beings and mice, the DMR of *Snurf-Snrpn* is heavily methylated on the maternally inherited allele and unmethylated on the paternally inherited allele (192). However, in the case of human and mice with AS imprinting defect, the DMR of the maternally inherited allele becomes unmethylated. The mice with AS-IC^{an} mutation used in our experiment were generated by inserting a targeting vector (pG12H6) at 13 kb upstream from *Snurf-Snrpn* exon 1 on mouse chromosome 7. The vector integrates a *puromycin* cassette in the reverse orientation to the *Snurf-Snrpn* transcript and generates a 6-kb genomic DNA duplication. Genotyping of mice with AS-IC^{an} mutation was carried out by PCR and Southern blot. The locations of primers and the probe are indicated in Figure 3-1a.

BXF4 and T7 amplify a 294 bp fragment from the AS-IC^{an} targeted allele, and BXF4 and BXR4 amplify a 533 bp fragment from both the targeted and the wild type alleles. PCR genotyping using DNA derived from AS-IC^{+/an} and AS-IC^{an/an} mice generate both 294-bp and 533-bp products, whereas PCR genotyping using DNA derived from wild type mice only generate the 533-bp product. Two litters (15 mice) from two 129/SvEv AS-IC^{an/an} females which were mated with a 129/SvEv wild type male were genotyped by PCR. Since these mice were offspring from homozygous females and the wild type male, all of the pups were heterozygous for the AS-IC^{an} allele (Figure 3-1b). Southern blot was used to further confirm the genotype of these mice and their parents. The wild type allele is detected as an 8.5-kb hybridization band, and the

targeted allele is detected as an 11.1-kb hybridization band (Figure 3-1a). Southern blot results showed that all the 15 pups were heterozygous for the AS-IC^{an} allele, consistent with the PCR findings.

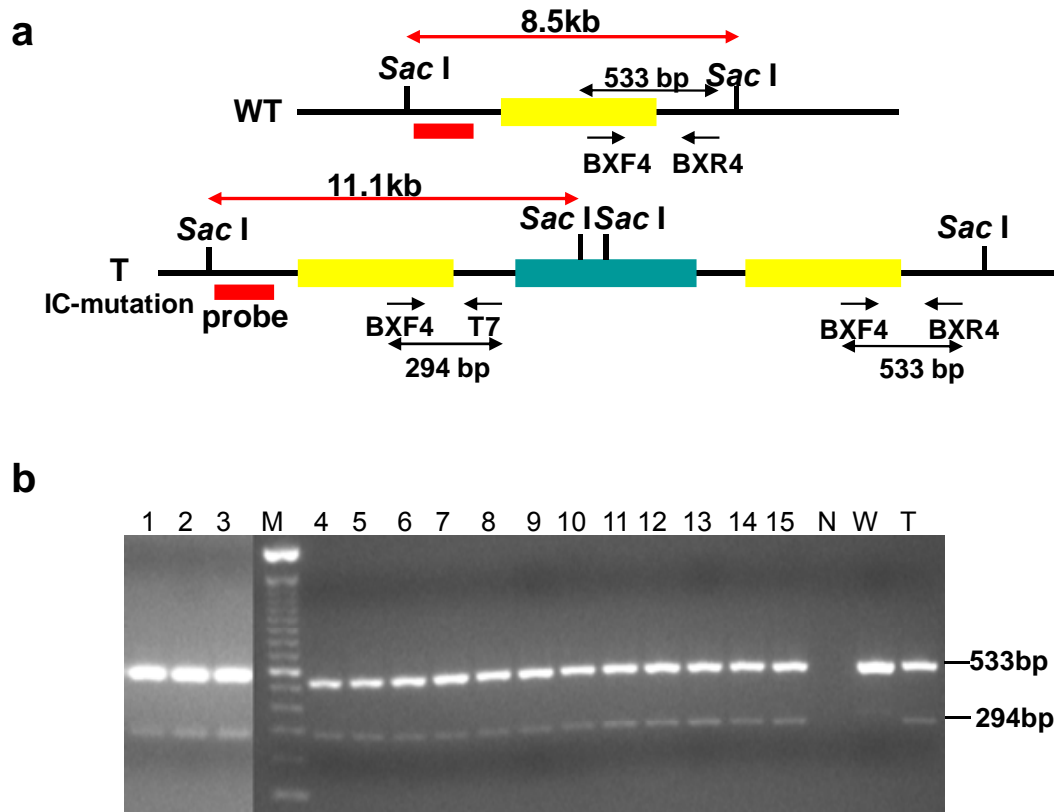


Figure 3-1 Genotyping mice with AS-IC^{an} mutation **a.** Schematic presentation of primers and probe used for genotyping of mice with AS-IC^{an} mutation by PCR and Southern blot. BXF4, BXR4 and T7 are primers used for PCR (Table 1 of appendices). Primers orientation and locations are indicated by arrows. The probe for Southern blot is indicated as a red rectangle. An 8.5-kb *SacI* fragment from the wild type allele (WT) and an 11.1-kb *SacI* fragment from the targeted allele (T) are detected by the probe. **b.** Fifteen mice numbered 1 through 15 were genotyped by PCR using primers BXF4, BXR4 and T7. PCR products were electrophoresed in a 2% agarose gel. PCR products from all the samples had two bands which were 533 bp and 294 bp. M: 100 bp DNA ladder; N: no template control; W: wild type control; T: heterozygote control.

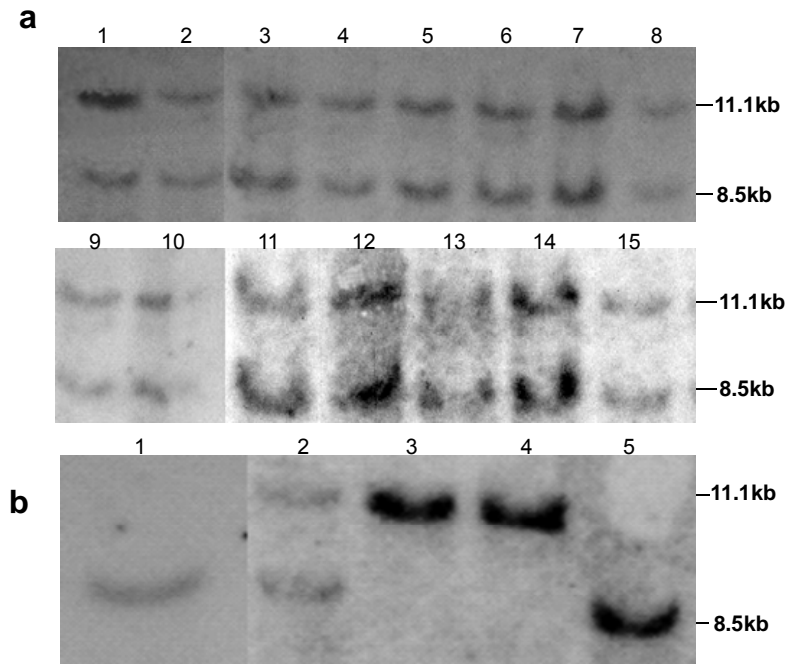


Figure 3-2 Genotyping mice with AS-IC^{an} mutation by Southern blot **a.** Fifteen mice were genotyped by Southern blot. Genomic DNA extracted from 15 mice was digested with *SacI* and analyzed by Southern blot. The location of the probe and the sizes of hybridization bands were indicated in Figure 3-1a. All the samples have both the 8.5-kb wild type and the 11.1-kb targeted alleles. **b.** The parents of the 15 mice were genotyped by Southern blot. Lane 1: the father; lane 2: AS-IC^{+/an} control; lanes 3 and 4: the two mothers; lane 5: wild type control.

To test whether these two AS-IC^{an/an} mice have AS imprinting defect, methylation patterns of *Snurf-Snrpn* DMR of these mice were examined by Southern blot using *HindIII* and a methylation sensitive restriction enzyme *SacII*. The methylated allele is detected as a 14-kb hybridization band, and the unmethylated allele is detected as an 11-kb hybridization band (Figure 3-3a). Southern blot results showed that these two mice had both 14-kb and 11-kb hybridization bands, suggesting that both of them have normal methylation patterns at *Snurf-Snrpn* DMR (Figure 3-3b). Among 26 F1 AS-IC^{m^{an}/p⁺} mice generated by crossing the 129/SvEv AS-IC^{an/an} female to 129/SvEv wild type male, 7 of them showed loss of methylation in their maternal allele of *Snurf-Snrpn* DMR (Figure 3-4, No. 3, 8, 13, 14, 17, 20, 25), and seizures could be induced among these mice by loud noise. These results are consistent with the expected

methylation pattern and phenotype of AS imprinting defect patients. These AS-IC m^{an}/p^{+} imprinting defect mice were smaller than their littermates and 5 of them died within three weeks after birth. AS-IC m^{an}/p^{+} imprinting defect male mice were fertile but female mice were sterile, whereas AS-IC m^{an}/p^{+} mice with normal methylation pattern at *Snurf-Snrpn* DMR were fertile regardless of gender. When the AS-IC m^{an}/p^{+} females with normal methylation pattern at *Snurf-Snrpn* DMR were crossed to wild type males, incomplete penetrance was also observed. Among 78 heterozygous offspring carrying the AS-IC^{an} mutation from maternal origin, 29 had both alleles of *Snurf-Snrpn* DMR unmethylated.

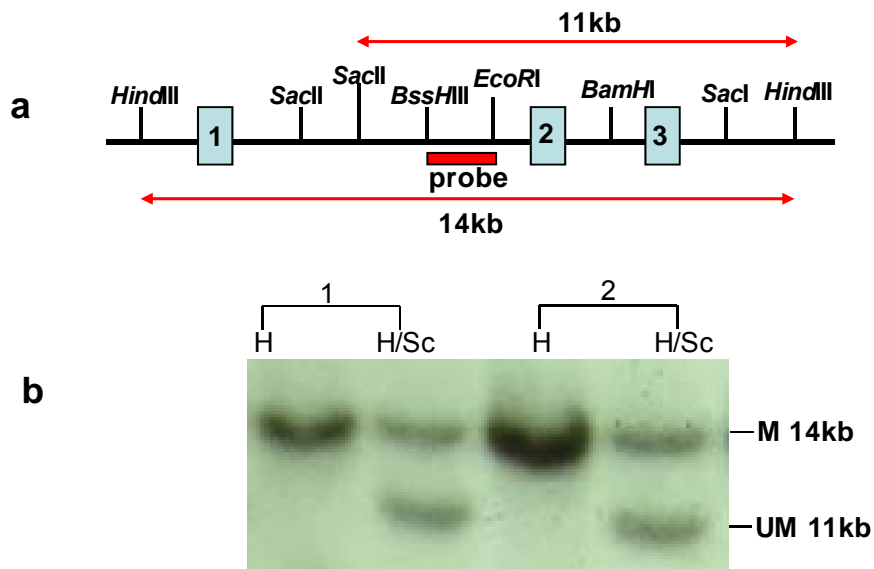


Figure 3-3 Methylation analysis of the two AS-IC^{an/an} mice **a.** Genomic DNA was digested with *HindIII* (H) alone, *HindIII* plus methylation sensitive enzyme *SacII* (H/Sc), and analyzed by Southern blot. The probe for Southern blot is indicated as a red rectangle. A methylated (M) fragment of 14 kb and an unmethylated (UM) fragment of 11 kb were detected by the probe. **b.** Both of the AS-IC^{an/an} mice (1 and 2) had normal methylation pattern with one allele methylated and one allele unmethylated at the *Snurf-Snrpn* DMR.

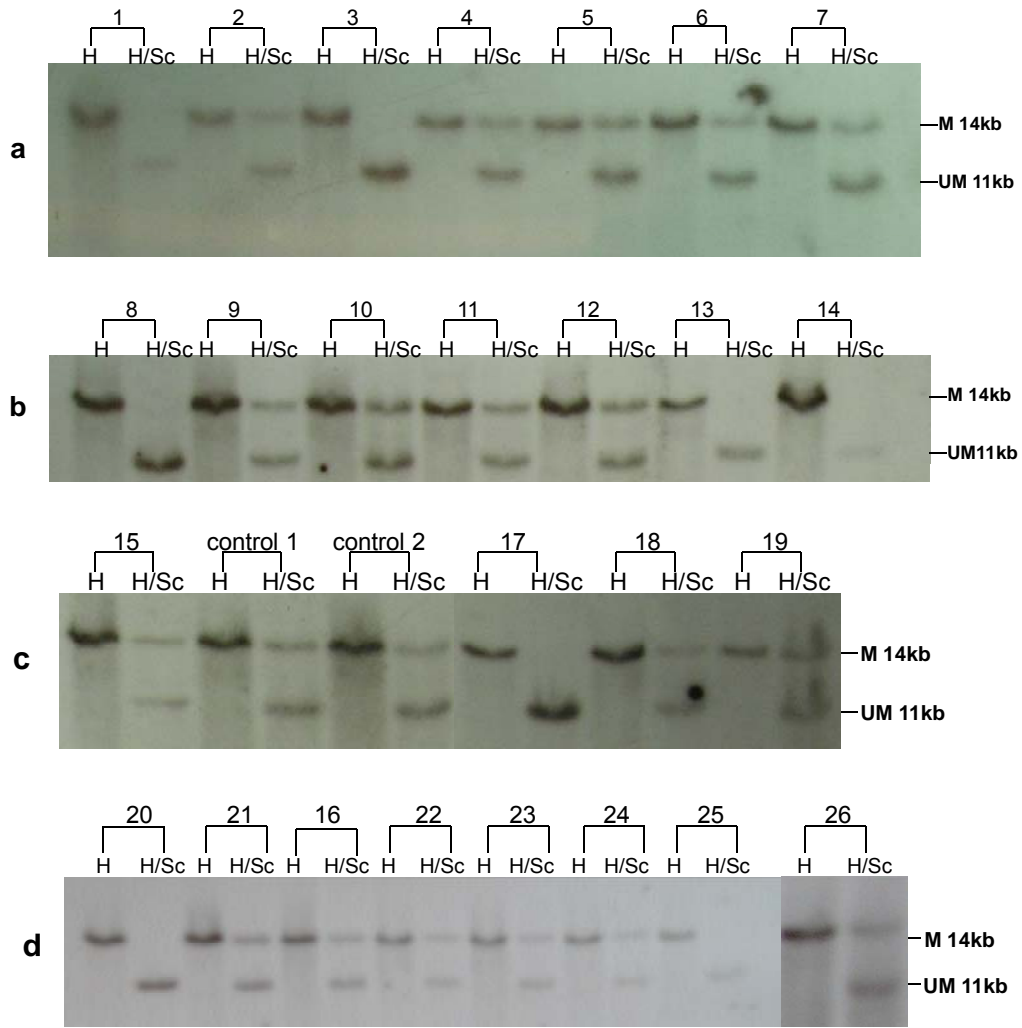


Figure 3-4 Methylation analysis of F1 AS-IC m^{an}/p^{+} mice generated from cross between AS-IC^{an/an} female and male Genomic DNA extracted from 26 mice generated from 129/SvEv AS-IC^{an/an} female and 129/SvEv male matings was digested with *Hind*III (H) alone, or *Hind*III plus methylation sensitive enzyme *Sac*II (H/Sc); and analyzed by Southern blot (films a-d). The probe is indicated in Figure 3-3a. Control 1 and control 2 from film c are mice carrying AS-IC^{an} mutation from paternal origin. M, methylated allele (14 kb); UM, unmethylated allele (11 kb).

To introduce polymorphism into mouse line to facilitate later experiments in section 3.2, PWK/PhJ wild type male was crossed to 129/SvEv AS-IC^{+/an} female. Similar to the matings in 129/SvEv background, incomplete penetrance was observed among F1 AS-IC m^{an}/p^{+} mice. Loss of methylation from the maternal allele of *Snurf-Snrpn* DMR was found in 12 (57%) out of the 21 F1 AS-IC m^{an}/p^{+} mice (Figure 3-5 shows one litter). These 12 AS-IC m^{an}/p^{+} imprinting defect mice became obese at three

months of age (Figure 3-6). Body weights of these mice were nearly twice as much as that of their wild type or AS-IC m^{an}/p^{+} littermates with normal methylation pattern; furthermore, these AS-IC m^{an}/p^{+} imprinting defect mice were sterile regardless of gender. The AS-IC m^{an}/p^{+} mice with normal methylation pattern had normal body weight as compared to their wild type littermates. One of the (129/SvEv AS-IC^{+/an} female \times PWK/PhJ male) F1 AS-IC m^{an}/p^{+} female with normal methylation patterns was crossed to a PWK/PhJ male (Figure 3-7a). Two litters, with a total of 11 mice, were generated. Among them, 6 (55%) were AS-IC m^{an}/p^{+} ; and 3 (50%) out of these 6 mice had AS imprinting defect, indicating that incomplete penetrance exists among F2 AS-IC m^{an}/p^{+} mice. When a (PWK/PhJ female \times 129/SvEv AS-IC^{+/an} male) F1 AS-IC m^{+}/p^{an} female was crossed to a PWK/PhJ male (Figure 3-7b), seven litters, with a total of 39 mice, were generated from this mating. Among them, 19 were AS-IC m^{an}/p^{+} mice. Surprisingly, all of the 19 (49%) AS-IC m^{an}/p^{+} mice had both alleles unmethylated at the DMR of *Snurf-Snrpn*, indicating complete penetrance among F2 AS-IC m^{an}/p^{+} mice.

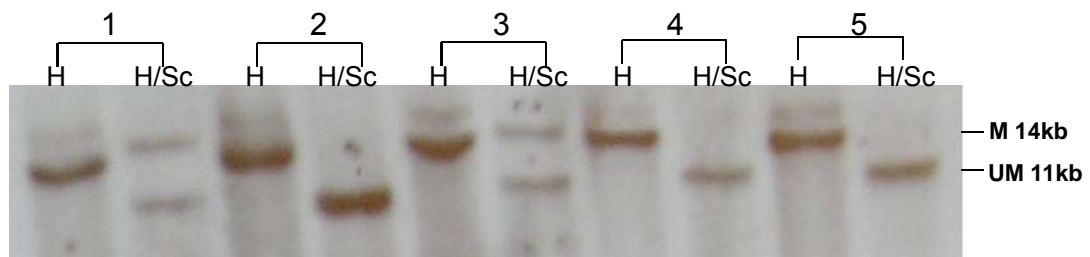


Figure 3-5 Methylation analysis of F1 mice derived from crosses between 129/SvEv AS-IC^{+/an} female and PWK/PhJ male Genomic DNA extracted from F1 mice generated from a cross between 129/SvEv AS-IC^{+/an} female and PWK/PhJ male was digested with *Hind*III (H) alone, or *Hind*III plus methylation sensitive enzyme *Sac*II (Sc); and then analyzed by Southern blot. The probe for methylation analysis is indicated in Figure 3-3a. Among 21 F1 AS-IC m^{an}/p^{+} mice, 12 of them had biallelic unmethylation at the *Snurf-Snrpn* DMR. Mice 1,2,4,5 are AS-IC m^{an}/p^{+} mice; mouse 3 is a wild type control. M, methylated allele (14 kb); UM, unmethylated allele (11 kb).

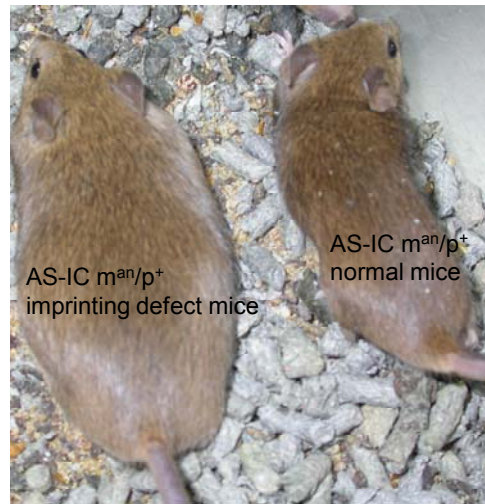


Figure 3-6 Typical example of AS-IC m^{an}/p^{+} mice with imprinting defect became obese A (129/SvEv AS-IC $^{+/an}$ female \times PWK/PhJ male) F1 AS-IC m^{an}/p^{+} mouse with imprinting defect is compared with a (129/SvEv AS-IC $^{+/an}$ female \times PWK/PhJ male) F1 AS-IC m^{an}/p^{+} mouse with normal methylation pattern at three months of age.

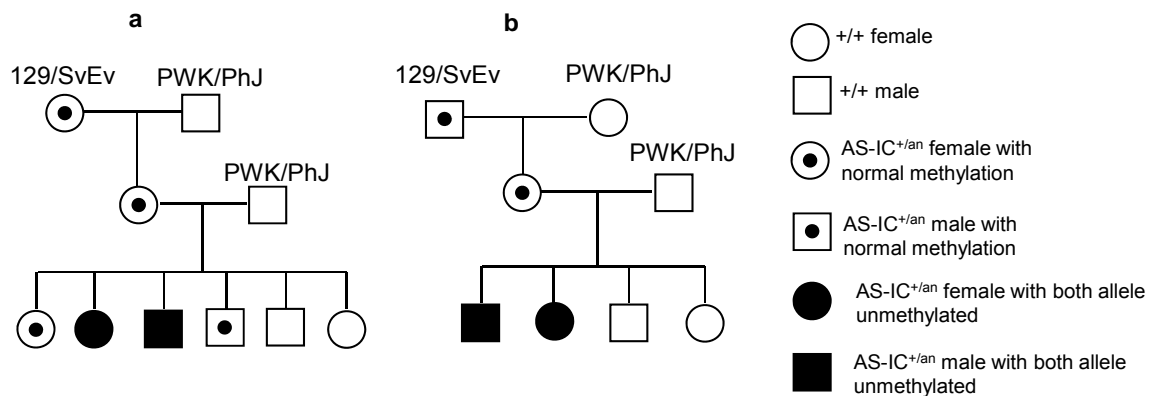


Figure 3-7 Examples of pedigree of 129/SvEv AS-IC $^{+/an}$ mice mating with PWK/PhJ mice **a.** A 129/SvEv AS-IC $^{+/an}$ female was mated with a PWK/PhJ male and the AS-IC m^{an}/p^{+} female offspring with normal methylation was crossed to a PWK/PhJ male. Incomplete penetrance was still observed among F2 AS-IC m^{an}/p^{+} mice. **b.** A 129/SvEv AS-IC $^{+/an}$ male was mated with a PWK/PhJ female. The AS-IC m^{+}/p^{an} female offspring was crossed to a PWK/PhJ male. Complete penetrance was observed among F2 AS-IC m^{an}/p^{+} mice.

Unlike AS-IC m^{an}/p^{+} mice in 129/SvEv background and in 129/PWK hybrid background, the AS-IC m^{an}/p^{+} mice in C57BL/6J background showed complete

penetrance (181). It appears that the effect of the targeting vector to the AS imprinting process is differentially regulated in different genetic background, resulting in variation in penetrance which is correlated with DNA methylation. To find out whether the incomplete penetrance is related with mice genetic background, a 129/SvEv AS-IC^{+an} female was mated with a C57BL/6J male and the AS-IC^{+an} female offspring with normal methylation was back-crossed to the C57BL/6J male for 5 generations. Incomplete penetrance was still observed even in the fifth generation. It is likely that 129/SvEv strain-specific modifiers suppress the effect of the targeting vector by an unknown mechanism. Biallelic unmethylation of *Snurf-Snrpn* DMR was found in all the tissues examined from AS-IC m^{an}/p⁺ imprinting defect mice (Figure 3-8), indicating that the effect of the targeting vector to AS imprinting process may occur before the germ cell lineage is established (193). Thus, the 129/SvEv strain-specific modifiers may also function at that time since the normal methylation pattern of *Snurf-Snrpn* DMR was observed in all the tissues assayed from AS-IC m^{an}/p⁺ mice without imprinting defect.

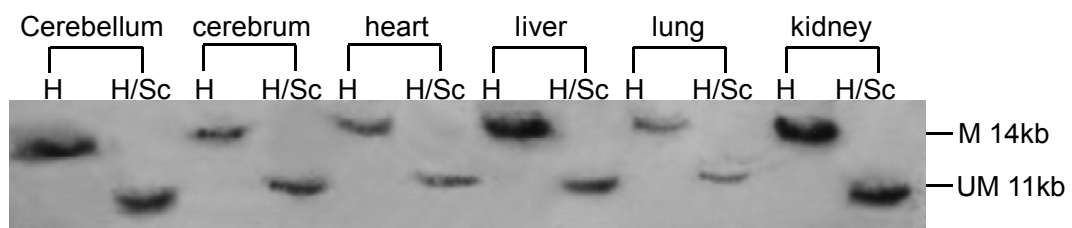


Figure 3-8 Methylation analysis in various tissues derived from AS-IC m^{an}/p⁺ imprinting defect mice Genomic DNA extracted from cerebellum, cerebrum, heart, liver, lung and kidney of AS-IC m^{an}/p⁺ imprinting defect mice was digested with *Hind*III (H) alone, or *Hind*III plus *Sac*II (Sc); and analyzed by Southern blot. The probe for methylation analysis is indicated in Figure 3-3a. Biallelic unmethylation was detected in all the tissues tested. M, methylated allele (14 kb); UM, unmethylated allele (11 kb).

3.2 Nucleotide polymorphisms between 129/SvEv and PWK/PhJ mice in the PWS-IC region

Allele-specific modification of DNA and chromatin can regulate imprinted gene expression. For example, differentially methylated histone H3K9 and K4 have been reported to be associated with the PWS-IC (104, 166, 194). Moreover, paternal and maternal alleles of imprinted genes have been shown to have differential chromatin conformation. In order to study histone H3K9 and H3K4 methylation status in the PWS-IC, 129/SvEv mice were crossed to PWK/PhJ mice to introduce polymorphisms into the F1 hybrids. To identify polymorphisms between the parental DNA, four sets of primers were used to amplify a 1534-bp fragment in PWS-IC region from 129/SvEv, PWK/PhJ and 129/PWK F1 hybrid mice. Through sequencing, seventeen nucleotide polymorphisms were identified between 129/SvEv and PWK/PhJ in the 1534-bp genomic region (Figure 3-9).

		1	50
129	(1)	AATCTGTGTGATGCTTGCAATCACTTGGGAGCAATTTTTTTAAAAAATTA	
pwk	(1)	AATCTGTGTGATGCTTGCAATCACTTGGGACAATTTTTTTAAAAAATTA	
Consensus	(1)	AATCTGTGTGATGCTTGCAATCACTTGGGACAATTTTTTTAAAAAATTA	
		51	100
129	(51)	AATGTATTTAGTAATAGGCAATTATATCCATTATTCCAGATTGACAGTGA	
pwk	(51)	AATGTATTTAGTAATAGGCAATTATATCCATTATTCCAGACTGACAGTGA	
Consensus	(51)	AATGTATTTAGTAATAGGCAATTATATCCATTATTCCAGATGACAGTGA	
		101	150
129	(101)	TTTTTTTTTTTAAATACACGCTCAAATTTCCGCACTAGGAATGCTCAAGC	
pwk	(101)	TTTTTTTTTTTA--AATACACGCTCAAATTTCCGTAGTAGGAATGTTCAAGC	
Consensus	(101)	TTTTTTTTTTTAAATACACGCTCAAATTTCCGCACTAGGAATGTCAAGC	
		151	200
129	(151)	ATTCCTTTTGGTAGCTGCCTTTTGGCAGGACATTCCGGTCAAGAGGGACAG	
pwk	(149)	ATTCCTTTTGGTAGCTGCCTTTTGGCAGGACATTCCGGTCAAGAGGGACAT	
Consensus	(151)	ATTCCTTTTGGTAGCTGCCTTTTGGCAGGACATTCCGGTCAAGGGACA	
		201	250

129	(201)	AGACCCCTGCATTGCGGCAAAAATGTGCGCATGTGCAGCCATTGCCTGGG
pwk	(199)	AGACCCCTGCATTGCGGCAAAAATGTGCGCATGTGCAGCCATTGCCTGGG
Consensus	(201)	AGACCCCTGCATTGCGGCAAAAATGTGCGCATGTGCAGCCATTGCCTGGG
		251 300
129	(251)	ACGCATGCGTAGGGAGCCGCGCGACAAACCTGAGCCATTGCGGCAAGACT
pwk	(249)	ACGCATGCGTAGGGAGCCGCGCGACAAACCTGAGCCATTGCGGCAAGACT
Consensus	(251)	ACGCATGCGTAGGGAGCCGCGCGACAAACCTGAGCCATTGCGGCAAGACT
		301 350
129	(301)	AGCGCAGAGAGGAGAGGGAGCCGGAGATGCCAGACGCTTGGTTCTGAGGA
pwk	(299)	AGCGCAGAGAGGAGAGGGAGCCGGAGATGCCAGACGCTTGGTTCTGAGGA
Consensus	(301)	AGCGCAGAGAGGAGAGGGAGCCGGAGATGCCAGACGCTTGGTTCTGAGGA
		351 400
129	(351)	GTGATTTGCAACGCAATGGAGCGAGGAAGGTCAGCTGGGCTTGTGGATTTC
pwk	(349)	GTGATTTGCAACGCAATGGAGCGAGGAAGGTCAGCTGGGCTTGTGGATTTC
Consensus	(351)	GTGATTTGCAACGCAATGGAGCGAGGAAGGTCAGCTGGGCTTGTGGATTTC
		401 450
129	(401)	TAGTAGTGAAAGTGCATCCTATTTGACCAAAACATTCTAGATTTGGGCTT
pwk	(399)	TAGTAGTGAAAGTGCATCCTATTTGACCAAAACATTCTAGATTTGGGCTT
Consensus	(401)	TAGTAGTGAAAGTGCATCCTATTTGACCAAAACATTCTAGATTTGGGCTT
		451 500
129	(451)	ATTAAGATTTTTGACAACCCAGATACCTTTATTTTTGAGAATTGGTGAGC
pwk	(449)	ATTAAGATTTTTGACAACCCAGATACCTTTATTTTTGAGAATTGGTGAGC
Consensus	(451)	ATTAAGATTTTTGACAACCCAGATACCTTTATTTTTGAGAATTGGTGAGC
		501 550
129	(501)	AATCCTTTGGAGCCGGCAGACGGACTCCTTGGGTGTGTTAGTGCGGCACC
pwk	(499)	AATCCTTTGGAGCCGGCAGACGGACTCCTTGGGTGTGTTAGTGCGGCACC
Consensus	(501)	AATCCTTTGGAGCCGGCAGACGGACTCCTTGGGTGTGTTAGTGCGGCACC
		551 600
129	(551)	TGCGTGTAACGCGTTGCCTTTATTATGGTGGTCTGAGGTTGTGACTGGGA
pwk	(549)	TGCGTGTAACGCGTTGCCTTTATTATGGTGGTCTGAGGTTGTGACTGGGA
Consensus	(551)	TGCGTGTAACGCGTTGCCTTTATTATGGTGGTCTGAGGTTGTGACTGGGA
		601 650
129	(601)	TCCTGGATGCAGGAGCTGTGTTGCCGCAGCGTGGGGGCTCCAGGATGCGG
pwk	(599)	TCCTGGATGCAGGAGCTGTGTTGCCGCAGCA TGGGGGCTCCAGGATGCGG
Consensus	(601)	TCCTGGATGCAGGAGCTGTGTTGCCGCAGC TGGGGGCTCCAGGATGCGG
		651 700
129	(651)	GACCTCTTTTGTGCGGGCCTCTGGACTCCTGGAAGTCAGAGCTGTGTTGC
pwk	(649)	GACCTCTTTTGTGCGGGCCTCTGGACTCCTGGAAGTCAGAGCTGTGTTGC
Consensus	(651)	GACCTCTTTTGTGCGGGCCTCTGGACTCCTGGAAGTCAGAGCTGTGTTGC
		701 750
129	(701)	CGCGACTTGTAGGTCCAGAGATTTTGGAACATTAACTGTGTGGCCTGTG

pwk	(699)	CGCGACTTGTAGGTCCAGAGATTTTGGAACATTAACTGTGTGGCCTGTG	
Consensus	(701)	CGCGACTTGTAGGTCCAGAGATTTTGGAACATTAACTGTGTGGCCTGTG	
		751	800
129	(751)	GCCTCCAGAATGCCGGAGCTCTGTTGGTTCTGGGGGTGGGTGTGGA	TAGA
pwk	(749)	GCCTCCAGAATGCCGGAGCTCTGTTGGTTCTGGGGGTGGGTGTGG	G
Consensus	(751)	GCCTCCAGAATGCCGGAGCTCTGTTGGTTCTGGGGGTGGGTGTGG	TAGA
		801	850
129	(801)	AGTTCTGTTGCCGCTGCAGGA	ACCTGTAGAGTCCGGGATTTTGTA
pwk	(799)	AGTTCTGTTGCCGCTGCAGG	G
Consensus	(801)	AGTTCTGTTGCCGCTGCAGG	ACCTGTAGAGTCCGGGATTTTGTA
		851	900
129	(851)	TACTGTGCGGCCTGTGGGCTCCAGGATGCAGGAGCTCTGTTGCCGCAGCC	
pwk	(849)	TACTGTGCGGCCTGTGGGCTCCAGGATGCAGGAGCTCTGTTGCCGCAGCC	
Consensus	(851)	TACTGTGCGGCCTGTGGGCTCCAGGATGCAGGAGCTCTGTTGCCGCAGCC	
		901	950
129	(901)	TGTGGGCTA	C
pwk	(899)	TGTGGGCTA	T
Consensus	(901)	TGTGGGCTA	G
		951	1000
129	(949)	GTTGATGCAGCCAGTGGGCTACAGGGCGTGGGAACTCTGCTGCCGCAGTG	
pwk	(949)	GTTGATGCAGCCAGTGGGCTACAGGGCGTGGGAACTCTGCTGCCGCAGTG	
Consensus	(951)	GTTGATGCAGCCAGTGGGCTACAGGGCGTGGGAACTCTGCTGCCGCAGTG	
		1001	1050
129	(999)	TCGCAGTCTGTTTTCTCCGCGGTGTGGGGGTGGGGGTGGGGAGGGAGCTC	
pwk	(999)	TCGCAGTCTGTTTTCTCCGCGGTGTGGGGGTGGGGGTGGGGAGGGAGCTC	
Consensus	(1001)	TCGCAGTCTGTTTTCTCCGCGGTGTGGGGGTGGGGGTGGGGAGGGAGCTC	
		1051	1100
129	(1049)	TGTTGCCGCAGCAGCCTATGTGCTACAGGGCATGAGAAATGGGCGGTTCGC	
pwk	(1049)	TGTTGCCGCAGCAGCCTATGTGCTACAGGGCATGAGAAATGGGCGGTTCGC	
Consensus	(1051)	TGTTGCCGCAGCAGCCTATGTGCTACAGGGCATGAGAAATGGGCGGTTCGC	
		1101	1150
129	(1099)	AGCTTGTGTGGTCTGGGGGATGGGAGCACCTTCAGGGGTCTGGGGA	ACTG
pwk	(1099)	AGCTTGTGTGGTCTGGGGGATGGGAGCACCTTCAGGGGTCTGGGGA	ACTG
Consensus	(1101)	AGCTTGTGTGGTCTGGGGGATGGGAGCACCTTCAGGGGTCTGGGGA	ACTG
		1151	1200
129	(1149)	GAGCTGTGTGGCGGTGGCCTGAGGGCTGGGAGCTTGTTGCCATGGCTTG	
pwk	(1149)	GAGCTGTGTGGCGGTGGCCTGAGGGCTGGGAGCTTGTTGCCATGGCTTG	
Consensus	(1151)	GAGCTGTGTGGCGGTGGCCTGAGGGCTGGGAGCTTGTTGCCATGGCTTG	
		1201	1250
129	(1199)	TGTGTTT	CAGGGTGGGGGCT
pwk	(1199)	TGTGTTT	CAGGGTGGGGGCT

Consensus	(1201)	TGTGTTTCAGGGTGGGGGC ACTGGAGTGCTGTTGCCGCGGCCTGCGGGCT	
		1251	1300
129	(1249)	ATGGGGGTGGTAGCTCCATTGCCACAGCCTGTGAGCCTAGGGTAGAGGGA	
pwk	(1249)	ATGGGGGTGGTAGCTCCATTGCCACAGCCTGTGAGCCTAGGGTAGAGGGA	
Consensus	(1251)	ATGGGGGTGGTAGCTCCATTGCCACAGCCTGTGAGCCTAGGGTAGAGGGA	
		1301	1350
129	(1299)	GCGGTAGCTCTGTGCGCTCTTAGTTCATGTTTGGGGGAGCTCTGCTGTTG	
pwk	(1299)	GCGGTAGCTCTGTGCGCTCTTAGTTCATGTTTGGGGGAGCTCTGCTGTTG	
Consensus	(1301)	GCGGTAGCTCTGTGCGCTCTTAGTTCATGTTTGGGGGAGCTCTGCTGTTG	
		1351	1400
129	(1349)	TGGCCTTTAGGCTGAGGGTGC GCGCAGGGTGTGGGGGATGGGGGCATTCT	
pwk	(1349)	TGGCCTTTAGGCTGAGGGTGC GCGCAGGGTGTGGGGGATGGGGGCATTCT	
Consensus	(1351)	TGGCCTTTAGGCTGAGGGTGC GCGCAGGGTGTGGGGGATGGGGGCATTCT	
		1401	1450
129	(1399)	GGGAGCTCTGTTGCTGCTTCATGTGGCTTCAAGGATGTCAGAGCTGTGTA	
pwk	(1399)	GGGAGCTCTGTTGCTGCTTCATGTGGCTTCAAGGATGTCAGAGCTGTGTA	
Consensus	(1401)	GGGAGCTCTGTTGCTGCTTCATGTGGCTTCAAGGATGTCAGAGCTGTGTA	
		1451	1500
129	(1449)	GTGGTGGTATGGTAGGGTGGAAGGTGAGCGCTAGTGGGTGATTTTCTCTG	
pwk	(1449)	GTGGTGGTATGGTAGGGTGGAAGGTGAGCGCTAGTGGGTGATTTTCTCTG	
Consensus	(1451)	GTGGTGGTATGGTAGGGTGGAAGGTGAGCGCTAGTGGGTGATTTTCTCTG	
		1501	1534
129	(1499)	AGATCTCTATAACTACTTCTCAAGATCATGTGGT	
pwk	(1499)	AGACCTCTATAACTACTTCTCAAGTCATGTGGT	
Consensus	(1501)	AGA CTCTATAACTACTTCTCAAG TCATGTGGT	

Figure 3-9 Nucleotide polymorphisms between 129/SvEv and PWK/PhJ mice in the PWS-IC region PCR products derived from 129/SvEv mice and PWK/PhJ mice were sequenced and the sequences were analyzed using Vector NTI. All the polymorphisms were confirmed by sequencing PCR products derived from (129/SvEv × PWK/PhJ) F1 hybrid mice.

3.3. Characteristics of AS-IC m^{an}/p^{+} imprinting defect mice

3.3.1 Complete loss of methylation spans the entire *Snurf-Snrpn* DMR

Methylation study of *Snurf-Snrpn* DMR using restriction enzyme digestion followed by Southern analysis can determine methylation status of one CpG dinucleotide, but bisulfite sequencing method can detect the methylation status of all the 16 CpG

dinucleotides in the *Snurf-Snrpn* DMR at the same time. To conduct bisulfite sequencing, genomic DNA of wild type mice, AS-IC m^{+}/p^{an} mice and AS-IC m^{an}/p^{+} mice with imprinting defect were treated with sodium bisulfite. Primers not containing any CpGs were designed according to the converted DNA sequence, and used to amplify the promoter/exon 1 (-307 to +115) of *Snurf-Snrpn*. Bisulfite modified DNA was used as template for nested PCR and PCR products were purified and fused to TA vector for sequencing. The plasmid/competent cells mixture was spread on pre-warmed LB selective agar plates directly. Among colonies derived from wild type (7) and AS-IC m^{+}/p^{an} mice (8), 4 out of 7 and 5 out of 8 colonies contained PCR fragments with nearly all the CpG dinucleotides methylated and 3 out of 7 and 3 out of 8 colonies contained PCR fragments with nearly all the CpG dinucleotides unmethylated, indicating that *Snurf-Snrpn* DMRs in these mice have normal methylation patterns (Figure 3-10b, left and middle). Sequencing results of colonies derived from the AS-IC m^{an}/p^{+} mice with imprinting defect showed that all the colonies contained PCR fragments with nearly all the CpG dinucleotides unmethylated, indicating that *Snurf-Snrpn* DMRs in these mice are biallelically unmethylated and that loss of methylation imprint from the maternally derived allele spans the entire DMR of *Snurf-Snrpn* (Figure 3-10b, right).

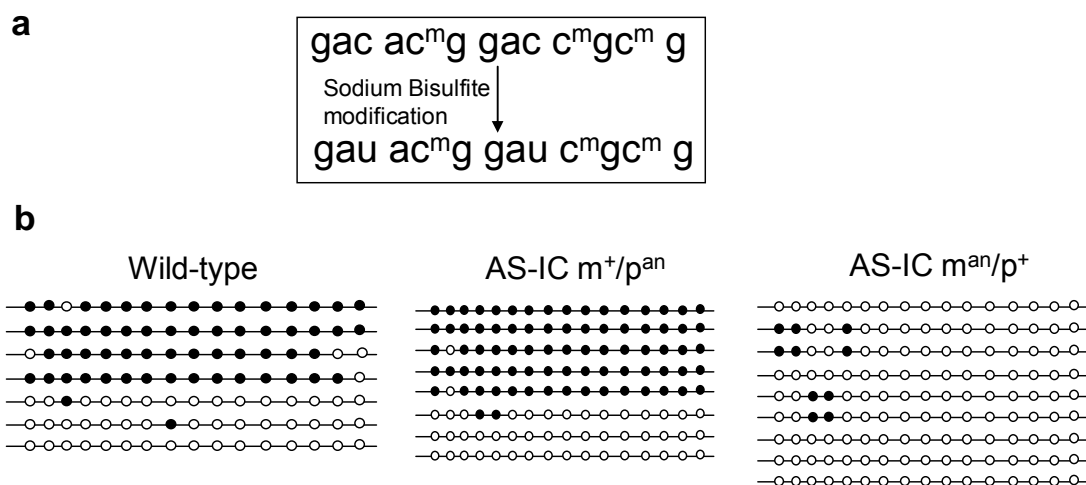


Figure 3-10 Loss of maternal methylation imprints at the *Snurf-Snrpn* DMR in AS-IC m^{an}/p⁺ imprinting defect mice **a.** Schematic depiction of the treatment of DNA with sodium bisulfite. Sodium bisulfite can convert cytosine to uracil. 5-Methyl cytosine is, however, protected from the bisulfite reaction because of the presence of the methyl group. **b.** Bisulfite sequencing analysis of methylation status of 16 CpG dinucleotides across the promoter/exon 1 (-307 to +115) of *Snurf-Snrpn* in wild type mice (left), heterozygous mice inheriting the AS-IC^{an} mutation paternally (middle), and AS-IC m^{an}/p⁺ mice with imprinting defect (right). Each line represents an individual colony sequenced. The 16 CpG dinucleotides are presented as circles. Closed circles represent methylated cytosine residues, whereas open circles represent unmethylated cytosine residues. The drawing is not to scale.

Genotyping of AS-IC m^{an}/p⁺ imprinting defect mice by Southern blot is laborious and time-consuming (refer to Chapter II Materials and Methods). Since loss of methylation from maternal allele of *Snurf-Snrpn* DMR is nearly complete and throughout the entire region, methylation specific PCR (MSP) was designed to make the identification of AS-IC m^{an}/p⁺ imprinting defect mice easier. As introduced previously, after sodium bisulfite treatment, sequences of two alleles of *Snurf-Snrpn* DMR differ depending on whether the DNA is originally methylated or unmethylated. MSP primers containing CpG dinucleotides were designed according to the converted DNA sequence in *Snurf-Snrpn* DMR, with one set of primers complementary to the methylated maternal allele and one set of primers complementary to the unmethylated

paternal allele (Figure 3-11a). In wild type mice (Figure 3-11b, lane 2) and AS-IC m^{an}/p^{+} mice with normal methylation (Figure 3-11b, lane 1), both methylated and unmethylated alleles were amplified, while in AS-IC m^{an}/p^{+} imprinting defect mice, only unmethylated allele was amplified since *Snurf-Snrpn* DMRs are biallelically unmethylated in these mice (Figure 3-11b, lane 3).

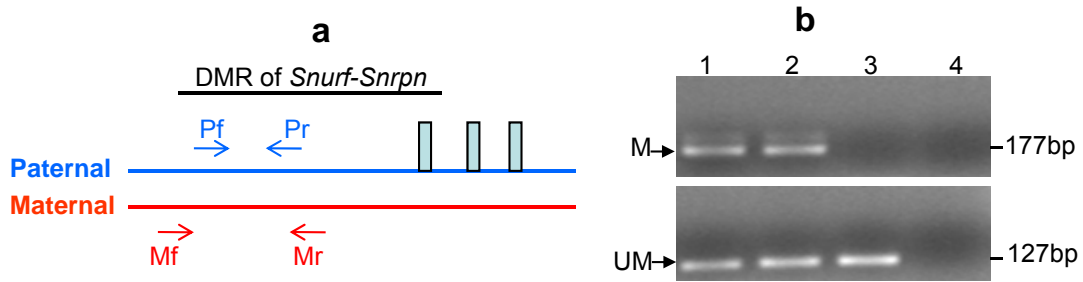


Figure 3-11 Identification of AS-IC m^{an}/p^{+} imprinting defect mice by MSP **a.** Schematic depiction of the locations of MSP primers. Mf and Mr are MSP primers specific for the amplification of the methylated maternal allele; Pf and Pr are MSP primers specific for the amplification of the unmethylated paternal allele. Red arrows and blue arrows indicate the orientation and locations of MSP primers. Three vertical blue bars represent exon 1-3 of *Snurf-Snrpn*. The horizontal black line indicates the DMR of *Snurf-Snrpn*. **b.** MSP followed by agarose gel electrophoresis is used to identify AS-IC m^{an}/p^{+} imprinting defect mice. Lane 1: AS-IC m^{an}/p^{+} mice with normal methylation pattern at DMR of *Snurf-Snrpn*; lane 2: wild type mice; lane 3: AS-IC m^{an}/p^{+} mice with imprinting defect; lane 4: no template control. M: MSP products from methylated allele; UM: MSP products from unmethylated allele.

3.3.2 *Snurf-Snrpn* transcript is biallelically expressed in AS-IC m^{an}/p^{+} imprinting defect mice

Methylation of DNA usually associates with silencing of genes, whereas loss of methylation usually reactivates silent genes. In wild type mice, the maternal allele of *Snurf-Snrpn* DMR is heavily methylated, and the maternal allele of *Snurf-Snrpn* is inactive and silent. In AS-IC m^{an}/p^{+} imprinting defect mice, the methylation of the maternal DMR of *Snurf-Snrpn* is lost. To determine whether loss of methylation on

the maternal allele of *Snurf-Snrpn* DMR is correlated with activation of imprinted genes which are normally silenced from the maternal allele, real time PCR was used to compare *Snurf-Snrpn* expression levels from wild type mice, AS-IC m^+/p^{an} mice, AS-IC m^{an}/p^+ mice with imprinting defect and AS-IC m^{an}/p^+ mice with normal methylation. The mRNA level of *Snurf-Snrpn* in AS-IC m^{an}/p^+ imprinting defect mice was nearly twice as much as that of others, indicating that loss of methylation on the maternal DMR of *Snurf-Snrpn* leads to activation of *Snurf-Snrpn* transcript from the maternal allele (Figure 3-12).

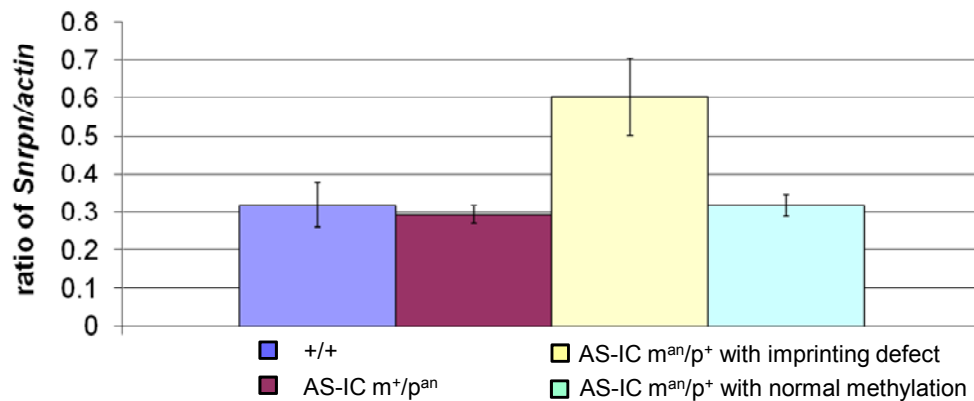


Figure 3-12 Real time PCR quantification of *Snurf-Snrpn* gene expression in mice cerebellum

Total RNA extracted from cerebellum of wild type mice, AS-IC m^+/p^{an} mice, AS-IC m^{an}/p^+ mice with imprinting defect and AS-IC m^{an}/p^+ mice with normal methylation patterns, was reverse transcribed into cDNA. The cDNA was used for real time PCR by standard curve method using β -actin as endogenous control. Blue column represents the *Snurf-Snrpn* expression level in wild type mice, purple column represents the *Snurf-Snrpn* expression level in AS-IC m^+/p^{an} mice, yellow column represents the *Snurf-Snrpn* expression level in AS-IC m^{an}/p^+ mice with imprinting defect and the light green column represents the *Snurf-Snrpn* expression level in AS-IC m^{an}/p^+ mice with normal methylation patterns. The mRNA level of *Snurf-Snrpn* in AS-IC m^{an}/p^+ imprinting defect mice is nearly twice as much as that of others.

3.3.3 Activation of *Snurf-Snrpn* upstream transcripts from maternal allele

In both human and mice, a brain-specific paternally expressed *Ube3a* antisense (*Ube3a-ATS*) has been proposed to repress the *Ube3a* gene that is expressed from the paternal allele in brain (195-197). Since the *Snurf-Snrpn* upstream transcripts display the same time course of expression as *Ube3a-ATS* during P19 neuronal differentiation and both are brain-specific and only expressed from paternal allele, it has been suggested that these transcripts may serve as initiation sites for the *IC-IPW/Ube3a-ATS*, and may contain the functional elements of AS-IC (169). Since *Snurf-Snrpn* transcript is expressed biallelically in AS-IC m^{an}/p^{+} imprinting defect mice, RT-PCR was carried out using F1 mice generated from cross between 129/SvEv AS-IC $^{+/an}$ female and PWK/PhJ male, and F1 from reciprocal cross, to detect the expression of these *Snurf-Snrpn* upstream transcripts (Figure 3-13). Total RNA was extracted from mice cerebellums and reverse transcribed into cDNA, and PCR was carried out using primer AH11 which is located in *Snurf-Snrpn* upstream exon 7 and primer AH10 which is located in *Snurf-Snrpn* exon 3. Two PCR products, 516 bp and 410 bp, were generated from cDNA derived from mice in 129/SvEv background, while only the 516-bp product was produced from cDNA derived from mice in PWK/PhJ background. Thus, these PCR products can be used to distinguish the expressed allele in a F1 mice generated from cross between 129/SvEv and PWK/PhJ (Figure 3-13b, sample 1 and 2). RT-PCR from (PWK/PhJ female \times 129/SvEv AS-IC $^{+/an}$ male) F1 AS-IC m^{+}/p^{an} mice generated two PCR products, 516 bp and 410 bp (Figure 3-13b, sample 3), which is the paternal 129/SvEv band pattern. RT-PCR from (129/SvEv AS-IC $^{+/an}$ female \times PWK/PhJ male) F1 AS-IC m^{an}/p^{+} mice with normal methylation patterns generated only 516-bp PCR product (Figure 3-13b, sample 4), which is the

same RT-PCR band pattern as that of (129/SvEv female \times PWK/PhJ male) F1 129/PWK wild type mice (Figure 3-13b, sample 5), which in turn, is the paternal PWK/PhJ band pattern. RT-PCR of (129/SvEv AS-IC^{+/^{an}} female \times PWK/PhJ male) F1 AS-IC m^{an}/p⁺ mice with AS imprinting defect generated two PCR products, 516 bp and 410 bp (Figure 3-13b, sample 6), which is the RT-PCR band pattern of the maternal allele of 129/SvEv. Both RT-PCR products from AS-IC m^{an}/p⁺ imprinting defect mice were sequenced and a single nucleotide polymorphism in U exon delta confirmed that the 410 bp PCR product was from 129/SvEv allele, but the 516-bp PCR product was only from PWK/PhJ allele. The splicing patterns of the 516-bp and 410-bp PCR products were shown as I and II (Figure 3-13a). RT-PCR using primer AH12 from U exon 5 and AH10 from *Snurf-Snrpn* exon 3 generated two RT-PCR products, 563 bp and 459 bp, from the cDNA of 129/SvEv mice, and no PCR product was detected from the cDNA of PWK/PhJ mice. Likewise, these two PCR products were generated from cDNA derived from (PWK/PhJ female \times 129/SvEv AS-IC^{+/^{an}} male) F1 AS-IC m⁺/p^{an} mice and (129/SvEv AS-IC^{+/^{an}} female \times PWK/PhJ male) F1 AS-IC m^{an}/p⁺ mice with AS imprinting defect. These PCR products were sequenced and the splicing patterns were shown as III and IV (Figure 3-13a). These results indicate that *Snurf-Snrpn* upstream transcripts are activated from the silent maternal allele in the AS-IC m^{an}/p⁺ imprinting defect mice, although it may not include all of the alternative splicing patterns.

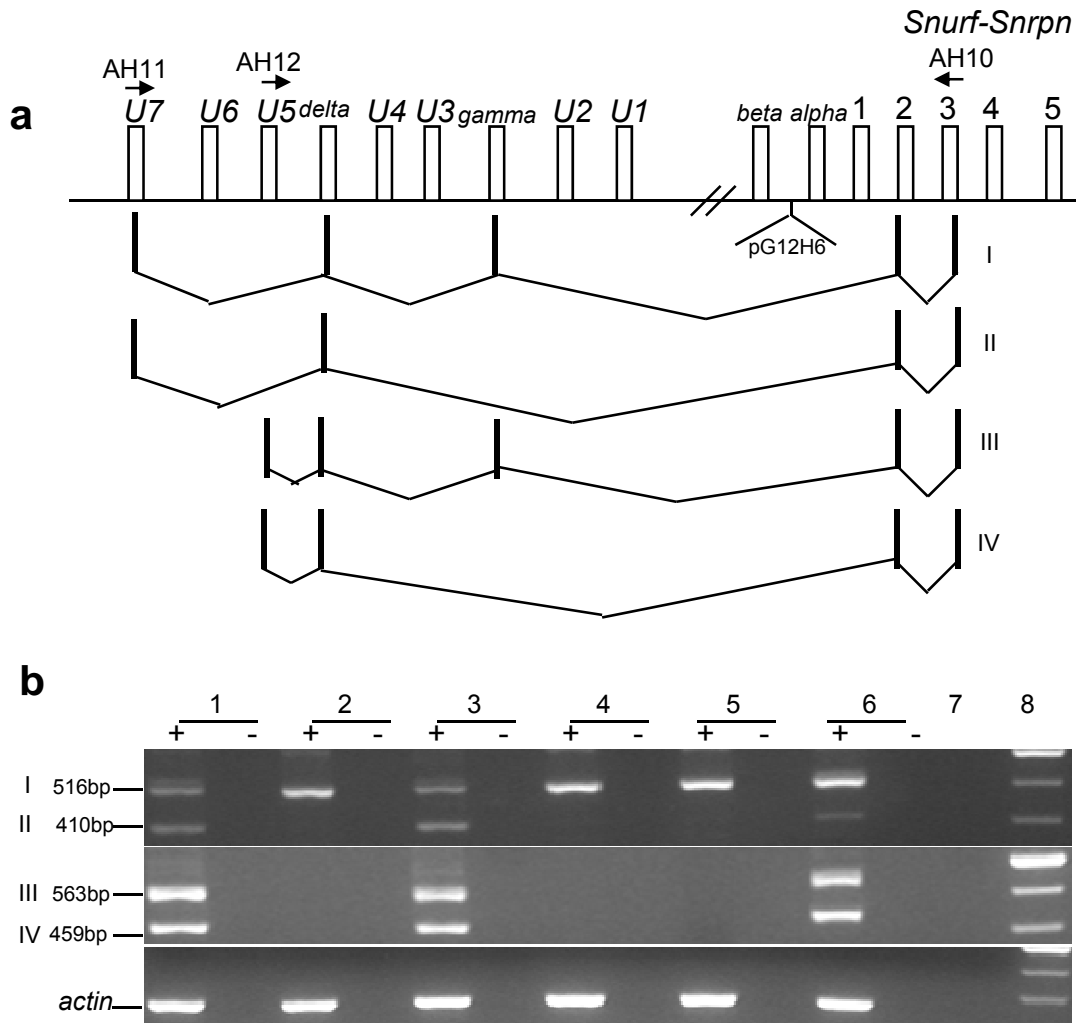


Figure 3-13 *Snurf-Snrpn* upstream transcripts are expressed from maternal allele in cerebellum of AS-IC m^{an}/p^{+} imprinting defect mice **a.** Schematic presentation of *Snurf-Snrpn* upstream exons and *Snurf-Snrpn* upstream transcripts with various splicing patterns. Primers AH10, AH11 and AH12 are derived from *Snurf-Snrpn* exon 3, U exon 7 and U exon 5, respectively. *Snurf-Snrpn* exons 1-5 and *Snurf-Snrpn* upstream exons are presented as small columns. Arrows indicate primers orientation and locations. I and II are splicing patterns of RT-PCR products from AH10 and AH11; III and IV are splicing patterns of RT-PCR products from AH10 and AH12. Exons of different splicing patterns are indicated. **b.** Expression of *Snurf-Snrpn* upstream transcripts. The first row of agarose gel picture shows PCR products from AH10 and AH11; second row shows PCR products from AH10 and AH12; third row shows PCR products of β -actin. 1: 129/SvEv wild type; 2: PWK/PhJ wild type; 3: (PWK/PhJ female \times 129/SvEv AS-IC $^{+/an}$ male) F1 AS-IC m^{+}/p^{an} mice; 4: (129/SvEv AS-IC $^{+/an}$ female \times PWK/PhJ male) F1 AS-IC m^{an}/p^{+} mice with normal methylation pattern; 5: (129/SvEv female \times PWK/PhJ male) F1 129/PWK wild type mice; 6: (129/SvEv AS-IC $^{+/an}$ female \times PWK/PhJ male) F1 AS-IC m^{an}/p^{+} mice with imprinting defect; 7: no template control; 8: 100 bp ladder. +: RT positive; -: RT negative. *Beta-actin* was used as RT-PCR endogenous control.

3.3.4 Histone epigenetic modifications on the maternal allele mimic that of the paternal allele

In PWS-IC region, histone H3K9 and K4 are methylated in a parental complementary pattern. Histone H3K9 is methylated only on the maternal allele, while histone H3K4 is methylated only on the paternal allele (104). In addition, maternal specific methylation of histone H3K9 in PWS-IC region is conserved between human and mice, so parental specific methylation of H3K9 and H3K4 is regarded as an epigenetic mark (198). To study the modification status of histone H3K9 and K4 in AS-IC m^{an}/p^{+} imprinting defect mice, tissues from F1 mice generated from crossing between 129/SvEv and PWK/PhJ mice were examined by chromatin immunoprecipitation (ChIP) assay.

The optimal average size of chromatin for ChIP is 300-500 bp, so chromatin sonication conditions were tested to optimize the condition. Four pieces of liver tissues of equal weight (30 mg) were fixed by formaldehyde and subjected to sonication in 4 different conditions. Sonicated chromatin was reversed cross-linked and DNA was electrophoresed in a 1% agarose gel (Figure 3-14). Conditions of lane 3 were chosen to perform ChIP experiments because it generated DNA fragment with an average size 500 bp. Although conditions of lane 4 showed the same results, there was foam generated during sonication.

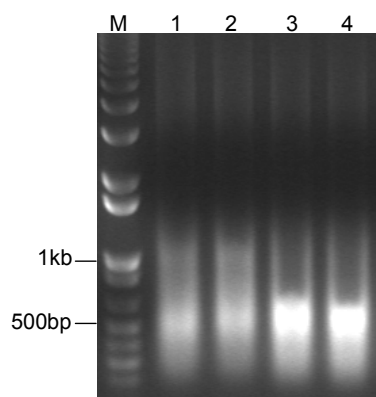


Figure 3-14 Optimization of mouse tissue sonication conditions Mouse liver (30 mg) was minced in a 2 ml tube and fixed with formaldehyde. The fixed samples were washed with PBS and suspended in SDS lysis buffer. The sonicated samples were reversed cross-linked and DNA samples were electrophoresed in a 1% agarose gel. Lane 1: 27 s/time for 1 time with 9.0 s on and 9.9 s off settings at 23% output power; lane 2: 27 s/time for 2 times with 9.0 s on and 9.9 s off settings at 23% output power; lane 3: 27 s/time for 3 times with 9.0 s on and 9.9 s off settings at 23% output power; lane 4: 27 s/time for 4 times with 9.0 s on and 9.9 s off settings at 23% output power. M: 1 kb ladder. Conditions of lane 3 gave an average chromatin size around 500 bp.

To investigate which parental alleles can be precipitated by the specific antibodies, primers that specifically amplify each parental allele were designed in the DMR of *Snurf-Snrpn* according to polymorphisms between 129/SvEv and PWK/PhJ in Figure 3-9. Primers AH20a and AH21a were used for the amplification of the PWK/PhJ allele, whereas AH22a and AH23a were used for amplifying the 129/SvEv allele. These two primer sets amplify the same DNA fragment. There is one base pair difference at 3' end between AH20a and AH22a, AH21a and AH23a to achieve allele-specific amplification for each parental strain. To determine the annealing temperature at which AH20a and AH21a can only amplify PWK/PhJ allele, and AH22a and AH23a can only amplify 129/SvEv allele, gradient PCR (annealing temperature from 55 °C to 64°C) was performed using genome DNA derived from 129/SvEv and PWK/PhJ, respectively. Figure 3-15a showed that primers AH20a and AH21a can amplify PWK/PhJ allele at all the annealing temperatures tested ranging

from 55°C to 64°C, but cannot amplify 129/SvEv allele under the same conditions. Figure 3-15b showed that primers AH22a and AH23a can amplify 129/SvEv allele at all the annealing temperatures tested and also amplify PWK/PhJ allele from 55°C to 58.5°C, so 60°C was chosen as the annealing temperature for the ChIP assays.

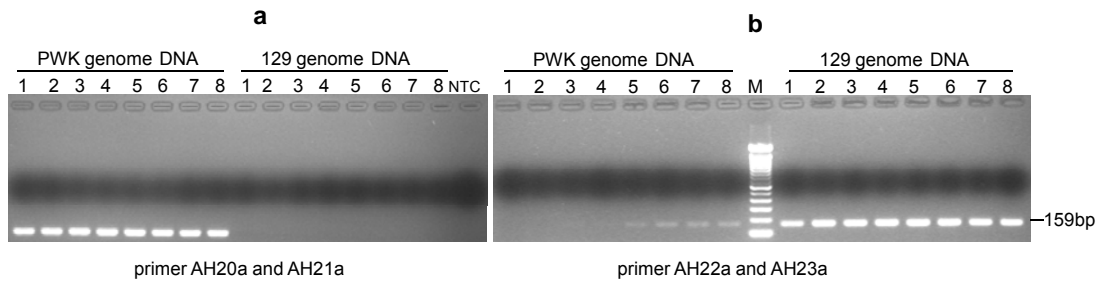


Figure 3-15 Determining primers annealing temperature by gradient PCR **a.** The PCR products of AH20a and AH21a were electrophoresed in a 2% agarose gel. **b.** The PCR products of AH22a and AH23a were electrophoresed in a 2% agarose gel. For each primer set, 16 PCR reactions were set up. Eight reactions used genomic DNA derived from 129/SvEv as template and eight reactions used genomic DNA derived from PWK/PhJ as template. Reactions were performed on a PCR machine setting with gradient annealing temperatures from 55 °C to 64 °C. The annealing temperatures from lane 1 to lane 8 is 64°C, 63.5°C, 62.5°C, 60.8°C, 58.5°C, 56.9°C, 55.8°C, 55°C, respectively. NTC: no template control. M: 100 bp ladder.

It has been reported that dimethylated histone H3K9 is associated with the inactive maternal allele and dimethylated histone H3K4 is associated with the active paternal allele at DMR of *Snurf-Snrpn* (165, 198), ChIP assay was carried out using liver from (129/SvEv × PWK/PhJ) F1 wild type mice with anti-dimethyl H3K4 and anti-dimethyl H3K9 to examine whether the same strategies can be apply to our case. Primers AH15 and AH16 universal to both parental sequences were used to amplify the DMR of *Snurf-Snrpn* from DNA precipitated by anti-dimethyl H3K4 and anti-dimethyl H3K9, respectively. It was found that AH15 and AH16 cannot generate any PCR product from DNA samples precipitated by anti-dimethyl H3K9 (Figure 3-16a, lane 3 and 4), but generate PCR products from DNA samples precipitated by anti-

dimethyl H3K4 (Figure 3-16a, lane 1 and 2). To test whether anti-dimethyl H3K9 can precipitate DMR of *Snurf-Snrpn* in central nerve systems, ChIP assay was carried out using mouse cerebellum with anti-dimethyl H3K9 and anti-trimethyl H3K9. It was found that DMR of *Snurf-Snrpn* of mouse cerebellum was precipitated by anti-trimethyl H3K9, but could not be precipitated by anti-dimethyl H3K9 (Figure 3-16b). *D13Mit55* is a locus near the centromere of mouse chromosome 13 and is known to be precipitated by anti-dimethyl H3K9 (198). To check whether the anti-dimethyl H3K9 antibody can work efficiently, primers AH24a and AH25a which are specific to *D13Mit55* region were used to perform PCR as a positive control. Results showed that primers AH24a and AH25a can generate PCR products from DNA samples precipitated by anti-dimethyl H3K9 from mouse cerebellum (Figure 3-16c, lane 2), indicating that anti-dimethyl H3K9 antibody works well. It is possible that differential modification of dimethyl H3K9 does not associate with the DMR of *Snurf-Snrpn* in mice, which is consistent with studies of another imprinting gene *Igf2r*. In the DMR2 of *Igf2r*, it has been shown that trimethyl H3K9 is involved in the regulation of imprinting expression of *Igf2r* (18).

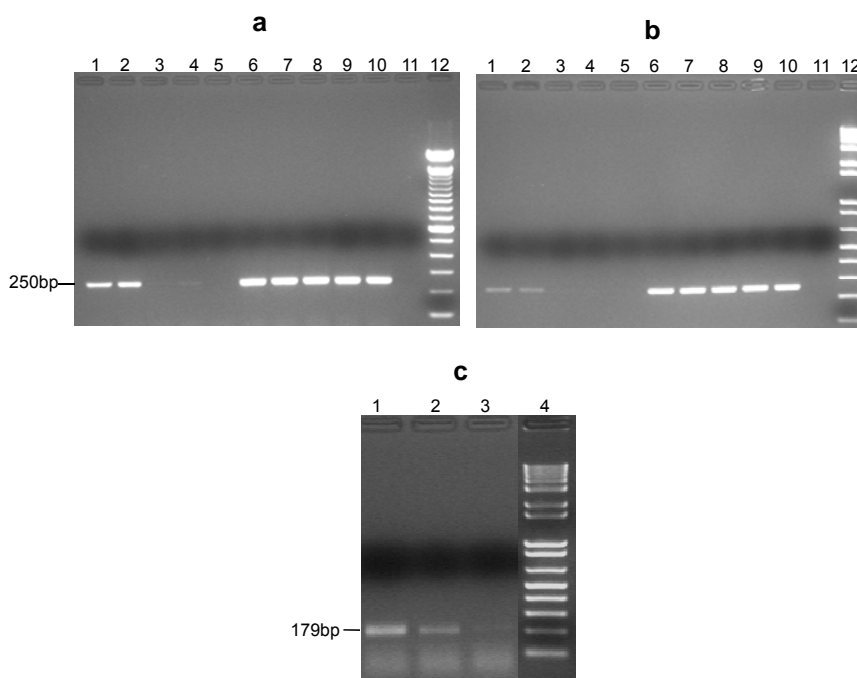


Figure 3-16 Trimethyl H3K9 not dimethyl H3K9 is enriched at the PWS-IC of mice **a.** ChIP assay using liver cells with anti-dimethyl H3K4 and anti-dimethyl H3K9. The input and precipitated DNA were subjected to PCR with primers AH15 and AH16. PCR products were electrophoresed in a 2% agarose gel. Lanes 1 and 2: ChIP DNA precipitated by anti-dimethyl H3K4; lanes 3 and 4: ChIP DNA precipitated by anti-dimethyl H3K9; lane 5: no antibody control; lanes 6-10: input control; lane 11: no template control; lane 12: 100 bp ladder **b.** ChIP assay using cerebellum cells with anti-dimethyl H3K9 and anti-trimethyl H3K9. Input DNA and precipitated DNA were subjected to PCR with primers AH15 and AH16. PCR products were electrophoresed in a 2% agarose gel. Lanes 1 and 2: ChIP DNA precipitated by anti-trimethyl H3K9; lanes 3 and 4: ChIP DNA precipitated by anti-dimethyl H3K9; lane 5: no antibody control; lanes 6-10: input control; lane 11: no template control; lane 12: 1 kb ladder. **c.** Anti-dimethyl H3K9 can precipitate *D13Mit55* in mice cerebellum. Input DNA and precipitated DNA from **b** were subjected to PCR with primers specific for *D13Mit55*. PCR products were electrophoresed in a 2% agarose gel. Lane 1: Input DNA; lane 2: ChIP DNA precipitated by anti-dimethyl H3K9; lane 3: no antibody control; lane 4: 1 kb ladder. *D13Mit55* can be precipitated by anti-dimethyl H3K9 in cerebellum.

Cerebellums from (129/SvEv and PWK/PhJ reciprocal cross) F1 wild type mice were subjected to ChIP assay with anti-dimethyl H3K4 and anti-trimethyl H3K9. Antibody precipitated DNA and input DNA were used to conduct allele-specific PCR using primers AH20a, AH21a, AH22a and AH23a in the presence of [α - 32 P] dCTP to compare which parental allele is enriched by the antibodies. The results showed that

the active paternal allele was enriched by anti-dimethyl H3K4 regardless of whether the paternal allele was from PWK/PhJ or 129/SvEv (Figure 3-17a). On the other hand, the inactive maternal allele was enriched by anti-trimethyl H3K9 regardless of whether the maternal allele was from 129/SvEv or PWK/PhJ (Figure 3-17b). Allele-specific modification of dimethyl H3K4 and trimethyl H3K9 is consistent with previous investigations, suggesting that dimethyl H3K4 and trimethyl H3K9 function as epigenetic mark in DMR of imprinting genes (104, 165). Since dimethyl H3K4 is specifically associated with the active paternal allele and trimethyl H3K9 is specifically associated with the inactive maternal allele at PWS-IC, both alleles should be enriched by anti-dimethyl H3K4 and the enrichment of maternal allele by anti-trimethyl H3K9 should be reduced in AS imprinting defect mice, because the inactive maternal allele behaves as the active paternal allele. ChIP assay results from cerebellum of AS-IC m^{an}/p^{+} imprinting defect mice with both anti-dimethyl H3K4 and anti-trimethyl H3K9 were consistent with our expectation (Figure 3-18).

To test whether the allele-specific association of dimethyl H3K4 and trimethyl H3K9 also exist in liver cells, ChIP assays were carried out with anti-dimethyl H3K4 and anti-trimethyl H3K9 in liver cells from (129/SvEv and PWK/PhJ reciprocal cross) F1 wild type mice and (129/SvEv AS-IC^{+/an} female \times PWK/PhJ male) F1 AS-IC m^{an}/p^{+} imprinting defect mice. In wild type mice, only the paternal allele was enriched by anti-dimethyl H3K4, whereas in AS-IC m^{an}/p^{+} imprinting defect mice, the enrichment by anti-dimethyl H3K4 was biallelic (Figure 3-19). ChIP assay of anti-trimethyl H3K9 was quantified by real time PCR using *Dl3Mit55* as an endogeneous control (Figure 3-20a). In AS-IC m^{an}/p^{+} imprinting defect mice, enrichment of the maternal allele by anti-trimethyl H3K9 was reduced compared to that of wild type mice. ChIP

assay results from both cerebellum and liver with anti-dimethyl H3K4 and anti-trimethyl H3K9 were summarized in Figure 3-20b. In liver and cerebellum from the wild type mice, paternal allele of *Snurf-Snrpn* DMR was enriched by anti-dimethyl H3K4 and maternal allele was enriched by anti-trimethyl H3K9. In AS-IC m^{an}/p^{+} imprinting defect mice, the inactive maternal allele of *Snurf-Snrpn* DMR is activated and behaves as the paternal allele, so both alleles were enriched by anti-dimethyl H3K4; and the enrichment of anti-trimethyl H3K9 from maternal allele was reduced when compared to that of wild type mice. These results suggest that the maternal DMR of *Snurf-Snrpn* gains the paternal histone modification characters in the AS-IC m^{an}/p^{+} imprinting defect mice.

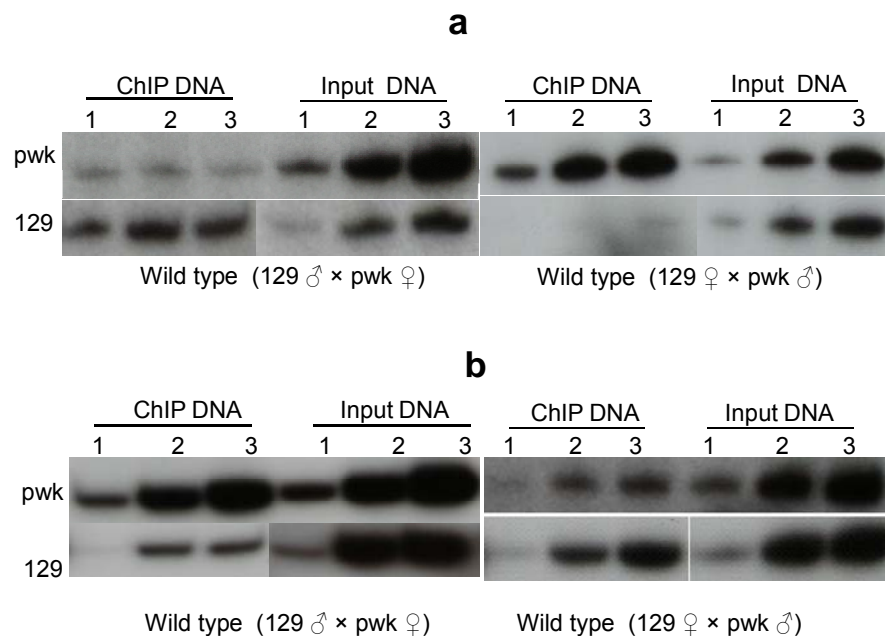


Figure 3-17 ChIP assay at the *Snurf-Snrpn* DMR in the cerebellum of wild type mice **a.** ChIP assay with anti-dimethyl H3K4 in (left: PWK/PhJ female × 129/SvEv male, right: 129/SvEv female × PWK/PhJ male) F1 wild type mice. The paternal allele (left: 129/SvEv allele, right: PWK/PhJ allele) was enriched by anti-dimethyl H3K4. **b.** ChIP assay with anti-trimethyl H3K9 in (left: PWK/PhJ female × 129/SvEv male, right: 129/SvEv female × PWK/PhJ male) F1 wild type mice. The maternal allele (left: PWK/PhJ allele, right: 129/SvEv allele) was enriched by anti-trimethyl H3K9. PCR products derived from ChIP precipitated DNA and input DNA are indicated. Lanes 1-3: 0.25 μ l, 1 μ l and 2 μ l of original DNA used for PCR, respectively.

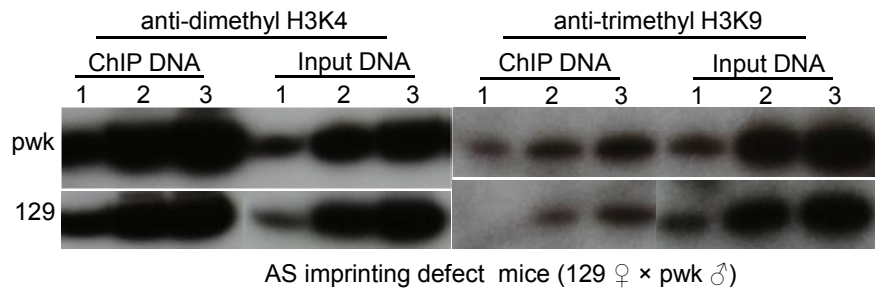


Figure 3-18 ChIP assay at the *Snurf-Snrpn* DMR in the cerebellum of AS-IC m^{an}/p^{+} imprinting defect mice Cerebellum from (129/SvEv AS-IC^{+an} female × PWK/PhJ male) F1 AS-IC m^{an}/p^{+} imprinting defect mice was used for ChIP with anti-dimethyl H3K4 (left) and anti-trimethyl H3K9 (right). Both alleles were enriched by anti-dimethyl H3K4 and the enrichment of maternal allele by anti-trimethyl H3K9 was reduced as compared to that of wild type mice. PCR products derived from ChIP precipitated DNA and input DNA are indicated. Lanes 1-3: 0.25 μ l, 1 μ l and 2 μ l of original DNA used for PCR, respectively.

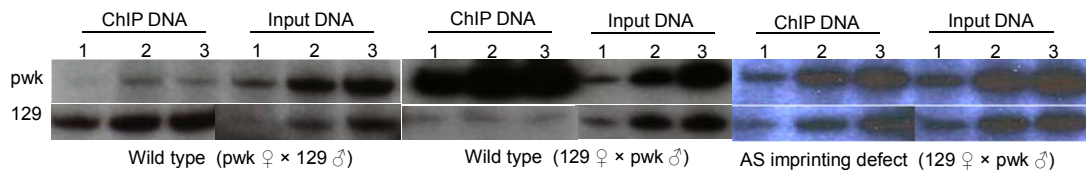


Figure 3-19 ChIP assay at the DMR of *Snurf-Snrpn* in liver cells with anti-dimethyl H3K4. Liver cells from (left: PWK/PhJ female × 129/SvEv male, middle: 129/SvEv female × PWK/PhJ male) F1 wild type mice and (129/SvEv AS-IC^{+an} female × PWK/PhJ male) F1 AS-IC m^{an}/p^{+} imprinting defect mice (right) were used for ChIP assay with anti-dimethyl H3K4. In the (129/SvEv × PWK/PhJ reciprocal cross) F1 wild type mice, the paternal allele was enriched by anti-dimethyl H3K4. In AS-IC m^{an}/p^{+} imprinting defect mice, both alleles were precipitated by anti-dimethyl H3K4. PCR products derived from ChIP precipitated DNA and input DNA are indicated. Lanes 1-3: 0.25 μ l, 1 μ l and 2 μ l of original DNA used for PCR, respectively.

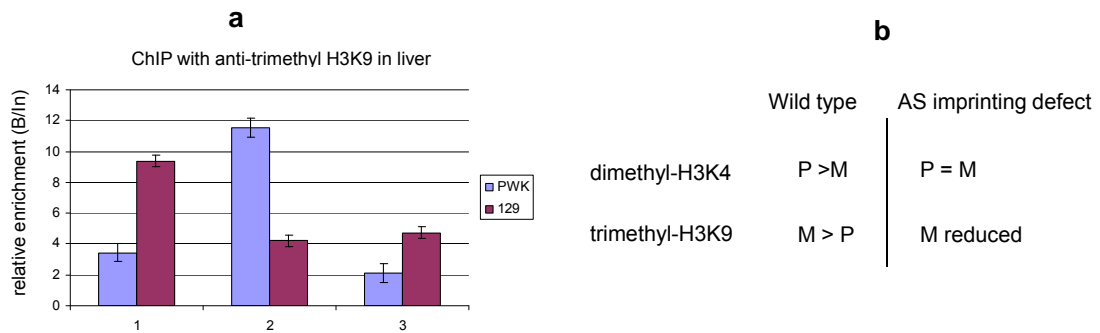


Figure 3-20 ChIP assay at the DMR of *Snurf-Snrpn* in liver with anti-trimethyl H3K9 and the summary of the ChIP assay results **a.** Liver cells from (1: 129/SvEv female \times PWK/PhJ male; 2: PWK/PhJ female \times 129/SvEv male) F1 wild type mice and (3: 129/SvEv AS-IC^{+/an} female \times PWK/PhJ male) F1 AS-IC m^{an}/p⁺ mice with imprinting defect were used for ChIP with anti-trimethyl H3K9. Real time PCR was used to quantify each allele of ChIP precipitated DNA and input DNA using *D13Mit55* as an endogenous control. In both the F1 wild type mice from 129/SvEv and PWK/PhJ reciprocal cross, the maternal allele was enriched by anti-trimethyl H3K9. In F1 AS-IC m^{an}/p⁺ imprinting defect mice, enrichment of maternal allele by anti-trimethyl H3K9 was reduced as compared to that of wild type mice. **b.** Summary of ChIP assay results in cerebellum and liver with anti-dimethyl H3K4 and anti-trimethyl H3K9. P: paternal allele; M: maternal allele.

3.3.5 Differential replication timing of the PWS/AS domain is decreased

FISH analysis using interphase nuclei is a sensitive method for studying replication timing. For most genomic regions, two single (SS) or two double (DD) hybridization spots per nucleus can be observed, indicating that both alleles replicate at about the same time in S phase. For imprinted genes and other monoallelically expressed genes, there is a high percentage (> 25%) of nuclei in which one allele has already replicated while the other has not (known as SD), indicating asynchronous replication of homologous chromosomes (180, 199). Allele-specific DNA asynchronous replication between homologous chromosomes has been observed in cells from normal individuals and in PWS and AS patients with chromosome 15 deletions, but has not been observed in PWS patients with maternal uniparental disomy (179). In the PWS/AS imprinting domain, the paternal allele replicates earlier than the maternal

allele (179). To study replication timing of the PWS/AS imprinting domain in the AS-IC m^{an}/p^{+} imprinting defect mice, FISH was performed using interphase nuclei from the liver of neonatal wild type and AS-IC m^{an}/p^{+} imprinting defect mice. The hybrid slides were observed under confocal microscope and cells with SS, SD and DD signatures were counted from three individual slides (Figure 3-21a-b). In wild type mice, the *Ndn* and PWS-IC regions showed asynchronous replication with more than 30% of cells detected with SD signature. In AS-IC m^{an}/p^{+} imprinting defect mice, the percentage of cells containing SD signature decreased, suggesting that the difference of replication timing between two alleles is not as obvious as that of wild type mice. The inserted targeting vector reduces the differential replication timing at the PWS/AS imprinting domain in AS-IC m^{an}/p^{+} imprinting defect mice.

The SS signature signifies that the probe detects the individual sequence on each of the homologous chromosomes before replication in the cell cycle, while the SD signature indicates that the sequence has replicated on only one allele, and DD signature indicates that both alleles has completed replication (200). Interestingly, in AS-IC m^{an}/p^{+} imprinting defect mice, the percentage of SS cells was increased regardless of whether it was detected with PWS-IC or *Ndn* probe, indicating that the replication timing of both loci in S phase is delayed compared to that of wild type mice (Figure 3-21c). This observation suggests that insertion of the targeting vector not only reduces the differential replication timing but also delays the replication of PWS/AS imprinting domain. It is likely that the decrease of differential replication timing in AS-IC m^{an}/p^{+} imprinting defect mice is not due to accelerating replication of the maternal allele, but is caused by delay of DNA replication of the paternal allele (201).

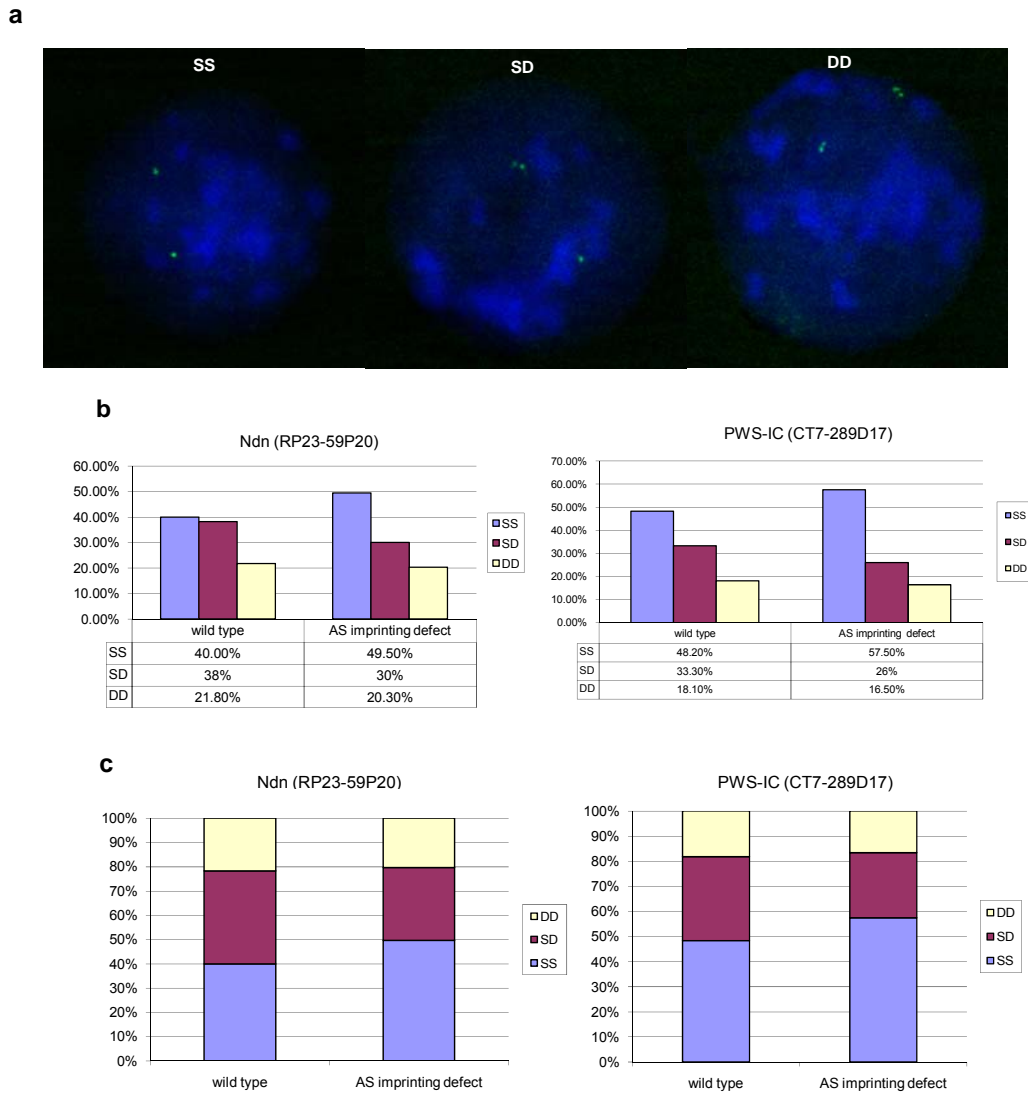


Figure 3-21 Differential replication timing is decreased at PWS/AS domain in AS-IC m^{an}/p^{+} imprinting defect mice FISH analysis was carried out in mice liver nuclei using SpectrumGreenTM labeled RP23-59P20 which overlaps *Ndn* and in another experiment using CT7-289D19 which overlaps the PWS-IC. In each experiment, at least 100 cells were analyzed by counting SS, SD and DD signatures. For each probe, the percentage of cells with SS signature is presented as a blue column, the percentage of cells with SD signature as a purple column and the percentage of cells with DD signature as a yellow column. **a.** Representative nuclei having two unreplicated alleles (SS), one replicated and one unreplicated alleles (SD) and both alleles replicated (DD). **b.** The percentage of cells having SS, SD and DD signatures in wild type and AS-IC m^{an}/p^{+} imprinting defect mice at the *Ndn* (RP23-59P20) and PWS-IC (CT7-289D17) loci in clustered column format. In AS-IC m^{an}/p^{+} imprinting defect mice, the cells containing SD signature is reduced as compared to that of wild type mice. **c.** The percentage of cells having SS, SD and DD signatures in wild type and AS-IC m^{an}/p^{+} imprinting defect mice at the *Ndn* (RP23-59P20) and PWS-IC (CT7-289D17) loci in stacked column format. The stacked column obviously indicates that the replication timing of *Ndn* and the PWS-IC is delayed in AS-IC m^{an}/p^{+} imprinting defect mice compared to that of wild type mice.

3.3.6 Biallelic interaction between the PWS-IC and Ndn in AS imprinting defect mice

Direct physical interactions and looping have been shown at the *H19/Igf2* imprinting domain. The physical interactions of the DMRs of *H19* and *Igf2* regulate the maternal and paternal chromatin into distinct loops, and thus leading to allelic expression of *Igf2* (114). It is still unclear how the PWS-IC and the AS-IC control the epigenetic dimension of such interaction. Chromosome conformation capture (3C) was carried out using cerebellum from wild type mice in C57BL/6J background to explore the potential long range interaction of the PWS-IC and *Ndn*, spanning 1.5 Mb apart. Figure 3-22 showed that *Bgl*III could digest fixed chromatin efficiently and the quality of the ligated DNA is good. PCR primers around *Bgl*III sites from *Ndn* and the PWS-IC region were designed (Figure 3-23a) and PCR experiments with various primer combinations were performed. PCR reaction of primer combination AH50 from *Ndn* and AH52 from the PWS-IC region reproducibly generated PCR products with expected length (Figure 3-23b). Sequence analysis of the amplified PCR product revealed a 133-bp sequence that matches 74-bp from the PWS-IC region and 59-bp from *Ndn* region (Figure 3-23c), suggesting that there is a physical interaction between the PWS-IC and *Ndn* gene.

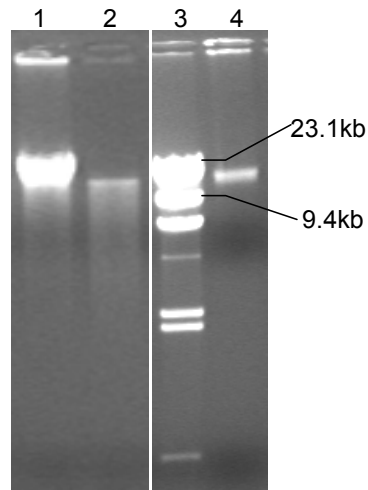


Figure 3-22 Electrophoresis of DNA derived from *Bgl/II* digested chromatin and 3C assay
 Freshly dissected cerebellum was meshed into DMEM media through a strainer and fixed with formaldehyde. The fixed chromatin was digested with *Bgl/II* overnight. An aliquot was reversed cross-linking to examine the digestion efficiency. Another aliquot was used to conduct 3C assay. Ligated DNA was reversed cross-linked and electrophoresed in a 1% agarose gel. Lane 1: DNA derived from chromatin without digestion; lane 2: DNA derived from chromatin after *Bgl/II* digestion; lane 3: λ DNA/*HindIII*; lane 4: 3C DNA.

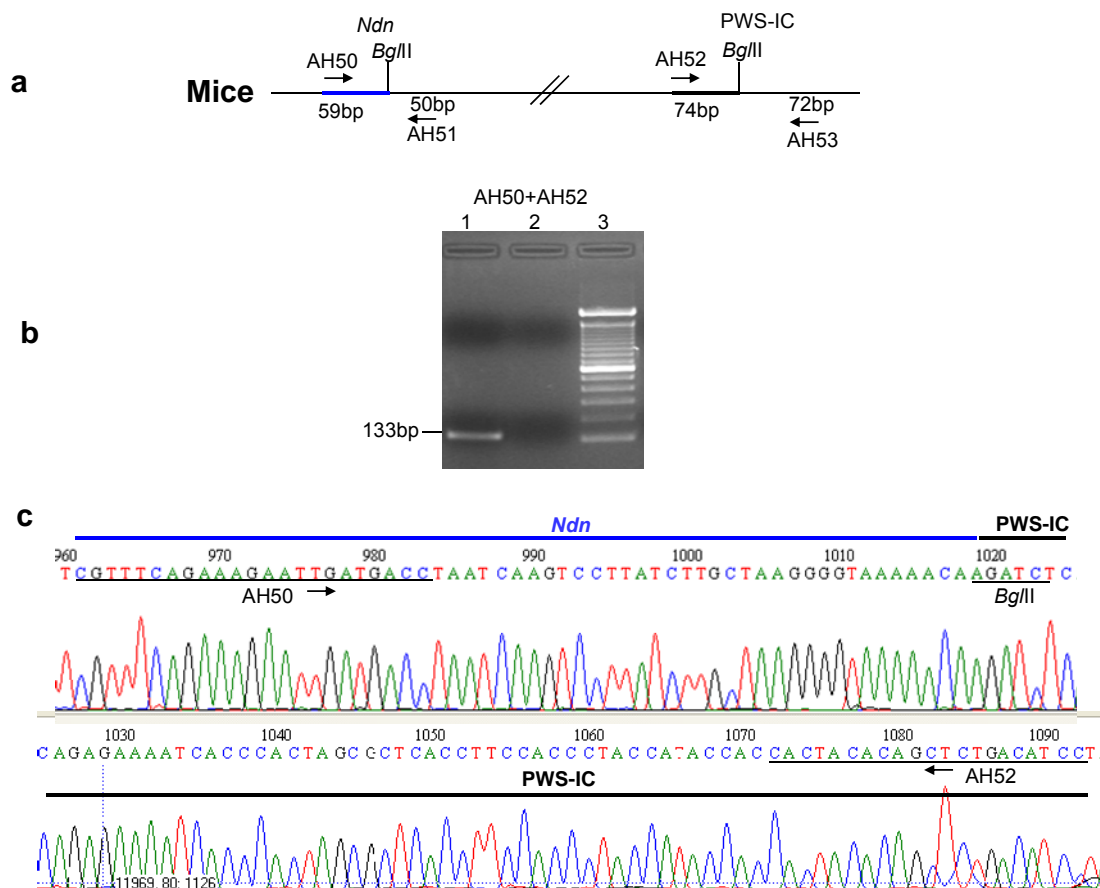


Figure 3-23 Interaction between the PWS-IC and *Ndn* in cerebellum of mice detected by 3C assay
a. Orientation of primers (arrows) and their distances to the *Bgl*II sites in *Ndn* and the PWS-IC regions are depicted. **b.** PCR products from 3C assay using primers combinations AH50 and AH52. Primer combination is shown above the agarose gel photograph. All individual PCR experiments were conducted three times using different batches of 3C assay DNA. Lane 1: PCR product of AH50-AH52; lane 2: no template control; lane 3: 100 bp ladder (Invitrogen). **c.** The sequence of the 133-bp PCR product obtained with primers AH50 in *Ndn* gene and AH52 in the PWS-IC region. Blue line indicates the DNA sequence derived from *Ndn* gene and black line indicates the DNA sequence derived from PWS-IC region.

Maternal inheritance of an AS-IC^{an} allele generated by insertion of a targeting vector 13 kb upstream of the PWS-IC along with a 6-kb genomic DNA duplication leads to AS imprinting defect. This suggests that the mouse AS-IC may locate within the 6-kb genomic region. Therefore, primers around the *Bgl*II sites within the 6-kb region were designed, combining with primers around the *Bgl*II site in *Ndn* gene to detect the potential interactions using 3C assay. However, no PCR product was generated from

these primers combinations (Figure 3-24a). In human, the AS-IC is located about 35 kb upstream from the PWS-IC, so the AS-IC of mice may not be limited to the 6-kb region, and may be located further upstream. Insertion of the targeting vector may influence its function by changing chromosome conformation. Therefore, primers around the *Bgl*II sites further upstream, one located 34 kb upstream from the PWS-IC, the other located 65 kb upstream from the PWS-IC, were combined with primers around the *Bgl*II sites in *Ndn* and the PWS-IC to detect the potential interactions using 3C assay (Figure 3-24b). No PCR product of expected size was obtained.

Ube3a is a tissue-specific maternally expressed imprinting gene (125, 202) and AS-IC may control its imprinting by direct physical interaction. Primers around *Bgl*II sites in the *Ube3a* gene were designed. One set of primers was at the 5' end of *Ube3a* and the other set was at the 3' end of *Ube3a* (Figure 3-24c). Primers from the 6-kb region and the PWS-IC region were combined with primers from *Ube3a* gene to perform 3C assay, and no expected PCR product was produced. These 3C assay results indicate that the AS-IC may not locate within these regions or it does not control its targeting genes by direct physical interaction.

3.3.7 Human PWS-IC and NDN physically interact

The PWS/AS imprinting domain is conserved between human and mice. To study whether the physical interaction of the PWS-IC and *Ndn* gene also occur in human, 3C assay was carried out using human untransformed fibroblast cell lines GM00364, GM09255 and GM04503. Primers around *Bgl*II sites in *NDN* and the PWS-IC regions were designed and PCR were carried out with various primer combinations. The primer combination of AH66 from *NDN* gene and AH71 from the PWS-IC region

generated a 140-bp PCR product of expected size (Figure 3-25). The sequencing result confirmed that the PCR product contained 39 bp from *NDN* gene and 101 bp from the PWS-IC region. This PCR product can be detected in all three human fibroblast cell lines tested. Therefore, it is concluded that the physical interaction of the PWS-IC and *NDN* gene is conserved between human and mice, and thus, the epigenetic interaction between the PWS-IC and *Ndn* may be required for the establishment and/or maintenance of the paternal specific chromatin conformation.

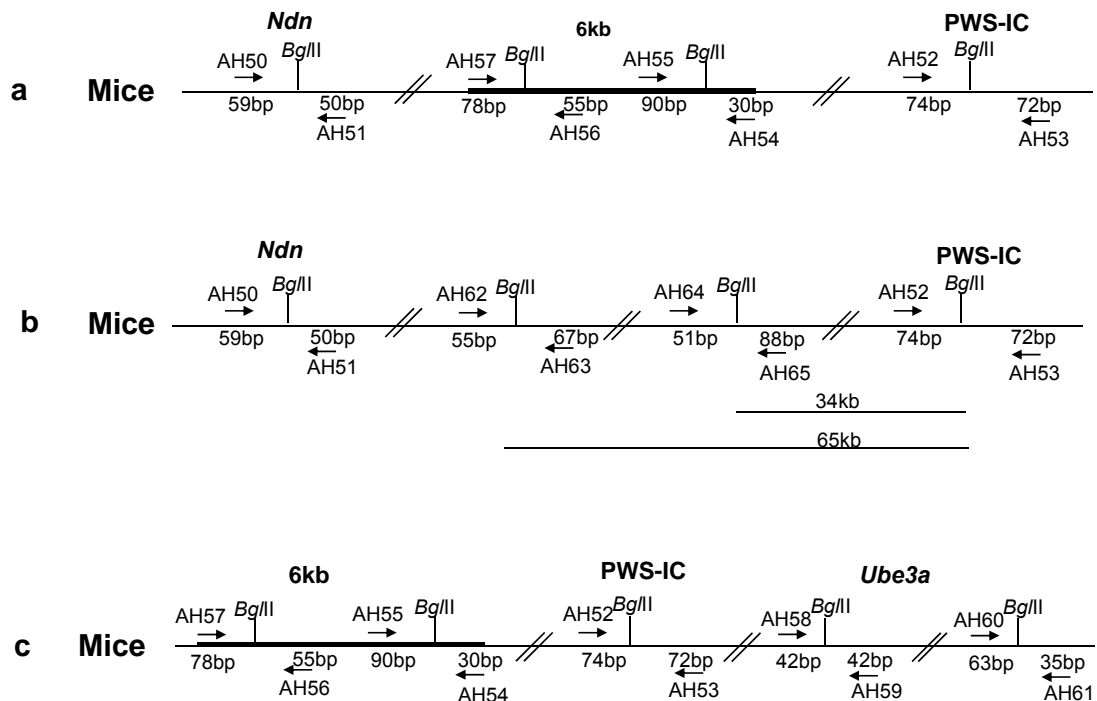


Figure 3-24 3C assay failed to detect other physical interactions in PWS/AS domain **a.** Orientation of primers (arrows) and their distances to the *Bgl*III sites in *Ndn* gene and the 6-kb region located 13 kb upstream from PWS-IC and PWS-IC regions. The thicker horizontal line indicates the 6-kb region. **b.** Orientation of primers (arrows) and their distances to the *Bgl*III sites in *Ndn* gene and the *Bgl*III sites adjacent to the PWS-IC region. The shorter horizontal line indicates 34 kb and the longer horizontal line indicates 65 kb. **c.** Orientation of primers (arrows) and their distances to *Bgl*III sites in the 6-kb region located 13 kb upstream of the PWS-IC and the *Bgl*III sites in *Ube3a* gene. The thicker horizontal line indicates the 6-kb region.

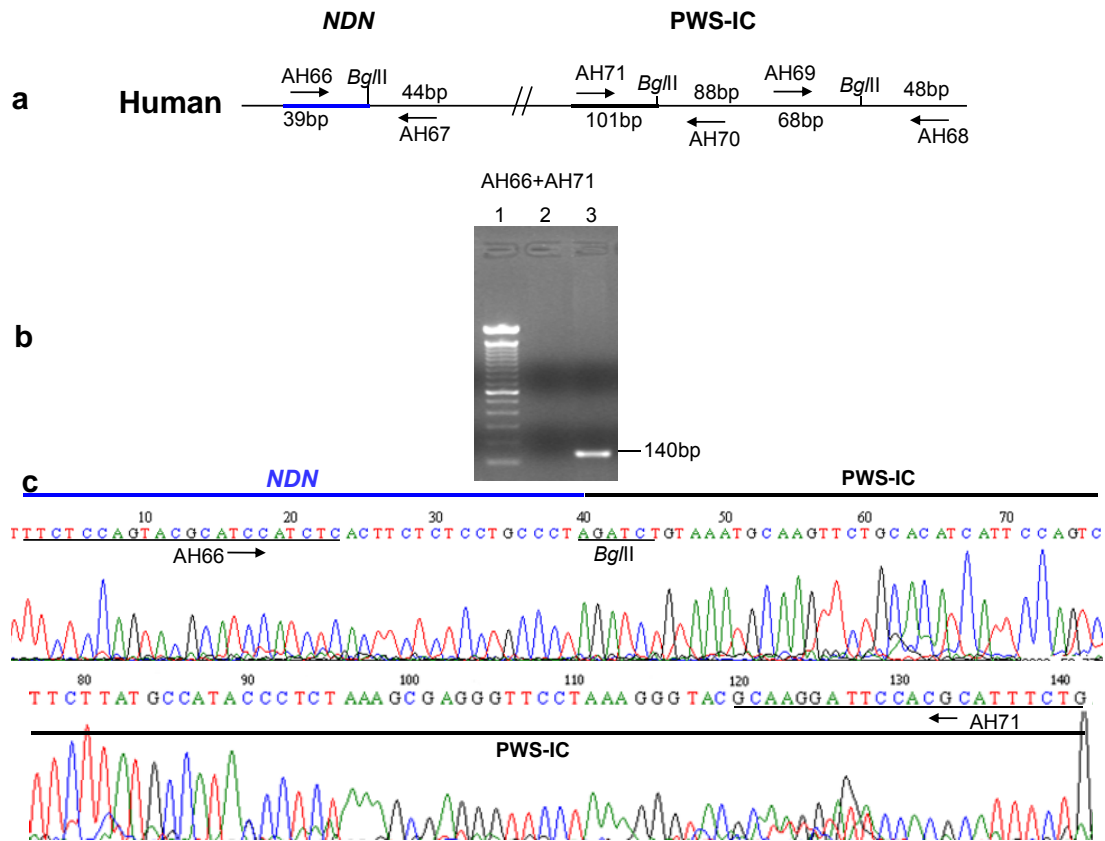


Figure 3-25 Interaction between PWS-IC and *NDN* gene in human fibroblast cells detected by 3C assay **a.** Orientation of primers (arrows) and their distances to the *Bgl*/II sites in *NDN* and the PWS-IC region are depicted. **b.** PCR products from 3C using primers combinations AH66 and AH71. Primer combination is shown above the agarose gel photograph. All individual PCR experiments were performed three times using different batches of 3C assay DNA. Lane 1: 100 bp ladder (Invitrogen); lane 2: no template control; lane 3: PCR product of AH66-AH71. **c.** The sequence of the 140-bp PCR product obtained with primers AH66 in *NDN* gene and AH71 in the PWS-IC region. Blue line indicates the DNA sequence derived from *NDN* gene and black line indicates the DNA sequence derived from the PWS-IC region.

Allele-specific interactions between *H19* DMR and *Igf2* DMRs have been demonstrated in mouse (114). To study whether the interaction of the PWS-IC and *Ndn* is allele-specific, (129/SvEv and PWK/PhJ reciprocal cross) F1 wild type mice were used for 3C assay. F1 AS-IC m^{an}/p^{+} (129/SvEv AS-IC^{+/an} female × PWK/PhJ male) hybrid mice with imprinting defect was also used for 3C assay to investigate whether there is any difference when compared to wild type mice. There is no

nucleotide polymorphism between 129/SvEv and PWK/PhJ around the *Bgl*II sites used previously in both *Ndn* and PWS-IC region, so the *Bgl*II sites cannot be used for 3C assay. Since not all the restriction enzymes can digest fixed chromatin efficiently, several restriction enzymes (*Pst*I, *Bam*HI, *Sac*I, *Xba*I, *Nde*I, *Sph*I, *Nco*I) near the polymorphisms between 129/SvEv and PWK/PhJ were screened for their ability to digest fixed chromatin (Figure 3-26). Among them, only *Nco*I can digest fixed chromatin efficiently; hence *Nco*I was used for subsequent 3C assay. Primers around the *Nco*I sites were designed from both the *Ndn* and PWS-IC region. Primers around the *Nco*I site in PWS-IC region span a single nucleotide polymorphism T→G between 129/SvEv and PWK/PhJ (Figure 3-27a). Primer combination of AH96 from the PWS-IC region and AH97 from *Ndn* gene generated the expected-size PCR products for all the DNA samples from F1 mice. AH96-AH97 PCR products were sequenced directly. The sequencing results showed that PCR products derived from (129/SvEv female × PWK/PhJ male) F1 wild type mice were from PWK/PhJ allele, and the PCR products derived from (PWK/PhJ female × 129/SvEv male) F1 wild type mice were from 129/SvEv allele, while the PCR products derived from (129/SvEv AS-IC^{+/an} female × PWK/PhJ male) F1 AS-IC m^{an}/p⁺ mice with imprinting defect were from both alleles (Figure 3-27b). These results indicate that the physical interaction of the PWS-IC and *Ndn* is paternal specific; however, in AS-IC m^{an}/p⁺ imprinting defect mice, the imprinting establishment and/or maintenance process of the maternal allele is abolished, and thus the maternal allele carries a paternal epigenotype, gaining the paternal specific chromatin loop.

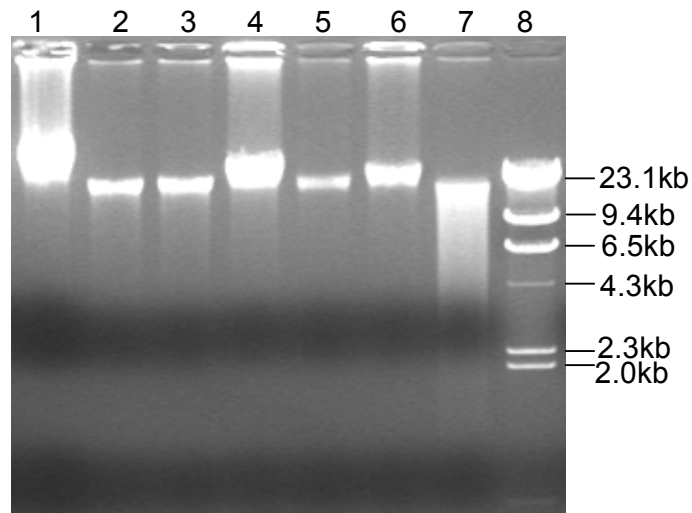


Figure 3-26 Restriction enzymes digest fixed chromatin with different efficiency Formaldehyde fixed nuclei (about 1×10^6) were extracted from freshly dissected mice cerebellum and then digested with *Xba*I, *Nde*I, *Sph*I, *Nco*I, respectively. Digested and original chromatin was reversed cross-linked and then DNA was electrophoresed in a 1% agarose gel. Lane 1: DNA from original chromatin; lanes 2 and 3: DNA from chromatin digested with *Xba*I; lanes 4 and 5: DNA from chromatin digested with *Nde*I; lane 6: DNA from chromatin digested with *Sph*I; lane 7: DNA from chromatin digested with *Nco*I; lane 8: λ /*Hind*III.

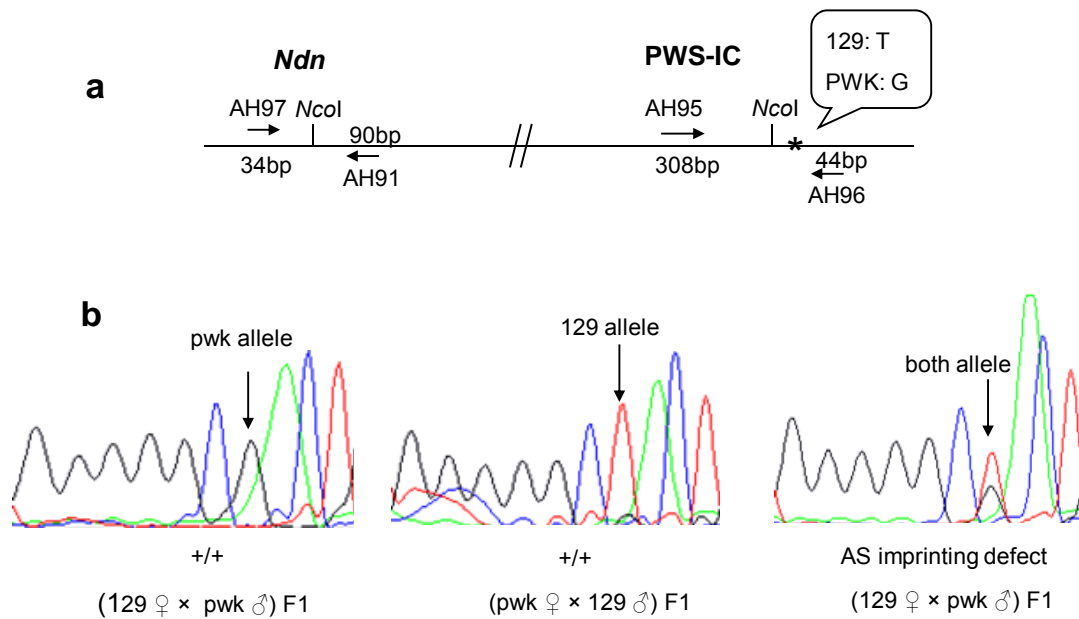


Figure 3-27 Interaction of the PWS-IC and *Ndn* is paternal-specific **a.** Orientation of primers (arrows) and their distances to *NcoI* sites in *Ndn* and the PWS-IC region are depicted. Asterisk indicates the location of T→G polymorphism. **b.** Depicted on the left chromatograph is AH97-AH96 PCR product derived from (129/SvEv female × PWK/PhJ male) F1 wild type mice, showing that only the paternally inherited PWK/PhJ allele is detected; the middle chromatograph shows the AH97-AH96 PCR product derived from (PWK/PhJ female × 129/SvEv male) F1 wild type mice, indicating that only the paternally inherited 129/SvEv allele is detected; the right chromatograph shows AH97-AH96 PCR product derived from (129/SvEv AS-IC^{+an} female × PWK/PhJ male) F1 AS-IC m^{an}/p⁺ mice with imprinting defect, indicating biallelic detection.

3.4 Mechanisms causing imprinting defect in AS-IC m^{an}/p⁺ mice

3.4.1 Effect of inserted active promoter on imprinting

Maternal transmission of an 80-kb deletion extending from the site of the AS-IC^{an} mutation shows either a normal methylation pattern, partial lack of methylation, or complete loss of methylation at *Snurf-Snrpn* DMR (181). Both the 80-kb deletion and the AS-IC^{an} mutation integrate promoters at 13 kb upstream of *Snurf-Snrpn* exon 1 on mouse chromosome 7. In mice carrying the 80-kb deletion, there is a phosphoglycerate kinase (PGK) promoter driving a *Hprt* minigene which is in the

same orientation as *Snurf-Snrpn* promoter. In mice carrying the AS-IC^{an} mutation, there is a PGK promoter driving a *puromycin* gene in the opposite orientation as *Snurf-Snrpn* promoter. It is possible that promoter activities from targeting vectors cause AS imprinting defect in both 80-kb deletion and AS-IC^{an} mouse lines. The activity of promoters may convert the inactive closed maternal chromatin to an active and open state, and thus make the maternal allele of PWS-IC accessible to transcriptional factors. To study the *puromycin* promoter activity in AS-IC^{an} mutation mouse line, RT-PCR was carried out using the RNA from liver or cerebellum of wild type mice, AS-IC m⁺/p^{an} mice, AS-IC m^{an}/p⁺ mice with imprinting defect, AS-IC m^{an}/p⁺ mice with normal methylation patterns and AS-IC^{an/an} homozygotes. It was found that *puromycin* gene was expressed in the liver and cerebellum of AS-IC m⁺/p^{an} and AS-IC^{an/an} mice (Figure 3-28, sample 2 and 5), as well as in the cerebellum of AS-IC m^{an}/p⁺ mice with imprinting defect (Figure 3-28, sample 3); but it was neither expressed in liver nor in cerebellum of AS-IC m^{an}/p⁺ mice with normal methylation patterns (Figure 3-28, sample 4). These results indicate that *puromycin* expression from maternal allele in cerebellum may contribute to the AS imprinting defect among AS-IC m^{an}/p⁺ mice. Real time PCR was performed to compare the *puromycin* expression levels in the cerebellums of AS-IC m^{an}/p⁺ imprinting defect mice and AS-IC m⁺/p^{an} mice. It was found that *puromycin* expression level in the cerebellum of AS-IC m^{an}/p⁺ imprinting defect mice was about one-fourth of the expression level in AS-IC m⁺/p^{an} mice (Figure 3-29). The result suggests that although the *puromycin* gene is expressed from maternal allele, the expression level is lower than that of paternally inherited allele.

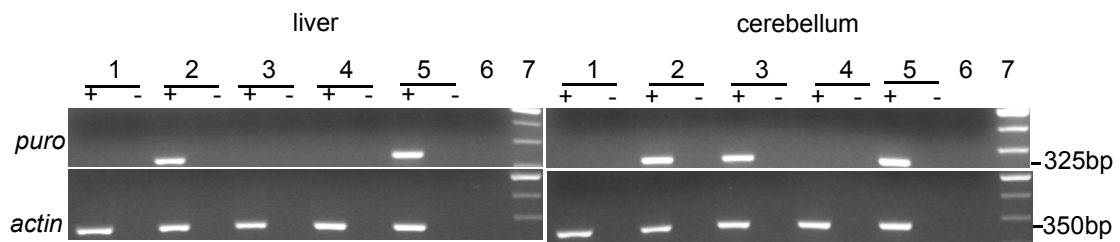


Figure 3-28 Analysis of *puromycin* gene expression in mice liver and cerebellum Total RNA extracted from liver and cerebellum of mice was analyzed by RT-PCR using *puromycin* gene-specific primers. β -actin was used as an endogenous control. 1: wild type mice; 2: AS-IC m^{+}/p^{an} mice; 3: AS-IC m^{an}/p^{+} mice with imprinting defect; 4: AS-IC m^{an}/p^{+} mice with normal methylation patterns; 5: AS-IC m^{an}/p^{an} homozygous mice; 6: no template control; 7: 100 bp ladder. +: RT positive; -: RT negative.

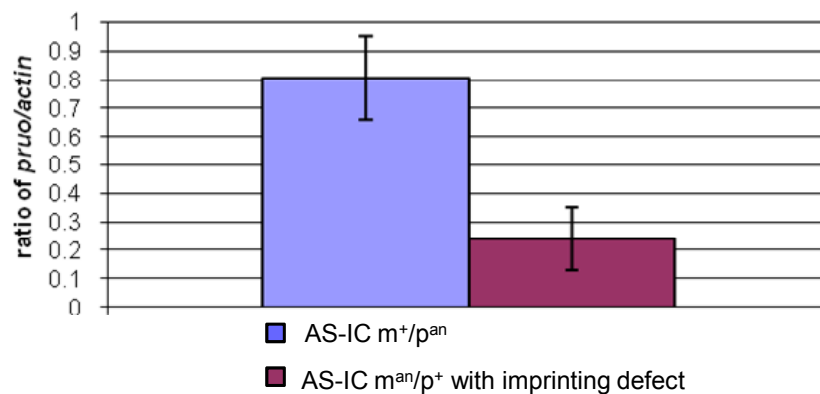


Figure 3-29 Real time PCR quantification of *puromycin* gene expression in mice cerebellum. Total RNA from cerebellum of AS-IC m^{+}/p^{an} and AS-IC m^{an}/p^{+} imprinting defect mice was used for real time PCR by standard curve method using β -actin as endogenous control. The expression level of *puromycin* gene in the cerebellum of AS-IC m^{an}/p^{+} imprinting defect mice is about 1/4 of the expression level in the cerebellum of heterozygous mice with paternally inherited AS-IC^{an} mutation.

3.4.2 *Snurf-Snrpn* upstream exons are spliced with 3'*Hprt* exons

Human 3' *Hprt* exons 3-9 was inserted into mouse genome with the targeting vector (pG12H6) in AS-IC^{an} mouse line (181). The 3' *Hprt* exons 3-9 has the splicing acceptor sequence, and can be spliced to 5' *Hprt* exons 1-2 to work as a selection marker. RT-PCR was performed using cerebellum RNA from two AS-IC m^{an}/p^{+}

imprinting defect mice and one AS-IC m^+/p^{an} mouse. Locations and orientation of primers used for RT-PCR are showed in Figure 3-30. Several PCR products were generated and sequenced. Sequencing results showed that three splicing patterns were obtained from AS-IC m^{an}/p^+ imprinting defect mice; alternative spliced transcripts II and III were obtained from the AS-IC m^+/p^{an} mice (Figure 3-30). The other PCR products appear to be heteroduplex. These results indicate that the 3' *Hprt* exons 3-9 can be spliced to *Snurf-Snrpn* upstream exons. The splicing may abolish *Snurf-Snrpn* upstream transcripts with certain splicing forms. For example, the 516 bp alternative splicing form I in Figure 3-13a was not detected from the maternal allele in AS-IC m^{an}/p^+ imprinting defect mice. It is possible that the U exons are alternatively spliced together with the 3' *Hprt* exons and is detected as the transcript represented as splicing form II as shown in Figure 3-30. These transcripts may play critical roles in AS imprinting establishment and/or maintenance.

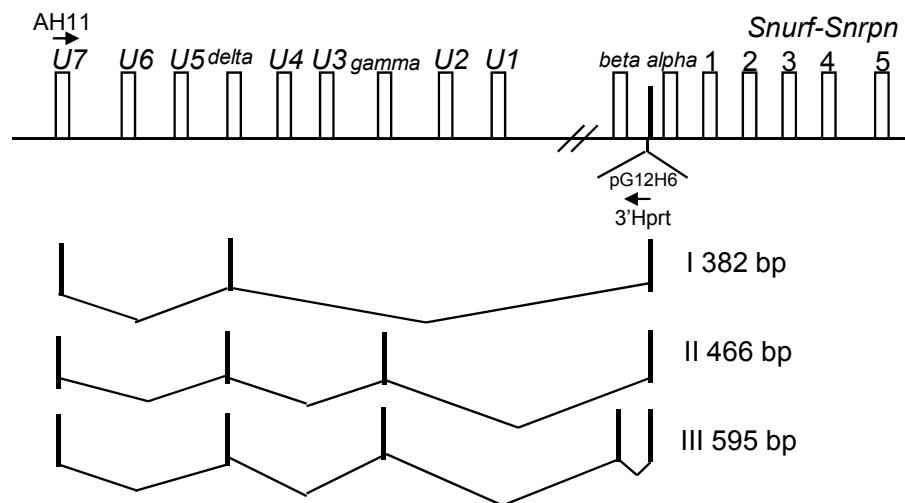


Figure 3-30 *Snurf-Snrpn* upstream exons are spliced with 3'*Hprt* exons Schematic presentation of *Snurf-Snrpn* upstream exons, 3'*Hprt* exons from targeting vector and various splicing patterns. *Snurf-Snrpn* exons 1-5 and *Snurf-Snrpn* upstream exons are shown as small columns. Arrows indicate primers orientation and locations. I, II and III are three splicing patterns between U exons and 3'*Hprt* exons. Location of the targeting vector pG12H6 is indicated.

3.4.3 A new targeting vector was constructed to delineate the mechanism of AS-IC^{an} imprinting defect

As mentioned previously, at least three mechanisms may explain the cause of imprinting defect upon maternal inheritance of the AS-IC^{an} allele. First, the promoter activity from the insertion vector may interfere with the *Snurf-Snrpn* upstream transcripts and disturb its role in establishing and/or maintaining of imprinting marks on maternally inherited chromosome (169, 182). Second, the insertion of the targeting vector may destroy the elements of AS-IC and thus leads to AS imprinting defect. Alternatively, the 6-kb duplication generated from homologous recombination may interfere with the AS imprinting process. These mechanisms are not necessary mutually exclusive. To determine the exact mechanisms involved, a new targeting vector pCMVH6 containing sequences from 129/SvEv genome, positive selection maker (neomycin resistant gene) and negative selection marker (TK) was constructed (Figure 3-31a). The new targeting vector is designed to integrate a CMV promoter driven β -geo gene with a reverse orientation to the *Snurf-Snrpn* promoter at the same locus as pG12H6, but will not generate chromosomal duplication. To verify in vivo expression of β -galactosidase, the new targeting vector was first transfected into human cell line HEK293F. Transfected cells were stained with X-gal. Blue color was observed in the positive control and the pCMVH6 transfected cells, indicating the expression of β -galactosidase gene in these cells (Figure 3-31b). Expression of β -geo, which is the fusion of neomycin resistant gene and β -galactosidase gene, was confirmed by Western blot with anti- β -galactosidase antibody. The molecular weight of β -galactosidase which was expressed in cells transfected with pCMVH6 was larger than that in cells transfected with pCMVSPORT β gal (Figure 3-32 a,b). This result

indicates that neomycin resistant gene and β -galactosidase gene are fused and expressed.

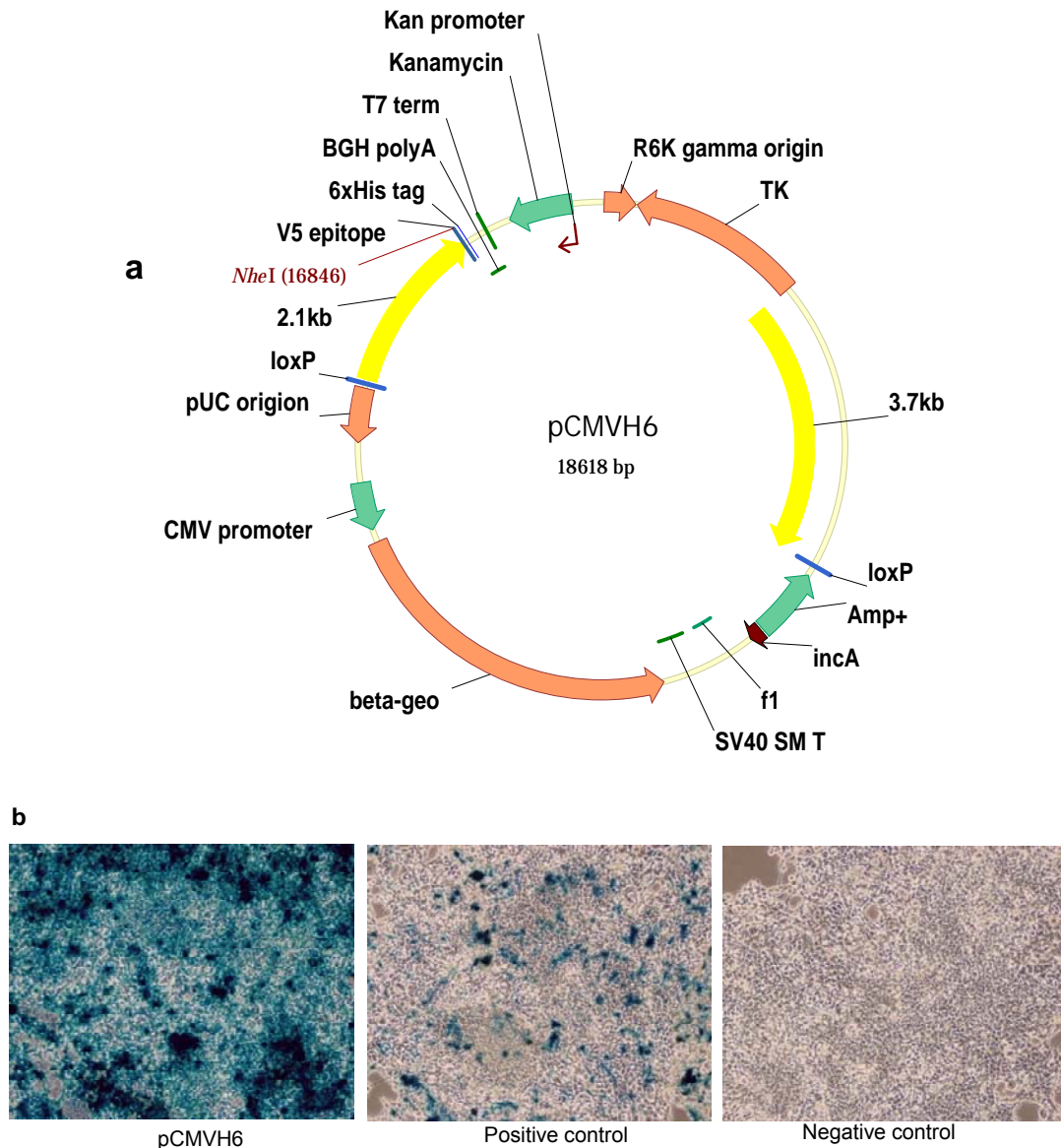


Figure 3-31 Analysis of β -galactosidase expression from the targeting vector **a.** Restriction map of the new targeting vector pCMVH6. **b.** Expression of β -galactosidase activity was visualized 48 hours after transfection of HEK293F cell with pCMVH6 (left), and transfection with the pCMVsport β gal plasmid was used as a positive control (middle). Lipofectamine and ddH₂O were used for transfection in negative control (right). Transfected cells were stained with X-gal. Cells transfected with pCMVH6 and pCMVsport β gal had β -galactosidase activity. No signal was detected in the negative control.

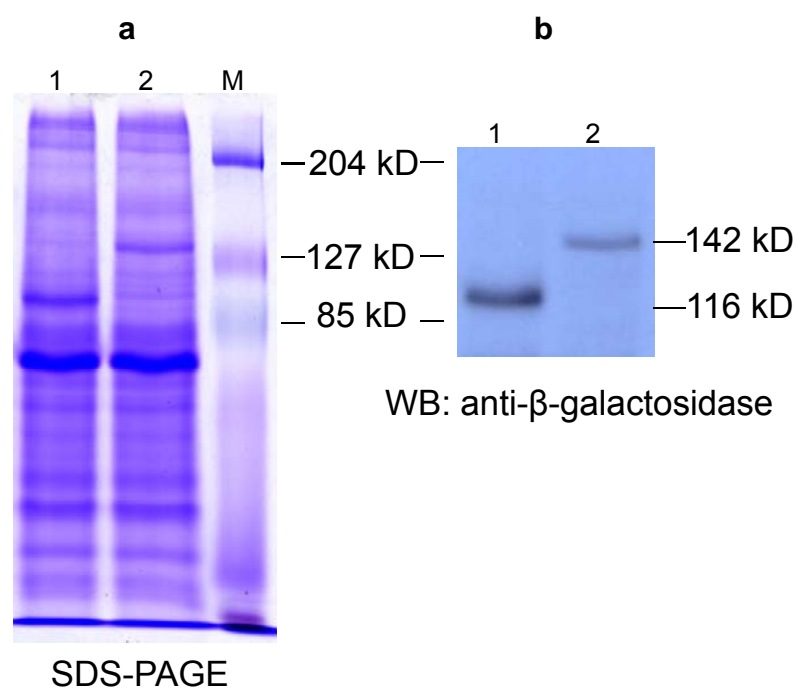


Figure 3-32 Expression of β -galactosidase gene and β -geo **a.** COS7 cells were transfected with pCMVH6 and pCMVSPORT β gal, and total cell lysate was separated in a 7.5% SDS-PAGE gel. Lane 1: cell lysate of pCMVSPORT β gal transfection; lane 2: cell lysate of pCMVH6 transfection. M: protein molecular weight standard. **b.** Western blot probed with anti- β -galactosidase antibody. The western blot results showed the expression of fused β -galactosidase and neomycin phosphotransferase genes.

Embryonic stem cells AB2.2 were electroporated with linearized pCMVH6. The targeting strategy of pCMVH6 was shown (Figure 3-33). The targeted region is detected as a 6-kb *Bam*HI fragment if there is no insertion, while it will be detected as a 9.5-kb *Bam*HI fragment after pCMVH6 insertion. Electroporations using the targeting vector were conducted 4 times and 600 colonies were picked and analyzed by Southern blot. However, no positive clone with the 9.5-kb *Bam*HI fragment was identified. PCR was also used to analyse these colonies. ES cell DNA was used for PCR with primers galA and galB which amplify a 250-bp fragment from the β -galactosidase gene of the targeting vector pCMVH6 (Figure 3-34). Among 96 DNA samples, 25 of them had 250-bp PCR products amplified, indicating that pCMVH6 is inserted into the ES cell genome. Primers AHF1 and AHR1 amplify the 5' junction of the vector as shown in Figure 3-33. Among those 25 galA-galB PCR positive DNA

samples, 19 of them generated PCR products with primers AHF1 and AHR1 (Figure 3-35a). Primers AHF2 and AHR2 amplify the 3' junction of the vector. Seven out of 19 AHF1 and AHR1 PCR positive DNA samples generated PCR products with primers AHF2 and AHR2 (Figure 3-35b). PCR with AHF2 and BXR4 did not generate any PCR product, indicating that none of the colonies have the desired insertion of the targeting vector. To further confirm the results, these 7 ES cell colonies were expanded in 6-well plates. DNA extracted from the 6-well plate culture was used for Southern blot with the probe described in Figure 3-33. Southern blot did not detect any hybridization band at 9.5 kb, suggesting that targeting vector inserts into ES cell genome randomly in these 7 colonies. All these results suggested that the screening system or the structure of the targeting vector may need to be optimized.

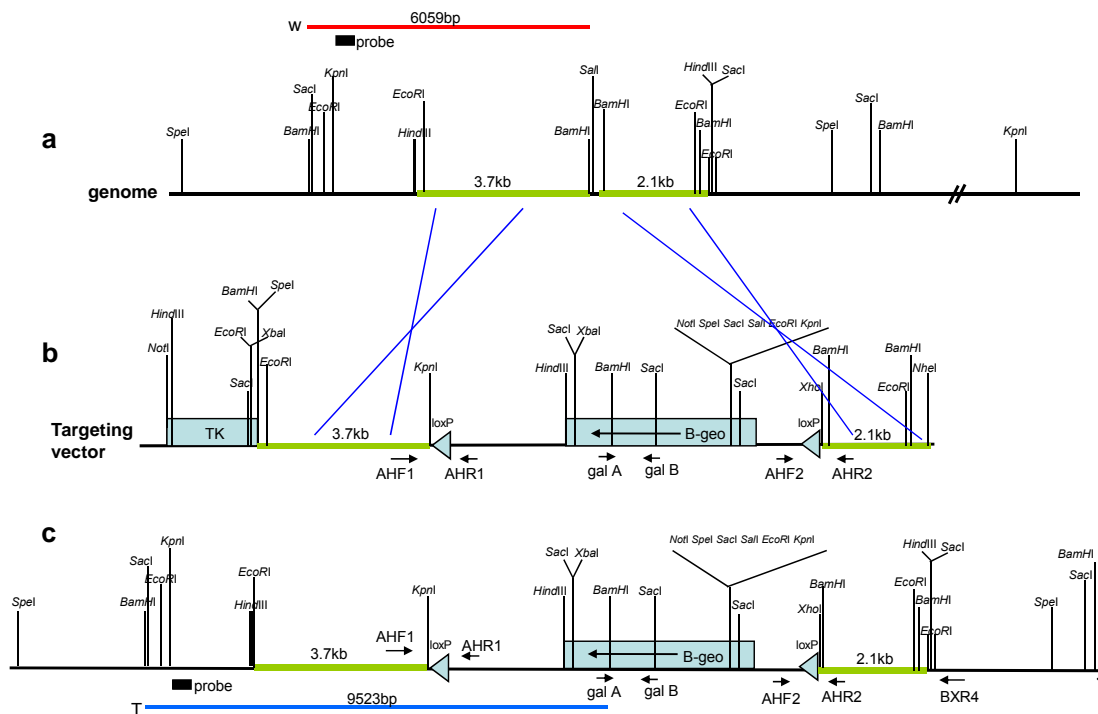


Figure 3-33 Schematic representation of pCMVH6 targeting strategy **a.** Restriction map of mice genomic region located 13 kb upstream of *Snurf-Snrpn* exon 1. 3.7 kb and 2.1 kb homologous arms are indicated with green color. **b.** The targeting construct was designed to insert β -geo into the mouse genome through homologous recombinations between homologous arms of the vector and mouse genomic DNA. The constructs include positive (*neo*) and negative (*TK*) selection cassettes. **c.** The targeted mouse locus following homologous recombinations. Black rectangle is the location of the probe used to identify homologous recombinants. The red line indicates the fragment detected as wild type allele (W) by the probe and the blue line indicates the fragment detected as targeted allele (T) by the probe. GalA and galB, AHF1 and AHR1, AHF2 and AHR2 are three sets of primers used for selection of positive colonies by PCR. AHF2 and BXR4 are used to confirm the desired insertion.

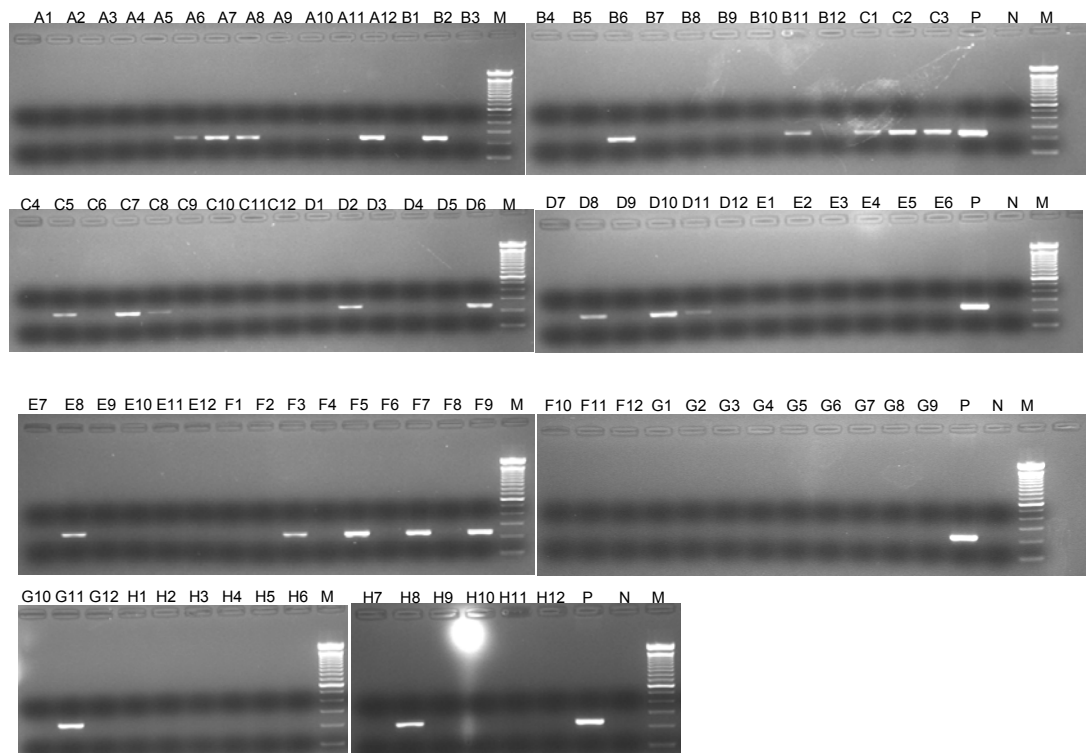


Figure 3-34 Selection of potential positive ES cell colonies by PCR β -galactosidase gene DNA was extracted from ES cells growing on a 96-well plate, and then was subjected to PCR with primers galA and galB. PCR products were electrophoresed in 2% agarose gels. Identification numbers of each ES cell colonies are labeled above the agarose gel photographs. P: pCMVH6 plasmid DNA used as the PCR positive control; N: no template control; M: 100 bp ladder (Invitrogen).

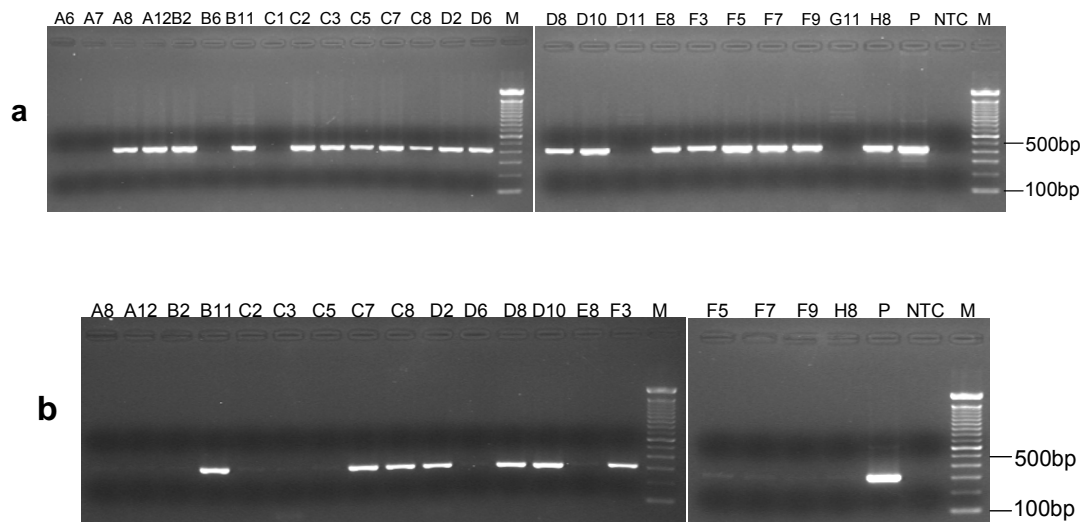


Figure 3-35 Selection of potential positive ES cell colonies by PCR 5' and 3' junctions a. PCR products amplified with AHF1 and AHR1 b. PCR products amplified with AHF2 and AHR2. P: pCMVH6 plasmid DNA was used as the PCR positive control; NTC: no template control; M: 100 bp ladder (Invitrogen).

3.5 Confirmation of PWS/AS deletion by microsatellite markers

The Prader-Willi and Angelman syndrome are two clinically distinct human neurogenetic diseases caused by the loss of function of oppositely imprinted genes in the chromosomal region 15q11-q13. To relay the animal project with actual examples of related human disease, DNA from eight PWS families were collected for genetic analysis.

Most of PWS and AS patients (65-75%) have a 4 Mb chromosome deletion of 15q11-q13 from either paternal or maternal allele (106). Some PWS cases (20%-30%) arise from maternal uniparental disomy (UPD) and a few AS cases (5%) arise from paternal uniparental disomy. Another 5% of PWS and AS patients have imprinting defect, and most of which are caused by microdeletion of IC. Among PWS and AS patients with deletion, there are four deletion types (203). The breakpoints (BP) of type I patients are BP1 (proximal) and BP3 (distal); those of type II patients are BP2 (proximal) and

BP3 (distal). Type I and type II are two major deletion types. The breakpoints of type III patients are BP1 (proximal) and BP4 (distal); those of type IV patients are BP1 (proximal) and BP5 (distal). Type III and type IV contribute to 5% of the PWS and AS patients with deletion. The clinical diagnosis of PWS and AS patients is evaluated by criteria derived from Holm *et al* (204). Cytogenetic techniques are frequently used for diagnosis of PWS/AS patients with common deletion. With probes in the critical region of PWS/AS domain, FISH is a quick and convenient method to screen whether there is a deletion at human chromosome 15q11-q13 (205). However, FISH can not be used as a single test for PWS or AS because it can not detect uniparental disomy, imprinting defect or translocation. Therefore, if there is no deletion detected by FISH, methylation specific PCR is used to determine whether there are methylation alterations. The microsatellite markers along the PWS/AS critical region make PCR diagnosis of UPD and determination of deletion size possible.

To further characterize the deletion breakpoints of these patients, 16 markers from chromosome 15q11-q13 were screened. Primers for microsatellite markers can be obtained from NCBI UniSTS database. The relative locations of the microsatellite markers are available from Ensembl. PCR products were first electrophoresed in 2% agarose gels to confirm the amplification, and then were fractionized by capillary electrophoresis (CE). Primers information is provided in Table 4 of the Appendices. Relative locations of these 16 markers are shown in Figure 3-36 and Figure 2 of Appendices.

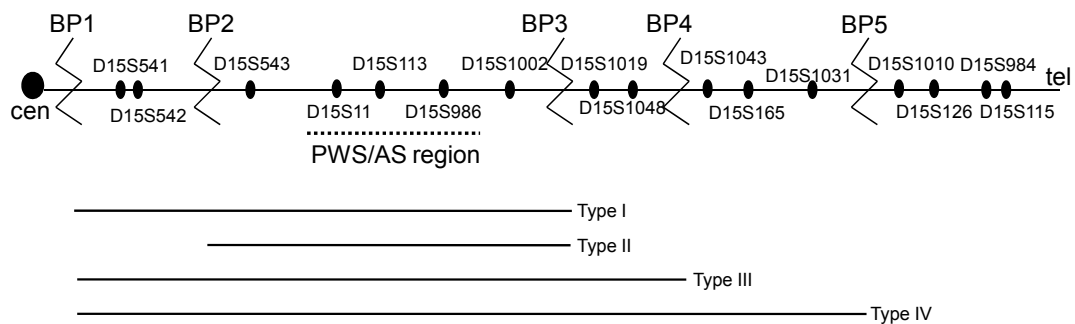


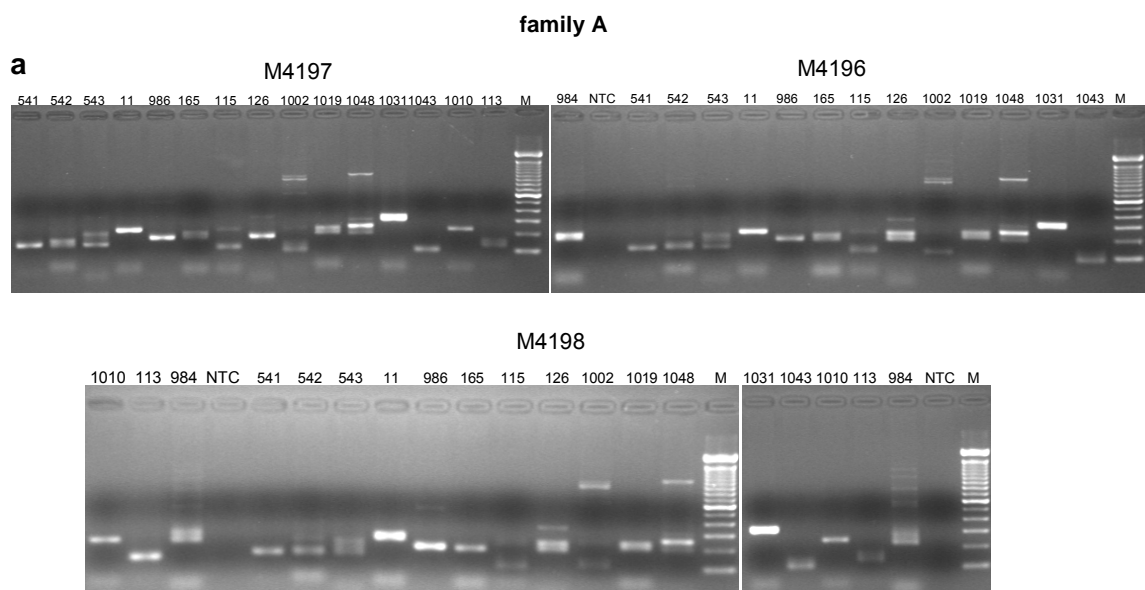
Figure 3-36 Schematic diagram showing locations of microsatellite markers Zigzag lines indicate the deletion breakpoints observed in PWS subjects. The deletion ranges of each deletion type are indicated. Adapted from Varela MC *et al* (203).

After capillary electrophoresis, the markers from patients were regarded as “normal” if they showed two alleles of distinct size and the two alleles were from mother and father, respectively. If the two alleles were both from one parent, the markers were regarded as “UPD”. The markers from patients showed only one size allele were scored as “deleted” (hemizygous) if inspection of the pedigree revealed noninheritance of a parental allele, or as “uninformative” if homozygosity could not be excluded. Table 3-1 shows genotyping data for family A. It is apparent that the patient inherited null alleles of D15S542, D15S113, D15S986 and D15S1002 from the father, which implies a deletion encompassing these markers. The patient inherited one allele each of D15S1031 and D15S984 from the father and the other allele from the mother, indicating that the patient has normal genotype at these markers. At D15S1019 and D15S1043, it is apparent that the patient inherited one allele from the father, given the fact that the patient has PWS, so the other allele should be derived from the mother. The rest of the markers were uninformative in this family. The agarose gel pictures of PCR products of all the markers and the CE profiles of all the informative markers are showed in Figure 3-37a-b. The diagnosis results of patient

M4196 are summarized in Figure 3-37c. Patient M4196 has deletion from BP1 to BP3 on the paternal chromosome 15 and belongs to type I deletion.

Table 3-1 Genotyping data for family A

Microsatellite markers	Allele size of microsatellite markers (bp)		
	Patient (M4196)	Father (M4197)	Mother (M4198)
D15S541	146	146	146
D15S542	148	142,154	148
D15S543	144	144	144,150
D15S11	244	244	244,260
D15S113	127	129,138	127,136
D15S986	188	182	188
D15S1002	144	103,118	105,144
D15S1019	205,222	205,222	205,218
D15S1048	199,221	199,221	199,226
D15S165	181,197	181,197	181
D15S1031	302,310	306,310	298,302
D15S1043	89,99	97,99	89,97
D15S1010	226,230	226	226,230
D15S126	185,205	185	185,205
D15S984	223,257	214,223	216,257
D15S115	109,113	113,115	92,109



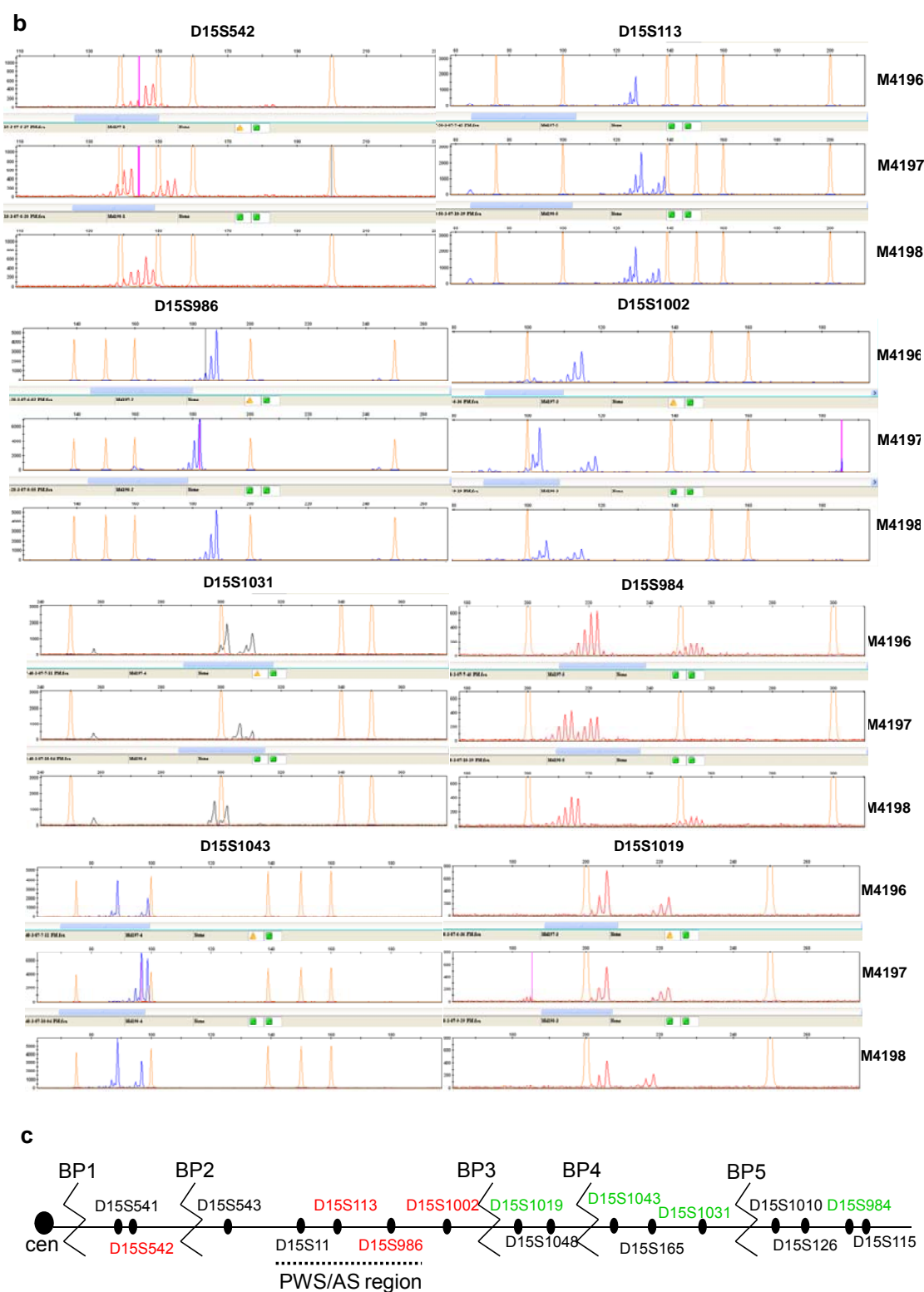
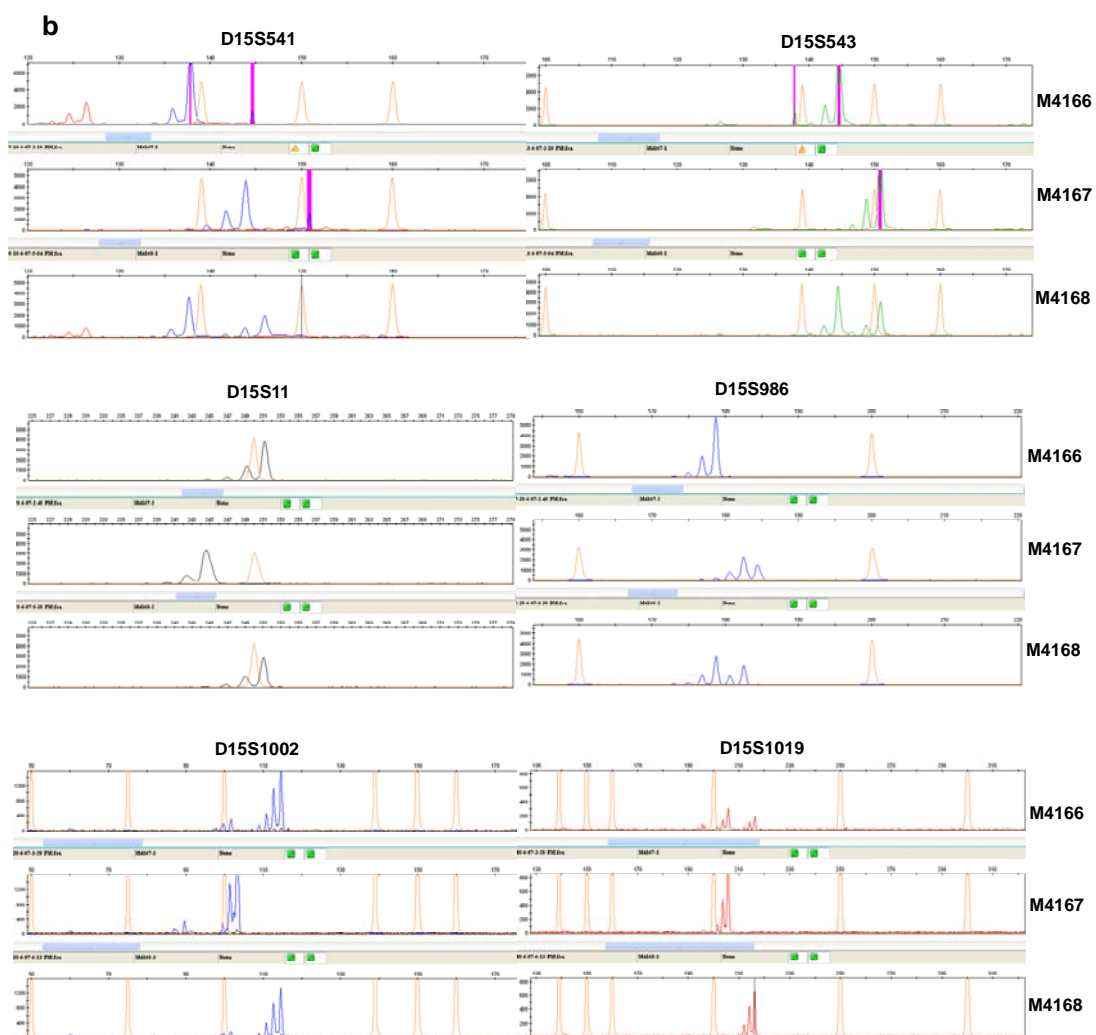
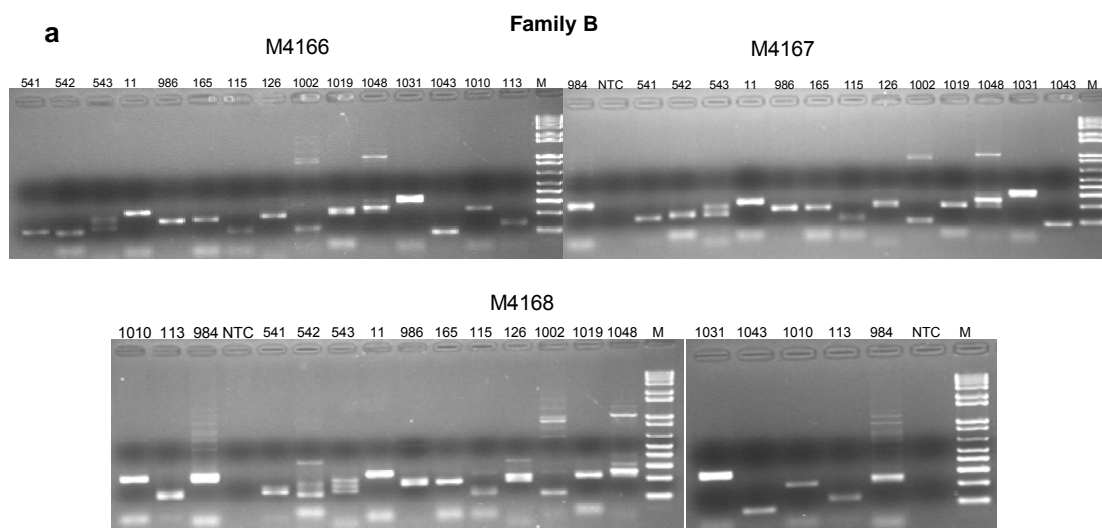


Figure 3-37 Diagnosis of patient M4196 from family A **a.** Agarose gel electrophoresis picture of PCR products from 16 microsatellite markers. M4196: patient; M4197: father; M4198: mother. M: 100 bp ladder. **b.** CE profiles of PCR products from the informative markers. Orange peaks represent GeneScan™-500LIZ™ size standard. **c.** Diagnosis results of patient M4196. Deleted markers are labeled in red. Normal markers are labeled in green. Non-informative markers are labeled in black. Patient M4196 has deletion from BP1 to BP3 on paternally inherited chromosome 15.

From genotyping data (Table 3-2) of family B, the patient inherited null alleles of D15S541, D15S543, D15S11, D15S986 and D15S1002 from the father, which implies a deletion encompassing these markers. The patient inherited one allele each of D15S1019, D15S1048, D15S1031, D15S1010 and D15S115 from the father and the other allele from the mother, indicating that the patient has normal genotype at these markers. The rest of the markers were uninformative in this family. The agarose gel pictures of PCR products of all the markers and the CE profiles of all the informative markers are showed in Figure 3-38a-b. Dignosis results are summarized in Figure 3-38c. Patient M4166 has deletion from BP1 to BP3 on paternally inherited chromosome 15 and belongs to type I deletion.

Table 3-2 Genotyping data for family B

Microsatellite markers	Allele size of microsatellite markers (bp)		
	Patient (M4166)	Father (M4167)	Mother (M4168)
D15S541	138	144	138,146
D15S542	126	153	126
D15S543	144	149,151	144,151
D15S11	251	245	251
D15S113	136	129,136	134,136
D15S986	179	184	179,183
D15S1002	115	103	115
D15S1019	206,216	206	216
D15S1048	214,224	199,224	214,222
D15S165	181,184	181,183	181
D15S1031	302,323	302,323	302,315
D15S1043	89	89	89
D15S1010	226,232	226,232	226
D15S126	197	197,205	185,197
D15S984	231,243	223,231	231,243
D15S115	110,112	112,116	110,116

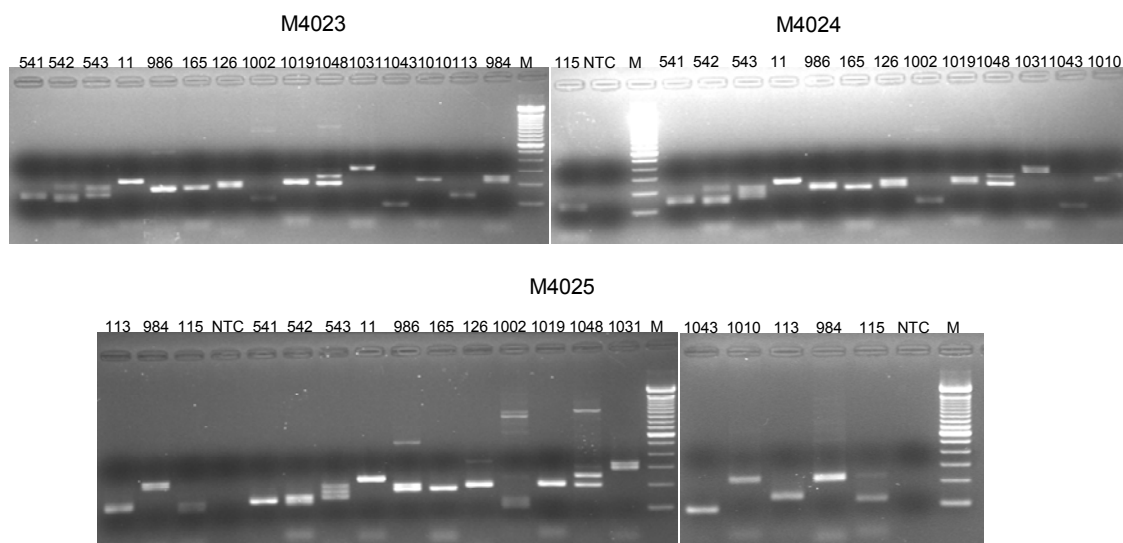


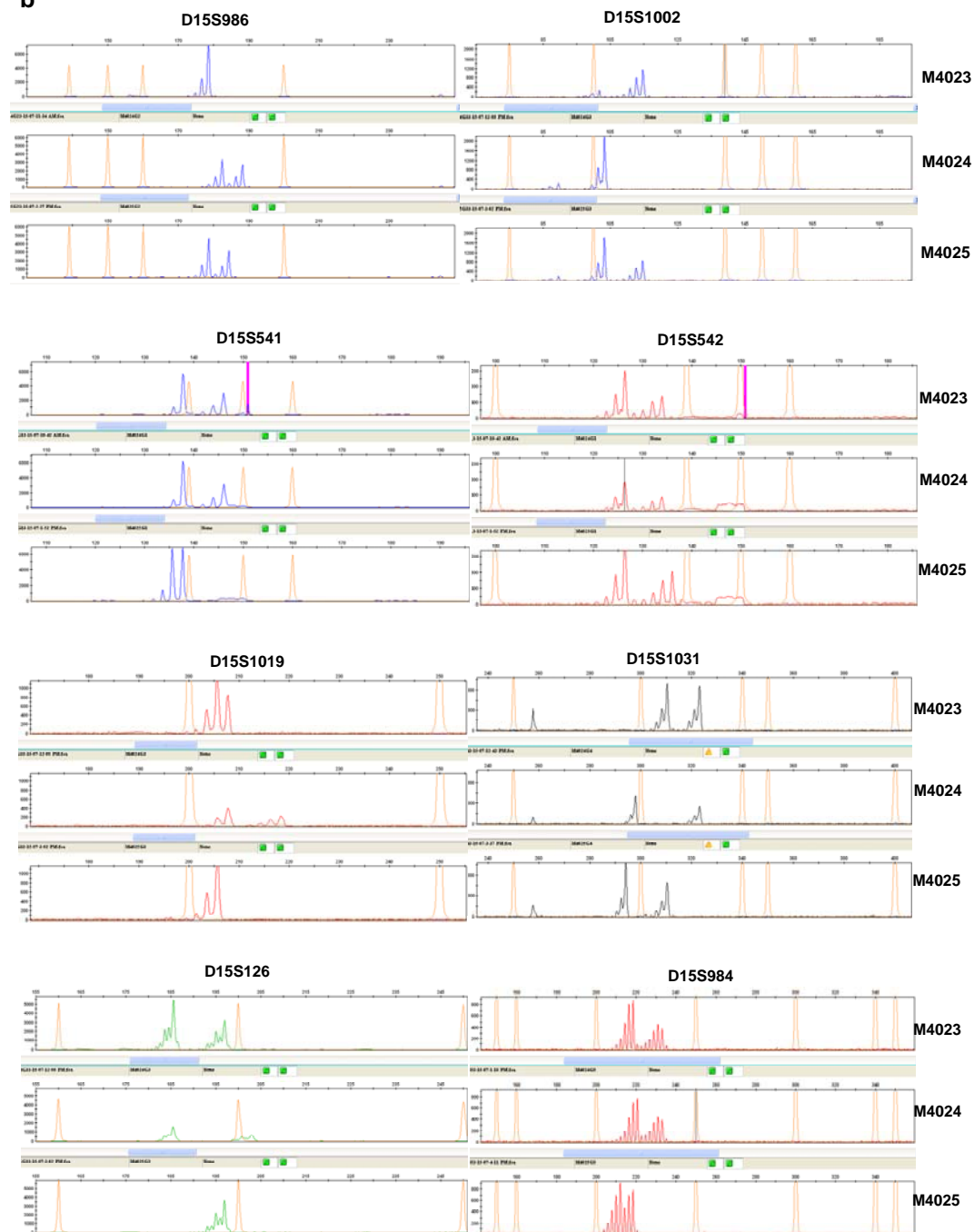
39c. Patient M4023 has deletion from BP2 to BP3 on paternally inherited chromosome 15 and belongs to type II deletion.

Table 3-3 Genotyping data for family C

Microsatellite markers	Allele size of microsatellite markers (bp)		
	Patient (M4023)	Father (M4024)	Mother (M4025)
D15S541	138,146	138,146	136,138
D15S542	126,134	126,134	126,136
D15S543	151	145,151	145,151
D15S11	245	245	245
D15S113	134	134,136	134,136
D15S986	179	182,188	179,184
D15S1002	115	103	103,115
D15S1019	206,208	208,218	206
D15S1048	199,258	199,258	199,258
D15S165	181,182	181,182	181,182
D15S1031	310,323	298,323	294,310
D15S1043	87,89	87,89	87,89
D15S1010	227	227,231	210,227
D15S126	185,197	185,203	197
D15S984	218,233	221,233	212,218
D15S115	112,119	112,119	112

a



b

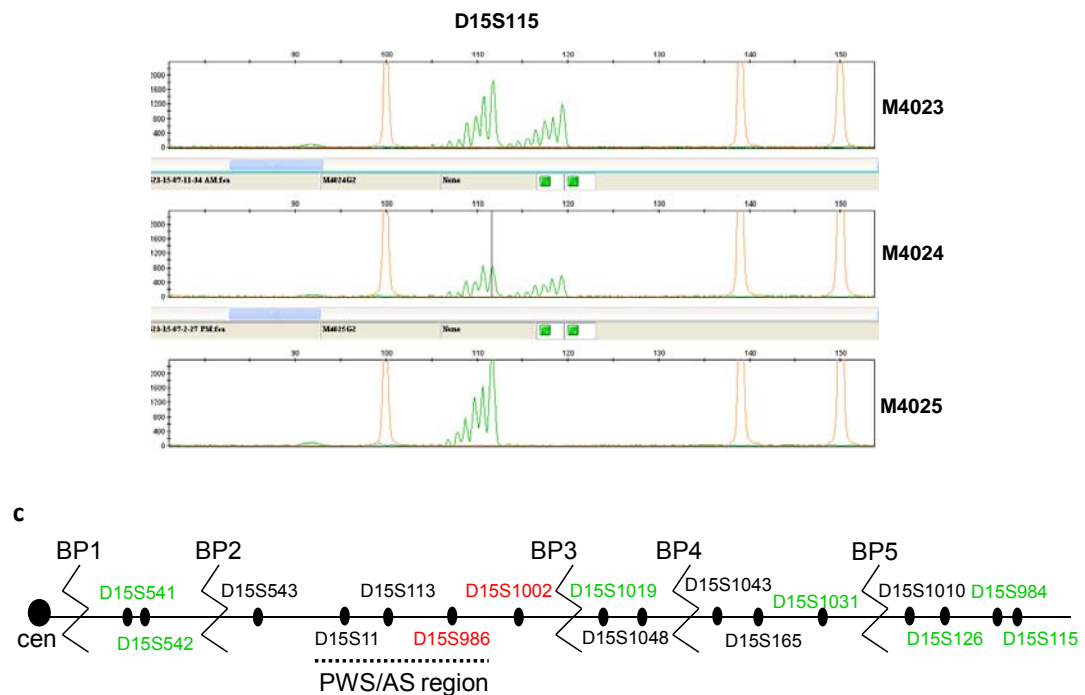
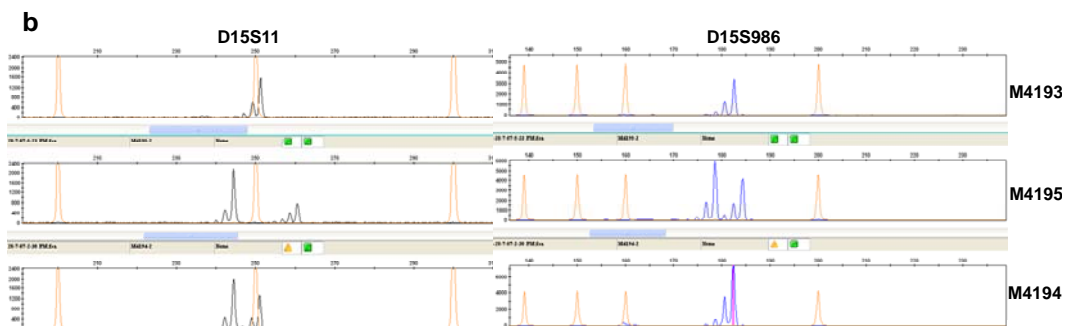
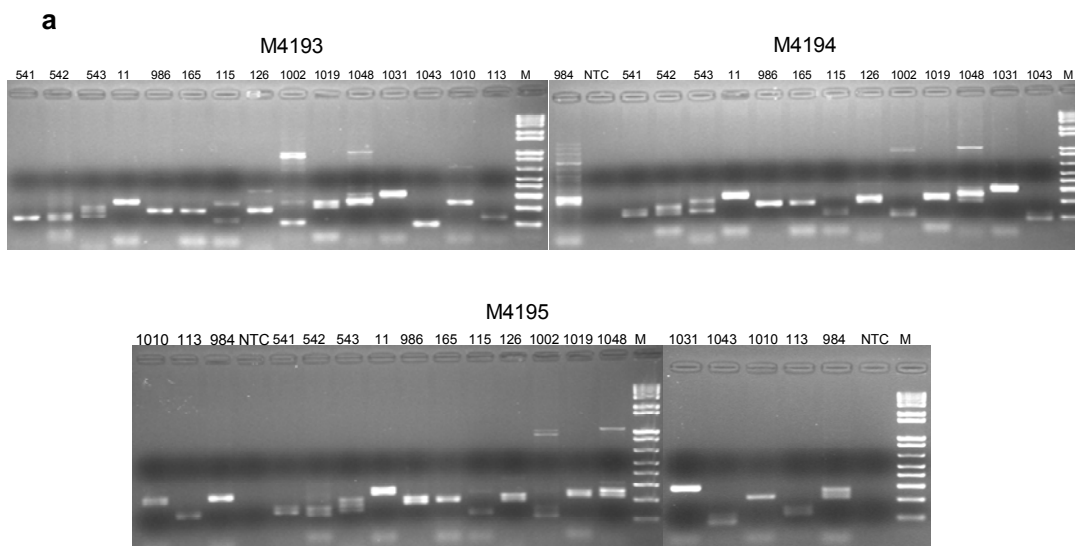


Figure 3-39 Diagnosis of patient M4023 from family C **a.** Agarose gel electrophoresis of PCR products from 16 microsatellite markers. M4023: patient; M4024: father; M4025: mother. M: 100 bp ladder. **b.** CE profiles of PCR products from informative markers. Orange peaks represent GeneScanTM-500LIZTM size standard. **c.** Diagnosis results of patient M4023. Deleted markers are labeled in red. Normal markers are labeled in green. Non-informative markers are labeled in black. Patient M4023 has deletion from BP2 to BP3 on paternally inherited chromosome 15.

From genotyping data (Table 3-4) of family D, the patient inherited null alleles of D15S11, D15S113, D15S986 and D15S1002 from the father, which implies a deletion encompassing these markers. The patient inherited one allele each of D15S541, D15S542, D15S1019, D15S1048 and D15S984 from the father and the other allele from the mother, indicating that the patient has normal genotype at these markers. The rest of the markers were uninformative in this family. The agarose gel pictures of PCR products of all the markers and the CE profiles of all the informative markers are showed in Figure 3-40a-b. Diagnosis results are summarized in Figure 3-40c. Patient M4193 has deletion from BP2 to BP3 on paternally inherited chromosome 15 and belongs to type II deletion.

Table 3-4 Genotyping data for family D

Microsatellite markers	Allele size of microsatellite markers (bp)		
	Patient (M4193)	Father (M4195)	Mother (M4194)
D15S541	136,138	138,146	136,144
D15S542	126,136	126,142	136,161
D15S543	144	144,151	144
D15S11	251	244,261	244,251
D15S113	134	129,138	134,136
D15S986	183	179,184	183
D15S1002	101	103,122	101,111
D15S1019	206,222	216,222	206,216
D15S1048	220,228	220	200,228
D15S165	181	181,183	181
D15S1031	294,302	302	294,302
D15S1043	89	89,99	89,97
D15S1010	226	226	210,226
D15S126	185	185,197	185,197
D15S984	227,248	217,248	227
D15S115	115	115,117	110,115



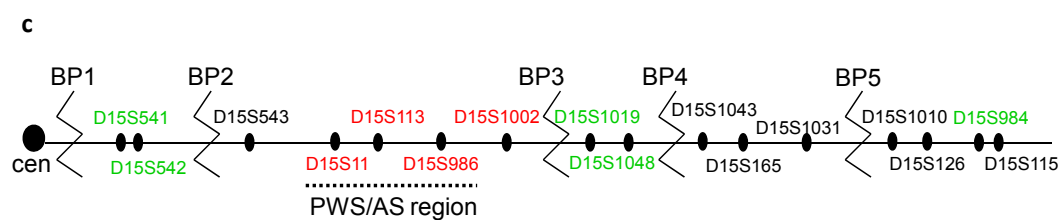
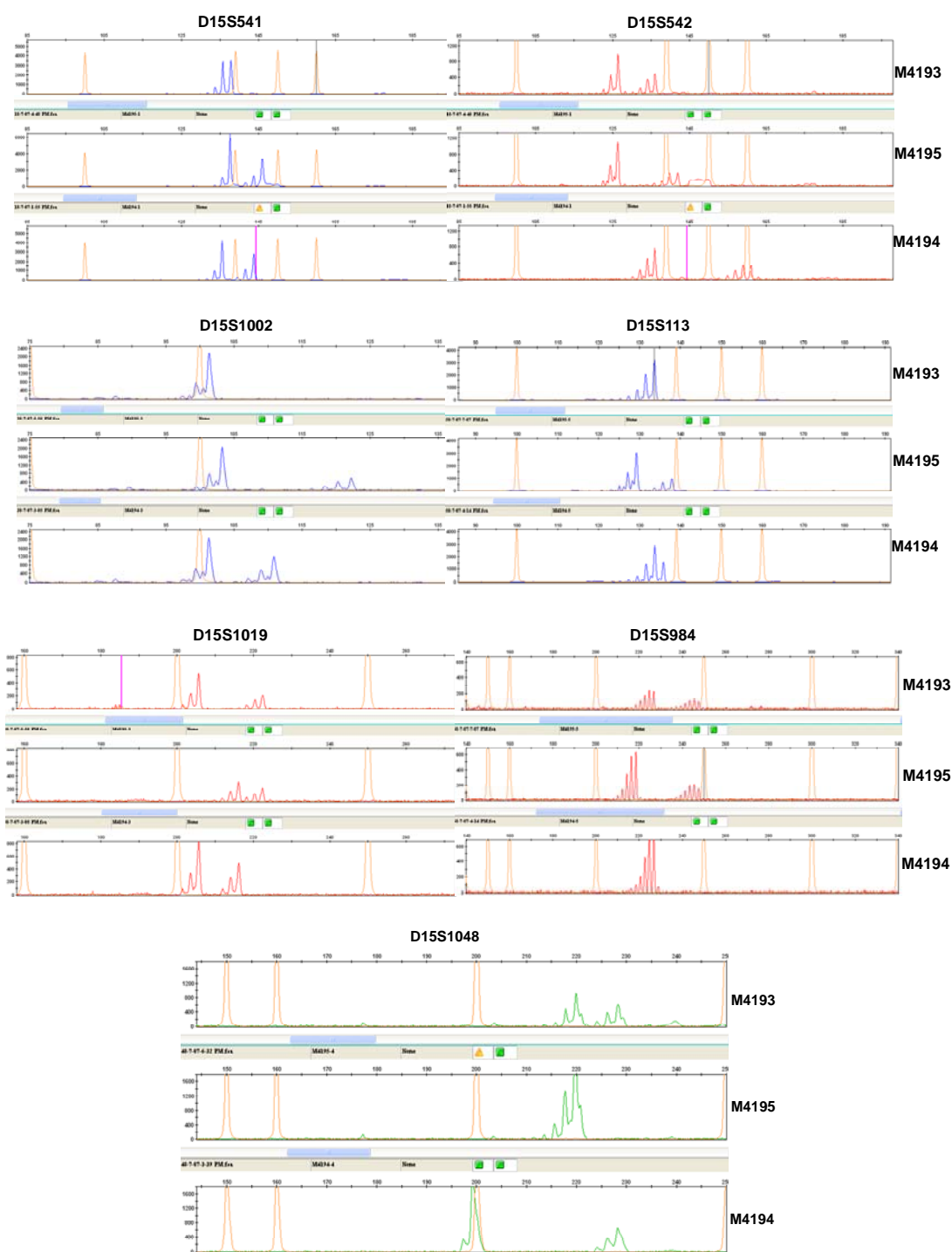
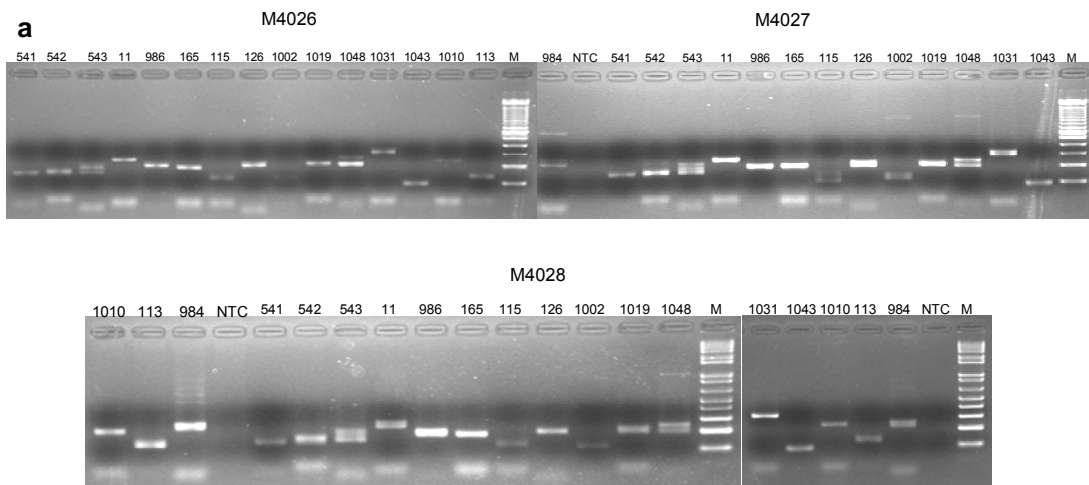


Figure 3-40 Diagnosis of patient M4193 from family D **a.** Agarose gel electrophoresis of PCR products from 16 microsatellite markers. M4193: patient; M4195: father; M4194: mother. M: 100 bp ladder. **b.** CE profiles of PCR products from informative markers. Orange peaks represent GeneScanTM-500LIZTM size standard. **c.** Diagnosis results of patient M4193. Deleted markers are labeled in red. Normal markers are labeled in green. Non-informative markers are labeled in black. Patient M4193 has deletion from BP2 to BP3 on paternally inherited chromosome 15.

From genotyping data (Table 3-5) of family E, the patient inherited null alleles of D15S543 and D15S986 from the father, which implies a deletion encompassing these markers. The patient inherited one allele each of D15S542, D15S1031, D15S1010, D15S984 and D15S115 from the father and the other allele from the mother, indicating that the patient has normal genotype at these markers. The rest of the markers were uninformative in this family. The agarose gel pictures of PCR products of all the markers and the CE profiles of some of the informative markers are showed in Figure 3-41a-b. Patient M4026 has deletion from BP2 to BP3 or BP4 on the paternally inherited chromosome 15. The diagnosis results are summarized in Figure 3-41c.

Table 3-5 Genotyping data for family E

Microsatellite markers	Allele size of microsatellite markers (bp)		
	Patient (M4026)	Father (M4027)	Mother (M4028)
D15S541	146	146	136,146
D15S542	144,155	144,149	136,155
D15S543	151	145,153	145,151
D15S11	244	244	244,268
D15S113	129	129,138	129,134
D15S986	192	182	182,192
D15S1002	116	103,113	116
D15S1019	206	206	206,218
D15S1048	199	199,220	199,218
D15S165	181,182	181,182	181,182
D15S1031	298,315	298,315	315
D15S1043	87,89	87,89	87,89
D15S1010	227,233	211,227	233
D15S126	197,201	185,197	197,201
D15S984	223,260	239,260	223,241
D15S115	115,117	92,117	115,119



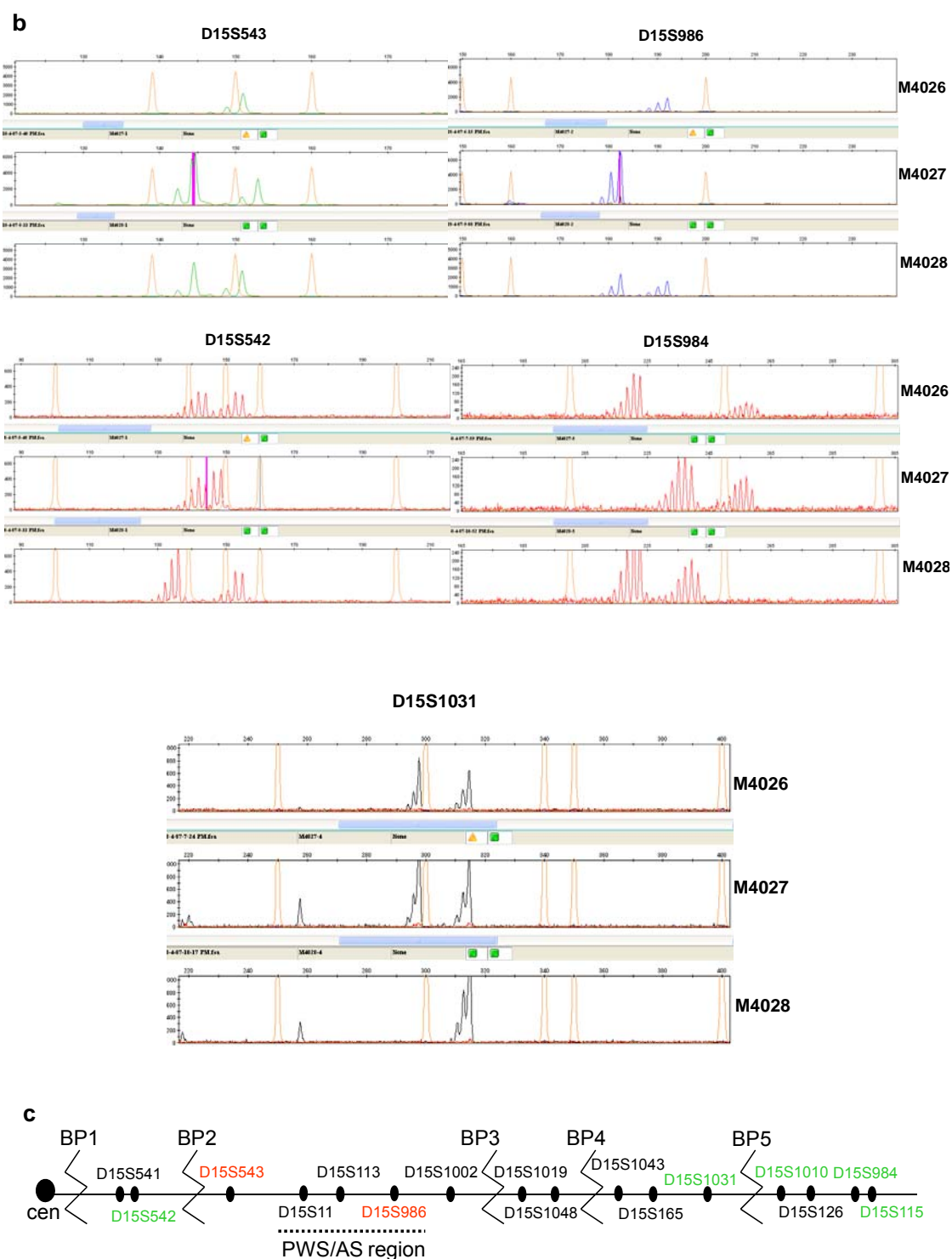


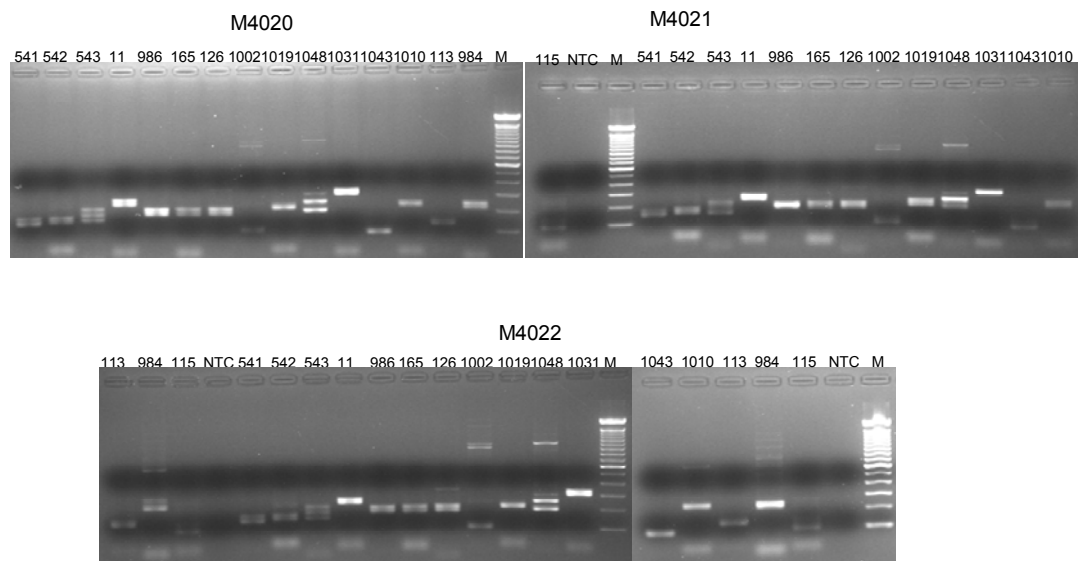
Figure 3-41 Diagnosis of patient M4026 from family E **a.** Agarose gel electrophoresis of PCR products from 16 microsatellite markers. M4026: patient; M4027: father; M4028: mother. M: 1 kb ladder. **b.** CE profiles of PCR products from informative markers. Orange peaks represent GeneScan™-500LIZ™ size standard. **c.** Diagnosis results of patient M4026. Deleted markers are labeled in red. Normal markers are labeled in green. Non-informative markers are labeled in black. Patient M4026 has deletion from BP2 to BP3 or BP4 on paternally inherited chromosome 15.

From the genotyping data of family F (Table 3-6), the patient inherited both alleles of D15S541, D15S986 and D15S1010 from the mother. Moreover, the patient carries the same size alleles as the mother at all the markers examined. Thus, patient M4020 is maternal uniparental disomy of chromosome 15. The agarose gel pictures of PCR products of all the markers and the CE profiles of all the informative markers are showed in Figure 3-42a-b. The diagnosis results are summarized in Figure 3-42c. Among 16 micorsatellite markers, 12 of them showed heterodisomy in the patient, so the chromosomal nondisjunction occurs at meiosis I during the maternal gametogenesis.

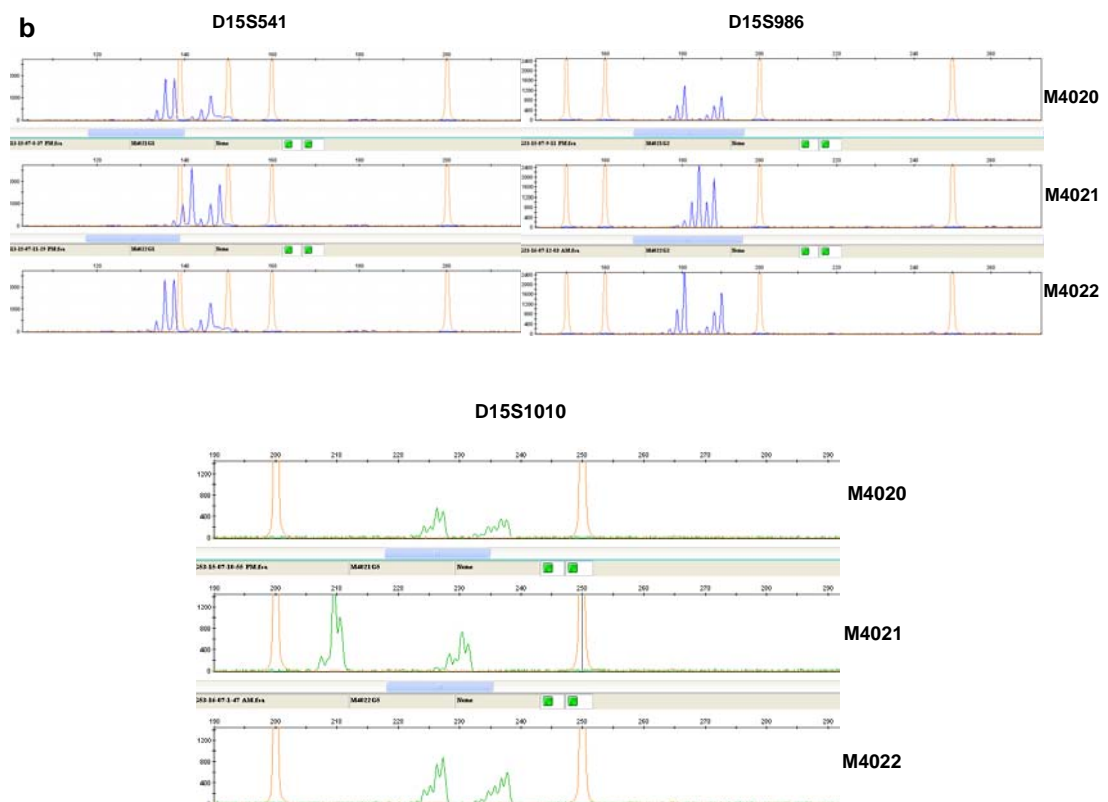
Table 3-6 Genotyping data for family F

Microsatellite markers	Allele size of microsatellite markers (bp)		
	Patient (M4020)	Father (M4021)	Mother (M4022)
D15S541	138,146	142,148	138,146
D15S542	144,148	148,154	144,148
D15S543	145,151	145,147	145,151
D15S11	245,261	245,261	245,261
D15S113	134	137,139	134
D15S986	181,190	184,188	181,190
D15S1002	101,103	103,111	101,103
D15S1019	218	206,220	218
D15S1048	199	199,222	199
D15S165	181,196	181,196	181,196
D15S1031	306,315	310,315	306,315
D15S1043	89	89,99	89
D15S1010	227,238	209,230	227,238
D15S126	186,197	186,197	186,197
D15S984	216,227	227,273	216,227
D15S115	91,111	91,109	91,111

a



b



c

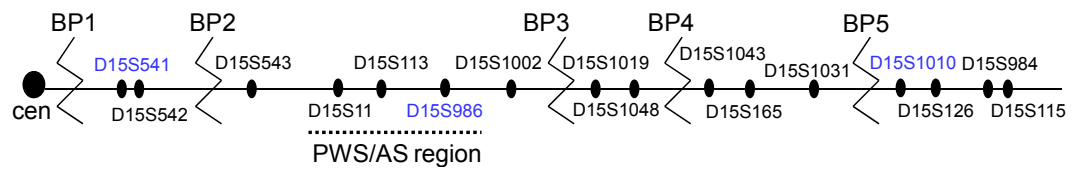


Figure 3-42 Diagnosis of patient M4020 from family F a. Agarose gel electrophoresis of PCR products from 16 microsatellite markers. M4020: patient; M4021: father; M4022: mother. M: 100 bp ladder. b. CE profiles of PCR products from informative markers. Orange peaks represent GeneScan™-500LIZ™ size standard. c. Diagnosis results of patient M4020. Uniparental disomy markers are labeled in blue. Non-informative markers are labeled in black.

From the genotyping data of family G (Table 3-7), the patient inherited both alleles of D15S1002 and D15S984 from the mother. In addition, at all the markers examined, the patient carries the same size alleles as the mother. Thus, patient M4169 is maternal uniparental disomy of chromosome 15. The agarose gel pictures of PCR products of all the markers and the CE profiles of all the informative markers are showed in Figure 3-43a-b. The diagnosis results are summarized in Figure 3-43c. Among 16 microsatellite markers, 14 of them showed heterodisomy in the patient, so the chromosomal nondisjunction occurs at meiosis I during the maternal gametogenesis.

Table 3-7 Genotyping data for family G

Microsatellite markers	Allele size of microsatellite markers (bp)		
	Patient (M4169)	Father (M4170)	Mother (M4171)
D15S541	138,146	138,146	138,146
D15S542	126,155	126,142	126,155
D15S543	145,151	145	145,151
D15S11	245,261	245	245,261
D15S113	131,136	129,136	131,136
D15S986	179,182	182,184	179,182
D15S1002	103,111	101,113	103,111
D15S1019	218,223	206,218	218,223
D15S1048	199,224	199,228	199,224
D15S165	181,196	181,196	181,196
D15S1031	298,315	315	298,315
D15S1043	89,99	89,99	89,99
D15S1010	226,232	226	226,232
D15S126	197	186,193	197
D15S984	229,242	223,227	229,242
D15S115	115	118	115

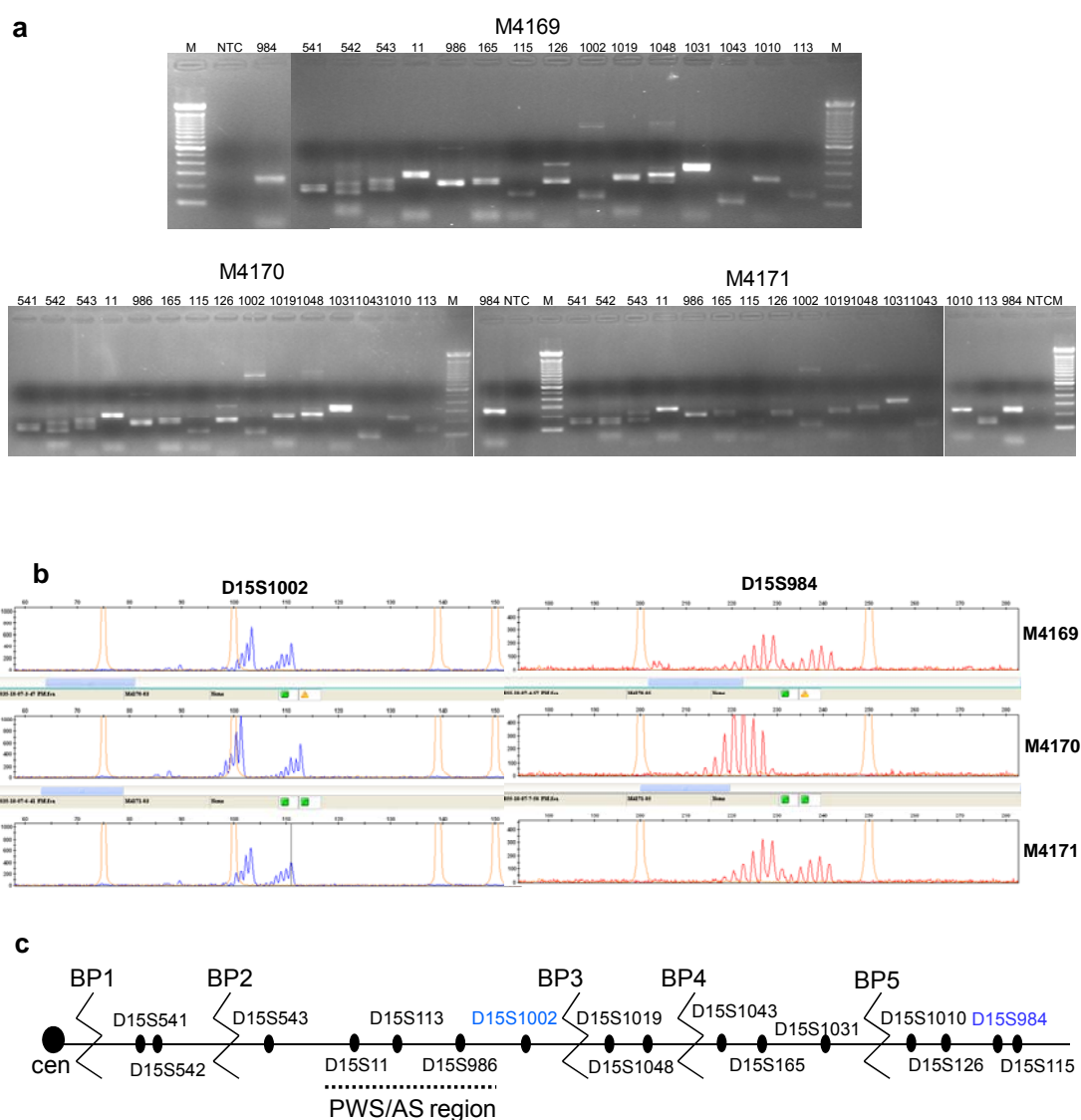


Figure 3-43 Diagnosis of patient M4169 from family G **a.** Agarose gel electrophoresis of PCR products from 16 microsatellite markers. M4169: patient; M4170: father; M4171: mother. M: 100 bp ladder. **b.** CE profiles of PCR products from informative markers. Orange peaks represent GeneScan™-500LIZ™ size standard. **c.** Diagnosis results of patient M4169. Uniparental disomy markers are labeled in blue. Non-informative markers are labeled in black.

From genotyping data of family H (Table 3-8), the patient inherited null alleles of D15S986 and D15S113 from the father, and only inherited one of the two alleles of the mother, which indicate that the patient has deletion on one of the chromosome 15 encompassing these two markers. The patient inherited both alleles of D15S984 and D15S115 from the mother, moreover, the patient carries the same size alleles as the mother at all the other markers. The results suggest that the patient is maternal

uniparental disomy of chromosome 15, and one of the chromosomes 15 has a deletion encompassing D15S986 and D15S113. Given the fact that the patient carries heterodisomy of 8 markers, the chromosomal nondisjunction occurs at meiosis I during the maternal gametogenesis. Figure 44a-b shows the agarose gel pictures of the PCR products of all the markers and the CE profiles of all the informative markers. The diagnosis results are summarized in Figure 44c.

Table 3-8 Genotyping data for family H

Microsatellite markers	Allele size of microsatellite markers (bp)		
	Patient (M4172)	Father (M4173)	Mother (M4174)
D15S541	146	138,146	146
D15S542	144	144,155	144
D15S543	145,151	145,151	145,151
D15S11	245	245,268	245
D15S113	129	134,136	129,134
D15S986	184	177	184,190
D15S1002	111	103,113	111
D15S1019	216,218	206,218	216,218
D15S1048	199,258	199,258	199,258
D15S165	181	181	181
D15S1031	306	304,319	306
D15S1043	89,99	89,99	89,99
D15S1010	226,232	226	226,232
D15S126	186,197	197,201	186,197
D15S984	212,231	210,223	212,231
D15S115	91,114	110	91,114

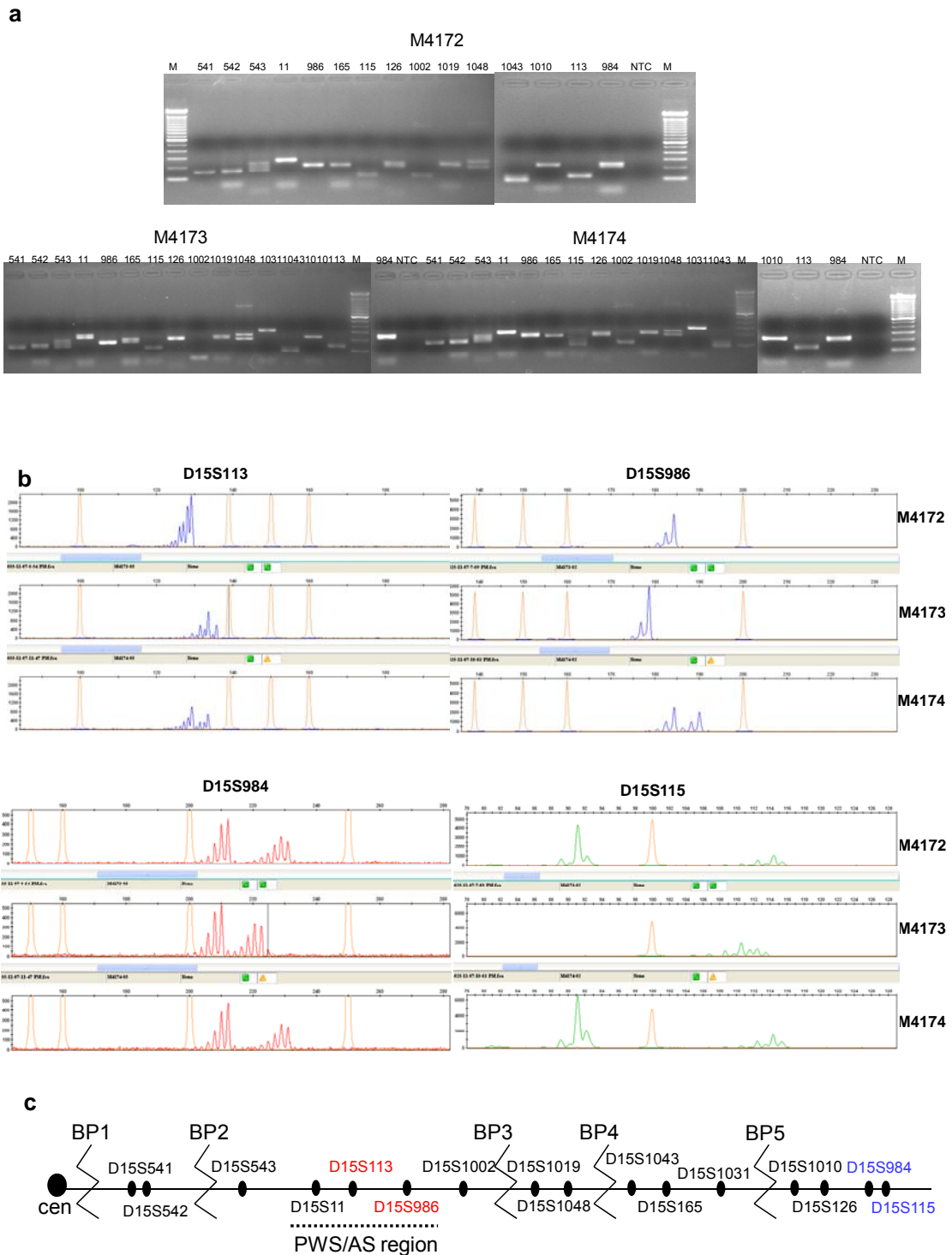


Figure 3-44 Diagnosis of patient M4172 from family H **a.** Agarose gel electrophoresis of PCR products from 16 microsatellite markers. M4172: patient; M4173: father; M4174: mother. M: 100 bp ladder. **b.** CE profiles of PCR products from informative markers. Orange peaks represent GeneScan™-500LIZ™ size standard. **c.** Diagnosis results of patient M4172. Uniparental disomy markers are labeled in blue. Non-informative markers are labeled in black. Deleted markers are labeled in red.

Genotyping results of the 8 PWS patients are summarized in Table 3-9.

Table 3-9 patient samples diagnosis by microsatellite DNA analysis

patient	Cytogenetic analysis	Microsatellite analysis	Extent of Deletion	Note
M4196	NA	D15S542, D15S113, D15S986, D15S1002, D15S1019, D15S1031, D15S1043, D15S984	Type I	none
M4166	NA	D15S541, D15S543, D15S11, D15S986, D15S1002, D15S1019, D15S1010, D15S1048, D15S1031, D15S115	Type I	none
M4023	deletion	D15S1002, D15S986, D15S541, D15S542, D15S1019, D15S1031, D15S126, D15S984, D15S115	Type II	none
M4193	NA	D15S541, D15S542, D15S11, D15S113, D15S1002, D15S986, D15S1019, D15S1048, D15S984	Type II	none
M4026	NA	D15S542, D15S543, D15S986, D15S115, D15S1010, D15S1031, D15S984	BP2 to BP3 or BP4	none
M4020	non-deletion	D15S541, D15S986, D15S1010, maternal UPD	none	Meiosis I
M4169	non-deletion, hemophilia	D15S984, D15S1002, maternal UPD	none	Meiosis I
M4172	non-deletion	D15S986, D15S113, D15S984, D15S115, show maternal UPD	D15S113, D15S986	Meiosis I

NA: not available

Chapter IV Discussion

4.1 The imprinting defect occur during oogenesis or fertilization in AS m^{an}/p^{+} mice

The AS-IC^{an} mice have been generated by inserting a targeting vector (pG12H6) 13 kb upstream of *Snurf-Snrpn* exon 1 on mouse chromosome 7. The offspring that inherit the mutant allele paternally are normal; whereas offspring that inherit the mutant allele maternally have AS imprinting defect in three mouse strains with different genetic backgrounds including 129/SvEv, C57BL/6J and PWK/PhJ.

In AS-IC m^{an}/p^{+} imprinting defect mice, the maternal chromosome carrying a paternal imprint could be inherited from the maternal grandfather or maternal grandmother. That mimics the phenomenon observed in AS imprinting defect patients. Studies of 18 AS imprinting defect patients without IC deletion have shown that 11 patients inherit the abnormal maternal allele from the maternal grandfather and 7 patients inherit the abnormal maternal allele from the maternal grandmother. It has been proposed that the imprinting defect happens after erasure of the parental imprint, probably due to the failure of establishing the maternal imprint during the oogenesis, or the failure to maintain the maternal imprint after the fertilization (122). This could also be the cause of the AS-IC m^{an}/p^{+} imprinting defect mice. The generation of AS-IC m^{an}/p^{+} imprinting defect mice suggests that AS imprinting mechanism is conserved between human and mice, although the exact sequence of the mouse AS-IC remains elusive. Some of AS imprinting defect patients without IC deletion (27%) are mosaic, but mosaicism has never been observed among AS-IC m^{an}/p^{+} imprinting defect mice. Biallelic unmethylation of the *Snurf-Snrpn* DMR is observed in all tissues tested from

AS-IC m^{an}/p^{+} imprinting defect mice. Therefore, the defect should occur during oogenesis or fertilization. It is possible, for example, that the primary gametic imprint (such as histone modifications) is not correctly established or not stable, and thus is not faithfully translated into CpG methylation; or that CpG methylation is not faithfully replicated during early embryogenesis. In both the AS imprinting defect patients and mice, the AS-IC fails to establish the maternal imprint on the PWS-IC during gametogenesis, leading to the maternally inherited chromosome carrying a paternal epigenotype. These observations further support the idea that the primary imprinting mark is established on AS-IC in the gametes and the imprinted AS-IC confers methylation on the maternal allele of PWS-IC after fertilization (177).

4.2 Incomplete penetrance of AS-IC^{an} in 129/SvEv background may due to strain-specific modifier

Although complete penetrance has been reported in C57BL/6J background (181), AS-IC m^{an}/p^{+} mice derived from matings in 129/SvEv background or in 129/PWK mix background show incomplete penetrance. These AS-IC m^{an}/p^{+} mice have normal methylation patterns at the DMR of *Snurf-Snrpn*, suggesting that the maternal imprint is established and maintained regardless of the integration of a targeting vector on the maternally inherited chromosome. In 129/SvEv background, both the AS-IC m^{an}/p^{+} imprinting defect mice and the AS-IC m^{an}/p^{+} normal mice could inherit the AS-IC^{an} mutant chromosome from the maternal grandmother or maternal grandfather. Therefore, the incomplete penetrance of the AS-IC^{an} mutation could not possibly be due to epigenetic inheritance. 129/SvEv and C57BL/6J are both inbred laboratory mice and they belong to the same species, but they are categorized into different

groups by SNP (206). Sixty-five percent of loci exhibited at least one polymorphism between 129 substrains and C57BL/6J (207). This difference may be the most plausible explanation for the variation in penetrance between the substrains. There might be a 129/SvEv strain-specific modifier repressed the effects of the inserted targeting vector, but such a modifier does not exist in C57BL/6J strain. It is also possible that such a modifier also exists in C57BL/6J strain, but the sequence variations affect its activity. Five nucleotide polymorphisms were identified between 129/SvEv and C57BL/6J in the 1500-bp genomic region upstream of *Snurf-Snrpn* promoter. A strain-specific modifier has been suggested to influence the survival rate of the PWS-IC deletion mice; moreover, the modifier is of maternal origin according to the hybrid background matings (208). To dilute the influence of the 129/SvEv strain-specific modifier, 129/SvEv AS-IC m^{an}/p^{+} female mice with normal methylation are backcrossed to C57BL/6J male for five generations. The offspring show incomplete penetrance even at the fifth generation, indicating that the effect of the 129/SvEv strain-specific modifier still exists. The epigenome is in a dynamic equilibrium: a change in the amount of modifier proteins can shift the balance between euchromatin and heterochromatin at a reporter locus (209). In the case of AS-IC^{an} mutation, the change of the amount of 129/SvEv strain-specific modifier might lead to incomplete penetrance of AS-IC^{an} mutation. Interestingly, incomplete penetrance has also been reported in AS imprinting defect patients. The affected patients have normal sisters or brothers despite carrying the same maternally inherited chromosome 15 (122). Thus, our AS imprinting defect mouse model recapitulates the incomplete penetrance phenomena observed in the AS imprinting defect families.

Incomplete penetrance is also observed among (129/SvEv AS-IC^{+an} female × PWK/PhJ male) F1 AS-IC m^{an}/p⁺ mice and it continues among F2 AS-IC m^{an}/p⁺ offspring from cross between (129/SvEv AS-IC^{+an} female × PWK/PhJ male) F1 AS-IC m^{an}/p⁺ female and PWK/PhJ male. However, complete penetrance is observed among F2 AS-IC m^{an}/p⁺ offspring from cross between (PWK/PhJ female × 129/SvEv AS-IC^{+an} male) F1 AS-IC m⁺/p^{an} female and PWK/PhJ male (Figure 3-7). PWK/PhJ mice are wild-derived inbred mice which have diverged from the original *M. m. musculus*. PWK/PhJ strain is evolutionary diverge from both 129/SvEv and C57BL/6J strains. In a 1534-bp genomic region of PWS-IC, there are 17 polymorphisms were identified between PWK/PhJ and 129/SvEv, and only 5 polymorphisms were identified between 129/SvEv and C57BL/6J. It is possible that the effect of 129/SvEv strain-specific modifier suppressor is repressed by the PWK/PhJ strain-specific modifier enhancer, which should be maternal origin. The PWK/PhJ maternal origin strain-specific modifier enhancer (for example, cytoplasmic factor in the oocytes) may function after fertilization and the effect is maintained during embryogenesis and gametogenesis, causing the failure in resetting the maternal imprint in the oocyte, and leading to the complete penetrance among the F2 offspring. Strain-specific modifier suppressors and enhancers affect the expression of transgenes in an insertion site-specific manner. Their effect may be developmental and/or parent-of-origin specific. The dominant influence of the BALB/c modifier occurs only when the transgene is introduced into the female BALB/c mice. It has been postulated that the modifier itself is down-regulated by a germline-specific imprint, and thus the paternally derived BALB/c allele fails to modify the transgene locus. Alternatively, the maternally and paternally derived alleles may be equivalent, but require an interaction with a BALB/c oocyte cytoplasmic factor (193). In the case of PWK/PhJ

modifier enhancer, the paternal transmission might be down-regulated or needs PWK/PhJ oocyte-specific factors to be functional. It is also possible that the 129/SvEv strain-specific modifier suppressor is lost in that particular mouse.

Obesity is observed among F1 AS-IC m^{an}/p^{+} (129/SvEv AS-IC^{+/an} female \times PWK/PhJ male) hybrid mice with imprinting defect, and is also observed among 129/SvEv AS-IC m^{an}/p^{+} imprinting defect mice, but at a later age of about 8 months old. The age difference may be because of different genetic background. Among the five classes of AS patients, UPD and imprinting defect patients show most striking increase of body weight, while *UBE3A* mutation patients show less increase (128). It is likely that the obesity has been caused by the loss of *UBE3A* gene expression, but *Ube3a*-mutant mice has not been observed with increased body weight (185). UPD and deletion mouse models of AS are associated with obesity (106, 210). Recently, obesity has also been reported in PWS-IC^{Hs/+} AS imprinting defect mice (186). Maternal inheritance of a deletion mapping to *Atp10c* leads to obesity in mice, suggesting that increased body weight in UPD, deletion and AS imprinting defect mice with AS-IC^{an} or PWS-IC^{Hs/+} mutation could be due to loss of maternal *Atp10c* expression (156). Although in all the cases, maternal *Atp10c* suppression has not yet been tested, the overlap of phenotype supports the possibility.

4.3 Characteristics of AS-IC m^{an}/p^{+} imprinting defect mice

The PWS-IC functions to activate the paternal patterns of gene expression, whereas the AS-IC functions in the female germline to silence the PWS-IC through methylation imprint and suppress the maternal alleles of paternally expressed genes (211). The PWS-IC methylation is not required for maintenance of *Snurf-Snrpn*

monoallelic expression in mouse ES cells (166). However, DNA methylation is still a hallmark of imprinting, although it may function as a secondary imprint. In the somatic cells of AS-IC m^{an}/p^{+} imprinting defect mice, complete loss of methylation spans the entire maternal allele of *Snurf-Snrpn* DMR, indicating that the AS-IC fails to set up methylation imprint at the PWS-IC during oogenesis, or fails to maintain the PWS-IC methylation after fertilization; and the defect is maintained throughout development. Identifying the sequence-specific binding factors involved in the regulation of methylation within the PWS-IC will assist in dissecting the mechanisms of imprinting centers. Dnmt family members are essential for the establishment and maintenance of methylation at many imprinted loci, but little is known about the other proteins that are involved in sequence-specific methylation. Studying of the methylation status of PWS-IC during oogenesis and embryogenesis of AS-IC^{an} mutant mice will facilitate the understanding of dynamics of methylation and identification of *trans*-acting factors involved in imprinted regulation in PWS/AS imprinting domain.

In somatic cells of both human and mice, at the PWS-IC region, histone H3K9 and K4 are methylated in a parental complementary pattern. Histone H3K9 is methylated only on the maternal allele, whereas histone H3K4 is methylated only on the paternal allele (104, 165). In our ChIP assay, the maternal allele of PWS-IC is enriched by anti-trimethyl H3K9 and the paternal allele is enriched by anti-dimethyl H3K4 in both cerebellum and liver of wild type mice. In cerebellum and liver of AS-IC m^{an}/p^{+} imprinting defect mice, both alleles of PWS-IC is enriched by anti-dimethyl H3K4, and the enrichment of the maternal allele by anti-trimethyl H3K9 is reduced. Results of the ChIP assay are consistent with the loss of differential methylation of PWS-IC and activation of *Snurf-Snrpn* transcripts from the maternal allele in AS-IC m^{an}/p^{+}

imprinting defect mice. It has been reported that the anti-dimethyl H3K9 antibody used in our study did not cross-react with trimethyl-H3K9 (212). The failure of anti-dimethyl H3K9 to enrich the maternal allele in wild type mice is probably because the trimethyl H3K9, instead of dimethyl H3K9, is the differential imprinting mark at the PWS-IC as reported by Vu *et al* at the DMR of *Igf2r* (18). The reason why anti-dimethyl H3K9 failed to enrich the maternal PWS-IC allele may also due to the limitations of ChIP. If dimethyl H3K9 is bound by other proteins, these proteins will be fixed to the chromatin by formaldehyde and prevent the access of anti-dimethyl H3K9 antibody to dimethyl H3K9, and thus the anti-dimethyl H3K9 antibody cannot precipitated PWS-IC region.

The observation that cytosine methylation of the PWS-IC occurs during or after fertilization in human, indicates that DNA methylation may not be the gametic imprint for the PWS/AS imprinting domain in human (163). In mouse ES cells, it has been shown that PWS-IC CpG island methylation depends on G9a H3K9/K27 methyltransferase, but H3K9 methylation is independent of CpG methylation. Furthermore, methylation of H3K9 is sufficient and CpG methylation is not required for the maintenance of *Snurf-Snrpn* monoallelic expression (166). In MeCP2 deficient mice, histone H3 acetylation and H3K4 methylation is increased while H3K9 methylation is reduced at the PWS-IC; however, there is no effect on DNA methylation (213). All these facts suggest that other than DNA methylation, histone modification is an essential epigenetic mark at PWS/AS domain. Investigations of imprinting on distal chromosome 7 in the placenta suggest that an evolutionary older imprinting mechanism, limited to extraembryonic tissues, is based on histone modifications, and that this mechanism is later made more stable for use in embryonic

lineages by the recruitment of DNA methylation (103). Investigation of DNA methylation and histone modification during the spermatogenesis stages preceding the genome-wide histone-to-protamine exchange shows that the paternally and maternally methylated imprinting center regions (ICRs) are marked by different combinations of histone modifications. It has been hypothesized that these pronounced differences could impact on how chromatin at these regions is assembled into specific structures during the final stages of spermiogenesis, and may determine the configuration in which the ICRs are transmitted to the fertilized egg (76). The finding further supports the idea that histone modifications are more primary imprint, compared to DNA methylation. Studying histone modifications during embryonic development of AS-IC^{an} mutant mice will help to elucidate the relationship of DNA methylation and histone modifications.

Besides histone modifications, chromatin histones may carry epigenetic information by other means. After fertilization, the genome wide DNA demethylation happens to the paternal pronucleus. However, the paternal methylated ICRs are resistant to this activity. A small percentage of the genomic DNA remains packaged with histones in the mature mouse sperms, making it possible that the paternal ICRs and other regions, which are protected against paternal DNA demethylation in the zygote, do not undergo the canonical histone-to-protamine exchange and remain nucleosomally organized in mature sperm (76). Histone variants may also carry certain epigenetic information. Investigation in *Drosophila* shows that nucleosomes containing H3.3 are specially assembled in paternal *Drosophila* chromatin after fertilization and before the first round of DNA replication, suggesting that paternal chromosomes with H3.3 may represent a primary epigenetic distinction between parental genomes in the zygote

(214). The paternal preference of H3.3 histone variant has also been reported in early mouse zygotes (215).

The preliminary data from 3C assay suggests that there is an epigenetically regulated chromatin interaction between PWS-IC and *Ndn* gene. In wild type mice, the chromatin interaction is paternal-allele specific, whereas in AS-IC m^{an}/p^{+} imprinting defect mice, the physical interaction of PWS-IC and *Ndn* is detected from both parental alleles. These results are consistent with the dysfunction of AS-IC, which cannot set up and/or maintain correct maternal imprints at PWS-IC, and thus causing the maternal chromosome to gain the paternal-specific active chromatin loop. Furthermore, results of 3C assay in human fibroblast cell lines suggest that the physical interaction of PWS-IC and *Ndn* is conserved between human and mice. As known, all the chromatin loops reported at imprinting loci are silent loops; for example, the allele-specific chromatin loop at *H19/Igf2* domain and the chromatin-derived 11-kb silent chromatin loop at the *Dlx5-Dlx6* locus (115, 216). Long range DNA interaction may not be faithfully reflected because of the limitations of 3C method. Firstly, when the nuclei were fixed with formaldehyde before restriction digestion, many restriction sites may be covered by DNA associated proteins and thus the DNA cannot be ligated following restriction digestion. Secondly, not all the restriction enzymes could digest formaldehyde fixed chromatin well. Furthermore, the restriction sites chosen might not be close enough to allow the DNA ends to be ligated. In this case, no PCR products will be generated. Using other methods for massively detecting and mapping interactions between genomic elements, such as chromosome conformation capture-on-chip (4C) and chromosome conformation capture carbon copy (5C) (217, 218), chromatin interactions other than PWS-IC and

Ndn might be detected. It is also possible that the physical interaction of PWS-IC and *Ndn* detected is simply because *Snurf-Snrpn* and *Ndn* share the same transcription factory, not because PWS-IC controls *Ndn* imprinting by direct physical interaction. Analyzing the sequences interacting with PWS-IC at various developmental stages of mouse may provide insight into the exact meaning of the physical interaction.

Although previous ChIP assay in human lymphoblast cells has indicated that CTCF may not interact with either the maternal or paternal alleles of the *SNURF-SNRPN* promoter, it is possible that CTCF binds to PWS-IC in other tissues other than lymphoblast (such as the germ line) since there are CTCF binding sites in PWS-IC region (168). It has been demonstrated that at the *H19/Igf2* imprinting locus CTCF binding in the maternal *H19* ICR regulates its interaction with MAR3 and DMR1 at *Igf2*, forming a tight loop around the maternal *Igf2* and contributing to its silencing (115). CTCF might function in the formation of a maternal silent loop at PWS/AS domain as it does at the *H19/Igf2* locus. The Rett syndrome and Angelman syndrome have epigenetic overlap. The epigenetic histone modifications at the PWS-IC is aberrant in both Rett syndrome and AS imprinting defect patients, suggesting that MeCP2 might be involved in the regulation of imprinting in the PWS/AS domain (213, 219). However, the ChIP-loop experiment with anti-Mecp2 fails to generate any PCR product with various primers combinations, indicating that Mecp2 may bind to the PWS-IC during the imprint establishment, and after that Mecp2 is no longer needed (data not shown).

3C assay fails to detect the physical interaction of *Ube3a* and the putative AS-IC region. This suggests that AS-IC may not control its targeting genes by direct

physical interaction, or that AS-IC interacts with PWS-IC and/or genes under its control only at specific developmental stages. Once the maternal imprint is set up, the maintenance machinery is no longer required. The organization of genome is not a rigid three-dimensional network, but in a dynamic organization with preferred conformation, changing through development and differentiation. It has been suggested that the nuclear interaction might not only be of gene-with-gene, gene-with-regulation element, but of two regulatory elements with each other (220). Analysis of chromatin interaction at various developmental stages will provide insights into the relationship between chromatin interaction and gene regulation.

Asynchronous replication has been observed as early as the pre-implantation embryo soon after fertilization and is erased before meiosis in the germ line, and then is reset in late gametogenesis in both the male and female, indicating that it may function as a primary epigenetic mark for distinguishing parental alleles (180). Although asynchronous replication timing still exists in AS-IC m^{an}/p^{+} imprinting defect mice, the asynchronous replication timing between two alleles is not as obvious as those of the wild type mice. Moreover, the replication timing in S phase of both PWS-IC and *Ndn* loci is later than those of wild type mice. Analysis of replication timing in Dnmt1- and Dnmt3L-deficient ES cells indicates that asynchronous replication is independent of differential DNA methylation, and imprinting centers regulates replication timing and subnuclear localization of nearby replicons (221). In AS-IC m^{an}/p^{+} imprinting defect mice, the targeting vector may interrupt the operation of AS-IC and perturb the movement of the maternal allele to particular nuclear compartments, changing the replication timing of the whole imprinting domain.

4.4 PGK promoter activity may responsible for the imprinting defect in AS-IC

m^{an}/p^{+} mice

The most likely cause for the AS-IC m^{an}/p^{+} imprinting defect mice is that the activity of the PGK promoter from the *puromycin* cassette of the targeting vector changes the chromatin conformation near the AS-IC and affects its function. The PGK promoter is expressed in both cerebellum and liver cells of AS-IC m^{+}/p^{an} mice, but expressed only in the cerebellum of AS-IC m^{an}/p^{+} mice with imprinting defect. PGK promoter is silent in both cerebellum and liver cells of AS-IC m^{an}/p^{+} mice with normal methylation patterns. These results indicate that *puromycin* gene expression is correlated with AS imprinting defect. In AS-IC m^{an}/p^{+} imprinting defect mice, biallelic unmethylation of *Snurf-Snrpn* DMR is detected from both liver and cerebellum, suggesting that *puromycin* expression is not dependent on PWS-IC unmethylation. Biallelic histone H3K4 dimethylation and decrease of histone H3K9 trimethylation from maternal allele are also detected from both liver and cerebellum, indicating that *puromycin* expression is not due to the abnormality of histone codes. Brain-specific expression of *puromycin* is likely related to *Snurf-Snrpn* upstream transcripts and *Ube3a-ATS*, considering that all of them are brain-specific.

Paternal inheritance of the PWS-IC deletion represses all paternal-specific transcripts including the *Ube3a-ATS* and activates paternal *Ube3a*, suggesting that *Ube3a-ATS* might regulate *Ube3a in cis* (196). The finding of brain-specific splicing of U exons directly to *Ube3a-ATS* excluding *Snurf-Snrpn*, resolves the contradiction that the *Snurf-Snrpn* expression is ubiquitous while *Ube3a-ATS* is brain-specific; and indicates that *Ube3a-ATS* is regulated by *Snurf-Snrpn* upstream exons (169). In the cerebellum of AS-IC m^{an}/p^{+} imprinting defect mice, the *Snurf-Snrpn* upstream transcripts are

activated and *Ube3a* is silenced from the maternally inherited chromosome, supporting the role of *Ube3a-ATS* in silencing *Ube3a* gene expression and the role of *Snurf-Snrpn* upstream transcripts in regulating *Ube3a-ATS* in brain.

It has been shown that the *Snurf-Snrpn* upstream transcripts are expressed in oocytes through an oocyte-specific promoter, which is different from the promoter initiating paternal expression of *Snurf-Snrpn* upstream transcript in brain under the control of PWS-IC. Considering the conserved structure and expression pattern of *Snurf-Snrpn* upstream transcripts in brain between human and mice, the oocyte-specific *Snurf-Snrpn* upstream transcripts have been indicated to function as an AS-IC *cis*-acting element to establish imprint at the PWS-IC on the maternal chromosome (222). In AS-IC m^{an}/p^{+} imprinting defect mice, the activation of *Snurf-Snrpn* upstream transcripts from the maternal allele only occurs in the brain where the *puromycin* gene is expressed, and where U exons are spliced together with 3' *Hprt* exons from the targeting vector. The most plausible explanation is that during oogenesis the inserted targeting vector alters the chromatin conformation of the AS-IC through the activity of the PGK promoter of *puromycin*. The 129/SvEv strain-specific modifier might function at the same time, so there is a balance between 129/SvEv strain-specific modifier which represses PGK promoter, and transcription factors which activate PGK promoter. Once the PGK promoter is activated, the whole PWS/AS domain will maintain in the open status which makes it accessible to more transcription factors. The oocyte-specific *Snurf-Snrpn* upstream promoter may be suppressed or certain transcripts are not spliced correctly, incorporating 3' *Hprt* exons in them. Therefore, AS-IC cannot set up maternal imprints (DNA methylation and histone modification) on the PWS-IC. Instead, the paternal imprint is established on the maternal

chromosome through PWS-IC. After fertilization, the brain-specific *Snurf-Snrpn* upstream transcripts are transcribed from the maternal allele together with *Ube3a-ATS*, leading to the silencing of maternal *Ube3a*. However, if the PGK promoter of *puromycin* is silenced by the 129/SvEv strain-specific modifier, the oocyte-specific promoter of *Snurf-Snrpn* upstream transcripts is recognized properly, and the oocyte-specific *Snurf-Snrpn* upstream transcripts are transcribed correctly. This will allow the AS-IC to set up maternal imprints at PWS-IC correctly and the maternal imprints will spread from PWS-IC to the whole PWS/AS domain.

To date, it is still not clear where the brain-specific *Snurf-Snrpn* upstream transcripts initiate from. More upstream exons have been reported, but whether these exons belong to the same large transcript remains unknown (223). However, *Snurf-Snrpn* upstream transcripts have strain-specific splicing patterns in mice. For example, a PCR product (516 bp) is generated using cDNA derived from PWK/PhJ mice with primers AH10 and AH11, whereas PCR products (410 bp and 516 bp) are generated using cDNA derived from 129/SvEv and C57BL/6J mice with the same sets of primers. Primers AH10 and AH12 cannot generate any PCR product from cDNA derived from PWK/PhJ mice, but PCR products (459 bp and 563 bp) are generated from cDNA derived from 129/SvEv. These upstream transcripts with different splicing patterns might have different functions, and they might be strain-specific or developmental stage-specific. Further studies will be required to elucidate the importance of these alternative transcripts and their relations to the imprinting establishment and maintenance.

The model of *Ube3a-ATS* silencing *Ube3a* gene expression *in cis* reconciles with the epigenetic silencing via antisense-mediated mechanism observed in X-inactivation and *Air* mediated *Igf2r* silencing (98, 224), and is consistent with the observation in PWS-IC^{Hs/+} AS imprinting defect mice (186). Landers *et al* disputes the notion of *Ube3a-ATS* in suppressing *Ube3a* expression *in cis* because it was observed that the maternal disruption of *Ube3a* led to increased *Ube3a-ATS*, suggesting that *Ube3a-ATS* is regulated by *Ube3a* *in trans*. One of the supporting evidences is that *UBE3A* has a preferential maternal expression in non-neuronal human tissues, such as fibroblasts and lymphoblasts, where *UBE3A-ATS* is not expressed (170). The other evidence is that *Air* does not regulate *Igf2r* imprinting because it was found that *Igf2r* was not imprinted in the brain despite the paternal-specific expression of *Air* in this tissue. However, analysis obtained using primary brain cell cultures shows that *Ube3a* and *Igf2r* are cell lineage-specific imprinting and non-imprinting. *Ube3a* is biallelically expressed in glial cells and fibroblasts, but expressed exclusively from the maternal allele only in neurons; while *Ube3a-ATS* is paternally expressed in neurons, but not expressed in other cells where *Ube3a* is biallelically expressed. *Igf2r* loses imprinting in neurons but not in glial cells and embryonic fibroblast, while *Air* is expressed in glial cells and embryonic fibroblast, but not in neurons. Primary brain cell culture not only confirms *Ube3a* neuron-specific imprinting, but also solves the confusing relationship of *Igf2r* imprinting and *Air* expression from the cell lineage level (151), thus providing additional evidence for the antisense-mediated imprinting silencing model. The repression of *Ube3a* expression from the maternal allele in AS-IC m^{an}/p⁺ imprinting defect mice further support the role of *Ube3a-ATS* in regulating *Ube3a* expression *in cis*. The increased expression of *Ube3a-ATS* in mice carrying the *Ube3a* mutant maternal chromosome observed by Landers *et al* might be that some of the

proteins regulating transcription of the *Ube3a-ATS in trans* may be degraded via the ubiquitin-proteasome proteolytic pathway. Dysfunction of Ube3A in mice may cause accumulation of these proteins or give these proteins more time to stay in cells, and thus more *Ube3a-ATS* mRNA is transcribed.

4.5 The new targeting vector has been constructed and the screening protocol for recombinant ES colonies needs further optimization

The fact that a targeting vector inserting into mouse chromosome 7C region generates a mouse with AS imprinting defect indicates that Angelman syndrome imprinting control machinery is conserved between human and mouse and has been localized by our targeting vector. The imprinting defect among the AS-IC m^{an}/p^{+} mice may be due to the effects of a structural rearrangement arising from the insertion of the puromycin resistance cassette, the duplication of the 6-kb genome DNA fragment in the region upstream of *Snurf-Snrpn*, or the disruption of a regulatory element which is required for establishing the maternal epigenotype. A new targeting vector pCMVH6 has been constructed to test these hypotheses. The new vector is designed to insert into the same locus as that of pG12H6, and will have the promoter in the same orientation as that of pG12H6, but will not cause chromosomal duplication. If the mouse carrying the newly-targeted chromosome from maternal origin develops AS imprinting defect, the duplication hypothesis will be excluded. The newly generated AS imprinting defect mouse will be crossed to a cyclization recombination recombinase (Cre)-carrying mouse. *Beta-geo* gene and its promoter will be deleted from chromosomes of their pups through Cre/LoxP mediated recombination. If pups carrying the targeted chromosome from the maternal origin still develop AS imprinting defect, the

insertion site hypothesis may be true. These mechanisms are not necessary mutually exclusive.

The linearized targeting vector pCMVH6 is electroporated into mouse ES cells. After 4 rounds of screening, more than 600 colonies with neomycin positive and FIAU negative are screened by PCR and Southern blots, but none of them have pCMVH6 integrated into the expected site of genome. In fact, most of the neomycin positive and FIAU negative colonies have no targeting vector inserted. This is probably because the concentration of the G418 and/or FIAU is not enough, since the plates containing ES cells electroporated without DNA have nearly the same number of colonies as the plates containing ES cells electroporated with DNA. The plates screened with only G418 have much more colonies than the plates screened with both G418 and FIAU, indicating that FIAU worked well. In the future, the concentration of G418 needs to be increased, but the concentration of FIAU does not. Some of the false positive colonies appear because the ES cells are screened in the selective plates for too long time (sometimes 14 days), and the cells without targeting vector may grow as satellite colonies. Another possible reason for the failure of screening is that the targeting vector pCMVH6 carrying a kanamycin cassette next to the TK gene. This kanamycin cassette may make cells resistant to G418 selection. Alternatively, more DNA may be needed for efficient electrophoration because of the size of the targeting vector (18.6 kb). The number of ES cells required for each electroporation also have to be optimized.

4.6 Microsatellite PCR can be used as a routine technique to diagnosis PWS/AS

UPD and gross DNA deletion contribute to more than 90% of PWS and AS. PWS patients carrying type I deletions lose more genes comparing to PWS patients carrying type II deletions. Butler *et al* has concluded that individuals with type I deletion have more behavioral and psychological problems than individuals with the type II deletions (225). It also has been found that hypopigmentation is more often seen in PWS patients with UPD than in PWS patients with deletion (226, 227). Distinguishing patients with UPD and deletion, and accurately defining the deletion extent in individual patient with deletion will give great help to clinical treatment. Traditional FISH method can only detect deletion but not UPD, so 16 sets of fluorescence labeled microsatellite primers were used to identify 8 PWS patients from Taiwan. Two were identified as type I deletion, two had type II deletion, one had a deletion from BP2 to BP3 or BP4, and three were identified as maternal UPD. Among the 16 microsatellite markers, fifteen of them are informative in at least one PWS families, and D15S165 is not informative in all the PWS families. In the future, these 15 microsatellite markers can be used to determine extent of deletion in PWS patients. Comparing to other methods, such as comparative genomic hybridization, FISH, BAC arrays and Southern blot, microsatellite PCR is an efficient and quick method to detect deletion and UPD among PWS and AS patients. However, microsatellite PCR cannot detect very small deletions due to limitations of microsatellite markers. For example, the right end of the deletion in patient M4026 cannot be determined because lack of informative microsatellite markers. To improve the accuracy of the diagnosis, more microsatellite markers are needed and more PCR reactions are needed, but that will make the diagnosis tedious and laborious. In addition, microsatellite PCR cannot distinguish trisomy samples with normal samples.

Multiplex amplifiable probe hybridization (MAPH) is demonstrated to simultaneously assess 40 human loci (228), but MAPH requires immobilization of sample nucleic acids and tedious washing of unbound probe, thus it is difficult to implement as a routine diagnosis setting. The recently developed multiplex ligation-dependent probe amplification (MLPA) method is sensitive to detect trisomy, UPD and deletion, even one exon deletion, but MLPA needs design special probes (229). Moreover, MLPA cannot determine parental origin of the deletion or UPD. Thus, microsatellite PCR is the best method for routine diagnosis setting. For detailed study of the exact deletion points in individual patient, it will be better to combine MLPA with microsatellite PCR. Microsatellite PCR is used to define the parental origin and the approximate extent of the deletion, and then MLPA can be used to determine the exact deletion point. Single nucleotide polymorphism (SNP) array is another newly developed method to detect regions with loss of heterozygosity without loss of gene dosage (230). SNP can perform genome wide diagnosis and is a potential method for genome screening of cancer and chromosome aberrations, but SNP need special Chip and software. Moreover, SNP is more expensive than MLPA and microsatellite PCR. Thus, SNP is difficult to use as a routine method for diagnosis of PWS and AS.

In summary, maternal inheritance of the AS-IC^{an} mutation causes AS imprinting defect with incomplete penetrance in the 129/SvEv mouse strain and 129/PWK hybrid. In AS-IC^{an} imprinting defect mice, the DMR of *Snurf-Snrpn* is biallelically unmethylated and the *Snurf-Snrpn* gene is biallelically expressed; moreover, the normally silent *Ube3a-ATS* is activated from the maternal allele, resulting in maternal *Ube3a* silencing. ChIP assay demonstrates that histone H3K4 dimethylation can be enriched from both parental alleles, and the enrichment of trimethyl H3K9 from

maternal allele is reduced when compared to wild type mice. The differential replication timing of PWS/AS domain is reduced in AS-IC^{an} imprinting defect mice. A paternal-specific physical interaction between PWS-IC and *Ndn* gene is detected in wild type mice. Interestingly, the interaction is detected from both parental alleles in AS-IC^{an} imprinting defect mice. The physical interaction of PWS-IC and *NDN* is conserved between human and mice, and thus may provide a new imprinting regulation mechanism for PWS/AS imprinting domain. The *puromycin* gene of the targeting vector only expresses from the cerebellum of AS-IC^{an} imprinting defect mice, even though cerebellum and liver cells have the same DNA methylation and histone modification patterns. A new targeting vector has been constructed to further elucidate the mechanism. Among 8 patients having PWS phenotype, two are identified to have type I deletion, two have type II deletion, one has deletion from BP2 to BP3 or BP4; three are identified to be maternal UPD and all the nondisjunction events occur during the meiosis I of maternal gametogenesis.

Reference

1. Waddington, C.H. (1957) *The Strategy of the Genes*. Allen & Unwin, London.
2. Russo, V.E.A., Martienssen, R.A. & Riggs, A.D. (1996) *Epigenetic Mechanisms of Gene Regulation*. Cold Spring Harbor Laboratory Press, Woodbury.
3. Bird, A. (2007) Perceptions of epigenetics. *Nature*, **447**, 396-398.
4. Reik, W. (2007) Stability and flexibility of epigenetic gene regulation in mammalian development. *Nature*, **447**, 425-432.
5. Riggs, A.D. (1975) X inactivation, differentiation, and DNA methylation. *Cytogenet Cell Genet*, **14**, 9-25.
6. Takai, D. and Jones, P.A. (2002) Comprehensive analysis of CpG islands in human chromosomes 21 and 22. *Proc Natl Acad Sci U S A*, **99**, 3740-3745.
7. Reik, W. and Walter, J. (2001) Genomic imprinting: Parental influence on the genome. *Nat Rev Genet*, **2**, 21-32.
8. Bestor, T.H. (1992) Activation of mammalian DNA methyltransferase by cleavage of a Zn binding regulatory domain. *EMBO J*, **11**, 2611-2617.
9. Li, E., Bestor, T.H. and Jaenisch, R. (1992) Targeted mutation of the DNA methyltransferase gene results in embryonic lethality. *Cell*, **69**, 915-926.
10. Howell, C.Y., Bestor, T.H., Ding, F., Latham, K.E., Mertineit, C., Trasler, J.M. and Chaillet, J.R. (2001) Genomic imprinting disrupted by a maternal effect mutation in the Dnmt1 gene. *Cell*, **104**, 829-838.
11. Okano, M., Bell, D.W., Haber, D.A. and Li, E. (1999) DNA methyltransferases Dnmt3a and Dnmt3b are essential for de novo methylation and mammalian development. *Cell*, **99**, 247-257.
12. Klimasauskas, S., Kumar, S., Roberts, R.J. and Cheng, X. (1994) HhaI methyltransferase flips its target base out of the DNA helix. *Cell*, **76**, 357-369.
13. Gowher, H., Liebert, K., Hermann, A., Xu, G. and Jeltsch, A. (2005) Mechanism of stimulation of catalytic activity of Dnmt3A and Dnmt3B DNA-(cytosine-C5)-methyltransferases by Dnmt3L. *J Biol Chem*, **280**, 13341-13348.

14. Bourc'his, D., Xu, G.L., Lin, C.S., Bollman, B. and Bestor, T.H. (2001) Dnmt3L and the establishment of maternal genomic imprints. *Science*, **294**, 2536-2539.
15. Lorincz, M.C., Schubeler, D., Hutchinson, S.R., Dickerson, D.R. and Groudine, M. (2002) DNA methylation density influences the stability of an epigenetic imprint and Dnmt3a/b-independent de novo methylation. *Mol Cell Biol*, **22**, 7572-7580.
16. Cheung, P., Tanner, K.G., Cheung, W.L., Sassone-Corsi, P., Denu, J.M. and Allis, C.D. (2000) Synergistic coupling of histone H3 phosphorylation and acetylation in response to epidermal growth factor stimulation. *Mol Cell*, **5**, 905-915.
17. Berger, S.L. (2007) The complex language of chromatin regulation during transcription. *Nature*, **447**, 407-412.
18. Vu, T.H., Li, T. and Hoffman, A.R. (2004) Promoter-restricted histone code, not the differentially methylated DNA regions or antisense transcripts, marks the imprinting status of IGF2R in human and mouse. *Hum Mol Genet*, **13**, 2233-2245.
19. Egger, G., Liang, G., Aparicio, A. and Jones, P.A. (2004) Epigenetics in human disease and prospects for epigenetic therapy. *Nature*, **429**, 457-463.
20. Wutz, A., Smrzka, O.W., Schweifer, N., Schellander, K., Wagner, E.F. and Barlow, D.P. (1997) Imprinted expression of the Igf2r gene depends on an intronic CpG island. *Nature*, **389**, 745-749.
21. Tufarelli, C. (2006) The silence RNA keeps: cis mechanisms of RNA mediated epigenetic silencing in mammals. *Philos Trans R Soc Lond B Biol Sci*, **361**, 67-79.
22. Tufarelli, C., Stanley, J.A., Garrick, D., Sharpe, J.A., Ayyub, H., Wood, W.G. and Higgs, D.R. (2003) Transcription of antisense RNA leading to gene silencing and methylation as a novel cause of human genetic disease. *Nat Genet*, **34**, 157-165.
23. Penny, G.D., Kay, G.F., Sheardown, S.A., Rastan, S. and Brockdorff, N. (1996) Requirement for Xist in X chromosome inactivation. *Nature*, **379**, 131-137.

24. Volpe, T.A., Kidner, C., Hall, I.M., Teng, G., Grewal, S.I. and Martienssen, R.A. (2002) Regulation of heterochromatic silencing and histone H3 lysine-9 methylation by RNAi. *Science*, **297**, 1833-1837.
25. Hall, I.M., Shankaranarayana, G.D., Noma, K., Ayoub, N., Cohen, A. and Grewal, S.I. (2002) Establishment and maintenance of a heterochromatin domain. *Science*, **297**, 2232-2237.
26. Grewal, S.I. and Elgin, S.C. (2007) Transcription and RNA interference in the formation of heterochromatin. *Nature*, **447**, 399-406.
27. Nakabayashi, K., Bentley, L., Hitchins, M.P., Mitsuya, K., Meguro, M., Minagawa, S., Bamforth, J.S., Stanier, P., Preece, M., Weksberg, R. *et al.* (2002) Identification and characterization of an imprinted antisense RNA (MESTIT1) in the human MEST locus on chromosome 7q32. *Hum Mol Genet*, **11**, 1743-1756.
28. Lee, Y.J., Park, C.W., Hahn, Y., Park, J., Lee, J., Yun, J.H., Hyun, B. and Chung, J.H. (2000) Mit1/Lb9 and Copg2, new members of mouse imprinted genes closely linked to Peg1/Mest(1). *FEBS Lett*, **472**, 230-234.
29. Yun, J., Park, C.W., Lee, Y.J. and Chung, J.H. (2003) Allele-specific methylation at the promoter-associated CpG island of mouse Copg2. *Mamm Genome*, **14**, 376-382.
30. Rivkin, M., Rosen, K.M. and Villa-Komaroff, L. (1993) Identification of an antisense transcript from the IGF-II locus in mouse. *Mol Reprod Dev*, **35**, 394-397.
31. Moore, T., Constancia, M., Zubair, M., Bailleul, B., Feil, R., Sasaki, H. and Reik, W. (1997) Multiple imprinted sense and antisense transcripts, differential methylation and tandem repeats in a putative imprinting control region upstream of mouse Igf2. *Proc Natl Acad Sci U S A*, **94**, 12509-12514.
32. Lee, M.P., DeBaun, M.R., Mitsuya, K., Galonek, H.L., Brandenburg, S., Oshimura, M. and Feinberg, A.P. (1999) Loss of imprinting of a paternally expressed transcript, with antisense orientation to KVLQT1, occurs frequently in Beckwith-Wiedemann syndrome and is independent of insulin-like growth factor II imprinting. *Proc Natl Acad Sci U S A*, **96**, 5203-5208.
33. Mitsuya, K., Meguro, M., Lee, M.P., Katoh, M., Schulz, T.C., Kugoh, H., Yoshida, M.A., Niikawa, N., Feinberg, A.P. and Oshimura, M. (1999) LIT1, an imprinted antisense RNA in the human KvLQT1 locus identified by

- screening for differentially expressed transcripts using monochromosomal hybrids. *Hum Mol Genet*, **8**, 1209-1217.
34. Smilinich, N.J., Day, C.D., Fitzpatrick, G.V., Caldwell, G.M., Lossie, A.C., Cooper, P.R., Smallwood, A.C., Joyce, J.A., Schofield, P.N., Reik, W. *et al.* (1999) A maternally methylated CpG island in KvLQT1 is associated with an antisense paternal transcript and loss of imprinting in Beckwith-Wiedemann syndrome. *Proc Natl Acad Sci U S A*, **96**, 8064-8069.
 35. Hernandez, A., Fiering, S., Martinez, E., Galton, V.A. and St Germain, D. (2002) The gene locus encoding iodothyronine deiodinase type 3 (Dio3) is imprinted in the fetus and expresses antisense transcripts. *Endocrinology*, **143**, 4483-4486.
 36. Rougeulle, C., Cardoso, C., Fontes, M., Colleaux, L. and Lalande, M. (1998) An imprinted antisense RNA overlaps UBE3A and a second maternally expressed transcript. *Nat Genet*, **19**, 15-16.
 37. Runte, M., Huttenhofer, A., Gross, S., Kieffmann, M., Horsthemke, B. and Buiting, K. (2001) The IC-SNURF-SNRPN transcript serves as a host for multiple small nucleolar RNA species and as an antisense RNA for UBE3A. *Hum Mol Genet*, **10**, 2687-2700.
 38. Jong, M.T., Gray, T.A., Ji, Y., Glenn, C.C., Saitoh, S., Driscoll, D.J. and Nicholls, R.D. (1999) A novel imprinted gene, encoding a RING zinc-finger protein, and overlapping antisense transcript in the Prader-Willi syndrome critical region. *Hum Mol Genet*, **8**, 783-793.
 39. Li, T., Vu, T.H., Zeng, Z.L., Nguyen, B.T., Hayward, B.E., Bonthron, D.T., Hu, J.F. and Hoffman, A.R. (2000) Tissue-specific expression of antisense and sense transcripts at the imprinted Gnas locus. *Genomics*, **69**, 295-304.
 40. Hayward, B.E. and Bonthron, D.T. (2000) An imprinted antisense transcript at the human GNAS1 locus. *Hum Mol Genet*, **9**, 835-841.
 41. Wroe, S.F., Kelsey, G., Skinner, J.A., Bodle, D., Ball, S.T., Beechey, C.V., Peters, J. and Williamson, C.M. (2000) An imprinted transcript, antisense to Nesp, adds complexity to the cluster of imprinted genes at the mouse Gnas locus. *Proc Natl Acad Sci U S A*, **97**, 3342-3346.
 42. Campbell, C.E., Huang, A., Gurney, A.L., Kessler, P.M., Hewitt, J.A. and Williams, B.R. (1994) Antisense transcripts and protein binding motifs within the Wilms tumour (WT1) locus. *Oncogene*, **9**, 583-595.

43. Malik, K.T., Wallace, J.I., Ivins, S.M. and Brown, K.W. (1995) Identification of an antisense WT1 promoter in intron 1: implications for WT1 gene regulation. *Oncogene*, **11**, 1589-1595.
44. Dallosso, A.R., Hancock, A.L., Brown, K.W., Williams, A.C., Jackson, S. and Malik, K. (2004) Genomic imprinting at the WT1 gene involves a novel coding transcript (AWT1) that shows deregulation in Wilms' tumours. *Hum Mol Genet*, **13**, 405-415.
45. Feinberg, A.P. (2007) Phenotypic plasticity and the epigenetics of human disease. *Nature*, **447**, 433-440.
46. Ehrlich, M. (2003) The ICF syndrome, a DNA methyltransferase 3B deficiency and immunodeficiency disease. *Clin Immunol*, **109**, 17-28.
47. Amir, R.E., Van den Veyver, I.B., Wan, M., Tran, C.Q., Francke, U. and Zoghbi, H.Y. (1999) Rett syndrome is caused by mutations in X-linked MECP2, encoding methyl-CpG-binding protein 2. *Nat Genet*, **23**, 185-188.
48. Feinberg, A.P. and Tycko, B. (2004) The history of cancer epigenetics. *Nat Rev Cancer*, **4**, 143-153.
49. Kane, M.F., Loda, M., Gaida, G.M., Lipman, J., Mishra, R., Goldman, H., Jessup, J.M. and Kolodner, R. (1997) Methylation of the hMLH1 promoter correlates with lack of expression of hMLH1 in sporadic colon tumors and mismatch repair-defective human tumor cell lines. *Cancer Res*, **57**, 808-811.
50. Varambally, S., Dhanasekaran, S.M., Zhou, M., Barrette, T.R., Kumar-Sinha, C., Sanda, M.G., Ghosh, D., Pienta, K.J., Sewalt, R.G., Otte, A.P. *et al.* (2002) The polycomb group protein EZH2 is involved in progression of prostate cancer. *Nature*, **419**, 624-629.
51. Lu, Q., Qiu, X., Hu, N., Wen, H., Su, Y. and Richardson, B.C. (2006) Epigenetics, disease, and therapeutic interventions. *Ageing Res Rev*, **5**, 449-467.
52. Gibbons, R.J. and Higgs, D.R. (2000) Molecular-clinical spectrum of the ATR-X syndrome. *Am J Med Genet*, **97**, 204-212.
53. Oostra, B.A. and Willemsen, R. (2002) The X chromosome and fragile X mental retardation. *Cytogenet Genome Res*, **99**, 257-264.
54. Nicholls, R.D., Saitoh, S. and Horsthemke, B. (1998) Imprinting in Prader-Willi and Angelman syndromes. *Trends Genet*, **14**, 194-200.

55. Goldstone, A.P. (2004) Prader-Willi syndrome: advances in genetics, pathophysiology and treatment. *Trends Endocrinol Metab*, **15**, 12-20.
56. Maher, E.R. and Reik, W. (2000) Beckwith-Wiedemann syndrome: imprinting in clusters revisited. *J Clin Invest*, **105**, 247-252.
57. Jones, P.A. and Baylin, S.B. (2002) The fundamental role of epigenetic events in cancer. *Nat Rev Genet*, **3**, 415-428.
58. Roberts, C.W. and Orkin, S.H. (2004) The SWI/SNF complex--chromatin and cancer. *Nat Rev Cancer*, **4**, 133-142.
59. Soejima, H., Nakagawachi, T., Zhao, W., Higashimoto, K., Urano, T., Matsukura, S., Kitajima, Y., Takeuchi, M., Nakayama, M., Oshimura, M. *et al.* (2004) Silencing of imprinted CDKN1C gene expression is associated with loss of CpG and histone H3 lysine 9 methylation at DMR-LIT1 in esophageal cancer. *Oncogene*, **23**, 4380-4388.
60. Claus, R. and Lubbert, M. (2003) Epigenetic targets in hematopoietic malignancies. *Oncogene*, **22**, 6489-6496.
61. Ausio, J., Levin, D.B., De Amorim, G.V., Bakker, S. and Macleod, P.M. (2003) Syndromes of disordered chromatin remodeling. *Clin Genet*, **64**, 83-95.
62. Li, E. (2002) Chromatin modification and epigenetic reprogramming in mammalian development. *Nat Rev Genet*, **3**, 662-673.
63. Ginsburg, M., Snow, M.H. and McLaren, A. (1990) Primordial germ cells in the mouse embryo during gastrulation. *Development*, **110**, 521-528.
64. Hajkova, P., Erhardt, S., Lane, N., Haaf, T., El-Maarri, O., Reik, W., Walter, J. and Surani, M.A. (2002) Epigenetic reprogramming in mouse primordial germ cells. *Mech Dev*, **117**, 15-23.
65. Yamazaki, Y., Mann, M.R., Lee, S.S., Marh, J., McCarrey, J.R., Yanagimachi, R. and Bartolomei, M.S. (2003) Reprogramming of primordial germ cells begins before migration into the genital ridge, making these cells inadequate donors for reproductive cloning. *Proc Natl Acad Sci U S A*, **100**, 12207-12212.
66. Morgan, H.D., Sutherland, H.G., Martin, D.I. and Whitelaw, E. (1999) Epigenetic inheritance at the agouti locus in the mouse. *Nat Genet*, **23**, 314-318.
67. Rakyan, V.K., Chong, S., Champ, M.E., Cuthbert, P.C., Morgan, H.D., Luu, K.V. and Whitelaw, E. (2003) Transgenerational inheritance of epigenetic

- states at the murine Axin(Fu) allele occurs after maternal and paternal transmission. *Proc Natl Acad Sci U S A*, **100**, 2538-2543.
68. Bhattacharya, S.K., Ramchandani, S., Cervoni, N. and Szyf, M. (1999) A mammalian protein with specific demethylase activity for mCpG DNA. *Nature*, **397**, 579-583.
 69. Detich, N., Theberge, J. and Szyf, M. (2002) Promoter-specific activation and demethylation by MBD2/demethylase. *J Biol Chem*, **277**, 35791-35794.
 70. Hamm, S., Just, G., Lacoste, N., Moitessier, N., Szyf, M. and Mamer, O. (2008) On the mechanism of demethylation of 5-methylcytosine in DNA. *Bioorg Med Chem Lett*, **18**, 1046-1049.
 71. Ng, H.H., Zhang, Y., Hendrich, B., Johnson, C.A., Turner, B.M., Erdjument-Bromage, H., Tempst, P., Reinberg, D. and Bird, A. (1999) MBD2 is a transcriptional repressor belonging to the MeCP1 histone deacetylase complex. *Nat Genet*, **23**, 58-61.
 72. Boeke, J., Ammerpohl, O., Kegel, S., Moehren, U. and Renkawitz, R. (2000) The minimal repression domain of MBD2b overlaps with the methyl-CpG-binding domain and binds directly to Sin3A. *J Biol Chem*, **275**, 34963-34967.
 73. Duncan, B.K. and Miller, J.H. (1980) Mutagenic deamination of cytosine residues in DNA. *Nature*, **287**, 560-561.
 74. Brandeis, M., Kafri, T., Ariel, M., Chaillet, J.R., McCarrey, J., Razin, A. and Cedar, H. (1993) The ontogeny of allele-specific methylation associated with imprinted genes in the mouse. *EMBO J*, **12**, 3669-3677.
 75. Kaneko-Ishino, T., Kohda, T. and Ishino, F. (2003) The regulation and biological significance of genomic imprinting in mammals. *J Biochem (Tokyo)*, **133**, 699-711.
 76. Delaval, K., Govin, J., Cerqueira, F., Rousseaux, S., Khochbin, S. and Feil, R. (2007) Differential histone modifications mark mouse imprinting control regions during spermatogenesis. *EMBO J*, **26**, 720-729.
 77. Kaneda, M., Okano, M., Hata, K., Sado, T., Tsujimoto, N., Li, E. and Sasaki, H. (2004) Essential role for de novo DNA methyltransferase Dnmt3a in paternal and maternal imprinting. *Nature*, **429**, 900-903.
 78. Judson, H., Hayward, B.E., Sheridan, E. and Bonthron, D.T. (2002) A global disorder of imprinting in the human female germ line. *Nature*, **416**, 539-542.

79. Hayward, B.E., De Vos, M., Judson, H., Hodge, D., Huntriss, J., Picton, H.M., Sheridan, E. and Bonthron, D.T. (2003) Lack of involvement of known DNA methyltransferases in familial hydatidiform mole implies the involvement of other factors in establishment of imprinting in the human female germline. *BMC Genet*, **4**, 2.
80. Adenot, P.G., Mercier, Y., Renard, J.P. and Thompson, E.M. (1997) Differential H4 acetylation of paternal and maternal chromatin precedes DNA replication and differential transcriptional activity in pronuclei of 1-cell mouse embryos. *Development*, **124**, 4615-4625.
81. Santos, F., Hendrich, B., Reik, W. and Dean, W. (2002) Dynamic reprogramming of DNA methylation in the early mouse embryo. *Dev Biol*, **241**, 172-182.
82. Morgan, H.D., Santos, F., Green, K., Dean, W. and Reik, W. (2005) Epigenetic reprogramming in mammals. *Hum Mol Genet*, **14**, R47-R58.
83. Rougier, N., Bourc'his, D., Gomes, D.M., Niveleau, A., Plachot, M., Paldi, A. and Viegas-Pequignot, E. (1998) Chromosome methylation patterns during mammalian preimplantation development. *Genes Dev*, **12**, 2108-2113.
84. Lane, N., Dean, W., Erhardt, S., Hajkova, P., Surani, A., Walter, J. and Reik, W. (2003) Resistance of IAPs to methylation reprogramming may provide a mechanism for epigenetic inheritance in the mouse. *Genesis*, **35**, 88-93.
85. Olek, A. and Walter, J. (1997) The pre-implantation ontogeny of the H19 methylation imprint. *Nat Genet*, **17**, 275-276.
86. Ferguson-Smith, A.C. and Surani, M.A. (2001) Imprinting and the epigenetic asymmetry between parental genomes. *Science*, **293**, 1086-1089.
87. Beaudet, A.L. and Jiang, Y.H. (2002) A rheostat model for a rapid and reversible form of imprinting-dependent evolution. *Am J Hum Genet*, **70**, 1389-1397.
88. Varmuza, S. and Mann, M. (1994) Genomic imprinting--defusing the ovarian time bomb. *Trends Genet*, **10**, 118-123.
89. Wilkins, J.F. and Haig, D. (2003) What good is genomic imprinting: the function of parent-specific gene expression. *Nat Rev Genet*, **4**, 359-368.
90. Constancia, M., Kelsey, G. and Reik, W. (2004) Resourceful imprinting. *Nature*, **432**, 53-57.

91. Reik, W., Constancia, M., Fowden, A., Anderson, N., Dean, W., Ferguson-Smith, A., Tycko, B. and Sibley, C. (2003) Regulation of supply and demand for maternal nutrients in mammals by imprinted genes. *J Physiol*, **547**, 35-44.
92. Tycko, B. and Morison, I.M. (2002) Physiological functions of imprinted genes. *J Cell Physiol*, **192**, 245-258.
93. Sibley, C.P., Coan, P.M., Ferguson-Smith, A.C., Dean, W., Hughes, J., Smith, P., Reik, W., Burton, G.J., Fowden, A.L. and Constancia, M. (2004) Placental-specific insulin-like growth factor 2 (Igf2) regulates the diffusional exchange characteristics of the mouse placenta. *Proc Natl Acad Sci U S A*, **101**, 8204-8208.
94. Frank, D., Fortino, W., Clark, L., Musalo, R., Wang, W., Saxena, A., Li, C.M., Reik, W., Ludwig, T. and Tycko, B. (2002) Placental overgrowth in mice lacking the imprinted gene *Ipl*. *Proc Natl Acad Sci U S A*, **99**, 7490-7495.
95. Curley, J.P., Barton, S., Surani, A. and Keverne, E.B. (2004) Coadaptation in mother and infant regulated by a paternally expressed imprinted gene. *Proc Biol Sci*, **271**, 1303-1309.
96. Reik, W. and Lewis, A. (2005) Co-evolution of X-chromosome inactivation and imprinting in mammals. *Nat Rev Genet*, **6**, 403-410.
97. Huynh, K.D. and Lee, J.T. (2003) Inheritance of a pre-inactivated paternal X chromosome in early mouse embryos. *Nature*, **426**, 857-862.
98. Okamoto, I., Otte, A.P., Allis, C.D., Reinberg, D. and Heard, E. (2004) Epigenetic dynamics of imprinted X inactivation during early mouse development. *Science*, **303**, 644-649.
99. Mak, W., Nesterova, T.B., de Napoles, M., Appanah, R., Yamanaka, S., Otte, A.P. and Brockdorff, N. (2004) Reactivation of the paternal X chromosome in early mouse embryos. *Science*, **303**, 666-669.
100. Engemann, S., Strodick, M., Paulsen, M., Franck, O., Reinhardt, R., Lane, N., Reik, W. and Walter, J. (2000) Sequence and functional comparison in the Beckwith-Wiedemann region: implications for a novel imprinting centre and extended imprinting. *Hum Mol Genet*, **9**, 2691-2706.
101. Stoger, R., Kubicka, P., Liu, C.G., Kafri, T., Razin, A., Cedar, H. and Barlow, D.P. (1993) Maternal-specific methylation of the imprinted mouse *Igf2r* locus identifies the expressed locus as carrying the imprinting signal. *Cell*, **73**, 61-71.

102. de Napoles, M., Mermoud, J.E., Wakao, R., Tang, Y.A., Endoh, M., Appanah, R., Nesterova, T.B., Silva, J., Otte, A.P., Vidal, M. *et al.* (2004) Polycomb group proteins Ring1A/B link ubiquitylation of histone H2A to heritable gene silencing and X inactivation. *Dev Cell*, **7**, 663-676.
103. Lewis, A., Mitsuya, K., Umlauf, D., Smith, P., Dean, W., Walter, J., Higgins, M., Feil, R. and Reik, W. (2004) Imprinting on distal chromosome 7 in the placenta involves repressive histone methylation independent of DNA methylation. *Nat Genet*, **36**, 1291-1295.
104. Xin, Z.H., Allis, C.D. and Wagstaff, J. (2001) Parent-specific complementary patterns of histone H3 lysine 9 and H3 lysine 4 methylation at the Prader-Willi syndrome imprinting center. *Am J Hum Genet*, **69**, 1389-1394.
105. Ferguson-Smith, A.C. (2000) Genetic imprinting: silencing elements have their say. *Curr Biol*, **10**, R872-875.
106. Nicholls, R.D. and Knepper, J.L. (2001) Genome organization, function and imprinting in Prader-Willi and Angelman syndromes. *Annu Rev Genomics Hum Genet*, **2**, 153-175.
107. Bielinska, B., Blaydes, S.M., Buiting, K., Yang, T., Krajewska-Walasek, M., Horsthemke, B. and Brannan, C.I. (2000) De novo deletions of SNRPN exon 1 in early human and mouse embryos result in a paternal to maternal imprint switch. *Nat Genet*, **25**, 74-78.
108. Szabo, P., Tang, S.H., Rentsendorj, A., Pfeifer, G.P. and Mann, J.R. (2000) Maternal-specific footprints at putative CTCF sites in the H19 imprinting control region give evidence for insulator function. *Curr Biol*, **10**, 607-610.
109. Kanduri, C., Pant, V., Loukinov, D., Pugacheva, E., Qi, C.F., Wolffe, A., Ohlsson, R. and Lobanenko, V.V. (2000) Functional association of CTCF with the insulator upstream of the H19 gene is parent of origin-specific and methylation-sensitive. *Curr Biol*, **10**, 853-856.
110. Bell, A.C. and Felsenfeld, G. (2000) Methylation of a CTCF-dependent boundary controls imprinted expression of the Igf2 gene. *Nature*, **405**, 482-485.
111. Hark, A.T., Schoenherr, C.J., Katz, D.J., Ingram, R.S., Levorse, J.M. and Tilghman, S.M. (2000) CTCF mediates methylation-sensitive enhancer-blocking activity at the H19/Igf2 locus. *Nature*, **405**, 486-489.

112. Constancia, M., Dean, W., Lopes, S., Moore, T., Kelsey, G. and Reik, W. (2000) Deletion of a silencer element in *Igf2* results in loss of imprinting independent of H19. *Nat Genet*, **26**, 203-206.
113. Eden, S., Constancia, M., Hashimshony, T., Dean, W., Goldstein, B., Johnson, A.C., Keshet, I., Reik, W. and Cedar, H. (2001) An upstream repressor element plays a role in *Igf2* imprinting. *EMBO J*, **20**, 3518-3525.
114. Murrell, A., Heeson, S. and Reik, W. (2004) Interaction between differentially methylated regions partitions the imprinted genes *Igf2* and H19 into parent-specific chromatin loops. *Nat Genet*, **36**, 889-893.
115. Kurukuti, S., Tiwari, V.K., Tavoosidana, G., Pugacheva, E., Murrell, A., Zhao, Z.H., Lobanenko, V., Reik, W. and Ohlsson, R. (2006) CTCF binding at the H19 imprinting control region mediates maternally inherited higher-order chromatin conformation to restrict enhancer access to *Igf2*. *Proc Natl Acad Sci USA*, **103**, 10684-10689.
116. Jiang, Y.H., Tsai, T.F., Bressler, J. and Beaudet, A.L. (1998) Imprinting in Angelman and Prader-Willi syndromes. *Curr Opin Genetics Dev*, **8**, 334-342.
117. Myers, S.E., Whitman, B.Y., Carrel, A.L., Moerchen, V., Bekx, M.T. and Allen, D.B. (2007) Two years of growth hormone therapy in young children with Prader-Willi syndrome: physical and neurodevelopmental benefits. *Am J Med Genet A*, **143**, 443-448.
118. van Woerden, G.M., Harris, K.D., Hojjati, M.R., Gustin, R.M., Qiu, S., de Avila Freire, R., Jiang, Y.H., Elgersma, Y. and Weeber, E.J. (2007) Rescue of neurological deficits in a mouse model for Angelman syndrome by reduction of α CaMKII inhibitory phosphorylation. *Nat Neurosci*, **10**, 280-282.
119. Chen, K.S., Manian, P., Koeuth, T., Potocki, L., Zhao, Q., Chinault, A.C., Lee, C.C. and Lupski, J.R. (1997) Homologous recombination of a flanking repeat gene cluster is a mechanism for a common contiguous gene deletion syndrome. *Nat Genet*, **17**, 154-163.
120. Robinson, W.P., Christian, S.L., Kuchinka, B.D., Penaherrera, M.S., Das, S., Schuffenhauer, S., Malcolm, S., Schinzel, A.A., Hassold, T.J. and Ledbetter, D.H. (2000) Somatic segregation errors predominantly contribute to the gain or loss of a paternal chromosome leading to uniparental disomy for chromosome 15. *Clin Genet*, **57**, 349-358.

121. Zogel, C., Bohringer, S., Gross, S., Varon, R., Buiting, K. and Horsthemke, B. (2006) Identification of cis- and trans-acting factors possibly modifying the risk of epimutations on chromosome 15. *Eur J Human Genet*, **14**, 752-758.
122. Buiting, K., Gross, S., Lich, C., Gillessen-Kaesbach, G., El-Maarri, O. and Horsthemke, B. (2003) Epimutations in Prader-Willi and Angelman syndromes: A molecular study of 136 patients with an imprinting defect. *Am J Hum Genet*, **72**, 571-577.
123. Maina, E.N., Webb, T., Soni, S., Whittington, J., Boer, H., Clarke, D. and Holland, A. (2007) Analysis of candidate imprinted genes in PWS subjects with atypical genetics: a possible inactivating mutation in the SNURF/SNRPN minimal promoter. *J Hum Genet*, **52**, 297-307.
124. Rougeulle, C., Glatt, H. and Lalonde, M. (1997) The Angelman syndrome candidate gene, UBE3A/E6-AP, is imprinted in brain. *Nat Genet*, **17**, 14-15.
125. Vu, T.H. and Hoffman, A.R. (1997) Imprinting of the Angelman syndrome gene, UBE3A, is restricted to brain. *Nat Genet*, **17**, 12-13.
126. Nawaz, Z., Lonard, D.M., Smith, C.L., Lev-Lehman, E., Tsai, S.Y., Tsai, M.J. and O'Malley, B.W. (1999) The Angelman syndrome-associated protein, E6-AP, is a coactivator for the nuclear hormone receptor superfamily. *Mol Cell Biol*, **19**, 1182-1189.
127. Krawczak, M. and Cooper, D.N. (1997) The human gene mutation database. *Trends Genet*, **13**, 121-122.
128. Lossie, A.C., Whitney, M.M., Amidon, D., Dong, H.J., Chen, P., Theriaque, D., Hutson, A., Nicholls, R.D., Zori, R.T., Williams, C.A. *et al.* (2001) Distinct phenotypes distinguish the molecular classes of Angelman syndrome. *J Med Genet*, **38**, 834-845.
129. Rapkins, R.W., Hore, T., Smithwick, M., Ager, E., Pask, A.J., Renfree, M.B., Kohn, M., Hameister, H., Nicholls, R.D., Deakin, J.E. *et al.* (2006) Recent assembly of an imprinted domain from non-imprinted components. *PLoS Genet*, **2**, e182.
130. Tsai, T.F., Jiang, Y.H., Bressler, J., Armstrong, D. and Beaudet, A.L. (1999) Paternal deletion from Snrpn to Ube3a in the mouse causes hypotonia, growth retardation and partial lethality and provides evidence for a gene contributing to Prader-Willi syndrome. *Hum Mol Genet*, **8**, 1357-1364.

131. Yang, T., Adamson, T.E., Resnick, J.L., Leff, S., Wevrick, R., Francke, U., Jenkins, N.A., Copeland, N.G. and Brannan, C.I. (1998) A mouse model for Prader-Willi syndrome imprinting-centre mutations. *Nat Genet*, **19**, 25-31.
132. Gray, T.A., Smithwick, M.J., Schaldach, M.A., Martone, D.L., Graves, J.A., McCarrey, J.R. and Nicholls, R.D. (1999) Concerted regulation and molecular evolution of the duplicated SNRPB'/B and SNRPN loci. *Nucleic Acids Res*, **27**, 4577-4584.
133. Tsai, T.F., Chen, K.S., Weber, J.S., Justice, M.J. and Beaudet, A.L. (2002) Evidence for translational regulation of the imprinted Snurf-Snrpn locus in mice. *Hum Mol Genet*, **11**, 1659-1668.
134. Gerard, M., Hernandez, L., Wevrick, R. and Stewart, C.L. (1999) Disruption of the mouse necdin gene results in early post-natal lethality. *Nat Genet*, **23**, 199-202.
135. Muscatelli, F., Abrous, D.N., Massacrier, A., Boccaccio, I., La Moal, M., Cau, P. and Cremer, H. (2000) Disruption of the mouse Necdin gene results in hypothalamic and behavioral alterations reminiscent of the human Prader-Willi syndrome. *Hum Mol Genet*, **9**, 3101-3110.
136. Tsai, T.F., Armstrong, D. and Beaudet, A.L. (1999) Necdin-deficient mice do not show lethality or the obesity and infertility of Prader-Willi syndrome. *Nat Genet*, **22**, 15-16.
137. Lee, S., Kozlov, S., Hernandez, L., Chamberlain, S.J., Brannan, C.I., Stewart, C.L. and Wevrick, R. (2000) Expression and imprinting of MAGEL2 suggest a role in Prader-Willi syndrome and the homologous murine imprinting phenotype. *Hum Mol Genet*, **9**, 1813-1819.
138. Bischof, J.M., Stewart, C.L. and Wevrick, R. (2007) Inactivation of the mouse Magel2 gene results in growth abnormalities similar to Prader-Willi Syndrome. *Hum Mol Genet*, **16**, 2713-2719.
139. Jong, M.T.C., Gray, T.A., Ji, Y.G., Glenn, C.C., Saitoh, S., Driscoll, D.J. and Nicholls, R.D. (1999) A novel imprinted gene, encoding a RING zinc-finger protein, and overlapping antisense transcript in the Prader-Willi syndrome critical region. *Hum Mol Genet*, **8**, 783-793.
140. Farber, C., Gross, S., Neesen, J., Buiting, K. and Horsthemke, B. (2000) Identification of a testis-specific gene (C15orf2) in the Prader-Willi syndrome region on chromosome 15. *Genomics*, **65**, 174-183.

141. Girard, A., Sachidanandam, R., Hannon, G.J. and Carmell, M.A. (2006) A germline-specific class of small RNAs binds mammalian Piwi proteins. *Nature*, **442**, 199-202.
142. Aravin, A., Gaidatzis, D., Pfeffer, S., Lagos-Quintana, M., Landgraf, P., Iovino, N., Morris, P., Brownstein, M.J., Kuramochi-Miyagawa, S., Nakano, T. *et al.* (2006) A novel class of small RNAs bind to MILI protein in mouse testes. *Nature*, **442**, 203-207.
143. Grivna, S.T., Beyret, E., Wang, Z. and Lin, H. (2006) A novel class of small RNAs in mouse spermatogenic cells. *Genes Dev*, **20**, 1709-1714.
144. Grivna, S.T., Pyhtila, B. and Lin, H. (2006) MIWI associates with translational machinery and PIWI-interacting RNAs (piRNAs) in regulating spermatogenesis. *Proc Natl Acad Sci U S A*, **103**, 13415-13420.
145. Buiting, K., Nazlican, H., Galetzka, D., Wawrzik, M., Gross, S. and Horsthemke, B. (2007) C15orf2 and a novel noncoding transcript from the Prader-Willi/Angelman syndrome region show monoallelic expression in fetal brain. *Genomics*, **89**, 588-595.
146. Ding, F., Prints, Y., Dhar, M.S., Johnson, D.K., Garnacho-Montero, C., Nicholls, R.D. and Francke, U. (2005) Lack of Pwcr1/MBII-85 snoRNA is critical for neonatal lethality in Prader-Willi syndrome mouse models. *Mamm Genome*, **16**, 424-431.
147. Runte, M., Varon, R., Horn, D., Horsthemke, B. and Buiting, K. (2005) Exclusion of the C/D box snoRNA gene cluster HBII-52 from a major role in Prader-Willi syndrome. *Hum Genet*, **116**, 228-230.
148. Gallagher, R.C., Pils, B., Albalwi, M. and Francke, U. (2002) Evidence for the role of PWCR1/HBII-85 C/D box small nucleolar RNAs in Prader-Willi syndrome. *Am J Hum Genet*, **71**, 669-678.
149. T. Sahoo, D.d.G., J.R. German, M. Shinawi, S.U. Peters, R. Person, A. Garnica, S.W. Cheung, A.L. Beaudet (2007) Prader-Willi syndrome is caused by paternal deficiency for the HBII-85 C/D box snoRNA cluster. *57th Annual Meeting of the American Society of Human Genetics*. San Diego, California, USA, p. 64.
150. F.Ding, H.L., S. Zhang, N. Solomon, S. Camper, E. Mignot, U. Francke (2007) SnoRNA Pwcr1/MBII-85 deletion mouse model for Prader-Willi syndrome shows growth retardation, hyperphagia and altered metabolism. *57th Annual*

- Meeting of the American Society of Human Genetics*. San Diego, California, USA, p. 64.
151. Kishino, T. (2006) Imprinting in neurons. *Cytogenet Genome Res*, **113**, 209-214.
 152. Meguro, M., Kashiwagi, A., Mitsuya, K., Nakao, M., Kondo, I., Saitoh, S. and Oshimura, M. (2001) A novel maternally expressed gene, ATP10C, encodes a putative aminophospholipid translocase associated with Angelman syndrome. *Nat Genet*, **28**, 19-20.
 153. Herzing, L.B., Kim, S.J., Cook, E.H., Jr. and Ledbetter, D.H. (2001) The human aminophospholipid-transporting ATPase gene ATP10C maps adjacent to UBE3A and exhibits similar imprinted expression. *Am J Hum Genet*, **68**, 1501-1505.
 154. Kashiwagi, A., Meguro, M., Hoshiya, H., Haruta, M., Ishino, F., Shibahara, T. and Oshimura, M. (2003) Predominant maternal expression of the mouse Atp10c in hippocampus and olfactory bulb. *J Hum Genet*, **48**, 194-198.
 155. Kayashima, T., Yamasaki, K., Joh, K., Yamada, T., Ohta, T., Yoshiura, K., Matsumoto, N., Nakane, Y., Mukai, T., Niikawa, N. *et al.* (2003) Atp10a, the mouse ortholog of the human imprinted ATP10A gene, escapes genomic imprinting. *Genomics*, **81**, 644-647.
 156. Dhar, M., Webb, L.S., Smith, L., Hauser, L., Johnson, D. and West, D.B. (2000) A novel ATPase on mouse chromosome 7 is a candidate gene for increased body fat. *Physiol Genomics*, **4**, 93-100.
 157. Gabriel, J.M., Gray, T.A., Stubbs, L., Saitoh, S., Ohta, T. and Nicholls, R.D. (1998) Structure and function correlations at the imprinted mouse Snrpn locus. *Mamm Genome*, **9**, 788-793.
 158. Glenn, C.C., Saitoh, S., Jong, M.T.C., Filbrandt, M.M., Surti, U., Driscoll, D.J. and Nicholls, R.D. (1996) Gene structure, DNA methylation, and imprinted expression of the human SNRPN gene. *Am J Hum Genet*, **58**, 335-346.
 159. Jong, M.T.C., Carey, A.H., Caldwell, K.A., Lau, M.H., Handel, M.A., Driscoll, D.J., Stewart, C.L., Rinchik, E.M. and Nicholls, R.D. (1999) Imprinting of a RING zinc-finger encoding gene in the mouse chromosome region homologous to the Prader-Willi syndrome genetic region. *Hum Mol Genet*, **8**, 795-803.

160. Lau, J.C.Y., Hanel, M.L. and Wevrick, R. (2004) Tissue-specific and imprinted epigenetic modifications of the human NDN gene. *Nucleic Acids Res*, **32**, 3376-3382.
161. Zeschnigk, M., Lich, C., Buiting, K., Doerfler, W. and Horsthemke, B. (1997) A single-tube PCR test for the diagnosis of angelman and Prader-Willi syndrome based on allelic methylation differences at the SNRPN locus. *Eur J Human Genet*, **5**, 94-98.
162. Soejima, H. and Wagstaff, J. (2005) Imprinting centers, chromatin structure, and disease. *J Cell Biochem*, **95**, 226-233.
163. El-Maarri, O., Buiting, K., Peery, E.G., Kroisel, P.M., Balaban, B., Wagner, K., Urman, B., Heyd, J., Lich, C., Brannan, C.I. *et al.* (2001) Maternal methylation imprints on human chromosome 15 are established during or after fertilization. *Nat Genet*, **27**, 341-344.
164. Geuns, E., De Rycke, M., Van Steirteghem, A. and Liebaers, I. (2003) Methylation imprints of the imprint control region of the SNRPN-gene in human gametes and preimplantation embryos. *Hum Mol Genet*, **12**, 2873-2879.
165. Fournier, C., Goto, Y.J., Ballestar, E., Delaval, K., Hever, A.M., Esteller, M. and Feil, R. (2002) Allele-specific histone lysine methylation marks regulatory regions at imprinted mouse genes. *EMBO J*, **21**, 6560-6570.
166. Xin, Z.H., Tachibana, M., Guggiari, M., Heard, E., Shinkai, Y. and Wagstaff, J. (2003) Role of histone methyltransferase G9a in CpG methylation of the Prader-Willi syndrome imprinting center. *J Biol Chem*, **278**, 14996-15000.
167. Schweizer, J., Zzynger, D. and Francke, U. (1999) In vivo nuclease hypersensitivity studies reveal multiple sites of parental origin-dependent differential chromatin conformation in the 150 kb SNRPN transcription unit. *Hum Mol Genet*, **8**, 555-566.
168. Rodriguez-Jato, S., Nicholls, R.D., Driscoll, D.J. and Yang, T.P. (2005) Characterization of cis- and trans-acting elements in the imprinted human SNURF-SNRPN locus. *Nucleic Acids Res*, **33**, 4740-4753.
169. Landers, M., Bancescu, D.L., Le Meur, E., Rougeulle, C., Glatt-Deeley, H., Brannan, C., Muscatelli, F. and Lalande, M. (2004) Regulation of the large (similar to 1000 kb) imprinted murine Ube3a antisense transcript by alternative exons upstream of Snurf/Snrpn. *Nucleic Acids Res*, **32**, 3480-3492.

170. Landers, M., Calcianno, M.A., Colosi, D., Glatt-Deeley, H., Wagstaff, J. and Lalande, M. (2005) Maternal disruption of Ube3a leads to increased expression of Ube3a-ATS in trans. *Nucleic Acids Res*, **33**, 3976-3984.
171. Ohta, T., Gray, T.A., Rogan, P.K., Buiting, K., Gabriel, J.M., Saitoh, S., Muralidhar, B., Bilienska, B., Krajewska-Walasek, M., Driscoll, D.J. *et al.* (1999) Imprinting-mutation mechanisms in Prader-Willi syndrome. *Am J Hum Genet*, **64**, 397-413.
172. Buiting, K., Lich, C., Cottrell, S., Barnicoat, A. and Horsthemke, B. (1999) A 5-kb imprinting center deletion in a family with Angelman syndrome reduces the shortest region of deletion overlap to 880 bp. *Hum Genet*, **105**, 665-666.
173. Ohta, T., Buiting, K., Kokkonen, H., McCandless, S., Heeger, S., Leisti, H., Driscoll, D.J., Cassidy, S.B., Horsthemke, B. and Nicholls, R.D. (1999) Molecular mechanism of Angelman syndrome in two large families involves an imprinting mutation. *Am J Hum Genet*, **64**, 385-396.
174. Perk, J., Makedonski, K., Lande, L., Cedar, H., Razin, A. and Shemer, R. (2002) The imprinting mechanism of the Prader-Willi/Angelman regional control center. *EMBO J*, **21**, 5807-5814.
175. Shemer, R., Hershko, A.Y., Perk, J., Mostoslavsky, R., Tsuberi, B., Cedar, H., Buiting, K. and Razin, A. (2000) The imprinting box of the Prader-Willi/Angelman syndrome domain. *Nat Genet*, **26**, 440-443.
176. Kantor, B., Kaufman, Y., Makedonski, K., Razin, A. and Shemer, R. (2004) Establishing the epigenetic status of the Prader-Willi/Angelman imprinting center in the gametes and embryo. *Hum Mol Genet*, **13**, 2767-2779.
177. Kantor, B., Shemer, R. and Razin, A. (2006) The Prader-Willi/Angelman imprinted domain and its control center. *Cytogenet Genome Res*, **113**, 300-305.
178. Buiting, K., Barnicoat, A., Lich, C., Pembrey, M., Malcolm, S. and Horsthemke, B. (2001) Disruption of the bipartite imprinting center in a family with Angelman syndrome. *Am J Hum Genet*, **68**, 1290-1294.
179. Knoll, J.H., Cheng, S.D. and Lalande, M. (1994) Allele specificity of DNA replication timing in the Angelman/Prader-Willi syndrome imprinted chromosomal region. *Nat Genet*, **6**, 41-46.
180. Simon, I., Tenzen, T., Reubinoff, B.E., Hillman, D., McCarrey, J.R. and Cedar, H. (1999) Asynchronous replication of imprinted genes is established in the gametes and maintained during development. *Nature*, **401**, 929-932.

181. Wu, M.Y., Chen, K.S., Bressler, J., Hou, A.H., Tsai, T.F. and Beaudet, A.L. (2006) Mouse imprinting defect mutations that model Angelman syndrome. *Genesis*, **44**, 12-22.
182. Bressler, J., Tsai, T.F., Wu, M.Y., Tsai, S.F., Ramirez, M.A., Armstrong, D. and Beaudet, A.L. (2001) The SNRPN promoter is not required for genomic imprinting of the PraderWilli/Angelman domain in mice. *Nat Genet*, **28**, 232-240.
183. Cattanach, B.M., Barr, J.A., Evans, E.P., Burtenshaw, M., Beechey, C.V., Leff, S.E., Brannan, C.I., Copeland, N.G., Jenkins, N.A. and Jones, J. (1992) A Candidate Mouse Model for Prader-Willi Syndrome Which Shows an Absence of Snrpn Expression. *Nat Genet*, **2**, 270-274.
184. Gabriel, J.M., Merchant, M., Ohta, T., Ji, Y., Caldwell, R.G., Ramsey, M.J., Tucker, J.D., Longnecker, R. and Nicholls, R.D. (1999) A transgene insertion creating a heritable chromosome deletion mouse model of Prader-Willi and Angelman syndromes. *Proc Natl Acad Sci U S A*, **96**, 9258-9263.
185. Jiang, Y.H., Armstrong, D., Albrecht, U., Atkins, C.M., Noebels, J.L., Eichele, G., Sweatt, J.D. and Beaudet, A.L. (1998) Mutation of the angelman ubiquitin ligase in mice causes increased cytoplasmic p53 and deficits of contextual learning and long-term potentiation. *Neuron*, **21**, 799-811.
186. Johnstone, K.A., DuBose, A.J., Futtner, C.R., Elmore, M.D., Brannan, C.I. and Resnick, J.L. (2006) A human imprinting centre demonstrates conserved acquisition but diverged maintenance of imprinting in a mouse model for Angelman syndrome imprinting defects. *Hum Mol Genet*, **15**, 393-404.
187. Peery, E.G., Elmore, M.D., Resnick, J.L., Brannan, C.I. and Johnstone, K.A. (2007) A targeted deletion upstream of Snrpn does not result in an imprinting defect. *Mamm Genome*, **18**, 255-262.
188. Li, L.C. and Dahiya, R. (2002) MethPrimer: designing primers for methylation PCRs. *Bioinformatics*, **18**, 1427-1431.
189. Friedrich, G. and Soriano, P. (1991) Promoter traps in embryonic stem cells: a genetic screen to identify and mutate developmental genes in mice. *Genes Dev*, **5**, 1513-1523.
190. Bradley, A.P.M.a.A. (1990) The Wnt-1 (int-1) proto-oncogene is required for development of a large region of the mouse brain. *Cell*, **62**, 1073.

191. Sambrook J., R.W.D. (2001) *Molecular Cloning: A laboratory Mannual. Third Edition*. Cold Spring Harbor Laboratory Press.
192. Zeschnigk, M., Schmitz, B., Dittrich, B., Buiting, K., Horsthemke, B. and Doerfler, W. (1997) Imprinted segments in the human genome: Different DNA methylation patterns in the Prader-Willi/Angelman syndrome region as determined by the genomic sequencing method. *Hum Mol Genet*, **6**, 387-395.
193. Allen, N.D., Norris, M.L. and Surani, M.A. (1990) Epigenetic Control of Transgene Expression and Imprinting by Genotype-Specific Modifiers. *Cell*, **61**, 853-861.
194. Nakayama J, R.J., Strahl BD, Allis CD, Grewal SI (2001) Role of histone H3 lysine 9 methylation in epigenetic control of heterochromatin assembly. *Science*, **292**, 110-113.
195. Rougeulle, C. and Lalonde, M. (1998) Angelman syndrome: how many genes to remain silent? *Neurogenetics*, **1**, 229-237.
196. Chamberlain, S.J. and Brannan, C.I. (2001) The Prader-Willi syndrome imprinting center activates the paternally expressed murine Ube3a antisense transcript but represses paternal Ube3a. *Genomics*, **73**, 316-322.
197. Yamasaki, K., Joh, K., Ohta, T., Masuzaki, H., Ishimaru, T., Mukai, T., Niikawa, N., Ogawa, M., Wagstaff, J. and Kishino, T. (2003) Neurons but not glial cells show reciprocal imprinting of sense and antisense transcripts of Ube3a. *Hum Mol Genet*, **12**, 837-847.
198. Xin, Z., Tachibana, M., Shinkai, Y. and Wagstaff, J. (2002) Role of histone methyltransferase, G9a in H3 Lys9 methylation and CpG methylation of the Prader-Willi imprinting center. *Am J Hum Genet*, **71**, 493-493.
199. Epner, E., Forrester, W.C. and Groudine, M. (1988) Asynchronous DNA replication within the human beta-globin gene locus. *Proc Natl Acad Sci U S A*, **85**, 8081-8085.
200. Simon, I., Tenzen, T., Mostoslavsky, R., Fibach, E., Lande, L., Milot, E., Gribnau, J., Grosveld, F., Fraser, P. and Cedar, H. (2001) Developmental regulation of DNA replication timing at the human beta globin locus. *EMBO J*, **20**, 6150-6157.
201. Kagotani, K., Takebayashi, S., Kohda, A., Taguchi, H., Paulsen, M., Walter, J., Reik, W. and Okumura, K. (2002) Replication timing properties within the

- mouse distal chromosome 7 imprinting cluster. *Biosci Biotechnol Biochem*, **66**, 1046-1051.
202. Albrecht, U., Sutcliffe, J.S., Cattanach, B.M., Beechey, C.V., Armstrong, D., Eichele, G. and Beaudet, A.L. (1997) Imprinted expression of the murine Angelman syndrome gene, Ube3a, in hippocampal and Purkinje neurons. *Nat Genet*, **17**, 75-78.
 203. Varela, M.C., Kok, F., Setian, N., Kim, C.A. and Koiffmann, C.P. (2005) Impact of molecular mechanisms, including deletion size, on Prader-Willi syndrome phenotype: study of 75 patients. *Clin Genet*, **67**, 47-52.
 204. Holm, V.A., Cassidy, S.B., Butler, M.G., Hanchett, J.M., Greenswag, L.R., Whitman, B.Y. and Greenberg, F. (1993) Prader-Willi syndrome: consensus diagnostic criteria. *Pediatrics*, **91**, 398-402.
 205. Teshima, I., Chadwick, D., Chitayat, D., Kobayashi, J., Ray, P., Shuman, C., SiegelBartelt, J., Strasberg, P. and Weksberg, R. (1996) FISH detection of chromosome 15 deletions in Prader-Willi and Angelman syndromes (vol 62, pg 216, 1996). *Am J Med Genet*, **64**, 527-527.
 206. Petkov, P.M., Ding, Y., Cassell, M.A., Zhang, W., Wagner, G., Sargent, E.E., Asquith, S., Crew, V., Johnson, K.A., Robinson, P. *et al.* (2004) An efficient SNP system for mouse genome scanning and elucidating strain relationships. *Genome Res*, **14**, 1806-1811.
 207. Simpson, E.M., Linder, C.C., Sargent, E.E., Davisson, M.T., Mobraaten, L.E. and Sharp, J.J. (1997) Genetic variation among 129 substrains and its importance for targeted mutagenesis in mice. *Nat Genet*, **16**, 19-27.
 208. Chamberlain, S.J., Johnstone, K.A., DuBose, A.J., Simon, T.A., Bartolomei, M.S., Resnick, J.L. and Brannan, C.I. (2004) Evidence for genetic modifiers of postnatal lethality in PWS-IC deletion mice. *Hum Mol Genet*, **13**, 2971-2977.
 209. Chong, S., Vickaryous, N., Ashe, A., Zamudio, N., Youngson, N., Hemley, S., Stopka, T., Skoultchi, A., Matthews, J., Scott, H.S. *et al.* (2007) Modifiers of epigenetic reprogramming show paternal effects in the mouse. *Nat Genet*, **39**, 614-622.
 210. Cattanach, B.M., Barr, J.A., Beechey, C.V., Martin, J., Noebels, J. and Jones, J. (1997) A candidate model for Angelman syndrome in the mouse. *Mamm Genome*, **8**, 472-478.

211. Brannan, C.I. and Bartolomei, M.S. (1999) Mechanisms of genomic imprinting. *Curr Opin Genetics Dev*, **9**, 164-170.
212. Liu, H., Kim, J.M. and Aoki, F. (2004) Regulation of histone H3 lysine 9 methylation in oocytes and early pre-implantation embryos. *Development*, **131**, 2269-2280.
213. Makedonski, K., Abuhatzira, L., Kaufman, Y., Razin, A. and Shemer, R. (2005) MeCP2 deficiency in Rett syndrome causes epigenetic aberrations at the PWS/AS imprinting center that affects UBE3A expression. *Hum Mol Genet*, **14**, 1049-1058.
214. Loppin, B., Bonnefoy, E., Anselme, C., Laurencon, A., Karr, T.L. and Couble, P. (2005) The histone H3.3 chaperone HIRA is essential for chromatin assembly in the male pronucleus. *Nature*, **437**, 1386-1390.
215. van der Heijden, G.W., Dieker, J.W., Derijck, A.A., Muller, S., Berden, J.H., Braat, D.D., van der Vlag, J. and de Boer, P. (2005) Asymmetry in histone H3 variants and lysine methylation between paternal and maternal chromatin of the early mouse zygote. *Mech Dev*, **122**, 1008-1022.
216. Horike, S., Cai, S.T., Miyano, M., Cheng, J.F. and Kohwi-Shigematsu, T. (2005) Loss of silent-chromatin looping and impaired imprinting of DLX5 in Rett syndrome. *Nat Genet*, **37**, 31-40.
217. Zhao, Z., Tavoosidana, G., Sjolinder, M., Gondor, A., Mariano, P., Wang, S., Kanduri, C., Lezcano, M., Sandhu, K.S., Singh, U. *et al.* (2006) Circular chromosome conformation capture (4C) uncovers extensive networks of epigenetically regulated intra- and interchromosomal interactions. *Nat Genet*, **38**, 1341-1347.
218. Dostie, J., Richmond, T.A., Arnaout, R.A., Selzer, R.R., Lee, W.L., Honan, T.A., Rubio, E.D., Krumm, A., Lamb, J., Nusbaum, C. *et al.* (2006) Chromosome Conformation Capture Carbon Copy (5C): a massively parallel solution for mapping interactions between genomic elements. *Genome Res*, **16**, 1299-1309.
219. Samaco, R.C., Hogart, A. and LaSalle, J.M. (2005) Epigenetic overlap in autism-spectrum neurodevelopmental disorders: MECP2 deficiency causes reduced expression of UBE3A and GABRB3. *Hum Mol Genet*, **14**, 483-492.
220. Fraser, P. and Bickmore, W. (2007) Nuclear organization of the genome and the potential for gene regulation. *Nature*, **447**, 413-417.

221. Gribnau, J., Hochedlinger, K., Hata, K., Li, E. and Jaenisch, R. (2003) Asynchronous replication timing of imprinted loci is independent of DNA methylation, but consistent with differential subnuclear localization. *Genes Dev*, **17**, 759-773.
222. Mapendano, C.K., Kishino, T., Miyazaki, K., Kondo, S., Yoshiura, K., Hishikawa, Y., Koji, T., Niikawa, N. and Ohta, T. (2006) Expression of the Snurf-Snrpn IC transcript in the oocyte and its putative role in the imprinting establishment of the mouse 7C imprinting domain. *J Hum Genet*, **51**, 236-243.
223. Buettner, V.I., Walker, A.M. and Singer-Sam, J. (2005) Novel paternally expressed intergenic transcripts at the mouse Prader-Willi/Angelman Syndrome locus. *Mamm Genome*, **16**, 219-227.
224. Wutz, A. and Barlow, D.P. (1998) Imprinting of the mouse Igf2r gene depends on an intronic CpG island. *Mol Cell Endocrinol*, **140**, 9-14.
225. Butler, M.G., Bittel, D.C., Kibiryeve, N., Talebizadeh, Z. and Thompson, T. (2004) Behavioral differences among subjects with Prader-Willi syndrome and type I or type II deletion and maternal disomy. *Pediatrics*, **113**, 565-573.
226. Gillessenkaesbach, G., Robinson, W., Lohmann, D., Kayawesterloh, S., Passarge, E. and Horsthemke, B. (1995) Genotype-Phenotype Correlation in a Series of 167 Deletion and Nondeletion Patients with Prader-Willi-Syndrome. *Hum Genet*, **96**, 638-643.
227. Cassidy, S.B., Forsythe, M., Heeger, S., Nicholls, R.D., Schork, N., Benn, P. and Schwartz, S. (1997) Comparison of phenotype between patients with Prader-Willi syndrome due to deletion 15q and uniparental disomy 15. *Am J Med Genet*, **68**, 433-440.
228. Armour, J.A.L., Sismani, C., Patsalis, P.C. and Cross, G. (2000) Measurement of locus copy number by hybridisation with amplifiable probes. *Nucleic Acids Res*, **28**, 605-609.
229. Schouten, J.P., McElgunn, C.J., Waaijer, R., Zwiijnenburg, D., Diepvens, F. and Pals, G. (2002) Relative quantification of 40 nucleic acid sequences by multiplex ligation-dependent probe amplification. *Nucleic Acids Res*, **30**, e57.
230. Gondek, L.P., Dunbar, A.J., Szpurka, H., McDevitt, M.A. and Maciejewski, J.P. (2007) SNP Array Karyotyping Allows for the Detection of Uniparental Disomy and Cryptic Chromosomal Abnormalities in MDS/MPD-U and MPD. *PLoS ONE*, **2**, e1225.

231. Ling, J.Q., Li, T., Hu, J.F., Vu, T.H., Chen, H.L., Qiu, X.W., Cherry, A.M. and Hoffman, A.R. (2006) CTCF mediates interchromosomal colocalization between Igf2/H19 and Wsb1/Nf1. *Science*, **312**, 269-272.

Appendices

Table 1 Primer sequences for genotyping/bisulfite/polymorphism/MSP/RT-PCR

name	sequence	note
BXF4	5'ATCCCTCCAAGTGATTCTGAGACA3'	primers for genotyping AS-IC ^{an} mice by PCR
BXR4	5'TTTGGCCATATAACAGGGCTCCAG3'	
T7	5'GTAATACGACTCACTATAGGGC3'	
SHF	5'CATACTCTACTTTGTGCAGTAA3'	
SHR	5'ACAAGGAATTTAGATGTATCAT3'	
		amplify probe for Southern detection of AS-IC ^{an} mice
AH4	5'AATCTGTGTGATGCTTGCAATC3'	129/SvEv and PWK/phJ polymorphism detection
AH5	5'CACTAACACACCCCAAGGAGTCC3'	
AH52	5'AGGATGTCAGAGCTGTGTAGTG3'	
AH53	5'CACAATCACTTCTCTGACTTGC3'	
AH44	5'GAACTATTAAGTGTGTGGCCTG3'	
AH5r	5' GGACTCCTTGGGTGTGTTAGTG3'	
AH45	5'GCCGCACAGTAACAGTTACA3'	
BIOF	5'TATGTAATATGATATAGTTTAGAAATTAG3'	DMR of <i>Snurf-Snrpn</i> bisulfite outside PCR primers
BIOR	5'AATAAACCCAAATCTAAAATATTTTAATC3'	
BIIF	5'AATTTGTGTGATGTTTGTAAATATTTGG3'	
BIIR	5'ATAAAATACACTTTCCTACTAAAATCC3'	
		DMR of <i>Snurf-Snrpn</i> bisulfite outside PCR primers
Mf	5'TTAATATACGTTTAAATTTTCG3'	MSP primers specific for maternal allele
Mr	5'TAACTCAAATTTATCGCGCG3'	
Pf	5'GTTGTTTTTTGGTAGGATATTTTGG3'	
Pr	5'CAATAACTCAAATTTATCACACAAC3'	
		MSP primers specific for paternal allele
AH10	5'CCTTGAATTCCACCACCTTG3'	at <i>Snurf-Snrpn</i> exon 3
AH11	5'CAGCAAGGCAATACAGCAAAT3'	
AH12	5'GAGGCAGGCAAACATGCCTCT3'	
Hprt	5'AATTACTTTTATGTCCCCTGTTGACTGG3'	
		at U exon 7
		at U exon 5
		at 3'Hprt exons of pG12H6
ksc3	5'GTGGGGAGAACTTGGTTTCAAT3'	<i>Snurf-Snrpn</i> gene specific primers for real time PCR
ksc4	5'TGCAGCGCCAGCAAGA3'	
purof	5'TGACCGAGTACAAGCCCACG3'	<i>Puromycin</i> gene specific primers for real time PCR
puror	5'AGGCCTTCCATCTGTTGCTG3'	
actinF	5'ACAACGGCTCCGGCATGTGC3'	<i>actin</i> gene specific primers for real time PCR
actinR	5'GGGTGTTGAAGGTCTCAAAC3'	

Table 2 Primer sequences for ChIP/ACT/5'RACE

name	sequence	note
AH20a	5'GATGCTTGCAATCACTTGGGAA3'	amplify DMR of <i>Snurf-Snrpn</i> PWK allele from ChIP DNA
AH21a	5'CAGCTACCAAAAGGAATGCTTGAA3'	
AH22a	5'GATGCTTGCAATCACTTGGGAG3'	amplify DMR of <i>Snurf-Snrpn</i> 129 allele from ChIP DNA
AH23a	5'CAGCTACCAAAAGGAATGCTTGAG3'	
AH24a	5'TCCTCAATATTAAGTCTAGCATGGTTA3'	amplify D13Mit55 region from ChIP DNA
AH25a	5'ATTAGATTTCATAAAAGGAAGGTGTGTG3'	
AH15	5' GGCAATTATATCCATTATTCCA3'	amplify both 129 and PWK alleles of DMR of <i>Snurf-Snrpn</i> from ChIP DNA
AH16	5' CTCTCCTCTCTGCGCTAGTCTT3'	
AH79	5'GCTGACCCTGAATTCGCACGTGCCTGTCGT TAGCGGACACAGGGCGATTAC3'	linker for ACT (231)
AH80	5'CGGTGAATC3'	
AH77	5'GCTGACCCTGAATTCGCACGTGCCT3'	out primers for ACT
AH81	5'GTTGCTGCTTCATGTGGCTTCAAGG3'	
AH78	5'GTCGTTAGCGGACACAGGGCGATT3'	inner primers for ACT

Table 3 Primers used in 3C assay

name	sequence	note
AH50	5'CGTTTCAGAAAGAATTGATGACC3'	flanking <i>Bg</i> /II site at 3' end of <i>Ndn</i> in mice
AH51	5'CTGTCAGAATAGTTTCGCTCATC3'	
AH52	5'AACCAATACCTCAGGACTGGAC3'	flanking <i>Bg</i> /II site at PWS-IC in mice
AH53	5'CACAATCACTTCTCTGACTTGC3'	
AH54	5'AACCAATACCTCAGGACTGGAC3'	flanking <i>Bg</i> /II site at 3' of 6-kb region in mice
AH55	5'CATAGAGTCTGATTCCCATTTG3'	
AH56	5'GAATATCCCACAACAAGCTATG3'	flanking <i>Bg</i> /II site at 5' of 6-kb region in mice
AH57	5'GTTAGGCCTACATGCAATACAC3'	
AH58	5'GGAATTATGATTAGAATGGTGC3'	flanking <i>Bg</i> /II site at 3' of <i>Ube3a</i> in mice
AH59	5'TTCTGCAGTAGACAATTTAAACTC3'	
AH60	5'TCCAATTTTATTCTCAGCATAGAT3'	flanking <i>Bg</i> /II site at 5' of <i>Ube3a</i> in mice
AH61	5'TCACATTTCTAAAACCTCAATC3'	
AH62	5'TATCCAGGATCTTGCTTCATAG3'	flanking <i>Bg</i> /II site at 65kb from PWS-IC in mice
AH63	5'GGTCTTTCTCCATCTTCTGAGG3'	
AH64	5'CACAAGCACATCACTATCAAGG3'	flanking <i>Bg</i> /II site at 34kb from PWS-IC in mice
AH65	5'ATTGGATGATTTAAAGGAAGT3'	
AH66	5'TTCTCCAGTACGCATCCATCTC3'	flanking <i>Bg</i> /II site of DMR of NDN in human
AH67	5'CACCTGCTGGGAGAGCGATC3'	
AH68	5'CGGCTCTACAGGGAGGAAGC3'	flanking <i>Bg</i> /II site at 3' of PWS-IC in human
AH69	5'GGTCTGTGTTGCGTCACTGCC3'	
AH70	5'CGACATAGCCTTCCAAGACCTG3'	flanking <i>Bg</i> /II site at 5' of PWS-IC in human
AH71	5'CAGAAATGCGTGGAATCCTTGC3'	
AH95	5'AGCTCTGTTGCCGCAGCCTGTG3'	flanking <i>Nco</i> I site at PWS-IC in mice
AH96	5'CCGCGGCAACAGCACTCCAG3'	
AH91	5'GCAGGAGGCCTGTCATGGGCATACGG3'	flanking <i>Nco</i> I site at DMR of <i>Ndn</i> in mice
AH97	5'CTGCACCTGAGGCTGACCAATC3'	

Table 4 Primers used in vector construction and selection of positive colonies

name	sequence	note
psportr	5'CTGTTCTCGCTATTATTCCA3'	sequencing of pCMVsport β galN ⁻ <i>NheI</i> site
AH26	5'GATTGCTGAGCGCCGGTCGCTACCATTACCAGTTGGTCTGGTGTTCAGGGGATCCCCCGGGCTGCAGCCAATATGGGATCGG3'	neo-pA <i>BlnI-HindIII</i> fragment amplification
AH27	5'GTACAAGCTTCATAGAGCCCACCGCATCCC3'	
galA	5'CAACAGCAACTGATGGAAAC3'	Sequencing junction of β -gal and neomycin fusion gene
2.3f-2	5'GATCGAGCTCGCTAGCCACCGTGTGTCTCAGAA TCAC3'	2.1kb homologous genome DNA amplification
2.3R	5'GCCACTCGAGGAGACTTTGCCAGGACTATATG3'	
2.1R	5'CATATAGTCCTGGCAAAGTCTC3'	Sequencing pUNI-2 to make sure TK cassette insertion direction is correct. Sequencing pCMVH6
3.7F	5'CACAGGTACCCCAAGACCCAGTATAGTCAGTG3'	3.7 kb homologous genome DNA amplification
3.7R	5'GGCCACTAGTTTCTGTTGAATAAGCTCTAAGC3'	
3.7Fr	5'CACTGACTATACTGGGTCTTGG3'	Sequencing pCMVH6
galB	5'GAACCTGCGTGCAATCCATC3'	Together with galA to select for galactosidase positive
AHF1	5'GCCAGAACCACATAGCTTGTGTG3'	Selection for 5' junction positive ES cell colonies
AHR1	5'CTGATAAATCTGGAGCCGGTGAGC3'	
AHF2	5'GCAAGCAGCAGATTACGCGCAG3'	Selection for 3' junction positive ES cell colonies
AHR2	5'GGATCCAGACCTTATTAGGCCTCT3'	

Tabel 5 Microsatellite markers for PWS diagnosis

name	forward primer sequences and label fluorescence	reverse primer sequences	length
D15S541	D15S541 F : 5'GCATTTTGGTTACCTGTATG3' 5' 6-FAM label blue	5' GTCTTCCAGGTTTATGGTTGTC3'	150bp
D15S542	D15S542 F: 5'AGCAGACTCCGGAACCTCATC3' 5' PET label red	5'CCTGCCTTCTTGCTGGGGCTG3'	140bp
D15S543	D15S543 F: 5'GCTGTGATCTGTTTCAACAGAG3' 5' VIC label green	5'GCTGTGTTCACTTTCCAGAG3'	140bp
D15S11	D15S11 F: 5'GACATGAACAGAGGTAAATTGGTGG3' 5' NED label black	5'GCTCTCTAAGATCACTGGATAGG3'	243bp
D15S986	D15S986 F: 5'GCAGGAATATGTCCAGGG3' 5' 6-FAM label blue	5'CATGGCTGGTCTTTAGGTG3'	182-196bp
D15S165	D15S165 F: 5'TAAAGTTTACGCCTCATGGA3' 5' PET label red	5'CACAGTCCCAAACCATTTTA3'	209bp
D15S126	D15S126 F: 5'GTGAGCCAAGATGGCACTAC3' 5' VIC label green	5'GCCAGCAATAATGGGAAGTT3'	188-218bp
D15S1002	D15S1002F: 5'GTATCCCAAGGCCATACCCT3' 5' 6-FAM label blue	D15S1002R: 5'CTCTTGCTAGAGACAGCAGG3'	105-129bp
D15S1019	D15S1019F: 5'TTCTGGACCACGCATACTA3' 5' PET label red	D15S1019R: 5'ATCAGGCCATCTTTCATTGT3'	208-218bp
D15S1048	D15S1048F: 5'AGCCGTCTTTGTGCCA3' 5'VIC label green	D15S1048R: 5'TGCAGCCACTGTGGAA3'	197-233bp
D15S1031	D15S1031F: 5'CAATCATGTGAGCCAATTCC3' 5'NED label black	D15S1031R: 5'ACCCTGCATCATCCTCGTT3'	299-321bp
D15S1043	D15S1043F: 5'GAACGGAAATAGGAGTACCA3' 5'6-FAM label blue	D15S1043R: 5'ATTATCATCTGTAACTGTGTCCTT3'	92-104bp
D15S1010	D15S1010F: 5'TAGGGGCAAATTCAATCTC3' 5'VIC label green	D15S1010R: 5'TTCACACAGCGTGGAAG3'	193-237bp
D15S113	D15S113F: 5'CATGTACTGTTTTATCCCTGTGGC3' 5'6-FAM label blue	D15S113R: 5'CTGCTGCTTATACTCTTCTCTATTC3'	130bp
D15S984	D15S984F: 5'GCAGACACGCTCGCAT3' 5'PET label red	D15S984R: 5'GAGGCTCCGAGGGCAG3'	204-256bp
D15S115	D15S115F: 5'TACACAAATGGTACACTTTCCA3' 5'VIC label green	D15S115R: 5'TGGCTGGGTCTCTACATTTA3'	115bp

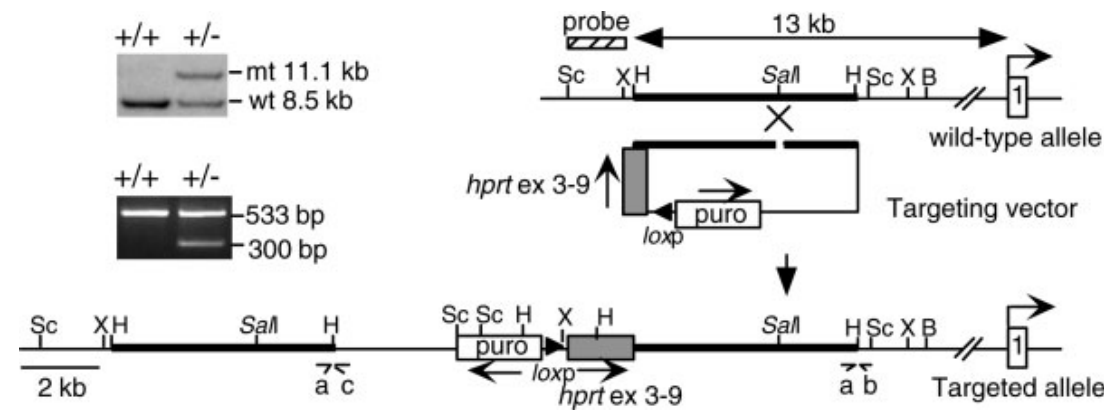


Figure 1 Generation of mice with an insertion/duplication (AS-IC^{an}) mutation 5' of *Snrpn* exon 1. Targeting strategy for generating the AS-IC^{an} mutation. The *Snrpn* genomic locus is at the top, the insertion targeting vector in the middle, and the final mutation at the bottom. The linearized targeting vector containing a 6 kb *Hind*III genomic DNA fragment, a puromycin resistance cassette (*puro*), a *loxP* site, and hypoxanthine phosphoribosyltransferase (*Hprt*) exons 3-9 was introduced into ES cells by homologous recombination. Left top: The targeting event in ES cells was analyzed using the 5' flanking probe (diagonally striped box) after digestion with *Sac*I. Left bottom: Integration of the vector was confirmed by PCR analysis using primers a and c to amplify a 300 bp fragment from the mutant allele and primers a and b to amplify a 533 bp fragment for a PCR control. ex, exon; Sc, *Sac*I; X, *Xba*I; H, *Hind*III; B, *Bam*HI.

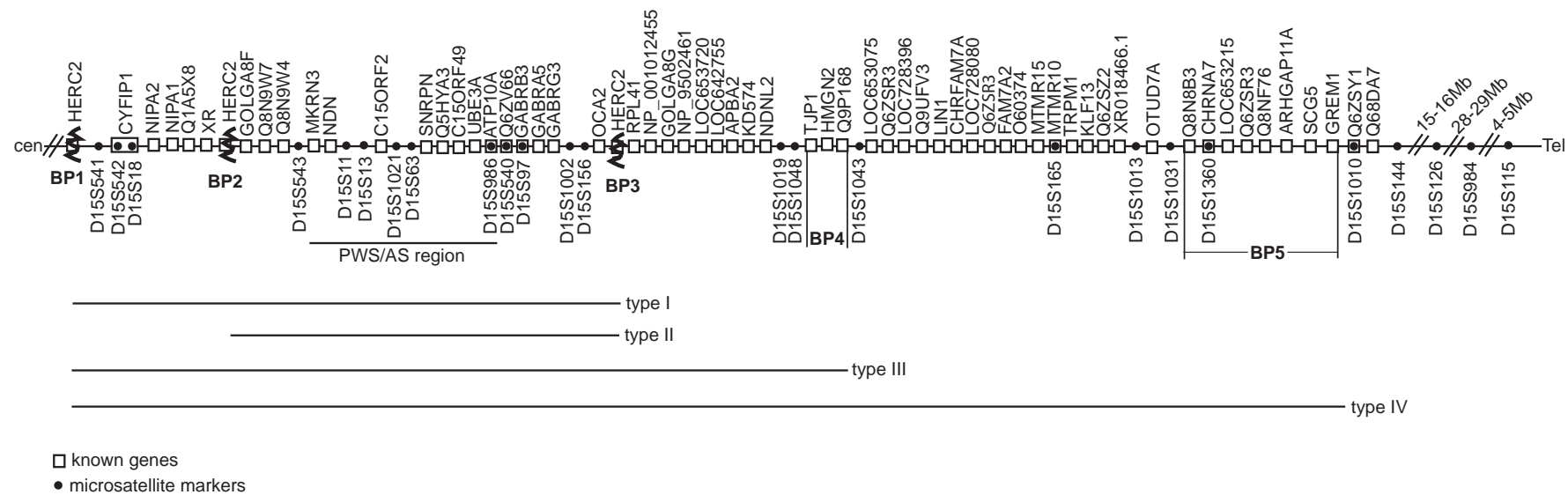


Figure 2 Schematic diagram showing the position of microsatellite markers and known genes at PWS/AS domain Zigzag lines indicate deletion breakpoints observed in PWS/AS patients. □: known genes; ●: microsatellite markers.